

Vol 14 No 1 (2010)

Vol 14 No 2 (2010)

### Malaysian Journal of Analytical Sciences Vol 14 No 1 2010

|    |   | Page |
|----|---|------|
| 1. | COUMARINS FROM MURRAYA PANICULATA (RUTACEAE)<br>(Koumarin daripada Murraya Paniculata (Rutaceae))<br>S. S. S. A. Aziz, M. A. Sukari, M. Rahmani, M. Kitajima, N. Aimi, N.J. Ahpandi   | 1    |
| 2. | CHEMICAL CONSTITUENTS FROM TWO WEED SPECIES OF SPERMACOCE (RUBIACEAE) (Kandungan Kimia daripada Dua Spesies Rerumput Spermacoce (Rubiaceae)) Neoh Bee Keat, Rahayu Utami Umar, Nordin Haji Lajis, Tai Yuen Chen, Tu Yen Li, Mawardi Rahmani, Mohd. Aspollah Sukari  | 6    |
| 3. | SURFACE EROSION AND SEDIMENT YIELDS ASSESSMENT FROM SMALL UNGAUGED CATCHMENT OF SUNGAI ANAK BANGI SELANGOR (Penilaian Hakisan Permukaan dan Muatan Sedimen Dari Kawasan Tadahan Sungai Anak Bangi Selangor)  Mohd Ekhwan Toriman, Md. Pauzi Abdullah, Mazlin Bin Mokhtar, Muhamad Barzani Gasim, Othman Karim   | 12   |
| 4. | EFFECTS OF INDUCED SALINITY ON BOD5 REACTION KINETICS OF RIVER WATER SAMPLES (Kesan Peningkatan Kemasinan Terhadap Kinetik Tindak Balas Keperluan Oksigen Biokimia 5 Hari Menggunakan Sampel Air Sungai)  Zaki Zainudin, Maketab Mohamed, Mohd. Rosslim Ramli   | 24   |
| 5. | ANALYSIS OF ESSENTIAL OILS OF ETLINGERA SPHAEROCEPHALA VAR. GRANDIFLORA BY TWO-DIMENSIONAL GAS CHROMATOGRAPHY WITH TIME-OF-FLIGHT MASS SPECTROMETRY (Analisis Minyak Pati Daripada Etlingera Sphaerocephala Var. Grandiflora Dengan Kromatografi Gas Dua Dimensi - Spektrometri Jisim Masa Terbang) M.A.A. Yahya, W.A. Yaacob, Laily B. Din, I. Nazlina | 32   |
| 6. | EFFECT OF HTAB CONCENTRATION ON THE SYNTHESIS OF NANOSTRUCTURED TiO2 TOWARDS ITS CATALYTIC ACTIVITIES (Kesan Kepekatan HTAB Terhadap Sintesis TiO2 Nanostruktur Ke Atas Aktiviti Pemangkinannya)  Ruslimie C. A, Mohd Hasmizam Razali and Wan M. Khairul  | 41   |

#### COUMARINS FROM MURRAYA PANICULATA (RUTACEAE)

(Koumarin daripada Murraya Paniculata (Rutaceae))

S. S. S. A. Aziz<sup>1</sup>, M. A. Sukari<sup>2</sup>\*, M. Rahmani<sup>2</sup>, M. Kitajima<sup>3</sup>, N. Aimi<sup>3</sup>, N.J. Ahpandi<sup>2</sup>

<sup>1</sup>Faculty of Science and Technology, Universiti Pendidikan Sultan Idris, 35900 Tanjung Malim, Perak Darul Ridzuan.

<sup>2</sup>Department of Chemistry, Universiti Putra Malaysia, 43400 UPM Serdang, Selangor Darul Ehsan.

<sup>3</sup>Faculty of Pharmaceutical Science, Chiba University, 1-33 Yayoi-Cho, Inage-Ku, Chiba 263, Japan.

\*Corresponding author: aspollah@science.upm.edu.my

#### Abstract

Phytochemical study on leaves of *Murraya paniculata* have yielded four coumarins of auraptene (1), *trans*-gleinadiene (2), 5,7-dimethoxy-8-(3-methyl-2-oxo-butyl)coumarin (3) and toddalenone (4). The compounds were isolated using chromatographic methods and identified using spectroscopic techniques. Antimicrobial activity evaluation on the crude extracts and pure compounds indicated chloroform extracts of the leaves exhibited moderate activity and only gleinadiene (2) showed moderate activity against *Bacillus cereus*. *trans*- Isomer of Gleinadiene (2) has never been reported from this plant previously.

Keywords: Murraya paniculata; auraptene; gleinadiene; antimicrobial

#### Abstrak

Kajian fitokimia terhadap daun *Murraya paniculata* telah menemui empat koumarin; auraptena (1), *trans*-gleinadiena (2), 5,7-dimetoksi-8-(3-metil-2-oks-butil)koumarin (3) dan toddalenon (4). Semua sebatian ini telah dipencilkan melalui kaedah kromatografi dan dikenalpasti melalui teknik spektroskopi. Penilaian aktiviti anti-mikrob terhadap ekstrak dan sebatian tulen menunjukkan bahawa ekstrak kloroform memperlihatkan aktiviti yang rendah dan hanya gleinadiena (2) menunjukkan aktiviti yang lemah terhadap *Bacillus cereus*. Isomer-*trans* bagi gleinadiena masih belum pernah dilaporkan daripada tumbuhan ini sebelum ini.

Katakunci : Murraya paniculata; auraptena; gleinadiena; antimikrob

#### Introduction

Rutaceae is a large family of trees, shrubs and climbers recognized easily from aromatic or lime-like smell of the broken twigs or fruits or of the crushed leaves. Some constituents of essential oils, such as citronella and bergamot, are obtained by distillation from plants of this family, and many species are used in native medicine. There are 16 from 161 genera and 60 from 1700 species occur in Malaysia, mostly found in lowland areas. *Murraya paniculata* which belong to Rutaceae family is one of the two genus species that can be found in West Malaysia. The plant which also well known as "kemuning" or orange jasmine also known as Chinese box in America and Canada [1]. The leaves are rather lather and dark shiny green. Their root bark is used as an anodyne or local anesthetic for the treatment of gout, contusion and bone ache [2].

The ground bark of *Murraya paniculata* is used in mixture of a drink and as antidote in snake bites and rubbed on the bitten limb. The ground bark of the root is eaten and rubbed on body to cure body ache. The powdered leaves is used as an application to fresh cuts, and decoction of the leaves is drunk in dropsy. They possess antibiotic activity against *Mycococcus pyogenes* and *Escherichia coli* [3, 4]. Both leaves and roots of the plant are used in folk medicine for the treatment of stomachache, toothache and gout [5], and treatment of diarrhea, dysentery and useful against rheumatism, cough and hysteria [3, 6, 7]. It is also reported that it is used to treat cuts, joint pain, body aches [8], and venereal disease [9]. Previous studies have reported several flavonoids and coumarins from the leaves and roots of *M. paniculata* [9, 10, 11]. Here we report the isolation and structural determination of coumarins from the leaf extracts of *M. paniculata* and their antimicrobial properties. The isolation of *trans*-isomer of gleinadiene from *M. paniculata* has never been reported previously.

#### **Experimental**

#### General procedure

Melting points were determined with Kofhler hot stage apparatus and were uncorrected. Infrared spectra were recorded with Perkin Elmer FTIR model 1725X spectrophotometer using KBr discs. Mass spectra were recorded on a Finnigen Mat SSQ710 spectrometer. <sup>1</sup>H-NMR spectra were obtained using 500 MHz JEOL spectrophotometer in CDCl<sub>3</sub>. <sup>13</sup>C-NMR spectra were determined in CDCl<sub>3</sub> operating at 125 MHz. TMS was used for internal standard while chemical shifts were reported in ppm. Vacuum column chromatography was employed by using silica gel Merck Kieselgel PF<sub>254</sub>. Preparative thin layer chromatography utilized Merck silica gel PF<sub>254</sub>. Analytical TLC was performed on commercially available TLC plastic sheets precoated with Kieselgel 60 F<sub>254</sub> (0.2 mm thickness).

#### Plant material

The plant sample was collected from Ipoh, Perak (Malaysia). A voucher specimen (No. RK 2954-96) was deposited in the Herbarium of the Department of Biology, Universiti Putra Malaysia.

#### **Extraction and isolation of compounds**

The leaves of *Murraya paniculata* were air-dried, ground to powder (1.5 kg) and extracted successively with petroleum ether, chloroform and methanol. The extracts were concentrated to produce semi solids weighed 21.6, 64.2 and 20.5 g of extracts respectively. The petroleum ether extract (19.6 g) was fractionated on a vacuum column chromatography of silica gel eluted with mixtures of petroleum ether, petroleum ether/chloroform and chloroform/methanol. A total of 50 fractions of 250 ml each were collected. Fraction 36 was rotary-evaporated, and the remaining solid was washed using ether and recrystallised with petroleum ether to yield auraptene (1); colourless crystals (65.2 mg),  $C_{19}H_{22}O_3$ , m.p. 64-65°C (Lit. [12] m.p. 67-68°C). MS m/z (% intensity): 298 (M<sup>+</sup>, 1), 163 (47), 162 (75), 136 (40), 93 (28), 81 (56), 69 (100), 41 (68). H- and <sup>13</sup>C-NMR data are in good agreement with the published data [12].

The chloroform extract (30.0 g) was chromatographed over a vacuum column chromatography on silica gel. The column was eluted with solvent mixtures of increasingly polarity (petroleum ether, petroleum ether/chloroform, chloroform/methanol) and 89 fractions of 250 ml each were collected. Solid obtained from fraction 29 upon washing with ether was recrystallised with methanol and gave gleinadiene (5,7-dimethoxy-8-[(E)-3'-methylbuta-1',3'-dienyl]coumarin) (2); yellow needles (261.3 mg),  $C_{16}H_{16}O_4$ , m.p. 138-141°C (Lit. [13] m.p. 120-121°C). IR  $v_{max}$  (cm<sup>-1</sup>, KBr disc); 2948, 1640, 1618, 1456, 1328, 1266, 1206, 1144, 1060, 992, 888, 746, 656. MS m/z, (% intensity); 272 (M<sup>+</sup>, 100), 257 (14), 241 (95), 226 (16), 213 (60), 198 (22), 182 (21), 155 (13), 141 (21), 128 (25), 115 (70), 91 (19); 77 (25), 63 (22), 51 (18). The <sup>1</sup>H-NMR and <sup>13</sup>C-NMR data are summarized in Table 1. Solid product of fractions 34-38 from chloroform extract was washed with ether and recrystallised with methanol to give 5,7-dimethoxy-8-(3-methyl-2-oxo-butyl)coumarin (3); colourless needles (32.5 mg),  $C_{16}H_{18}O_5$ , m.p. 124-126°C (Lit. [14] m.p.121-122°C). MS m/z (% intensity) 290 (M<sup>+</sup>, 12), 272 (1), 219 (100), 205 (2), 176 (3), 161 (30), 133 (6), 118 (6), 89 (4), 77 (5), 51 (3). <sup>1</sup>H- and <sup>13</sup>C-NMR data are in good agreement with the published data [14].

Fractions 58-59 from chloroform extract were rotary evaporated to give solid which was washed with ether and recrystallised with ethanol to give toddalenone (4); yellow needles (22.4 mg),  $C_{15}H_{14}O_5$ , m.p. 225-229°C (Lit.[12], m.p. 244-246°C). MS m/z (% intensity): 274 (M $^+$ , 34), 259 (52), 243 (100), 231 (31), 216 (35), 215 (9), 188 (29), 173 (43), 160 (6), 145 (18), 117 (10), 115 (21), 89 (18), 77 (12), 63 (21), 51 (12).  $^{1}H_{-}$  and  $^{13}C_{-}$  NMR are in good agreement with the published data [12].

#### **Antimicrobial assay**

Crude extracts and isolated compounds from *Murraya paniculata* were tested against one gram positive bacteria (*Bacillus cereus*) and 4 fungi (*Saccharomyces cerevisiae*, *Candida lypolytica*, *Saccharomyces lypolytica* and *Aspergillus ochraceous*) using the disc diffusion assay as described previously [15].

#### **Result and Discussion**

Extraction followed by chromatographic fractionation on the extracts of leaves of *Murraya paniculata* have yielded four coumarins; auraptene (1), gleinadiene (2), 5,7-dimethoxy-8-(3-methyl-2-oxo-butyl)coumarin (3) and toddalenone (4). The structures of the compounds were elucidated based on similarities of their spectral and physical data with the literature values. Out of four coumarins isolated, only compound (2) has not been

reported previously from this plant species. The characterization of compound (2) are described here besides the antimicrobial activity of the plant extracts.

Figure 1. Structure of coumarins isolated from Murraya paniculata

The IR spectrum of (2) showed peak at 1728 cm<sup>-1</sup> assigned as C=O group, while signal at 1618 cm<sup>-1</sup> was due to the presence of double bonds. The MS showed the presence of a molecular ion at m/z 272 corresponding to the molecular formula  $C_{16}H_{16}O_4$ .

The integration of the  $^1$ H NMR spectrum of (2) indicated the presence of 16 protons. A pair of doublets at  $\delta$  7.98 (J=9.7 Hz) and 6.16 (J=9.7 Hz) were characteristic of H-4 and H-3 in a coumarin nucleus, while another pair of doublets at  $\delta$  6.81 (J=16.3 Hz) and 7.37 (J=16.3 Hz) were assigned to H-2' and H-1', respectively. Coupling constant 16.3 Hz indicates that the structure has *trans* configuration. A methyl group signal at  $\delta$  2.02 and a two doublets due to two methylene protons at  $\delta$  5.16 and 5.07 (H-4') indicated that the coumarin contained a 3'-methylbuta-1',3'-dienyl side chain. The aromatic proton at H-6 occurs as a singlet at  $\delta$  6.32 to the upfield because of shielding effect of two methoxyl groups. The singlets at  $\delta$  3.96 and 3.94 were due to the presence of two methoxy groups at C-5 and C-7 in the aromatic ring respectively.

The assignments of  $^{1}$ H- and  $^{13}$ C-NMR data were confirmed by HMQC spectrum. The HMBC spectrum revealed H-4 at  $\delta$  7.98 correlated with carbon signal for C-2 (161.2 ppm) and C-5 (153.5 ppm). The proton signal at  $\delta$  7.37 (H-1') showed cross-peak with carbon signals at 103.8 ppm (C-8), 117.1 ppm (C-2') and 143.3 ppm (C-3'). H-2' at  $\delta$  6.81 found to correlate with C-1' (135.7 ppm) and C-3' (143.3 ppm). The proton signal at  $\delta$  6.32 (H-6) showed cross-peak with carbon signals at 161.1 ppm (C-7), 103.8 ppm (C-8) and 107.2 ppm (C-10). In addition, proton signal at  $\delta$  6.16 (H-3) correlated with carbon signal at 155.6 ppm (C-9) and 107.2 ppm (C-10). The complete NMR data of the compound (2) are displayed in Table 1. The structure of this compound was established based on the similarity of its spectral and physical data to those of gleinadiene previously isolated from *M. gleinei* root as reported by Kumar *et al.* [13]. However, there were inexplicable differences in the melting points for both compounds. The *cis* isomer of gleinadiene, (5,7-dimethoxy-8-[(Z)-3'-methylbutan-1',3'-dienyl]coumarin) which had been isolated from *Murraya paniculata* by Kinoshita and Firman [16] had coupling constant of 12.1 Hz. Our data demonstrated a larger value (16.3 Hz) which we suggest corresponds to *trans*-isomer of the compound. The melting point of toddalenone (4) in the present report was also found to be rather

far from the reported value [14]. The difference in melting points of several diastereoisomers of coumarins isolated from *Murraya* species are rather common phenomena [13].

| Table 1: <sup>1</sup> H- and <sup>13</sup> C-NMR Chemical Shifts (δ) and Coupling Patterns of the Protons and Correlations |
|--|
| in HMBC Techniques of Compound (2)   |

| Carbon no.         | <sup>13</sup> C (ppm)          | <sup>1</sup> <b>H</b> (ppm)   | HMBC                          |
|--------------------|--------------------------------|-------------------------------|-------------------------------|
|                    | (CDCl <sub>3</sub> , 67.9 MHz) | (CDCl <sub>3</sub> , 500 MHz) | Correlation                   |
| 2                  | 161.2                          | -                             | -                             |
| 3                  | 110.9                          | 6.16, d                       | C-9, C-10                     |
| 4                  | 138.7                          | 7.98, d                       | C-5, C-2                      |
| 5                  | 153.5                          | -                             | -                             |
| 6                  | 90.3                           | 6.32, s                       | C-7, C-8, C-10                |
| 7                  | 161.1                          | -                             | -                             |
| 8                  | 103.8                          | -                             | -                             |
| 9                  | 155.6                          | -                             | -                             |
| 10                 | 107.2                          | -                             | -                             |
| 1'                 | 135.7                          | 7.37, d                       | C-8, C-2', C-3'<br>C-1', C-3' |
| 2'                 | 117.1                          | 6.81, d                       | C-1', C-3'                    |
| 3'                 | 143.3                          | -                             | -                             |
| 4'                 | 117.0                          | 5.16, d                       | -                             |
|                    |                                | 5.07, d                       |                               |
| 5'                 | 18.3                           | 2.02, s                       | -                             |
| 5-OCH <sub>3</sub> | 56.0                           | 3.96, s                       | -                             |
| 7-OCH <sub>3</sub> | 55.9                           | 3.94, s                       | -                             |

All of the extracts and pure compounds were tested against gram positive bacteria and fungi. The chloroform extract of the leaves of *Murraya paniculata* demonstrated weak activity against *Bacillus cereus* and *Saccharomyces cerevisiae* with inhibition zone of 9 and 8 mm. respectively. No activity was observed against other microbes. In addition, all other extracts of the plant were found to be non active against all the microbes used in the test. Of all the isolated compounds, only compound (2) exhibited weak antimicrobial activity against *Bacillus cereus* (8 mm inhibition zone). Thus, the antibacterial activity of the chloroform extract may be due to the synergistic effect of compound (2) since compounds (1), (2) and (3) were isolated from chloroform whereas (1) was obtained from *petroleum ether extract*.

#### References

- 1. Bailey, L.H. (1978). The standard Encylopedia of Horticulture Vol II, Mac Milan.
- 2. Kinoshita, T., Tahara, S., Ho, F.C. and Sakawa, U. (1989). 3-Prenylindoles from *Murraya paniculata* and Their Biogenetic Significance. *Phytochemistry*. **28**(1): 147-151.
- Sastri, B.N. (1962). The Wealth of India: New Delhi. Council of Scientific and Industrial Research, Vol VI, p. 446.
- 4. Perry, L.M. (1980). Medicinal Plants of East and Southeast Asia. M.I.T. Press Cambridge, p. 367.
- 5. Rahman, A.U., Shabbir, M., Sultani, S.Z., Jabbar, A. and Choudhary, M.I. (1997). Cinnamates and Coumarins from the Leaves of *Murraya paniculata*. *Phytochemistry*. **44**(4): 683-685.
- 6. Chopra, R.N., Nayar, S.L. and Chopra, I.C. (1956). Glossary of India Medicinal Plants. India, CSIR, p. 171.
- 7. Ghani, A. (2003). Medicinal Plants of Bangladesh: Chemical constituents and Uses. Second edition. Dhaka. Asiatic Society of Bangladesh, 309-310.
- 8. Parotta, J.A. (2001). Healing Plants of Peninsular India New York, CABI Publishing, p. 917.
- 9. Kinoshita, T. and Firman, K. (1996). Highly Oxygenated Flavonoids from *Murraya paniculata*. *Phytochemistry*, **42**: 1207-1210.
- 10. Sukari, M.A., Azziz, S.S.S.A., Rahmani, M., Ali, A.M., Aimi, N. and Kitajima, M. (2003). Polysubstituted Flavonoid from the Leaves of *Murraya paniculata* (Rutaceae). *Natural Product Science*. **9**(2): 56-59.
- 11. De Silva, L.B., De Silva, U.L.L, Mahendran, M. and Jennings, R.C. (1980). 4'-Hydroxy-3,5,6,7,3',5'-hexamathoxyflavone from *Murraya paniculata*. *Phytochemistry*. **19**: 2794.

- 12. Ishii, H., Ishikawa, T., Mihara M. and Akaike, M. (1983). The Chemical Constituents of *Xantoxylum ailanthoides. Yakugaku Zasshi*. **103**(3): 279-292.
- 13. Kumar, V., Reisch, J., Wickremaratne, D.B.M., Adesina, K.S., Hussain, R. and Balasubramaniam, S. (1987). Gleinene and Gleinadiene. 5,7-dimethoxycoumarins from *Murraya gleinei* root. *Phytochemistry*. **26**(2): 511-514.
- 14. Imai, F., Itoh, K.N., Kinoshita, T. and Sakawa, U. (1989). Constituents of the Root Bark of *M. paniculata* Collected in Indonesia. *Chem. Pharm. Bull.* 37: 119-123.
- 15. MacKeen, M.M., Ali, A.M., El-Sharkawy, S.H., Manap, M.Y., Salleh, K.M., Lajis, N.H., Kawazu, K. (1997). Antimicrobial and Cytotoxic Properties of Some Malaysian Traditional Vegetables. *International Journal of Pharmacognosy*, **35**: 174-178.
- 16. Kinoshita, T. and Firman, K. (1996). Prenylcoumarin Derivatives from the Leaves of an Indonesian Medicinal Plant *Murraya paniculata* (Rutaceae). *Chem. Pharm. Bull.* **44**(6): 1261-1262.

#### CHEMICAL CONSTITUENTS FROM TWO WEED SPECIES OF SPERMACOCE (RUBIACEAE)

(Kandungan Kimia daripada Dua Spesies Rerumput *Spermacoce* (Rubiaceae))

Neoh Bee Keat<sup>1</sup>, Rahayu Utami Umar<sup>2</sup>, Nordin Haji Lajis<sup>2</sup>, Tai Yuen Chen<sup>2</sup>, Tu Yen Li<sup>2</sup>, Mawardi Rahmani<sup>2</sup>, Mohd. Aspollah Sukari<sup>2\*</sup>

<sup>1</sup>Sime Darby Technology Centre, 2, Jalan Tandang, 46050 Petaling Jaya, Selangor <sup>2</sup>Chemistry Department, Faculty of Science, Universiti Putra Malaysia, 43400 Serdang, Selangor, Malaysia

\*Corresponding author: aspollah@science.upm.edu.my

#### Abstract

Spermacoce articularis and Spermacoce exilis are weeds commonly growing in wastelands but widely used as traditional medicines. The separation works on the two plant species had been carried out using various solvents and chromatographic methods. The structures of the isolated compounds were determined by using spectroscopic methods such as IR, MS, <sup>1</sup>H NMR, <sup>13</sup>C NMR, 2D-NMR and by comparison with the data reported previously. Extracts from Spermacoce articularis gave two compounds, identified as ursolic acid (1) and stigmasterol, while extracts from Spermacoce exilis yielded four compounds, ursolic acid (1), benzo[g]isoquinoline-5,10-dione (2), stigmasterol and hexadecanoic acid (3). There was no previous phytochemical investigation on Spermacoce exilis.

Keywords: weed; Spermacoce; Rubiaceae; ursolic acid

#### Abstrak

Spermacoce articularis dan Spermacoce exilis adalah rerumput yang selalunya tumbuh di tanah terbiar tetapi banyak digunakan meluas sebagai ubatan tradisional. Proses pemisahan telah dijalankan ke atas dua spesies tumbuhan tersebut menggunakan pelbagai pelarut dan kaedah kromatografi. Struktur sebatian yang telah dipencilkan ditentukan dengan kaedah spektroskopi seperti IM, JS, RMN <sup>1</sup>H, RMN <sup>13</sup>C, RMN-2D serta membandingkan dengan data yang dilaporkan sebelumnya. Ekstrak daripada Spermacoce articularis memberikan dua sebatian, dikenali sebagai asid ursolik (1) dan stigmasterol. manakala ekstrak daripada Spermacoce exilis memberikan empat sebatian, asid ursolik (1), benzo[g]isokuinolin-5,10-dion (2), stigmasterol and asid heksadekanoik (3). Tiada siasatan mengenai fitokimia bagi spesies Spermacoce exilis dilaporkan selama ini.

Katakunci: rerumput; Spermacoce; Rubiaceae; asid ursolik

#### Introduction

Rubiaceae is one of the larger plant families and comprises of some 650 genera and 10,500 species. Most of the members are mainly distributed in the tropical and subtropical regions, with a few exceptions in temperate regions. There are 80 genera and 555 species in the Malay Peninsular. Several famous members of this family of economic importance are coffee (*Coffea*) and quinine (*Cinchona*), as well as *Gardenia*, cultivated for its fragrant flowers. *Spermacoce* is a relatively large genus of herbs or half-shrubby plants. This genus consists of about 100 species distributed throughout the tropics. Several of them are united with *Borreria*, so that some of the Malayan species have synonyms [1].

Spermacoce articularis (shaggy button weed) is a diffused herb found in tropical Asia and Peninsular Malaysia. It is commonly seen growing in sandy wastelands often in the coastal areas. A poultice of this plant is used to heal leg ulcers, wounds, headaches, toothaches and found to be highly antioxidative [2]. Previous phytochemical studies on S. articularis originated from India indicated the presence of flavonoids [3], triterpenoids [4] and ursolic acid [5]. Spermacoce exilis is also found throughout Peninsular Malaysia. It commonly grows in wastelands and garden paths. It is used to treat headache, fever and ulcers. This herb contains coumarins and is used in Java for poultice. Despite all the applications in the medicinal plant practices, the chemical constituents of this plant have never been investigated. Thus, here we report the phytochemical studies on Spermacoce articularis and Spermacoce exilis.

#### **Experimental**

#### General

Melting points were determined using Kohfler melting points apparatus and were uncorrected. The IR spectra were recorded using KBr discs on Perkin Elmer FTIR spectrophotometer 1650. <sup>1</sup>H and <sup>13</sup>C NMR spectra were obtained on JEOL spectrometer at 400 and 100 MHz, respectively with tetramethylsilane (TMS) as internal standard. Mass spectra were recorded on an AE1-MS12 spectrometer. Separation by column chromatography was carried out using silica gel (Merck 7749 and 9385), while silica gel 60PF<sub>254</sub> was used for TLC analysis.

#### Plant material

Both Spermacoce articularis and Spermacoce exilis were collected from Sungkai Reverse Forest in Perak in 2005 and identified by Mr. Shamsul Khamis, Institute of Bioscience (IBS), Universiti Putra Malaysia and voucher specimens were deposited at the IBS Herbarium. The voucher specimen numbers of Spermacoce articularis is SK 607/03 while Spermacoce exilis is SK 608/03.

#### **Extraction and isolation**

The finely ground air-dried *Spermacoce articularis* (600 g) was extracted with 90% ethanol for 72 hours to give 30.5 g of crude extract. The extract was partitioned with various solvents and concentrated under reduced pressure to give hexane (12.5 g), dichloromethane (3.75 g) and ethyl acetate (12.6 g) extracts. Ten gram of hexane extract was subjected to column chromatography eluted with mixtures of hexane, ethyl acetate and ethanol as eluents to give 25 fractions. Purification by trituration with MeOH of fraction 8 and fraction 12 gave stigmasterol (18 mg) and compound 1 (1.45 g), respectively. While the finely ground air-dried *Spermacoce exilis* (600 g) was similarly extracted with 90% ethanol for 72 hours to give 21.1 g of crude extract. The extract was partitioned with various solvents and concentrated under reduced pressure to give hexane (1.1 g), dichloromethane (4.5 g) and ethyl acetate (0.98 g) extracts. One gram of hexane extract was subjected to column chromatography eluted with mixtures of hexane, ethyl acetate and ethanol as eluents to give 41 fractions. Fraction 4 was futher purified by using smaller scale column chromatography to give compound 2 (8 mg) and stigmasterol (23 mg). Recrystalization of solid obtained from fraction 7 gave compound 3 (15 mg). Further isolation work on 4 gram of dichloromethane extract gave compound 1 (0.30 g).

*Ursolic acid* (1); colourless crystals,  $C_{30}H_{48}O_{3}$ , m.p 270-272 °C (lit. [6], m.p. 276-279 °C). IR (cm<sup>-1</sup>, KBr)  $v_{max}$ : 3446, 2392, 1698, 1456, 1382, 1244, 1036, 998, 664. <sup>1</sup>H NMR (400 MHz, DMSO) δ : 5.14 (1H, m, H-12), 3.05 (1H, dd, J=11.0, 4.6 Hz, H-3), 2.11 (1H, d, J=11.9 Hz, H-18), 1.94 (1H, m, H-16α), 1.85 (2H, m, H-11), 1.83 (1H, m, H-15α), 1.59 (1H, m, H-22), 1.53 (1H, m, H-16β), 1.50 (2H, m, H-2), 1.49 (1H, m, H-6α), 1.47 (1H, m, H-9), 1.45 (1H, m, H-7α), 1.44 (1H, m, H-21α), 1.36 (1H, m, H-21β), 1.30 (1H, m, H-19), 1.27 (1H, m, H-6β), 1.26 (1H, m, H-7β), 1.03 (3H, s, H-27), 0.93 (1H, m, H-15β), 0.92 (1H, m, H-20), 0.88 (2H, m, H-1), 0.88 (3H, d, d) =6.4 Hz, H-30), 0.87 (3H, d), H-23), 0.86 (3H, d), H-25), 0.83 (3H, d), d) =6.4 Hz, H-29), 0.76 (3H, d), H-26), 0.69 (3H, d), H-24), 0.69 (1H, d), d) =6.4 Hz, H-5). <sup>13</sup>C NMR, (100 MHz, DMSO) δ : 181.7 (C-28), 139.6 (C-13), 126.9 (C-12), 79.7 (C-3), 56.7 (C-5), 54.4 (C-18), 49.2 (C-9), 48.6 (C-17), 43.2 (C-14), 40.8 (C-8), 40.4 (C-19), 40.4 (C-20), 40.0 (C-4), 39.8 (C-1), 38.1 (C-10), 38.1 (C-22), 34.3 (C-7), 31.8 (C-21), 29.2 (C-23), 28.8 (C-15), 27.8 (C-2), 25.3 (C-16), 24.3 (C-27), 24.0 (C-11), 21.6 (C-30), 19.5 (C-6), 17.8 (C-29), 17.7 (C-26), 16.4 (C-24), 16.0 (C-25). EI-MS m/z (% intensity): 456 (M<sup>+</sup>, 3), 438 (1), 423 (1), 248 (100), 219 (18), 203 (42).

Benzo[g]isoquinoline-5, 10-dione (2); green needle-shaped crystals,  $C_{13}H_7NO_2$ , m.p 178-180 °C (lit [7], m.p. 178-179 °C). IR (cm<sup>-1</sup>, KBr)  $v_{max}$ : 3582, 2920, 2850, 1678, 1578, 1302, 1142, 1022, 946, 922, 858, 792, 702. <sup>1</sup>H NMR (400 MHz, CDCl<sub>3</sub>) δ: 9.61 (1H, s, H-1), 9.15 (1H, d, d) d=7.5 Hz, H-3), 8.37 (1H, d), 8.37 (1H, d), 8.11 (1H, d), d=7.5 Hz, H-4), 7.91 (2H, d), d=7.5 NMR (100 MHz, CDCl<sub>3</sub>) δ: 182.8 (C-10), 182.8 (C-5), 155.7 (C-3), 150.0 (C-1), 138.7 (C-4a), 135.3 (C-8), 134.9 (C-7), 133.3 (C-5a), 133.3 (C-9a), 127.7 (C-6), 127.6 (C-9), 126.6 (C-10a), 119.3 (C-4). EI-MS m/z (% intensity): 209 (M<sup>+</sup>, 100), 181 (57), 153 (99), 126 (71), 99 (12).

*Hexadecanoic acid* (3); white crystal,  $C_{16}H_{32}O_2$ , m.p 38-40 °C (lit [8], m.p. 38-40 °C). IR (cm<sup>-1</sup>, KBr)  $v_{max}$ : 3438, 2920, 2850, 1738, 1468, 1174, 724. <sup>1</sup>H NMR (400 MHz, CDCl<sub>3</sub>): 2.32 (2H, t, J=7.3 Hz, H-2), 1.60 (2H, m, H-3), 1.27 (2H, m, H-15), 1.26 (22H, br s, H-4 to H-14), 0.85 (3H, t, J=7.3 Hz, H-16). <sup>13</sup>C NMR (100 MHz, CDCl<sub>3</sub>) δ: 179.2 (C-1), 34.0 (C-2), 31.9 (C-14), 29.0-29.7 (C-4 to C-13), 24.7 (C-3), 22.7 (C-15), 14.1 (C-16). EI-MS m/z (% intensity): 256 ( $M^{+}$ , 44), 242 (2), 227 (88), 185 (22), 129 (67), 85 (42), 55 (100).

#### **Results and Discussion**

Extraction and fractionation works on the extracts of *Spermacoce articularis* and *Spermacoce exilis* have afforded ursolic acid (1) as the major constituent besides benzo[g]isoquinoline-5,10-dione (2), hexadecanoic acid (3) and stigmasterol. The structures of the compounds were elucidated using spectroscopic techniques. The isolations works on *Spermacoce articularis* and *Spermacoce exilis* originated from Perak, Malaysia have never been reported previously.

The EI-MS spectrum of compound 1 showed molecular ion peak at m/z 456 that corresponds to molecular formula  $C_{30}H_{48}O_3$ . IR spectrum showed the presence of hydroxyl group as broad peak at 3346 cm<sup>-1</sup>, while peak at 1698 cm<sup>-1</sup> revealed the existence of carbonyl group. Peak at 1382 cm<sup>-1</sup> exhibited the presence of trisubstituted olefinic group. The <sup>1</sup>H NMR spectrum showed the presence of 48 protons. Higher field signals in the region of  $\delta$  0.69 to  $\delta$  2.11 indicated the characteristic of triterpene skeleton. An olefinic proton peak at  $\delta$  5.14 was assigned to H-12 which correlated to C-14 in HMBC spectrum. A signal represented H-3 was observed at lower field at  $\delta$  3.05 due to the attachment of a hydroxyl group to C-3. The COSY spectrum displays that H-15 $\alpha$  ( $\delta$ 1.83) showed cross peak with H-16 $\alpha$  ( $\delta$  1.53) while H-15 $\beta$  ( $\delta$  0.93) showed cross peak with H-16 $\beta$  ( $\delta$  1.94). Besides that, the COSY spectrum also showed that H-2 coupled to H-3 and H-18 coupled to H-19. The <sup>13</sup>C NMR spectrum accounted of 30 carbons. The peaks at  $\delta$  181.7 indicated the presence of a carbonyl group, assigned as C-28. A pair of sp<sup>2</sup> carbon (C-12 and C-13) was indicated at δ 126.9 and 139.6. The prominent peaks at higher field of  $\delta$  29.2, 16.4, 16.0, 17.7, 24.4, 17.8 and 21.6 were attributed to methyl carbons of C-23, C-24, C-25, C-26, C-27, C-29 and C-39, respectively. Some of the important HMBC correlations were shown by the cross peak between methyl proton peaks at  $\delta$  0.87 (H-23) and  $\delta$  0.69 (H-24) with carbon signal at  $\delta$  40.0 (C-4), Proton signals at δ 0.83 (H-29) and δ 0.88 (H-30) also correlated to carbon signal at δ 40.4 (C-19 and C-20). The complete assignments of NMR data are displayed in Table 1. Thus, compound 1 was determined as ursolic acid [5]. Ursolic acid was previously isolated and elucidated from *Ilex paraguariensis* [9] and also reported as the main compound present in apple (Malus domestica) cuticular wax as well as in the leaves [10].

Table 1: NMR spectral data for ursolic acid (1)

| Position, | <sup>13</sup> C | $^{1}\mathrm{H}$ | НМВС        | COSY        |
|-----------|-----------------|------------------|-------------|-------------|
| C         | (δ)             | $(\delta)$       | Correlation | Correlation |
| 1         | 39.8            | 0.88, m          | C-2, C-5    |             |
| 2         | 27.9            | 1.50, <i>m</i>   | C-10        | H-3         |

## Neoh Bee Keat et al: CHEMICAL CONSTITUENTS FROM TWO WEED SPECIES OF *SPERMACOCE* (RUBIACEAE)

| 3  | 79.7  | 3.05, <i>dd</i> , <i>J</i> =11.0, 4.6 Hz |                             | H-2  |
|----|-------|--|-----------------------------|------|
| 4  | 40.0  |  |                             |      |
| 5  | 56.7  | 0.69, <i>d</i> , <i>J</i> =6.4 Hz        |                             |      |
| 6  | 19.5  | 1.27, <i>m</i><br>1.49                   | C-10                        |      |
| 7  | 34.3  | 1.26, <i>m</i><br>1.45                   | C-14, C-26                  |      |
| 8  | 40.8  |  |                             |      |
| 9  | 49.2  | 1.47, m                                  | C-10, C-11, C-14            |      |
| 10 | 38.1  |  |                             |      |
| 11 | 24.1  | 1.85, m                                  | C-9, C-13                   | H-12 |
| 12 | 126.9 | 5.14, <i>m</i>                           | C-14                        | H-11 |
| 13 | 139.6 |  |                             |      |
| 14 | 43.2  |  |                             |      |
| 15 | 28.8  | 0.93, <i>m</i><br>1.83                   | C-13, C-17                  | H-16 |
| 16 | 25.3  | 1.53, <i>m</i><br>1.94                   | C-14                        | H-15 |
| 17 | 48.6  |  |                             |      |
| 18 | 54.4  | 2.11, <i>d</i> , <i>J</i> =11.9 Hz       | C-13, C-17, C-19 C-14, C-20 | H-19 |
| 19 | 40.4  | 1.30, <i>m</i>                           |                             | H-18 |
| 20 | 40.4  | 0.92, m                                  |                             |      |
| 21 | 31.8  | 1.36, <i>m</i><br>1.44                   |                             |      |
| 22 | 38.1  | 1.59, m                                  |                             |      |
| 23 | 29.2  | 0.87, s                                  | C-3, C-4, C-5, C-24         |      |
| 24 | 16.4  | 0.69, s                                  | C-4, C-3, C-5, C-23         |      |
| 25 | 16.0  | 0.86, s                                  | C-10, C-5                   |      |
| 26 | 17.7  | 0.76, s                                  | C-7                         |      |
| 27 | 24.4  | 1.03, s                                  | C-13                        |      |
| 28 | 181.7 |  |                             |      |
| 29 | 17.8  | 0.83, <i>d</i> , <i>J</i> =6.4 Hz        | C-19, C-18, C-20            |      |
| 30 | 21.6  | 0.88, <i>d</i> , <i>J</i> =6.4 Hz        | C-20, C-19                  |      |

Compound 2 exhibited a molecular formula of C<sub>13</sub>H<sub>7</sub>NO<sub>2</sub> from its EI-MS. The IR spectrum exhibited the presence of C=O stretching peak at 1678 cm<sup>-1</sup>, while 1578 cm<sup>-1</sup> was due benzene skeleton ring. Peaks at 1302 and 1142 cm<sup>-1</sup> indicated the presence of C=N and C-N groups. The <sup>1</sup>H NMR spectrum exhibited a total of seven protons. The aromatic region of the <sup>1</sup>H NMR spectrum indicated the presence of an A<sub>2</sub>B<sub>2</sub> system in ring A. Multiplets appearing at  $\delta$  8.37 and  $\delta$  7.91 integrating each for two protons were attributed to H-6/9 and H-7/8, respectively. A set of doublet at  $\delta$  9.15 (J=7.5 Hz) and  $\delta$  8.11 (J=7.5 Hz) were due to *ortho*-coupled H-3 and H-4 protons, which also showed correlation in COSY spectrum. In addition, one singlet intregated for one proton at  $\delta$  9.61 was assigned to H-1. The <sup>13</sup>C NMR spectrum gave absorption peaks representing all aromatic and carbonyl carbons. The presence of two carbonyl groups were indicated by overlapping peak at δ 182.8 (C-5/10). The locations of the C=O were suggested by HMBC correlation between H-4 and H-6 with C-5, and between H-9 with C-10. Other aromatic carbons of rings A and C were represented by signals between δ 119.3 and 155.7. Among the prominent HMBC cross peaks representing <sup>2</sup>J correlations were observed between H-6 and C-7, C-5a; H-7 and C-6; H-8 and C-9 and between H-9 and C-8, C-9a. The complete NMR data are summarized in Table 2. Based on the comparison of these spectral and physical data, compound 2 has thus been identified as benzo[g]isoquinoline-5,10-dione, which was previously isolated from Mitracarpus scaber [7]. This is the first report on the isolation of the compound from this plant species.

Table 2: NMR spectral data for benzo[g]isoquinoline-1,5-dione (2)

| Position, | <sup>13</sup> C | <sup>1</sup> H                    | НМВС                      | COSY        |
|-----------|-----------------|-----------------------------------|---------------------------|-------------|
| C         | $(\delta)$      | $(\delta)$                        | Correlation               | Correlation |
| 1         | 150.0           | 9.61, s                           | C-10a, C-3, C-4a          |             |
| 3         | 155.7           | 9.15, <i>d</i> , <i>J</i> =7.5 Hz | C-4, C-1, C-4a            | H-4         |
| 4         | 119.3           | 8.11, <i>d</i> , <i>J</i> =7.5 Hz | C-3, C-5, C-10a           | H-3         |
| 4a        | 138.7           |                                   |                           |             |
| 5         | 182.8           |                                   |                           |             |
| 5a        | 133.3           |                                   |                           |             |
| 6         | 127.7           | 8.37, m                           | C-7, C-5a, C-5, C-8, C-9a | H-7         |
| 7         | 134.9           | 7.91, <i>m</i>                    | C-6, C-5a, C-9            | H-6         |
| 8         | 135.3           | 7.91, <i>m</i>                    | C-6, C-9, C-9a            | H-9         |
| 9         | 127.6           | 8.37, m                           | C-8, C-9a, C-7, C-10      | H-8         |
| 9a        | 133.3           |                                   |                           |             |
| 10        | 182.8           |                                   |                           |             |
| 10a       | 126.6           |                                   |                           |             |

The EI-MS spectrum of compound 3 exhibited molecular ion at m/z 256, which corresponds to a molecular formula of  $C_{16}H_{32}O_2$ . The IR spectrum indicated the presence of asymmetric and symmetric methylene stretching bonds at 2920 and 2850 cm<sup>-1</sup>, respectively. Two absorptions at 1738 and 1468 cm<sup>-1</sup> represent carbonyl and methylene groups, respectively. The <sup>1</sup>H NMR spectrum showed the characteristic of aliphatic carboxylic acid at region between  $\delta$  0.80 to 2.40. The spectrum indicated the presence of a long chain methylene protons representing eleven methylene groups overlapped as broad peak at  $\delta$  1.26. The <sup>13</sup>C NMR spectrum showed the presence of seven peaks. The terminal methyl proton C-16 appeared at  $\delta$  14.1 attached to methylene carbon C-15 ( $\delta$  22.7). Another methylene carbon resonates at  $\delta$  31.9 (C-14), while methylene carbons C-14 and C-13 overlapped at between  $\delta$  29.7 – 29.0. The existence of carbonyl signal was observed at  $\delta$  179.2. The NMR

## Neoh Bee Keat et al: CHEMICAL CONSTITUENTS FROM TWO WEED SPECIES OF SPERMACOCE (RUBIACEAE)

data are shown in Table 3. The structure of compound 3 was therefore characterized as hexadecanoic acid. This fatty acid had been reported as one of constituents that was isolated from *Lysimachia fordiana* [11].

<sup>13</sup>C Position,  $^{1}H$ **HMBC**  $\mathbf{C}$ (δ) (δ) Correlation 179.2 1 2 34.0 2.32, t, J=7.3 Hz C-1, C-3, C-4 3 24.7 1.60, mC-1, C-2, C-4 4-13 29.0-29.7 1.26, br s 14 31.9 C-15 15 22.7 1.27, mC-13, C-14 16 14.1 0.85, t, J=7.3 Hz

Table 3: NMR spectral data for hexadecanoic acid (3)

#### Acknowledgements

We wish to express our thanks to Ministry of Science, Technology and Innovation (MOSTI) for financial assistance under E-Science Fund and to Universiti Putra Malaysia (UPM) for all facilities provided.

#### References

- Burkill, I.H. 1935. Dictionary of Economic Products from Malay Peninsular, Vol. I-II. The Ministry of Agriculture & Cooperatives, Kuala Lumpur, 1297.
- Saha, K., Lajis, N.H., Israf, D.A., Hamzah, A.S., Khozirah. S., Khamis, S. & Syahida, A. 2004. Evaluation
  of antioxidant and nitric oxide inhibitory activities of selected Malaysian medicinal plants. *Journal of Ethnopharmacology*, 92: 263-267.
- 3. Purushothaman, K.K. & Kalyani, K. 1979. Isolation of isorhamnetin from *Borreria hispida Linn. JRMYH*, **14**(1): 131-132.
- 4. Mukherjee, K.S., Manna, T.K., Laha, S. & Chakravorty, C.K. 1993. Phytochemical investigation af *Spermacoce articularis. Journal of Indian Chemical Society*, **70**: 609-610.
- 5. Kapoor, S.K., Prakash, L., Asif, Z. 1969. Chemical constituents of *Borreria hispida*. *Indian Journal of Applied Chemistry*, **32**(6): 402.
- 6. Tkachev, A.V., Denisov, A.Y., Gatilov, Y.V., Bagryanskaya, I.Y., Shevtsov, S.A. & Rybova, T.V. 1994. Stereochemistry of hydrogen peroxide-acetic acid oxidation of ursolic acid and related compounds. *Tetrahedron*, **50**(39): 11459-11488.
- 7. Okunade, A. L., Clark, A. M., Hufford, C. D. and Oguntimein, B. O. 1999. Azaanthraquinone: An antimicrobial alkaloid from *Mitracarpus scaber*. *Planta Medica*, **65**: 447–448.
- 8. Patra, A. and Chauduri. S.K. 1988. Chemical Constituents of *Impatiens balsamina Linn. Journal of The Indian Chemical Society*, **65**: 367-368.
- 9. Gnoatto, S. C. B., Klimpt, A. D., Nascimento, S. D., Galera, P., Boumediene, K., Gosmann, G., Sonnet, P., Moslemi, S. 2008. Evaluation of ursolic acid isolated from *Ilex paraguariensis* and derivatives on aromatase inhibition. *European Journal of Medicinal Chemistry*, **43**: 1865-1877.
- Belding, R. D., Blankenship, S. M., Young, E., & Leidy, R. B. 1998. Composition and variability of epicuticular waxes in apple cultivars. *Journal of the American Society for Horticultural Science*, 123(3): 348–356
- 11. Huang, X. A., Yang, R. Z., 2004. A new hydroquinone diglucoside from *Lysimachia fordiana*. *Chemistry of Natural Compounds*, **4**(5): 457-459.

#### SURFACE EROSION AND SEDIMENT YIELDS ASSESSMENT FROM SMALL UNGAUGED CATCHMENT OF SUNGAI ANAK BANGI SELANGOR

(Penilaian Hakisan Permukaan dan Muatan Sedimen Dari Kawasan Tadahan Sungai Anak Bangi Selangor)

Mohd Ekhwan Toriman<sup>1\*</sup>, Md. Pauzi Abdullah<sup>2</sup>, Mazlin Bin Mokhtar<sup>3</sup>, Muhamad Barzani Gasim<sup>4</sup>, Othman Karim<sup>5</sup>

<sup>1</sup> Fakulti of Social Sciences and Humanities
<sup>2,4</sup> Faculty of Science and Technology
<sup>3</sup> Institute of Environment and Development (LESTARI)
<sup>5</sup> Faculty of Engineering and Built Environment
Universiti Kebangsaan Malaysia, 43600 UKM BANGI, Selangor, Malaysia

\*Corresponding author: ikhwan@ukm.my

#### **Abstract**

This study was performed to estimate surface erosion and suspended yield in the forested catchment of Sungai Anak Bangi using USLE and numerical analyses from September-November 2006. The value of erosion rate, as dominated by *Serdang* and *Prang* series is moderate at 84.88 tons/ha/yr. Meanwhile, three major data were measured namely the rainfall depth, the suspended sediment concentration and river discharge (Q) at two sampling stations along the river. 12 rainfall events were recorded with highest rainfall of 36.7 mm was received on October 02, 2006 while the lowest rainfall depth was recorded on October, 08, 2006 (1.9 mm). Almost all the rainfall events occurred within the short and moderate durations (< 7 hours). Meanwhile, the daily Q sampled range from 172.8 m³/day to 6220.8 m³/day or 172, 800 and 6220, 800 L/day. The average suspended sediment concentration values recorded for both stations are considered low with 19.47 mg/l and 25.23 mg/l were recorded at Station 1 and Station 2, respectively. When converted to average suspended sediment yield per day, Sungai Anak Bangi was recorded of 75.0415 kg/day at Station 1 while at Station 2 was 103.256 kg/day. When converted into per square km, the gross value of suspended sediment yield leaved from Sungai Anak Bangi is estimated about 27.907 kg/km²/day or 10, 186 kg/km²/yr¹¹.

Keywords: Suspended sediment concentration, rainfall, river discharge, concentration, Sungai Anak Bangi

#### Abstrak

Kajian ini dibuat bagi menganggar hakisan permukaan dan muatan sedimen terampai di kawasan tadahan Sungai Anak Bangi menggunakan rumus USLE dan analisis numerical dari bulan September-November 2006. Kadar hakisan yang direkodkan oleh tanih jenis Serdang dan Prang ialah sederhana iaitu 84.88 tons/ha/yr. Sementara itu, tiga data utama telah diukur, iaitu kedalaman hujan, konsentrasi sedimen terampai dan luahan sungai (Q) di dua stesen pencerapan di sepanjang sungai. 12 kejadian hujan telah direkodkan dengan hujan tertinggi ialah 36.7 mm yang diterima pada 2 Oktober, 2006 sementara hujan terendah dicatatkan pada 08 Oktober 2006 (1.9 mm). Kebanyakan kejadian hujan berlaku dalam tempoh singkat dan sederhana (< 7 jam). Sementara itu, nilai Q harian adalah diantara 172.8 ke 6220.8 m³/hari atau 172, 800 and 6220, 800 L/hari. Purata nilai konsentrasi sedimen terampai yang direkodkan bagi kedua-dua stesen adalah rendah, iaitu masing-masing 19.47 mg/l dan 25.23 mg/l yang direkodkan bagi Stesen 1 dan 2. Nilai ini bila ditukarkan kepada penghasilan muatan sedimen terampai bagi Sungai Anak Bangi ialah 75.0415 kg/hari di Stesen 1 manakala di Stesen 2 ialah 103.256 kg/hari. Angka ini jika ditakrifkan kepada setiap kilometer persegi menunjukkan anggaran sedimen yang diangkut keluar melalui Sungai Anak Bangi ialah 27.907 kg/ km²/hari atau 10, 186 kg/ km²/tahun.

Kata kunci: Penghasilan muatan sedimen terampai, hujan, luahan sungai, konsentrasi, Sungai Anak Bangi

#### Introduction

In a natural environment, soil erosion is a worldwide issue all over the globe. Soil erosion is a two-phase process, consisting of the detachment of individual particles from soil mass and transport by erosive agent such as sediment water [1]. It is a natural process, erosion begun before the history of man's existence on earth. However, disturbance from human activities further aggravates the soil erosion process especially at steep slopes. In general most

## Mohd Ekhwan Toriman: SURFACE EROSION AND SEDIMENT YIELDS ASSESSMENT FROM SMALL UNGAUGED CATCHMENT OF SUNGAI ANAK BANGI SELANGOR

sediment in surface waters derives from surface erosion and comprises a mineral component, arising from the erosion of bedrock, and an organic component arising during soil-forming processes.

Surface erosion and sediments play an important role in elemental cycling in the aquatic environment. As studied by many researchers [2,3,4,5] sediments are responsible for transporting a significant proportion of many nutrients and contaminants. They also mediate their uptake, storage, release and transfer between environmental compartments.

The studies of the surface erosion and subsequent impacts of sediment on alluvial rivers have been explored significantly all over the world. Most of the studies concentrate on the impacts of land reclamation on sediment concentration at downstream rivers [6,7], agriculture activities and increase in sediment load [8], logging activity in hilly forest [9] and sediment-river water quality [10]. Presently, rivers contribute 95 percent of sediments entering the ocean [11]. Most of studies agreed that over sediment flux may result changes on water quality and flow regimes [12,13,14].

The trend of sediment production may be increase in future times due to rapid economic activities particularly those from developing countries. Such activities are land use change, reservoir construction, sediment control programmes and mining activity. The main objectives of the research are twofold, namely to estimate surface erosion generated by individual rainfall and to calculate suspended sediment yield from Sungai Anak Bangi.

#### Study Area

The study was conducted at Sungai Anak Bangi in Bangi Forest Reserve, Selangor (02° 55′ 44.0″ N latitude and 101° 47′ 12.6″E longitude, Figure 1). The total catchment area for Bangi Forest Reserve is 34 km², while for Sungai Air Anak Bangi is 3.7 km². A description of the physical and climatic features of the catchments is given in Table 1.

Table 1: Physical and climatic features of Sungai Anak Bangi

| River catchment detail                       | value  |
|--|--------|
| Physical fectures                            |        |
| catchment size (km <sup>2</sup> ): Station 1 | 1.5    |
| : Station 2                                  | 2.2    |
| Elevation (m): Max                           | 200    |
| : Min  | 100    |
| Catchment length (km)                        | 2.5    |
| $\Sigma$ stream length (km)                  | 3.6    |
| Stream order                                 | 3      |
| Drainage density                             | 1.29   |
| Catchment width ratio                        | 0.8    |
| Climatic fectures                            |        |
| Annual rainfall (mm)                         | 2250.7 |
| No of raindays                               | 158    |
| Relative humidity (%)                        | 85     |
| Temperature (°C): Max                        | 33     |
| : Min  | 24.6   |

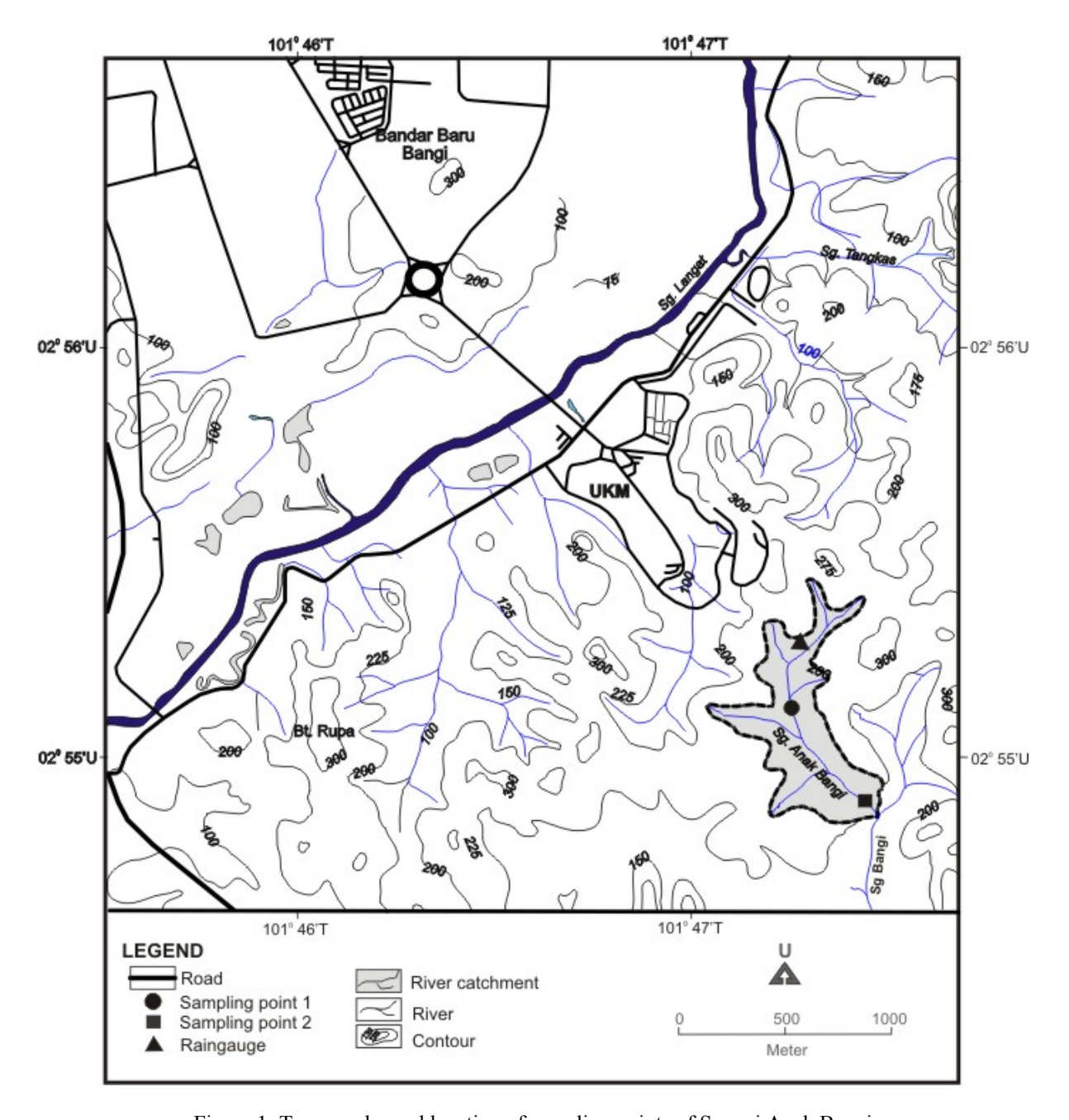


Figure 1: Topography and location of sampling points of Sungai Anak Bangi

The geology of the area is predominantly of granitic rocks. The soil texture ranges from coarse to fine sandy clay with Muchong-Seremban being the major soil series. The land cover of the study area is mostly hill dipterocarp forest. This forest has been logged in late 1960s and early 1970s. Towards downstream, the catchment has been transformed by oil palm plantations and development of Pekan Bangi Lama (Figure 2)

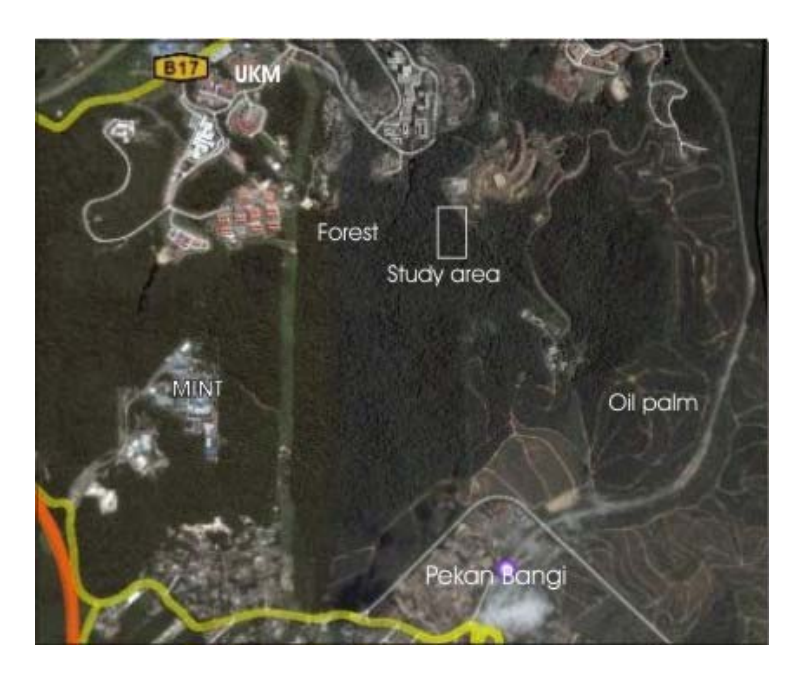


Figure 2: Existing land use surrounding the study catchment

#### **Material and Methods**

Soil erosion, based on tons/ha/yr was estimated using the Universial Soil Loss Equation [15]. (Wischmeier and Smith, 1978). The formulae for USLE estimation is,

 $A = R*K*LS*C*P \dots (1)$ 

where: A is the computed soil loss

R is the computed son ross
R is the rainfall erosivity index
K is the soil erodibility index
L is the slope length factor
S is the slope steepness factor
C is the vegetation/cover factor and
P is the soil conservation practices factor.

Meanwhile, rainfall was measured using the manual tipping bucket raingauge located at the Hutan Pendidikan Alam, UKM (02° 55′ 123.0″ N latitude and 101° 47′ 65.2″E longitude). It consists of a large copper cylinder set into the ground with funnel at the top of the cylinder to collects and channels the precipitation. This raingauge was installed temporary over two months of study period (September-November 2006).

Observed discharge was measured manually using mean-mid technique [16, 17, 18], at two water sampling points, namely the Station 1 and Station 2. Station 1 located at the upper reach of Sungai Anak Bangi while Station 2 is just before the river joint with Sungai Bangi. In this study, discharge calculation was estimated using the equation:

Q = sum of 
$$Q_n = W_1D_1V_1 + W_2D_2V_2 + \dots W_nD_nV_n$$
 .....(2)

where  $W_n$  is the width of the section (m),  $D_n$  the depth of the section at the midpoint (m), and  $V_n$  mean velocity of the section at the midpoint (m/s). Water samples were taken using the grab sampler method during rainy and storm events at both stations. Water samples were analysed for suspended concentration following the procedure outlined by Rainwater and Thatcher [19] and Morgan [20]. (1995). The residue remaining on the filter paper was oven dried at  $105^{\circ}$ C for 24 hours, cooled in a dessicator and weighed. The total amount of suspended sediment yield in kg/day then was calculated by multiplying the weighed suspended sediment with the stream discharge (m<sup>3</sup>s<sup>-1</sup>) during samplings [21].

#### **Results and Discussion**

#### **Surface erosion**

Calculation of rainfall erosivity index, soil erodibility index, slope length factor, slope steepness factor, vegetation/cover factor and soil conservation practices factor based on tons/ha/yr are tabulated in Table 2.

| Symbol | Parameter                                       | Unit   | Value            |
|--------|---|--------|------------------|
| R      | rainfall erosivity index                        | (J/ha) | 1654.55          |
| K      | soil erodibility index (Serdang & Prang series) | (t/J)  | 0.32             |
| L,S    | slope length factor                             | %      | 10.02            |
| C      | vegetation/cover factor                         | Index  | 0.02             |
| P      | soil conservation practices                     | Index  | 0.80             |
|        | -   |        |                  |
|        |   | A =    | 84.88 tons/ha/yr |

Table 2: Results of Surface erosion

The calculation of soil erosion based on USLE model show that Bangi Forest Reserve was 84.88 tons/ha/yr. Most of the forested area occurred in the west and northern part of the watershed and most of the human activities occurred in the east and southern region. The steepest slopes within the watershed occur to the west and northern part of watershed. On the basis of Soil Loss Tolerance Rates in Department of Environment [22], Serdang, and Prang Series have moderate rate of soil loss. These Soil Series areas are located under oil palm, rubber and forest area. Due to some part of forest area, the value of erosion yield can be considered as moderate.

#### **Sediment Concentration and yields**

The two sampling stations along Sungai Anak Bangi were selected in order to gain some idea of sediment yield between upstream and downstream sites. Generally speaking, the sediment productions at Sungai Anak Bangi are very much relied to rainfall events. During the study period, 12 rainfall events were recorded with highest rainfall of 36.7 mm was received on October 02, 2006 while the lowest rainfall depth was recorded on October 08, 2006 (1.9 mm). Most of the rainfall events occurred within the short and moderate durations (< 7 hours) from 75 to 405 minutes. The daily rainfall depth pattern during the study period exhibited fairy similar pattern compared with average 10 years mean daily rainfall depth recorded at Universiti Kebangsaan Malaysia Rainfall stations (240°N 101° 44'E) (Figure 3). The relationships when expressed into statistical showing positive significant relationship with R<sup>2</sup> = 0.5625 (Figure 4). Nevertheless, certain observed days recorded highest than the long term average namely day-4, day-5 and day-9, while others recorded less than the long term average rainfall. Detailed of rainfall depth and results of individual stations on suspended sediment production is tabulated in Table 3.

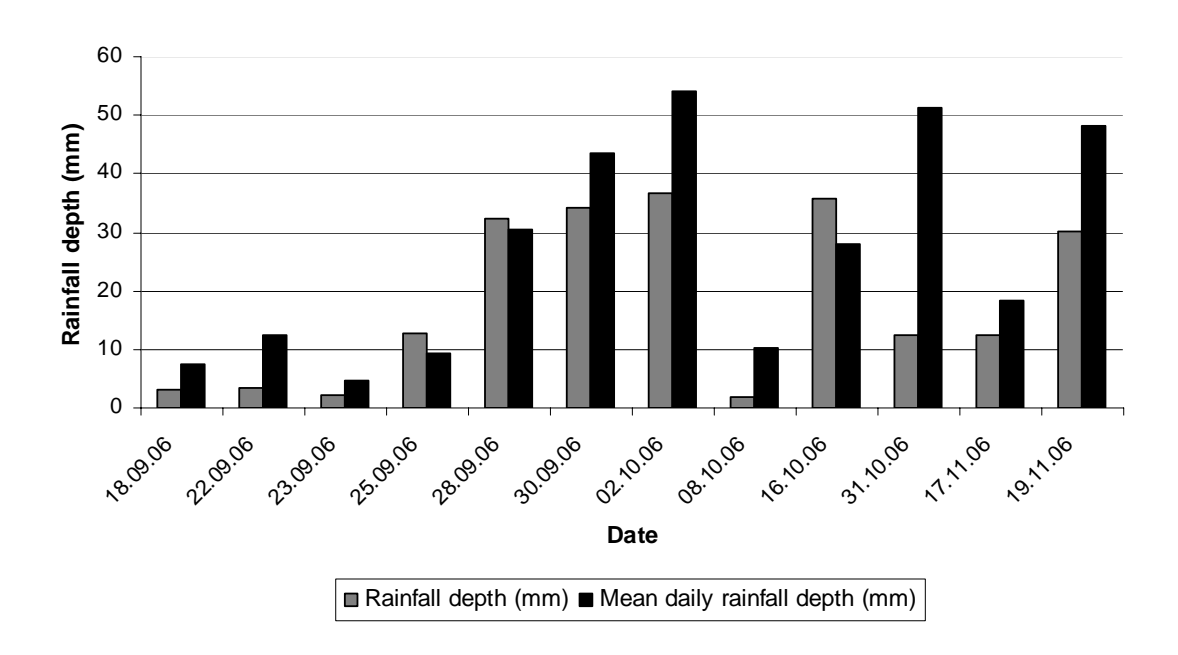


Figure 3: Daily rainfall depth recorded at study site and UKM rainfall station

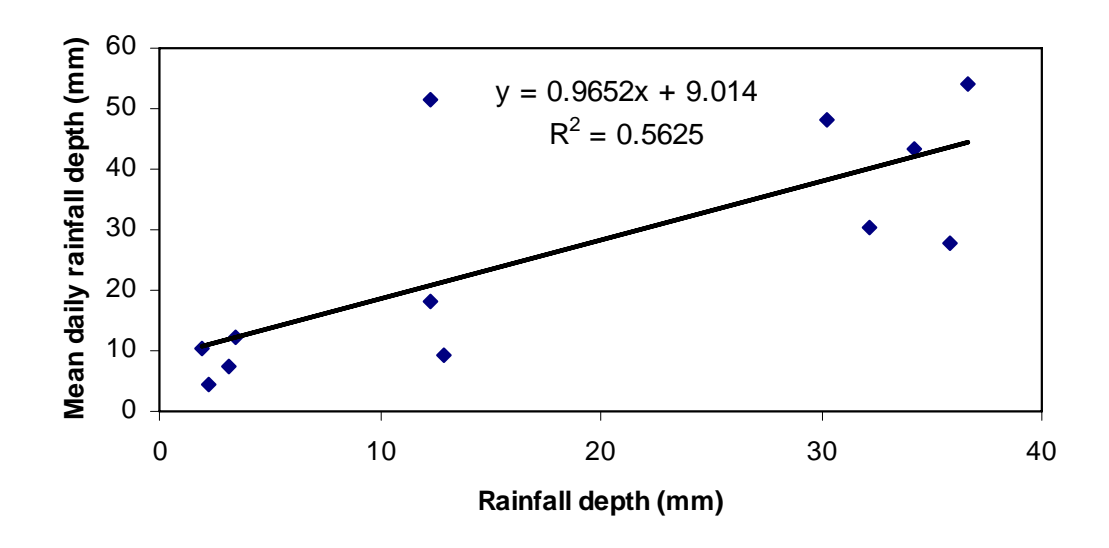


Figure 4: The relationships between observed rainfall depth and mean daily rainfall depth

Table 3: Rainfall duration, rainfall depth and suspended sediment concentration at Sungai Anak Bangi

| Rainfall events | Rainfall duration | Rainfall depth | SSC     | (mg/l)  |
|-----------------|-------------------|----------------|---------|---------|
|                 | (minute)          | (mm)           | Stnt. 1 | Stnt. 2 |
| 18.09.06        | 125               | 3.1            | 8.4     | 9.2     |
| 22.09.06        | 22.09.06 140      |                | 12.1    | 18.5    |
| 23.09.06        | 45                | 2.2            | 2.2     | 7.1     |
| 25.09.06        | 120               | 12.9           | 13.7    | 17.5    |
| 28.09.06        | 28.09.06 210      |                | 34.2    | 42.5    |
| 30.09.06        | 240               | 34.2           | 32.4    | 40.3    |
| 02.10.06        | 300               | 36.7           | 43.5    | 48.1    |
| 08.10.06        | 75                | 1.9            | 8.6     | 15.8    |
| 16.10.06        | 103               | 3.1            | 12.3    | 14.1    |
| 31.10.06        | 90                | 35.8           | 10.4    | 14.2    |
| 17.11.06        | 18                | 12.3           | 1.2     | 5.5     |
| 19.11.06        | 405               | 30.3           | 54.6    | 69.8    |
| Σ               | 31 hrs            | 208.2          | 233.6   | 302.6   |
| Average         | 155.92            | 17.35          | 19.47   | 25.23   |
| Max             | 405               | 36.7           | 54.6    | 69.8    |
| Min             | 18                | 1.9            | 1.2     | 5.5     |

From the Table 3, weighted suspended sediment concentration (SSC) discharge from the two sampling stations varied from minimum 1.2 to maximum 54.6 mg/l (Station 1) and 5.5 to 69.8 mg/l (Station 2). Both maximum SSC were recorded during the prolonged rainy day on 19.11.06 while the minimum SSC for both stations were recorded on 17.11.06. The average values recorded for both stations were considered low compared with other study areas. For example, average SSC recorded for Sungai Air Terjun (CA = 28 km²) was 111.04 mg/l (Wan Ruslan 1996), Bebar (CA = 36.2 km²) was 104.2 mg/l [23], while 12.27 mg/l was recorded at Chini River (CA = 4.36 km²) [24].

The results show that the present of stable density forest canopy of the Bangi Forest Reserve plays an important role in minimising surface erosion which is expected as one of a major contributor on sediment yield in rivers. The successive layers of the canopy were act as a great filter through interception process [25], and reducing the impact from splash erosion by rain drops [26]. Changed in land use from forested to other human activities may lead to higher sediment yield particularly during unstable condition. For example, [27] reported that the erosion rate on newly constructed was 154.8 t/ha/yr at logging areas while [28], reveals that the transformation from forest to urban catchment will leave the soil surface more exposed to erosion.

In the context of catchment physical characteristics, the size of the catchment and topography of the land surface also have significant relation to sediment yield production. It is clear from field studies that the dominant response mechanisms behind the link, along with the sediment yield itself, was the process of sediment being transported from the source to the outlet. This includes the sediment transport modes (wash load, bed load or suspended load), sediment properties (size and shape of grain), bedforms (ripple, dunes and antidunes), bed roughness, ks and effective shear stress,  $\tau b$ . Combination of these factors with other physical aspects such as basin area scale and hydro-meteorological conditions have been shown to influence the sediment yield of many catchment areas as studied by [29,30,31,32,33,34].

The regime of the Sungai Anak Bangi reflects the rainfall events associated with north-east monsoon occurred during the study period. Using equation (1), detailed observed discharge (Q) and estimated daily Q calculated for each sampling points during water collection were tabulated in Table 4. At Station 1, the daily Q sampled ranged

from 172.8  $\text{m}^3$ /day to 6220.8  $\text{m}^3$ /day. This when converted to L/day is 172, 800 and 6220, 800 L/day. Meanwhile at Station 2, daily Q sample ranged from 432.0  $\text{m}^3$ /day to 7862.4  $\text{m}^3$ /day or 432, 000 to 7862, 400 L/ day. All together, the mean observed Q and daily Q ( $\text{m}^3$ /day) for Station 1 and Station 2 are 0.024  $\text{m}^3$ /s, 0.029  $\text{m}^3$ /s, 2052  $\text{m}^3$ /day and 2484  $\text{m}^3$ /day, respectively.

| Date     | Observed Q |           | Q Estimated daily Q (m³/day) |         | Estimated daily Q (L/day) |           |  |
|----------|------------|-----------|------------------------------|---------|---------------------------|-----------|--|
|          | (m         | $n^3/s$ ) |                              |         |                           |           |  |
|          | Stnt. 1    | Stnt. 2   | Stnt. 1                      | Stnt. 2 | Stnt. 1                   | Stnt. 2   |  |
| 18.09.06 | 0.012      | 0.013     | 1036.8                       | 1123.2  | 1036, 800                 | 1123, 200 |  |
| 22.09.06 | 0.013      | 0.013     | 1123.2                       | 1123.2  | 1123, 200                 | 1123, 200 |  |
| 23.09.06 | 0.004      | 0.005     | 345.6                        | 432.0   | 345, 000                  | 432, 000  |  |
| 25.09.06 | 0.013      | 0.015     | 1123.2                       | 1296.0  | 1123, 200                 | 1296, 000 |  |
| 28.09.06 | 0.035      | 0.052     | 3024.0                       | 4492.8  | 3024, 000                 | 4492, 800 |  |
| 30.09.06 | 0.042      | 0.043     | 3628.8                       | 3715.2  | 3628, 800                 | 3715, 200 |  |
| 02.10.06 | 0.051      | 0.052     | 4406.4                       | 4492.8  | 4406, 400                 | 4492, 800 |  |
| 08.10.06 | 0.005      | 0.010     | 432.0                        | 864.0   | 432, 000                  | 864, 000  |  |
| 16.10.06 | 0.032      | 0.036     | 2764.8                       | 3110.4  | 2764, 800                 | 3110, 400 |  |
| 31.10.06 | 0.004      | 0.010     | 345.6                        | 864.0   | 345, 600                  | 864, 000  |  |
| 17.11.06 | 0.002      | 0.005     | 172.8                        | 432.0   | 172, 800                  | 432, 000  |  |
| 19.11.06 | 0.072      | 0.091     | 6220.8                       | 7862.4  | 6220, 800                 | 7862, 400 |  |

Table 4: Hydrological data for Sungai Anak Bangi

There are also significant correlations between observed Q and the present of suspended sediment concentration for both sampling stations (Figures 5 and 6). At Station 1, observed Q was correlated as positive slope with SSC ( $R^2$ = 0.910) showing that the highest the Q will follow with an increase in suspended sediment concentration. Meanwhile at Station 2, the measurement of observed Q and SSC showed a statistically significant relationship between both variables ( $R^2$  = 0.909).

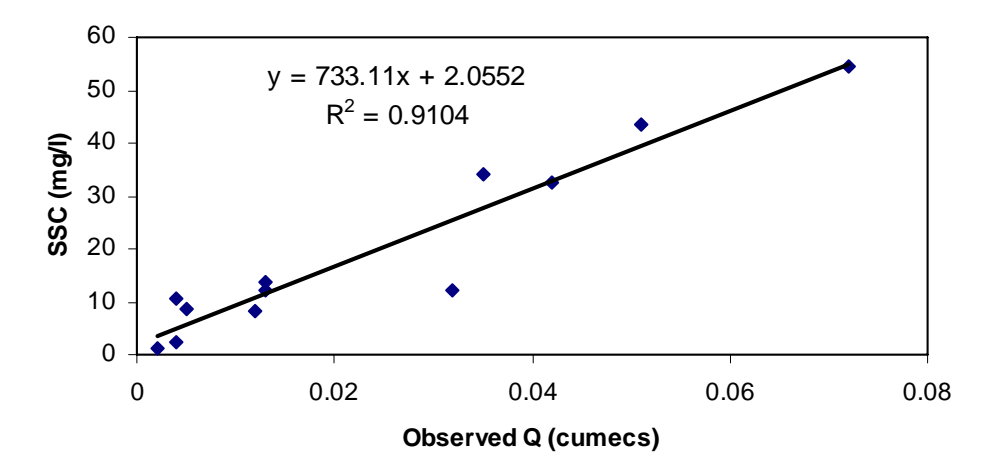


Figure 5: Relationship between observed Q and SSC at Station 1

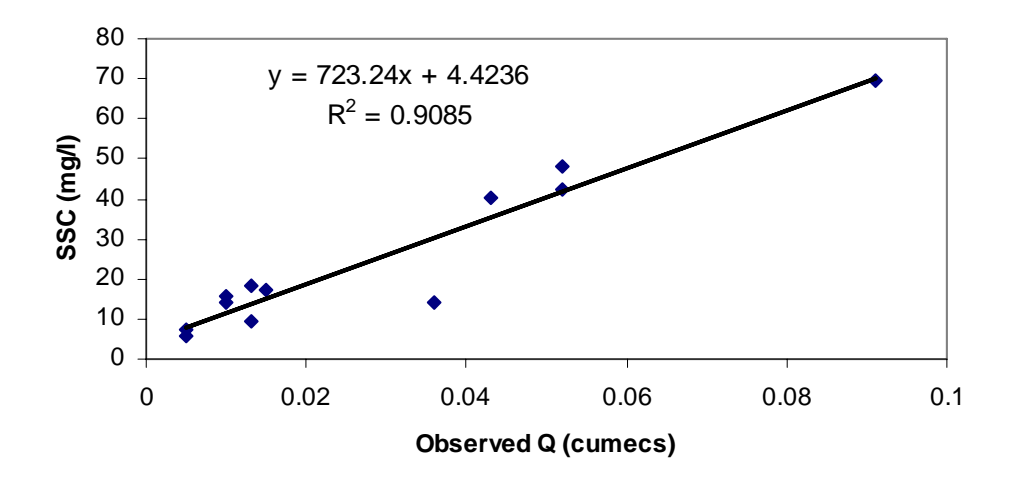


Figure 6: Relationship between observed Q and SSC at Station 2

To gain the suspended sediment yield in the river, the daily suspended sediment concentration was calculated. It is the gross amount of suspended sediments carried past the sampling stations over a 24 hour period. The information is important because of the fact that sediment yield from the catchments is that portion of the eroded soil which leaves the catchment. The result is presented in Table 5. Average suspended sediment yield estimated at Station 1 was 75.0415 kg/day while at Station 2 was 103.2559 kg/day. As the volume of sediments at Station 1 are flowing to Station 2, it can be estimated that gross amount of sediment yields produced at Station 2 (103.2559 minus 75.0415= 28.21 kg/day) is much lesser than the amount of sediment yield calculated at Station 1. At Station 1, suspended sediment yields were recorded between 0.76 kg/day to 339.66 kg/day while at Station 2, suspended sediment yields ranged from 2.38 kg/day to 548.79 kg/day, respectively. The large sediment yield on the latter occasion (19.11.06) was partly derived from high discharge occurred on that day. Total catchment area for Sungai Anak Bangi is 3.7 km². This is the estimated area of which sediment leaved the catchment. When converted into per square km, the gross value of suspended sediment yield leaved from Sungai Anak Bangi is estimated about 27.907 kg/ km²/day or 10, 186 kg/ km²/yr.

#### Conclusion

The study shows the importance of forest covers in reducing the surface erosion. The present of Bangi Reserve Forest plays a vital role in controlling surface erosion and rainfall interception. At a same time, sediment concentration is closely related to rainfall events which increase river regimes especially in terms of river discharge. Suspended sediment yields carried out by the Sungai Anak Bangi are much smaller than those reported for other rivers in Malaysia. This indicates that erosion although occurred in the study area but still within the acceptable value. It is extremely important to preserve the forest as well as Sungai Anak Bangi as one of the best practices in controlling over sediment yield in the study area.

#### Acknowledgements

This work was carried out under the Kampus Lestari sub-committee lead by Prof. Dr Mazlin Mokhtar. Special thank to students assisted with fieldwork namely Mr. Nizam Abdullah and Miss Nor Aseken Rosley. Also special thanks to Mr. Sharif Mohd Nasir, lab assistant of PPSPP which carried out most of the laboratory analyses.

Table 5: Suspended sediment yield per day in Sungai Anak Bangi

| Date     | Estimated daily Q (L/day) |           | SSC     |         | SSC       |           | SSC yield |          |
|----------|---------------------------|-----------|---------|---------|-----------|-----------|-----------|----------|
|          |                           |           | (mg/l)  |         | (kg/l)    |           | (kg/day)  |          |
|          | Stnt. 1                   | Stnt. 2   | Stnt. 1 | Stnt. 2 | Stnt. 1   | Stnt. 2   | Stnt. 1   | Stnt. 2  |
| 18.09.06 | 1036, 800                 | 1123, 200 | 8.4     | 9.2     | 0.0000084 | 0.0000092 | 8. 7091   | 10.3334  |
| 22.09.06 | 1123, 200                 | 1123, 200 | 12.1    | 18.5    | 0.0000121 | 0.0000185 | 13.5907   | 20.7792  |
| 23.09.06 | 345, 000                  | 432, 000  | 2.2     | 7.1     | 0.0000022 | 0.0000071 | 0.759     | 3.0672   |
| 25.09.06 | 1123, 200                 | 1296, 000 | 13.7    | 17.5    | 0.0000137 | 0.0000175 | 15.3878   | 22.6800  |
| 28.09.06 | 3024, 000                 | 4492, 800 | 34.2    | 42.5    | 0.0000342 | 0.0000435 | 103.4208  | 195.4368 |
| 30.09.06 | 3628, 800                 | 3715, 200 | 32.4    | 40.3    | 0.0000324 | 0.0000403 | 117.5731  | 149.7226 |
| 02.10.06 | 4406, 400                 | 4492, 800 | 43.5    | 48.1    | 0.0000435 | 0.0000481 | 191.6784  | 216.1037 |
| 08.10.06 | 432, 000                  | 864, 000  | 8.6     | 15.8    | 0.0000086 | 0.0000158 | 3.7152    | 13.6512  |
| 16.10.06 | 2764, 800                 | 3110, 400 | 12.3    | 14.1    | 0.0000123 | 0.0000141 | 34.0070   | 43.8566  |
| 31.10.06 | 345, 600                  | 864, 000  | 10.4    | 14.2    | 0.0000104 | 0.0000142 | 3.5942    | 12.2688  |
| 17.11.06 | 172, 800                  | 432, 000  | 1.2     | 5.5     | 0.0000012 | 0.0000055 | 2.074     | 2.3760   |
| 19.11.06 | 6220, 800                 | 7862, 400 | 54.6    | 69.8    | 0.0000546 | 0.0000698 | 339.6557  | 548.7955 |
| Average  | 258900                    | 1929600   | 19.5    | 25.2    | 0.0000195 | 0.0000253 | 75.0415   | 103.2559 |

#### References

- 1. Morgan, R.P.C. 2005. Soil erosion and conservation. Oxford: Blackwell Publisher.
- 2. Bruijnzeel, L.A. 1990. Hydrology of moist tropical forests and effects of conversion: A state of knowledge review. UNESCO. Paris. 224.
- 3. Wan Ruslan Ismail, 1996. The role of tropical storms in the catchment sediment removal. *Journal of Bioscience*. 7 (2), 153-168.
- 4. Mohd Ekhwan Toriman, 2004. The analysis of sediment mobility in the Kemaman River estuary, Terengganu: A preliminary investigation. *Prosiding* Persidangan Kebangsaan Sains Teknologi dan Sains Sosial 2004. Penerbit UiTM Pahang. Pahang. 135-141.
- 5. Mohd Ekhwan Toriman, Mazlin Bin Mokhtar, Othman Karim, M. Barzani Gasim & Raihan Taha. 2009. Short term sediment yields from small catchment of Sungai Anak Bangi Selangor. . *Bull. Geol. Soc. Mal.75. August.* 55-59.
- 6. Lane, A. 2004. Bathymetric evolution of the Mercey estuary, UK. Causes and effects. *Estuarine Coastal Shelf Sci.* 59. 249-263.
- 7. Mohd Ekhwan Toriman. 1997. The effects of urbanization on river bank and lateral channel change of the Chorlton Brook Manchester England. *Journal Ilmu Alam.* 23. 115-132.
- 8. Subramaniam, V. 1993. Sediment load of Indian Rivers. Curr. Science. 64. 928-930.
- 9. Baharuddin Kasran. 1988. Effect of logging on sediment yield in a hill dipterocarp forest in Peninsular Malaysia. *Journal of Tropical Forest Science* 1(1). 56 66.
- 10. Li, Y.H. 1976. Denudation of Taiwan Island since Pliocene epoch. *Geology*. 4. 105-107.
- 11. Chakrapani, G.J. 2005. Factors controlling variations in river sediment loads. *Current science*. Vol. 88 (4). 569-575.
- 12. Holland, H.D. 1981. River transport to the oceans. In Emiliani, C (ed.). *The ocean lithosphere*. Wiley. Vol.7.763-800.
- 13. Bruijnzel, L.A. 1996. Hydrology of moist tropical forests and effects of conversion: A state of knowledge review. UNESCO. Paris. 22.
- 14. Mohd Ekhwan Toriman, 2003. Processes of channel planform change on meandering channel: Implication for river restoration on the Langat River, In Mokhtar Jaafar (eds.). *Prosiding* Persidangan cabaran pembangunan dilema persekitaran. Penerbit Pusat Pengajian Sosial, Pembangunan dan Persekitaran, UKM. Bangi. 21-28.
- 15. Wischmeier, W. H. & Smith, D.D. 1978. Predicting rainfall erosion losses. USDA Agricultural Research Service Handbook 537.
- 16. Wan Ruslan Ismail, 1994. Pengantar hidrologi. Kuala Lumpur: Dewan Bahasa dan Pustaka.
- 17. Mohd Ekhwan Toriman & Haryati Che Lah. 2007. Ciri Hidrologi dan hakisan tebing sungai di Sungai Lendu, Alor Gajah, Melaka. *Journal E-Bangi*. Vol. 2 (2),1-19.
- 18. Philip, B.B, Wayne, C.H & Baxter, E.V. 2008. *Hydrology and floodplain analysis*. New Jersey: Prentice Hall.
- 19. Rainwater, F.H & Thatcher, L.L.1995. Methods for collection and analysis of water samplers. *United States Geological Survey Water-Supply Paper*. 1454.
- 20. Morgan, R.P.C. 2005. Soil erosion and conservation. Oxford: Blackwell Publisher.
- 21. Bartham, J & Ballance, R. 1996. Water quality monitoring- A practical guide to the design and implementation of freshwater quality studies and monitoring programmes. UNEP/WHO.
- 22. Department of Environment. 1996. Guidelines for Prevention and Control of Soil Erosion and Siltation in Malaysia. *Ministry of Science, Technology and Environment, Malaysia*.
- 23. Mohd Ekhwan Toriman, 2005. Hydrometeorological conditions and sediment yield in the upstream reach of Sungai Bebar, Pekan Forest Reserve. Pahang. PSF Technical Series No.4. Peat Swamp Forest Project. UNDP/GEF. 41-46.
- 24. Mohd Barzani Gazim, Mohd Ekhwan Toriman, Sahibin Abd. Rahim, Mir Sujaul Islam, Tan Choon Chek & Hafizan Juahir. 2006. Hydrology and Water Quality Assessment of Tasik Chini's Feeder Rivers, Pahang Malaysia. *Geografia*. Vol 3 (3), 1-16.
- 25. Mohd Ekhwan Toriman & Shukor Md. Nor. 2006. An analysis of rainfall interception on the selected experimental plot of Pangkor Hill Reserved Forest. *Journal Wildlife and National Park*. Disember 2006.169-178.
- 26. Pinet, P & Souriau, M. 1988. Continental erosion and large-scale relief. *Tectonic*. 563-582.
- 27. Hamilton, L.S. & King, P.N. 1983. *Tropical forest watersheds. Hydrologic and soil response to major uses of conservation.* A Westview Replica Edition. Westview Press, Colorado. 168

## Mohd Ekhwan Toriman: SURFACE EROSION AND SEDIMENT YIELDS ASSESSMENT FROM SMALL UNGAUGED CATCHMENT OF SUNGAI ANAK BANGI SELANGOR

- 28. Douglas, I. 1984. Water and sediment issues in the Kuala Lumpur ecosystem. In Y.h. Yip & K.S.Low (eds.). *Urbanisation and ecodevelopment with special reference to Kuala Lumpur*. Institute of Advance Studies. University of Malaya. 101-121.
- Bruijnzeel, L.A. 1990. Hydrology of moist tropical forests and effects of conversion: A state of knowledge review. UNESCO. Paris. 224.
- 30. Wan Ruslan Ismail, 1996. The role of tropical storms in the catchment sediment removal. *Journal of Bioscience*. 7 (2), 153-168.
- 31. Mohd Ekhwan Toriman. 1997. The effects of urbanization on river bank and lateral channel change of the Chorlton Brook Manchester England. *Journal Ilmu Alam.* 23. 115-132.
- 32. Mohd Ekhwan Toriman & Noorazuan Md. Hashim. 2003. Construction of channel instability and channel changes using GIS approach along the Langat River, Peninsular Malaysia, In Noorazuan Md. Hashim & Ruslan Rainis (eds). *Urban ecosystem studies in Malaysia: A study of change*. Universal Publishers. Florida 186-198.
- 33. Mohd Barzani Gazim, Mohd Ekhwan Toriman, Sahibin Abd. Rahim, Mir Sujaul Islam, Tan Choon Chek & Hafizan Juahir. 2006. Hydrology and Water Quality Assessment of Tasik Chini's Feeder Rivers, Pahang Malaysia. *Geografia*. Vol 3 (3), 1-16.
- 34. Mohd. Ekhwan Toriman, 2002. Stream channel erosion and bank protection on Langat River Basin, In Chan Ngai Weng (eds.). *Proceeding*. Rivers: towards sustainable development. Universiti Sains Malaysia publisher. 291-299.

## EFFECTS OF INDUCED SALINITY ON BOD<sub>5</sub> REACTION KINETICS OF RIVER WATER SAMPLES

(Kesan Peningkatan Kemasinan Terhadap Kinetik Tindak Balas Keperluan Oksigen Biokimia 5 Hari Menggunakan Sampel Air Sungai)

Zaki Zainudin<sup>1\*</sup>, Maketab Mohamed<sup>2</sup>, Mohd. Rosslim Ramli<sup>3</sup>

<sup>1</sup>Water Resources Technical Division, Institution of Engineers Malaysia, 46720 Petaling Jaya, Selangor Darul Ehsan <sup>2</sup>Faculty of Chemical and Natural Resources Engineering, Universiti Teknologi Malaysia, 81310 Skudai, Johor, Malaysia <sup>3</sup>Faculty of Chemical Engineering, Universiti Teknologi MARA, 40450 Shah Alam, Selangor, Malaysia

\*Corresponding author: zakizainudin@gmail.com

#### **Abstract**

Biochemical Oxygen Demand (BOD) is a typical parameter used in assessing organic pollution strength in surface waters and is normally tested over a 5-day period at an incubation temperature of  $20^{\circ}$ C (BOD<sub>5</sub>). The accuracy of this constituent, in assessing organic contamination under brackish conditions has always been known to be somewhat limited as elevated concentrations of chloride (Cl<sup>-</sup>) disrupts microbial activity from osmotic cellular degradation, causing the bottle decay rate,  $k_1$ , to be effected. The aim of this study was to quantify the effects of induced salinity on  $k_1$ , with varying levels of sodium chloride (NaCl) concentration (5 – 25 ppt), towards six mildly polluted to polluted tropical river water samples. The observed variations ranged between 0.10 - 0.25/day of  $k_1$  for the stipulated samples using the Thomas graphical method for determination of the  $k_1$  rate constant. Sg. Rawang depicted the highest quantum of difference in  $k_1$ , with decrement from 0.754/day (0 ppt) to 0.513/day (25 ppt), whereas Sg. Klang showed the lowest quantum, from 0.306/day (0 ppt) to 0.265/day (25 ppt).

Keywords: BOD<sub>5</sub> saline, brackish, estuarine, bottle decay rate

#### Abstrak

Keperluan Oksigen Biokimia (BOD) adalah metodologi biasa yang digunakan untuk menilai kekuatan pencemaran bahan organik dalam air dan biasanya diuji dalam jangka masa 5 hari pada suhu inkubasi  $20^{\circ}$ C (BOD<sub>5</sub>). Ketepatan BOD<sub>5</sub>, untuk menilai kontaminasi organik dalam air masin sememangnya diketahui agak terhad akibat daripada kandungan klorida (Cl) tinggi yang mengganggu aktiviti mikrob, di mana berlakunya pelupusan sel dari proses osmosis, yang seterusnya menyebabkan gangguan terhadap kadar pereputan dalam botol ( $k_1$ ). Tujuan kajian ini adalah untuk menghisab kesan kemasinan terhadap  $k_1$ , dengan meningkatkan kepekatan Natrium Klorida (NaCl) secara berperingkat, antara 5-25 bpj, terhadap enam sampel air sungai yang diklasifikasikan sebagai sedikit tercemar hingga tercemar. Didapati variasi  $k_1$  umumnya berada antara 0.10-0.25/sehari menggunakan metodologi pengukuran grafikal Thomas. Sg. Rawang menunjukkan perbezaan ketara dalam nilai  $k_1$ , dengan kejatuhan daripada 0.754/sehari (0 bpj) ke 0.513/sehari (25 bpj), manakala Sg. Klang pula menunjukkan perbezaan paling minima dari 0.306/sehari (0 bpj) ke 0.265/sehari (25 bpj).

Katakunci: BOD<sub>5</sub> air masin, pencemaran organik di kawasan kuala sungai, kadar pereputan dalam botol

#### Introduction

Biochemical Oxygen Demand (BOD) is a fundamental parameter used in the assessment of organic contaminants present in water and wastewater. The parameter was first used in the early 1900s as an indicator of organic contamination from sewage sources in the United Kingdom (UK). An incubation time of 5 days at 20°C for testing, brought about the acronym BOD<sub>5</sub>, with the primary justification that the maximum retention time of organic pollutants from sewerage sources of rivers in the UK was in accordance to these conditions [1]. The test itself inturn, is primarily governed by three things; (1) the amount of biodegradable organic matter present, (2) mix culture of microbial population that propagates the degradation and (3) acceptable dissolved oxygen levels for microbial aerobic respiration. The amount of biodegradable organic matter present (left hand side of the Eq. 1.1), is the primary constituent of concern measured in the test, as excess amounts of organic matter may contribute towards instream oxygen depletion, commonly referred to as the DO sag [2];

## Zaki Zainudin et al: EFFECTS OF INDUCED SALINITY ON BOD<sub>5</sub> REACTION KINETICS OF RIVER WATER SAMPLES

$$C_n H_a O_b N_c + (n + \frac{a}{4} - \frac{b}{2} - \frac{3}{4}c)O_2 \rightarrow nCO_2 + (\frac{a}{2} - \frac{3}{2}c)H_2O + cNH_3 + NewCells$$
 (1)

A universal qualifier used in BOD testing is that, only the carbonaceous fraction (or cBOD), is measured as this portion truly reflects the biodegradable organics present. The resulting ammonia, NH<sub>3</sub>-N, which is a product of the degradation, exhibits its own oxygen demand after a few days, during the transformation of NH<sub>3</sub>-N to NO<sub>2</sub>-N and NO<sub>3</sub>-N (nitrification). This oxygen demand is referred to as nitrogenous BOD or nBOD. In order to inhibit the effects of nBOD, nitrification inhibitors such as TCMP (2-chloro-6-(trichloro-methyl) pyridine) is utilized [3]. Throughout the degradation process, there must be sufficient levels of dissolved oxygen (DO) in the BOD test bottle, preferably above 2 mg/l. Depletion of DO below this value at any time during the test, will incur anoxic conditions, causing stress to the microbial population, hence affecting the BOD readings. If the value falls below 2 mg/l on the fifth day, the sample will simply be rejected and not considered to be part of the result. This is why many analytical references on BOD testing often recommend preparation of serial dilutions of the same sample, where incubation is done simultaneously [1].

The final variable for consideration is the quantity and type of microorganisms present. The microorganisms, which drive the degradation process can either be introduced through seeding or assumed to be already present in ambient water sample. As an added precautionary measure, seeding is often recommended by analytical references [3]. Though being the case, the quantification of the microbial population in the BOD tests remains arbitrary in many practices. This does not mean that this variable is unimportant; after all it is the microorganisms that incur DO depletion in the test bottle. Any disturbance, whether it is natural or otherwise, to microbial growth, will disrupt the first-order reaction kinetics and hence affect the BOD results [4].

#### **Problem Statement**

The presence of reagents such as chlorine (Cl<sub>2</sub>), widely used as a disinfectant, in water and wastewater treatment plants in many developing countries, is a good example of the disturbances discussed above. Chlorine is effective in removing coliform organisms such as *Escherichia coli* (*E. coli*) and *Enterococcus spp.*, by incurring osmotic cellular protoplasmic decomposition [5]. The effects of these types of disinfectants on microbes are widely recognized, though little is known on the implications towards the BOD test itself, when samples due for testing contain elevated levels of the constituent. A chlorine check is typically recommended prior to commencement of BOD<sub>5</sub> analysis [3].

Another perspective is, to look at this in terms of application of the BOD test for assessment of ambient water quality, particularly at the estuarine zone where salinity levels, as a result of chloride (NaCl) is predominant. It has been long accepted that BOD, as a parameter of assessment for organic contamination under such conditions is not preferable, where Total Organic Carbon (TOC) analysis is more preferred [6]. To what extent the chloride content affects the BOD test under brackish conditions, remains ambiguous. TOC analysis though providing a viable, more representative alternative is not necessarily a cost-effective solution, due to limited facilities and equipment [7]. This is even more so true when a comprehensive monitoring network is already in place. It is on this basis that the extent of chloride influences on the BOD<sub>5</sub> test, or more specifically the reaction kinetics involved needs to be further scrutinized.

#### Methodology

Prior to conducting the analysis, suitable locations for grab sample collection were identified. Since the BOD<sub>5</sub> test is a bio-assay procedure, where the sensitivity of the analysis is directly related to the DO margin between the first and fifth day, it was therefore necessary, to choose locations where organic contamination was known to be significant; in order to encapsulate the maximum degradation, and hence view clear and distinct variations between runs. This was done qualitatively, by correlation to specific land uses. Rivers and streams in the state of Selangor, Peninsular Malaysia that receive significant amount of organic contributions, such as from sullage or greywater, sewage and industrial sources were the best candidates to collect the grab samples. Based on historical monitoring data, these stations were also known to exhibit significant BOD. Five sampling stations were identified; Sg. Rawang (Rawang

river), Sg. Serendah (Serendah river), Sg. Klang (Klang river) and Sg. Damansara (Damansara river, 2 stations, upstream and downstream). The geographical coordinates of these stations are shown in Table 1 below:

Table 1: Location of Sampling Stations

| River                         | Basin   | Description  | Latitude<br>(N) | Longitude<br>(E) | Station<br>ID |
|-------------------------------|---|--|-----------------|------------------|---------------|
| Sg. Rawang                    | Sg.<br>Selangor   | Predominantly receives sewerage pollution input from Rawang town, a tributary of Sg. Serendah.   | 3° 19'00''      | 101° 4'00''      | S1            |
| Sg. Serendah                  | Sg.<br>Selangor   | Identified as most polluting tributary within Sg. Selangor particularly for organic contaminants such as BOD, COD and NH <sub>3</sub> -N | 3° 21'00''      | 101° 33'00''     | S2            |
| Sg. Klang                     | Sg.<br>Klang  | Receives input from various types of pollution sources in Selangor state, border transcends to Kuala Lumpur.                             | 3° 2'50"        | 101° 30'43"      | S3            |
| Sg. Damansara<br>(Upstream)   | Sg.<br>Klang  | A tributary of Sg. Klang, station is prior to receiving industrial effluent from Shah Alam industrial zone, located near TTDI Jaya.      | 3° 4'25''       | 101° 33'16"      | S4            |
| Sg. Damansara<br>(Downstream) | Station located after industrial zone input, but prior to Sg. Klang confluence. |  | 3° 3'17"        | 101° 32'56"      | S5            |

All samples collected were incubated at 4°C for about 2 hours, during transit from site to the laboratory. The actual BOD<sub>5</sub> analysis was conducted in accordance with the American Public Health Association (APHA) Standard Methods for the Examination of Water and Wastewater, Method 5210B.

Prior to incubation and analysis, sodium chloride (NaCl) solutions were prepared and mixed with the dilution water. This was done with by using gravimetric method, factoring in the solubility limit of the constituent in a 300 ml BOD<sub>5</sub> test bottle under varying salinity levels from 5 parts per thousand (ppt) to 25 ppt for each of the sample collected, at different dilutions. Table 2 below illustrates the amount of NaCl addition required to the achieve the desired salinity;

Table 2: Amount of Sodium Chloride (NaCl) added to 300ml BOD<sub>5</sub> Test Bottle

| Desired Salinity (ppt) | NaCl addition (g) |  |  |
|------------------------|-------------------|--|--|
| 5                      | 1.5               |  |  |
| 10                     | 3.0               |  |  |
| 15                     | 4.5               |  |  |
| 20                     | 6.0               |  |  |
| 25                     | 7.5               |  |  |

## Zaki Zainudin et al: EFFECTS OF INDUCED SALINITY ON BOD<sub>5</sub> REACTION KINETICS OF RIVER WATER SAMPLES

Lide [10], showed that the solubility of NaCl, at an incubation temperature of  $20^{\circ}$ C, based on the above desired salinity levels should be close to 100%. DO levels in each of the BOD bottles were monitored daily, to view any variation in decay rate,  $k_1$  and daily BOD. There are many proposed methodologies pertaining to  $k_1$  determination, the one employed in this study is the Thomas' graphical method [8]. This method relies on the following BOD rate equation:

$$BOD_{t} = L_{0}(kt)[1 + (1/6)kt]^{-3}$$
(2)

Rearranging this equation, and taking the cube root of both sides yields;

$$\left(\frac{t}{BOD_{t}}\right)^{1/3} = \frac{1}{(kL_{0})^{1/3}} + \frac{(k)^{2/3}}{6(L_{0})^{1/3}}(t)$$
(3)

A plot of  $(t/BOD_t)^{1/3}$  over time is linear. The intercept and slope are defined as:

$$\mathbf{A} = (\mathbf{kL}_0)^{-1/3} \tag{4}$$

$$B = \frac{(k)^{2/3}}{6(L_0)^{1/3}}$$
 (5)

Finally solving for  $L_0^{1/3}$ , in Eq. 3.11 by substitution of Eq. 3.12 yields:

$$k = 6 \left( \frac{B}{A} \right) \tag{6}$$

To summarize, in calculating the bottle decay rate, k or  $k_1$ ,  $(t/BOD_t)^{1/3}$  versus time is plotted on an arithmetic graph and a best-fit straight line is drawn, after which the intercept (A) and slope (B) from the plot is determined and finally k, is calculated based on Eq. 6.

#### **Results and Discussion**

Referring to Figure 1 below, unsurprisingly, there is a noticeable difference for the BOD samples tested with varying degrees of salinity. Generally, the bottle decay rate,  $k_1$ , decreases as salinity increases, which in turn is an indicator that the chloride is disrupting microbial activity. This hypothesis has been previously established, what is interesting though, is the extent of the effect on the samples tested. After the fifth day, the margin, for Sg. Damansara (downstream) and Sg. Klang samples, exhibited the maximum observable deficiency in BOD ( $\Delta$ BOD), between lowest and highest salinity at 8 mg/l each (Sg. Damansara (downstream); 0 ppt BOD<sub>5</sub> = 15 mg/l, 25 ppt BOD<sub>5</sub> = 7 mg/l; Sg. Klang; 0 ppt BOD<sub>5</sub> = 16 mg/l, 25 ppt BOD<sub>5</sub> = 8 mg/l), a reduction of more than 50%. The lowest variation was in the Sg. Serendah sample at about 1.5 mg/l (25%) which can be considered negligible as the standard error for the BOD test is about 2 mg/l [3].

It should be noted that not all of samples followed the same inverted BOD-salinity relationship. There were also some discrepancies, where higher salinity levels, actually incurred higher BOD (particularly for Sg. Rawang). This phenomenon relates back to the fact that the BOD test is a bioassay procedure, and heterogeneous distribution of organics and microbial populous, may be the root cause. Further observations are required to determine the root cause of the anomaly.

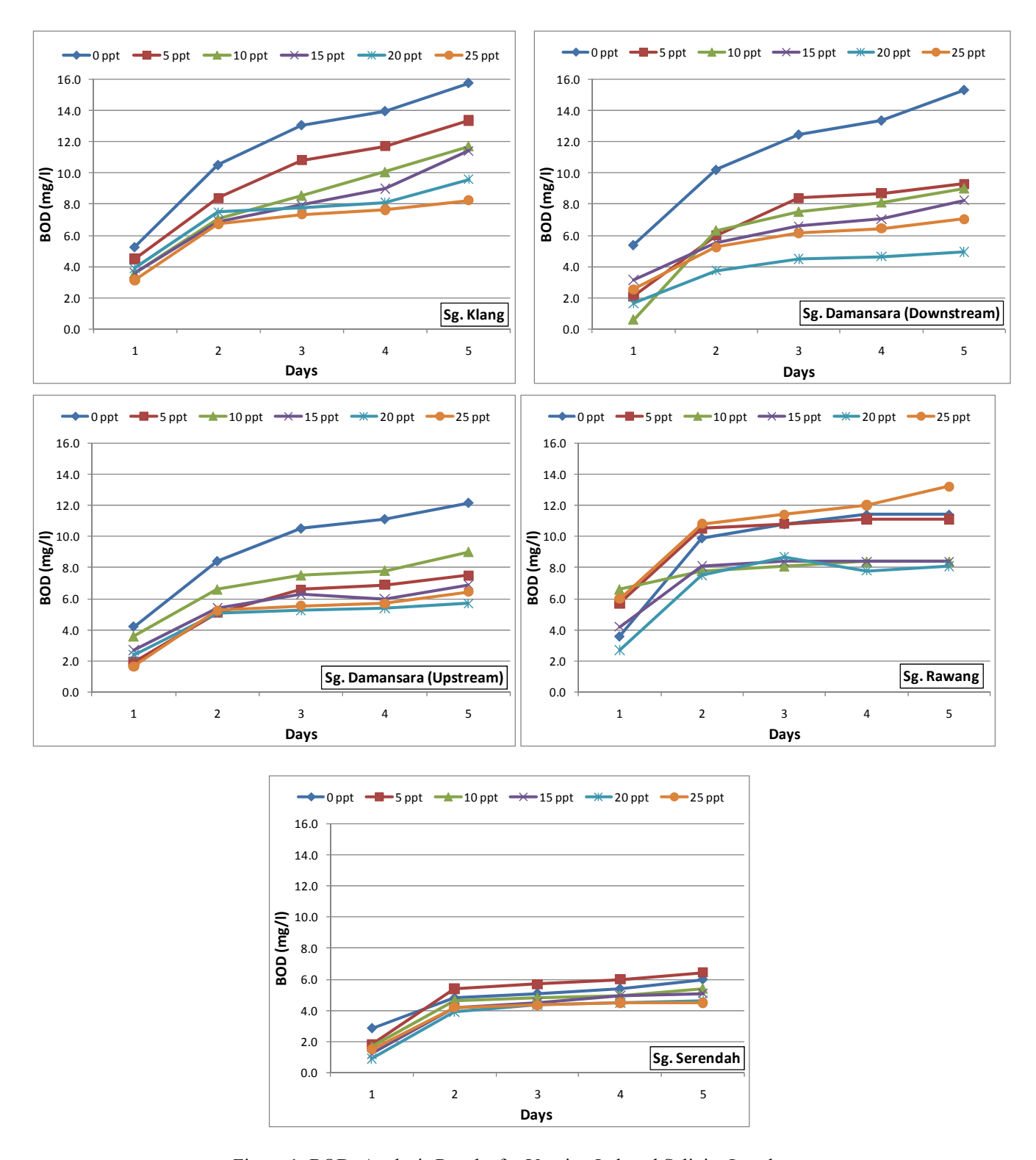


Figure 1: BOD<sub>5</sub> Analysis Results for Varying Induced Salinity Levels

## Zaki Zainudin et al: EFFECTS OF INDUCED SALINITY ON BOD<sub>5</sub> REACTION KINETICS OF RIVER WATER SAMPLES

The decay rate analysis,  $k_1$ , in accordance with the Thomas graphical method was then conducted, the results of which are summarized in Table 3 and illustrated in Figure 2:

|                | BOD Decay Rate, k <sub>1</sub> (1/day) |              |           |                             |                            |  |
|----------------|--|--------------|-----------|-----------------------------|----------------------------|--|
| Salinity (ppt) | Sg. Rawang                             | Sg. Serendah | Sg. Klang | Sg. Damansara<br>(Upstream) | Sg. Damansara (Downstream) |  |
| 0              | 0.754                                  | 0.798        | 0.306     | 0.466                       | 0.420                      |  |
| 5              | 0.719                                  | 0.663        | 0.299     | 0.444                       | 0.390                      |  |
| 10             | 0.691                                  | 0.533        | 0.265     | 0.416                       | 0.390                      |  |
| 15             | 0.670                                  | 0.662        | 0.257     | 0.401                       | 0.383                      |  |
| 20             | 0.577                                  | 0.626        | 0.260     | 0.440                       | 0.251                      |  |
| 25             | 0.513                                  | 0.626        | 0.265     | 0.243                       | 0.234                      |  |

0.041

13.39%

0.223

47.85%

0.186

44.29%

0.172

21.55%

0.241

31.96%

 $%\Delta k_1/k_{1(s=0)}$ 

Table 3: BOD Decay Rate, k<sub>1</sub>, Analysis Summary

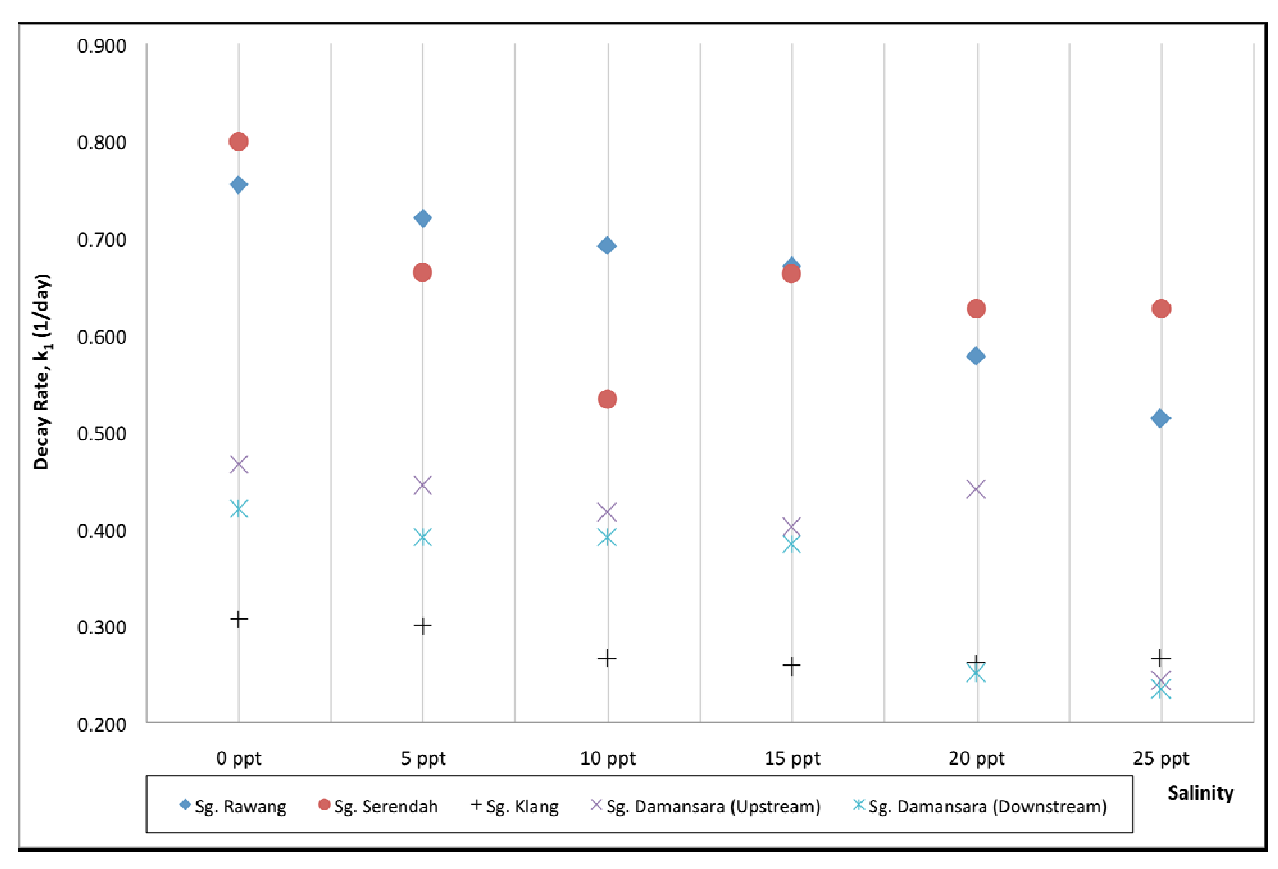


Figure 2: BOD Decay Rate, k<sub>1</sub>, Graphical Analysis

Again, it is apparent there is a decrement in the bottle decay rate,  $k_1$ , with regards to increasing salinity. The highest quantum was observed in Sg. Rawang at 0.241/day, followed by Sg. Damansara (upstream) at 0.223/day, whereas the lowest quantum was observed at Sg. Klang at 0.041/day. At first glance, this may seem anomalous, because, as mentioned previously, Sg. Klang and Sg. Damansara (downstream) exhibited the highest reduction in terms of overall BOD in the analytical proceedings. What needs to be understood here is that although there seems to be a significant reduction in  $k_1$ , (denoted as  $\Delta k_1$ ), the influence on the overall in-stream BOD magnitude, still remains relative to the overall/original decay rate, vis- $\dot{a}$ -vis, the ratio  $\Delta k_1/k_{1(s=0)}$  is a more indicative contributor of the influence of chloride towards overall BOD reduction. Sg. Rawang for example, though exhibiting a  $\Delta k_1$  of 0.241/day, only has a relative reduction or  $\Delta k_1/k_{1(s=0)}$  of 32% whereas Sg. Damansara (downstream) on the other hand exhibited a  $\Delta k_1/k_{1(s=0)}$  of about 44%, an even more significant reduction than the former.

The rate of decrement itself ( $\Delta k_1$ ), varies from one sample to the next, which again may be attributed to the mix of microbial populations already present in the sample, as well as the composition and biodegradability of the organic constituents present, which more likely than not, is site specific and relative to input sources. However, it is clear, for there to be any significant reduction in oxygen demand exerted by microbial organisms when stabilizing biodegradable organic matter by salinity/chloride, the margin of relative reduction to the original decay rate ( $\Delta k_1/k_{1(s=0)}$ ) must be significant, whereas the magnitude of reduction ( $\Delta k_1$ ) alone is insufficient.

The decay rate in the bottle,  $k_1$  is often misinterpreted as  $k_d$ , which is the in-stream decay rate.  $k_d$  can differ to  $k_1$  by as much as ten times [8], due to the unrestricted supply of oxygen transfer, occurring at the air-water interface, attributed to re-aeration as well as photosynthesis. Therefore it would also be safe to assume that the decay rate ratio affecting the bottle decay also applies under these conditions as well. The only unaccounted factor relating to BOD kinetics under estuarine conditions is therefore tidal dilution of organic contaminants, which of course has a substantial effect [9]. Albeit being the case, this case study has clearly shown that BOD is not a suitable parameter for assessment of saline waters; the bio-kinetics is simply skewed, as elaborated above.

#### Conclusion

From the preliminary study conducted above, there is a significant drop in BOD as a result of increasing salinity in all the river water samples collected. This was directly attributed to the influence of chloride in relation to microbial cellular decomposition. Although the magnitude of  $\Delta k_1$  varies from one sample to the next, the end results subject BOD to further scrutiny as a suitable water quality parameter for monitoring of estuarine zones. In consequence of this observation, other water quality applications which cannot avoid using BOD as an indicator for organic matter, such as in water quality modeling, need to account for the effects of salinity towards microbial activity [6]. A reasonable approximation pertaining to the reduction in decay rate, in particular for tropical rivers can be done using the above results.

#### References

- Zainudin, Z. (2008). "The Many Intricacies of Biochemical Oxygen Demand (BOD)", Institution of Engineers Malaysia (IEM), Featured Article, Jurutera Monthly Bulletin, ISSN 0126-9909, KPDN PP 1050/09/2008 (010721), November 2008.
- 2. Sawyer, C. N., McCarty, P. L. and Parkin G. F. (2003). "Chemistry for Environmental Engineering and Science: Fifth Edition". In: Biochemical Oxygen Demand. McGraw-Hill Professional., USA.
- 3. American Public Health Association (APHA), American Water Works Association (AWWA) and Water Environment Federation (WEF), 2005. "Standard Methods For The Examination of Water and Wastewater: 21st Edition", APHA, AWWA and WEF.
- 4. Rasmussen, P. P. and Ziegler, A. C., (2003). "Comparison and Continuous Estimates of Fecal Coliform and Escherichia Coli Bacteria in Selected Kansas Streams". United States Geographical Survey (USGS).
- 5. Metcalf and Eddy, Inc. (2004), Revised by: Tchobanoglous, G., Burton, F. L. and Stensel, H. D. "Wastewater Engineering: Treatment and Reuse, Fourth Edition", McGraw-Hill.
- Zainudin, Z., Mazlan N. F. and Abdullah, N. (2008). "Low Flow Integration Effects on Water Quality Modeling of Sg. Selangor River Basin with Emphasis on Sewage Pollution Sources", International Conference and Expo on Environmental Management and Technologies (ICEEMAT'08), Putra World Trade Center (PWTC), December 2008.

## Zaki Zainudin et al: EFFECTS OF INDUCED SALINITY ON BOD<sub>5</sub> REACTION KINETICS OF RIVER WATER SAMPLES

- 7. Baginda, A. R. A. and Zainudin, Z (2009). "Keynote Paper: Moving Towards Integrated River Basin Management (IRBM) in Malaysia", Institution of Engineers Malaysia (IEM), Proceedings, 11th Annual IEM Water Resources Colloquium, ISBN 978-967-5048-46-3.
- 8. Davis, M. L. and Cornwell, D. A. (1998). "Introduction to Environment Engineering: 3rd Edition", McGraw Hill.
- 9. Mills, W. B., Bowie, G. L., Grieb, T. M., Johnson, K. M. and Whittemore, R. C. (1986). "Handbook: Stream Sampling for Waste Load Allocation Applications". United States Environmental Protection Agency (US EPA), Washington D. C., USA.
- 10. Lide, D. R. (2008). "CRC Handbook of Chemistry and Physics, 89th Edition", CRC Press/Taylor and Francis, Boca Raton, FL.

# ANALYSIS OF ESSENTIAL OILS OF *ETLINGERA SPHAEROCEPHALA* VAR. *GRANDIFLORA* BY TWO-DIMENSIONAL GAS CHROMATOGRAPHY WITH TIME-OF-FLIGHT MASS SPECTROMETRY

(Analisis Minyak Pati Daripada *Etlingera Sphaerocephala* Var. *Grandiflora* Dengan Kromatografi Gas Dua Dimensi - Spektrometri Jisim Masa Terbang)

M.A.A. Yahya<sup>1</sup>, W.A. Yaacob<sup>1</sup>, Laily B. Din<sup>1</sup>, I. Nazlina<sup>2</sup>

<sup>1</sup>School of Chemical Sciences and Food Technology, <sup>2</sup>School of Bioscience and Biotechnology, Faculty of Science and Technology, Universiti Kebangsaan Malaysia, 43600 Bangi, Selangor, Malaysia.

#### Abstract

Hydrodistillation using a Clevenger-type apparatus of the *Etlingera sphaerocephala* var. *grandiflora* rhizomes, stem, leaves and whole plant yielded oils of respective 0.03, 0.02, 0.17 and 0.05%. Forty two compounds (or 97%), 32 (81%), 40 (63%) and 36 (80%) of the rhizome, stem, leaf and whole plant oils gave good matches in GCXGC-TOFMS analysis. The major components in the rhizome oil: 1,8-cineole (16.8%), α-phellandrene (12.7%) and β-trans-ocimene (8.9%); the stem: 1,8-cineole (17.4%), α-phellandrene (9.7%) and 1*S*-α-pinene (9.5%); the leaf: α-phellandrene (12.3%) and diprene (10.3%); and in the whole: β-pinene (12.2%), α-pinene (8.6%), p-menth-1-en-8-ol (8.5%) and α-phellandrene (8.5%). Monoterpenes constituted the richest components (76% average) in all of the four oils followed by sesquiterpenes (4%) and non-terpenes (0.2%). Three clusters of 1,8-cineole and α-phellandrene; β-pinene and 1,8-cineole; and α-phellandrene were obtained in cluster and principal component analyses.

Keywords: Etlingera sphaerocephala var. grandiflora, essential oils, GCXGC-TOFMS

#### Abstrak

Penyulingan air dengan radas jenis-Clevenger rizom, batang, daun dan keseluruhan tumbuhan menghasilkan minyak masing-masing sebanyak 0.03, 0.02, 0.17 dan 0.05%. Empat puluh dua sebatian (atau 97%), 32 (81%), 40 (63%), dan 36 (80%) minyak rizom, batang, daun dan keseluruhan tumbuhan memberikan padanan yang baik dalam analisis KGXKG-SJMP. Komponen utama dalam minyak rizom: 1,8-sineol (16.8%), α-felandrena (12.7%) dan β-trans-osimena (8.9%); batang: 1,8-sineol (17.4%), α-felandrena (9.7%) dan 1S-α-pinena (9.5%); daun: α-felandrena (12.3%) dan diprena (10.3%); dan dalam keseluruhan: β-pinena (12.2%), α-pinena (8.6%), p-ment-1-en-8-ol (8.5%) dan α-felandrena (8.5%). Monoterpena menjuzukkan komponen terkaya (purata 76%) dalam kesemua empat minyak diikuti seskuiterpena (4%) dan bukan-terpena (0.2%). Tiga kluster 1,8-sineol dan α-felandrena; β-pinena dan 1,8-sineol; dan α-felandrena diperolehi dalam analisis kluster dan komponen utama.

Kata kunci: Etlingera sphaerocephala var. grandiflora, minyak pati, GCXGC-TOFMS

#### Introduction

There are 151 Zingiberaceae species belonging to 18 genera found in Peninsular Malaysia [1]. The largest Zingiberaceae genus is *Alpinia* (23 species), whereas *Etlingera* (10) ranks sixth. The number of *Etlingera* species has now increased to 15 [2]. *Etlingera* species are tall forest plants, with larger species reaching up to 6 m in height [3]. Holttum [4] described *E. sphaerocephala* var. *grandiflora* by its subterranean inflorescence with flowers appearing at soil level; its stature is 2.5 m; its leaves when young also suffused purple below; its labellum is 6 cm or more in length and 2.7 cm wide, the base is red in colour. *Etlingera sphaerocephala* var. *grandiflora* can be found in many parts of the Peninsular Malaysia and Borneo [5], mainly in lowland forests and at moderate elevation on the mountains. No uses have ever been recorded for *E. sphaerocephala* var. *grandiflora* [6].

To date, several studies have been carried out on *Etlingera* essential oils. Lechat-Vahirua et al. [7] found methyl eugenol (47.4%) and (*E*)-methyl isoeugenol (18.2%) as major components in the rhizome essential oil of *Etlingera* cevuga. The respective dry flower and flower axis essential oils of the Brazilian *E. elatior* contained dodecanol (42.5, 34.6%), dodecanal (14.5, 21.5%) and  $\alpha$ -pinene (22.2, 6.3%) as their major constituents [8].  $\beta$ -Pinene (19.2%), caryophyllene (15.4%) and (*E*)- $\beta$ -farnesene (27.9%) represented the major components of the leaf essential oil of

# M. A. A. Yahya et al: ANALYSIS OF ESSENTIAL OILS OF *ETLINGERA SPHAEROCEPHALA* VAR. *GRANDIFLORA* BY TWO-DIMENSIONAL GAS CHROMATOGRAPHY WITH TIMEOF-FLIGHT MASS SPECTROMETRY

the Malaysian *E. elatior* whereas 1,1-dodecanediol diacetate (34.3%) and (*E*)-5-dodecene (27%) largely dominated the stem essential oil. The flower and rhizome essential oils of the Malaysian *E. elatior* comprised the major constituents of 1,1-dodecanediol diacetate and cyclododecane [9]. Nine components were identified from the rhizome essential oil of the Thai *Etlingera punicea* from which the phenolic compound of methyl chavicol (95.7%) represented the major constituent [10].

#### **Materials and Methods**

#### **Plant Material**

Rhizome, stem, leaf and whole plant samples of the *Etlingera sphaerocephala* var. *grandiflora* were collected in January 2009 from Genting Peras, Hulu Langat, Selangor, Malaysia and kept fresh in the freezer. A voucher specimen of WYA 386 for the plant was deposited at the Universiti Kebangsaan Malaysia Hebarium.

#### **Isolation Procedure**

Each of the fresh parts and the whole plant of the *Etlingera sphaerocephala* var. *grandiflora* was cut into small pieces, blended in distilled water and hydrodistilled in a Clevenger-type apparatus for 3 hours. The volatile oils obtained were dried over anhydrous sodium sulfate and stored in a cold room. Each of the oils was dissolved in dicholoromethane for analysis using GCXGC-TOFMS.

#### **GCXGC-TOFMS System**

#### **GCXGC**

GCXGC analyses were carried out using Agilent 6890N GC equipped with a LECO thermal modulator (technology under license from Zoex Corporation). Two columns were employed: Rtx-5MS (30 m, 0.10 mm id, film thickness 0.25  $\mu$ m) and DB-WAX (1 m, 0.1 mm id, film thickness 0.1  $\mu$ m). Operating conditions for both columns were as follows: initial oven temperature, 45 °C for 2 min, then to 230 °C (for Rtx-5MS) and 50 °C for 2 min, then to 235 °C (for DB-WAX) at 6 °C/min then held for 5 min; inlet temperature, 230 °C; carrier gas, 1 ml/min He; injection size, 1.0  $\mu$ l splitless; modulator temperature, 30 °C offset from main oven; modulation frequency, 5 s with a 1 s hot pulse time.

#### MS

The GC-TOF-MS software of the LECO Pegasus was used to find all peaks in the raw GCXGC chromatogram. Significant operating parameters: ionization voltage, EI at 70 eV; source temperature 200 °C; scan mass range, 50-400 U; acquisition rate, 100 spectra/s

#### **Compounds Identification**

Compounds were identified by computer using their MS data compared to the NIST mass spectral library. The components which have similarity, reverse and probability of more than 800, 800 and 1000 respectively were considered as good matches.

#### **Statistical Analysis**

The percentage composition of the major components of the essential oils was used to determine the relationship among different parts using hierarchical cluster analysis (SPSS software computer package). The cluster analysis was constructed on the basis of agglomerative grouping and average linkage between the groups employing the clustering method based on squared Euclidean distances.

#### **Results and Discussion**

The hydrodistillation of the rhizomes of *Etlingera sphaerocephala* var. *grandiflora* gave a pale yellowish viscous oil in 0.03% yield (w/w). The same proved true for the stem and whole plant oils but they gave 0.02 and 0.05% yields. The leaves produced a colorless non-viscous oil in 0.17% yield. With the yield ratio for the leaves: whole plant: rhizomes: stem of 8.5: 2.5: 1.5: 1, the leaves contained far more oil than the others.

GCXGC-TOFMS analysis of the *Etlingera sphaerocephala* var. *grandiflora* rhizome, stem, leaf and whole plant oils has shown the presence of respective 42, 32, 40 and 36 components which comprised of 97, 81, 63 and 80% of the total constituents of the oils (Table 1). There were 70 different compounds present in those four oils.

All the major compounds of the Etlingera sphaerocephala var. grandiflora oils as presented below were of the terpenic, whereby the rhizomes gave 1,8-cineole (16.8%), α-phellandrene (12.7%) and β-trans-ocimene (8.9%); the stem produced 1,8-cineole (17.4%), α-phellandrene (9.7%) and 1S-α-pinene (9.5%); the leaves yielded αphellandrene (12.3%) and diprene (10.3%); and the whole plant gave  $\beta$ -pinene (12.2%),  $\alpha$ -pinene (8.6%), p-menth-1-en-8-ol (8.5%) and  $\alpha$ -phellandrene (8.5%) (Figure 1). From the above eight main components, it is obvious that  $\alpha$ phellandrene was found in all four oils whereas 1.8-cineole occurred only in the rhizomes and the stem. The major compounds of the Malaysian Etlingera elatior leaf oil were also of the terpenic, comprising of (E)-\(\theta\)-farnesene (27.9%),  $\beta$ -pinene (19.2%) and caryophyllene (15.4%). Notice that the major  $\beta$ -pinene found in the whole plant oil of the Etlingera sphaerocephala var. grandiflora was also a main component in the Malaysian Etlingera elatior leaf oil. On the other hand, the flower and flower axis oils of the Brazilian Etlingera elatior each contained one terpenic compound of α-pinene (22.2 and 6.3%) out of three major components besides the non-terpenic dodecanol (42.5 and 34.6%) and dodecanal (14.5 and 21.5%). Coincidently, the oils of the Brazilian Etlingera elatior and the Etlingera sphaerocephala var. grandiflora whole plant contained a similar major component, α-pinene. Other main compounds of the Etlingera volatile oils were all non-terpenic such as methyl eugenol (47.4%) and (E)-methyl isoeugenol (18.2%) of the Etlingera cevuga rhizome oil; 1,1-dodecanediol diacetate (34.3%) and (E)-5-dodecene (27%) of the Malaysian E. elatior stem oil; 1,1-dodecanediol diacetate (47.3%) and cyclododecane (34.5%) of the Malaysian E. elatior rhizome oil; cyclododecane (40.3%) and 1,1-dodecanediol diacetate (24.4%) of the Malaysian E. elatior flower oil; and methyl chavicol (95.7%) of the Thai Etlingera punicea rhizome oil.

Out of the 70 different components that occurred in the four oils, 16 (23%) were found in each of the oils. They were  $\alpha$ -phellandrene, o-cymene,  $\alpha$ -terpinolene,  $\beta$ -pinene, camphene,  $\beta$ -cis-ocimene,  $\alpha$ -p-dimethylstyrene, 1,8-cineole, p-menth-1-en-8-ol, 4-terpineol, linalool, borneol, exo-fenchol,  $\alpha$ -humulene, epi- $\beta$ -santalene and 3,5-dimethyloctane.  $\alpha$ -Santalene and copaene were available in all of the oils of E. sphaerocephala var. grandiflora except in the rhizomes. 3-Pinanone and myrtenal were found in the all oils of E. sphaerocephala var. grandiflora but not in the stem. Limonene,  $\delta$ -cadinene,  $\alpha$ -muurolene and  $\alpha$ -bergamotene were present in all of the oils of E. sphaerocephala var. grandiflora except in the leaves.

On average, monoterpenes represented the most abundant constituents (76%) in all four oils followed by sesquiterpenes (4%) and non-terpenes (0.2%). Previous studies on the Etlingera essential oils found that they were not rich in monoterpenes, as shown in the Etlingera cevuga rhizome (20.1%); Brazilian Etlingera elatior flower (25.3%) and flower axis (6.8%); Malaysian Etlingera elatior leaf (38.8%), stem (4.8%), flower (7.5%) and rhizome (0.5%); and Thai Etlingera punicea rhizome (4.2%), compared to the current study on the E. sphaerocephala var. grandiflora rhizome (89.9%), stem (77%), leaf (61.2%) and whole plant (75.9%). Eight, four and fifteen compounds of the sesquiterpenes comprising 4.1, 1.2 and 6.8% of the whole components were identified in the Etlingera cevuga, E. punicea and E. sphaerocephala var. grandiflora rhizome oils whereas the Malaysian Etlingera elatior rhizome oil had no sesquiterpenes. The sesquiterpene percentages in the Malaysian Etlingera elatior leaf and stem oils (45.7 and 11.3%) were higher than those in the E. sphaerocephala var. grandiflora leaf and stem oils (1.1 and 4.2%). The sesquiterpenes were found in small percentages in the oils of Brazilian Etlingera elatior flower (3.2%), Malaysian Etlingera elatior flower (5.8%) and E. sphaerocephala var. grandiflora whole plant (3.7%) whereas the one found in Brazilian Etlingera elatior flower axis yielded 22.5%. The non-terpenes represented the high percentages in the essential oils from the Etlingera cevuga rhizome (72.9%); Brazilian Etlingera elatior flower (66.6%) and flower axis (65.2%); Malaysian Etlingera elatior stem (86.8%), flower (81.1%) and rhizome (82.8%); and Thai Etlingera punicea rhizome (95.7%). The non-terpenes which were found in the Malaysian Etlingera elatior leaf oil gave 3.5%. The non-terpene percentages were considerably very low in all parts of the E. sphaerocephala var. grandiflora.

The hierarchical cluster analysis of the major volatile constituents from the rhizomes, stem, leaves and whole plant grouped those oils into three main two-part clusters (Fig. 1 and Fig. 2). The first cluster is formed of oils of the rhizomes (16.8%) and stem (17.4%) contained 1,8-cineole as the main component. The second cluster constructed

# M. A. A. Yahya et al: ANALYSIS OF ESSENTIAL OILS OF *ETLINGERA SPHAEROCEPHALA* VAR. *GRANDIFLORA* BY TWO-DIMENSIONAL GAS CHROMATOGRAPHY WITH TIMEOF-FLIGHT MASS SPECTROMETRY

by oils of the leaves and whole plant comprised  $\alpha$ -phellandrene (12.3%) and  $\beta$ -pinene (12.2%) as the major components, while the third cluster consisted of oils of the rhizomes and leaves and contained 1,8-cineole (16.8%) and  $\alpha$ -phellandrene (12.3%) as the main components.

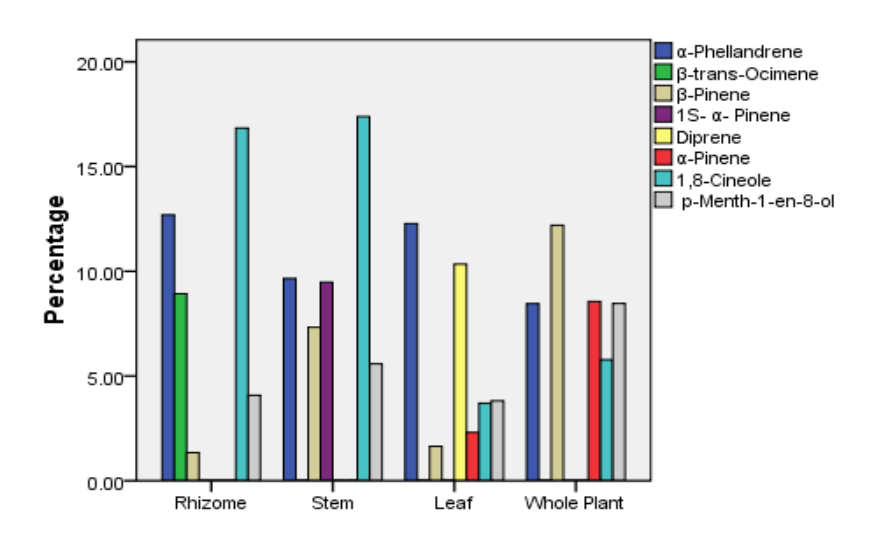


Figure 1: The percentages of the main compounds in the essential oils of the rhizomes, stem, leaves and whole plant of the *Etlingera sphaerocephala* var. *grandiflora*.

Rescaled Distance Cluster Combine

# C A S E 0 5 10 15 20 25 Label Num +-----+ Rhizome 1 Stem 2 Leaf 3 Whole Plant 4

Figure 2: Dendrogram generated by hierarchical cluster analysis of the percentage composition of eight major components of the essential oils from rhizomes, stem, leaves and whole plant of *Etlingera sphaerocephala* var. *grandiflora*, clustering method based on squared Euclidean distances.

Table 1: Components of essential oils obtained from the rhizomes, stem, leaves and whole plant of *Etlingera sphaerocephala* var. *grandiflora*.

|                                 | _                      | Rhizon | <u>ne</u> |      |       | _                      | Stem |     |      |      | _                      | Leaf |     |      |       |                        | /hole p | lant |      |      |
|---------------------------------|------------------------|--------|-----------|------|-------|------------------------|------|-----|------|------|------------------------|------|-----|------|-------|------------------------|---------|------|------|------|
| Compound                        | R.t.<br>1<br>R.t.<br>2 | S      | R         | P    | %     | R.t.<br>1<br>R.t.<br>2 | S    | R   | P    | %    | R.t.<br>1<br>R.t.<br>2 | S    | R   | P    | %     | R.t.<br>1<br>R.t.<br>2 | S       | R    | P    | %    |
| Monoterpene hydrocarbon         |                        |        |           |      |       | -                      |      |     |      |      |                        |      |     |      |       | -                      |         |      |      |      |
| α-Phellandrene                  | 9.83333<br>0.730       | 919    | 929       | 6954 | 12.69 | 9.83333<br>0.720       | 922  | 922 | 7235 | 9.66 | 9.75<br>0.700          | 938  | 938 | 8759 | 12.28 | 9.75<br>0.670          | 934     | 934  | 8743 | 8.45 |
| β-trans-Ocimene                 | 8.16667<br>0.670       | 913    | 913       | 3633 | 8.93  |                        |      |     |      | -    |                        |      |     |      | -     |                        |         |      |      | -    |
| (3Z)-2,7-Dimethyl-3-octen-5-yne | 8.25<br>0.710          | 813    | 821       | 1603 | 7.33  |                        |      |     |      | -    |                        |      |     |      | -     | 8.16667<br>0.710       | 838     | 845  | 1638 | 5.40 |
| Pseudolimonene                  | 9.16667<br>0.740       | 811    | 827       | 2404 | 7.04  |                        |      |     |      | -    | 9.1666<br>0.750        | 813  | 828 | 2196 | 4.65  | 0.710                  |         |      |      | -    |
| Sabinene                        | 9.16667<br>0.670       | 912    | 912       | 6176 | 5.27  |                        |      |     |      | -    | 9.25<br>0.670          | 900  | 901 | 5709 | 5.13  |                        |         |      |      | -    |
| o-Cymene                        | 10.3333<br>0.740       | 947    | 952       | 5596 | 4.82  | 10.3333<br>0.760       | 942  | 947 | 5084 | 6.60 | 10.3333<br>0.740       | 935  | 944 | 5014 | 3.18  | 10.25<br>0.690         | 953     | 956  | 5648 | 4.72 |
| Limonene                        | 10.3333<br>0.700       | 896    | 896       | 2564 | 3.50  | 10.3333<br>0.700       | 876  | 892 | 3612 | 4.70 | 0.710                  |      |     |      | -     | 10.3333<br>0.680       | 805     | 824  | 4483 | 1.46 |
| α-Terpinolene                   | 11.8333<br>0.690       | 938    | 940       | 3220 | 2.00  | 11.8333<br>0.700       | 939  | 941 | 3987 | 2.22 | 11.8333<br>0.710       | 938  | 942 | 2756 | 1.90  | 11.8333<br>0.670       | 955     | 957  | 4265 | 2.01 |
| β-Pinene                        | 9.5<br>0.700           | 912    | 912       | 4821 | 1.34  | 9.16667<br>0.690       | 957  | 960 | 5609 | 7.33 | 9.50<br>0.710          | 919  | 910 | 5000 | 1.64  | 9.25<br>0.670          | 927     | 931  | 3910 | 12.2 |
| Camphene                        | 8.58333<br>0.640       | 963    | 966       | 5823 | 1.21  | 8.58333<br>0.640       | 963  | 966 | 5983 | 1.30 | 8.58333<br>0.640       | 958  | 961 | 5416 | 0.56  | 8.58333<br>0.630       | 962     | 965  | 5754 | 0.96 |
| α-Terpine                       | 10.0833<br>0.680       | 882    | 889       | 2006 | 1.08  | 0.010                  |      |     |      | -    | 0.010                  |      |     |      | -     | 10.0833<br>0.660       | 888     | 895  | 2012 | 0.55 |
| β-cis-Ocimene                   | 10.8333<br>0.710       | 929    | 929       | 3919 | 0.52  | 10.8333<br>0.730       | 896  | 896 | 2638 | 0.31 | 10.8333<br>0.720       | 892  | 892 | 2254 | 0.15  | 10.8333<br>0.690       | 902     | 902  | 2951 | 0.40 |
| α, <i>p</i> -Dimethylstyrene    | 11.8333<br>0.870       | 918    | 918       | 3568 | 0.23  | 11.8333<br>0.850       | 924  | 938 | 4153 | 0.38 | 11.8333<br>0.880       | 898  | 899 | 2482 | 0.30  | 11.8333<br>0.820       | 905     | 905  | 3910 | 0.27 |
| 1 <i>S</i> - α-Pinene           | 0.070                  |        |           |      | -     | 8.25<br>0.680          | 931  | 931 | 3856 | 9.48 | 0.000                  |      |     |      | -     | 0.020                  |         |      |      | -    |
| Moslene                         |                        |        |           |      | -     | 10.0833<br>0.680       | 874  | 874 | 3737 | 1.00 |                        |      |     |      | -     |                        |         |      |      | -    |
| Diprene                         |                        |        |           |      | -     | 0.000                  |      |     |      | -    | 10.5<br>0.940          | 810  | 810 | 1655 | 10.34 |                        |         |      |      | -    |
| Sabinane                        |                        |        |           |      | -     |                        |      |     |      | -    | 8.25<br>0.820          | 893  | 893 | 2002 | 3.68  |                        |         |      |      | -    |
| D-Limonene                      |                        |        |           |      | -     |                        |      |     |      | -    | 10.3333<br>0.700       | 878  | 878 | 3255 | 2.37  |                        |         |      |      | -    |
| α-Pinene                        |                        |        |           |      | -     |                        |      |     |      | -    | 8.16667                | 968  | 968 | 5101 | 2.31  | 8.16667                | 939     | 939  | 3754 | 8.56 |

# M. A. A. Yahya et al: ANALYSIS OF ESSENTIAL OILS OF *ETLINGERA SPHAEROCEPHALA* VAR. *GRANDIFLORA* BY TWO-DIMENSIONAL GAS CHROMATOGRAPHY WITH TIME-OF-FLIGHT MASS SPECTROMETRY

| Pinene hydrochloride   |                  |     |      |           | _      |                  |     |     |            | _       | 0.660<br>13.5833 | 928 | 936  | 7228      | 0.08   | 0.650<br>13.5833 | 898 | 903  | 5221      | 0.12   |
|------------------------|------------------|-----|------|-----------|--------|------------------|-----|-----|------------|---------|------------------|-----|------|-----------|--------|------------------|-----|------|-----------|--------|
| i mone ny droemoriae   |                  |     |      |           |        |                  |     |     |            |         | 0.670            | ,20 | 750  | 7220      | 0.00   | 0.630            | 070 | 703  | 3221      | 0.12   |
| 3-Carene               |                  |     |      |           | -      |                  |     |     |            | -       | 14.8333<br>0.710 | 843 | 845  | 1442      | 0.04   |                  |     |      |           | -      |
| 1 <i>R</i> -α-Pinene   |                  |     |      |           | -      |                  |     |     |            | -       |                  |     |      |           | -      | 8.16667<br>0.740 | 959 | 959  | 4468      | 8.03   |
| Thuja-2,4(10)-diene    |                  |     |      |           | -      |                  |     |     |            | -       |                  |     |      |           | -      | 8.66667<br>0.640 | 827 | 827  | 3147      | 0.16   |
|                        |                  |     | (Sub | o-total 5 | 5.96%) |                  |     | (Su | ıb-total 4 | 12.98%) |                  |     | (Sul | o-total 4 | 8.61%) |                  |     | (Sub | -total 53 | 3.29%) |
| Oxygenated monoterpene |                  |     |      |           |        |                  |     |     |            |         |                  |     |      |           |        |                  |     |      |           |        |
| 1,8-Cineole            | 10.5<br>0.830    | 856 | 886  | 8092      | 16.84  | 10.5<br>0.810    | 864 | 891 | 8515       | 17.39   | 10.4167<br>0.710 | 909 | 909  | 9499      | 3.70   | 10.5<br>0.760    | 879 | 906  | 8578      | 5.78   |
| β-Terpinyl acetate     | 10.4167<br>0.780 | 899 | 901  | 4058      | 5.93   | 10.4167<br>0.770 | 893 | 897 | 4047       | 6.59    |                  |     |      |           | -      |                  |     |      |           | -      |
| p-Menth-1-en-8-ol      | 14.25<br>0.910   | 946 | 946  | 6693      | 4.08   | 14.25<br>0.920   | 948 | 948 | 6672       | 5.58    | 14.25<br>0.930   | 955 | 955  | 6806      | 3.82   | 14.25<br>0.820   | 947 | 947  | 6756      | 8.46   |
| 3-Pinanone             | 13.9167<br>0.750 | 917 | 917  | 5957      | 2.18   |                  |     |     |            | -       | 13.9167<br>0.740 | 928 | 931  | 6769      | 1.71   | 13.9167<br>0.710 | 917 | 917  | 4760      | 1.22   |
| 4-Terpineol            | 13.9167<br>0.810 | 886 | 886  | 5817      | 1.95   | 13.9167<br>0.800 | 901 | 901 | 6568       | 1.57    | 13.9167<br>0.82  | 919 | 919  | 6433      | 1.64   | 13.9167<br>0.750 | 838 | 849  | 5438      | 3.45   |
| Linalool               | 12.0833<br>0.860 | 896 | 896  | 7321      | 1.03   | 12,0833<br>0.860 | 898 | 898 | 7519       | 1.18    | 12.0833<br>0.850 | 899 | 899  | 7498      | 0.69   | 12.0833<br>0.800 | 890 | 890  | 7150      | 1.50   |
| Borneol                | 13.6667<br>0.840 | 920 | 920  | 3130      | 0.72   | 13.6667<br>0.850 | 944 | 944 | 3233       | 0.98    | 13.6667<br>0.840 | 934 | 934  | 3098      | 0.37   | 13.75<br>0.790   | 925 | 925  | 3076      | 1.12   |
| exo-Fenchol            | 12.4167<br>0.810 | 915 | 915  | 5904      | 0.29   | 12.4167<br>0.800 | 932 | 932 | 5858       | 0.69    | 12.4167<br>0.800 | 937 | 937  | 6307      | 0.20   | 12.5<br>0.760    | 923 | 923  | 5327      | 0.46   |
| L-Pinocarveol          | 13.0833<br>0.830 | 854 | 854  | 8669      | 0.29   |                  |     |     |            | -       |                  |     |      |           | -      |                  |     |      |           | -      |
| Myrtenol               | 14.4167<br>0.900 | 862 | 862  | 7201      | 0.23   |                  |     |     |            | -       |                  |     |      |           | -      |                  |     |      |           |        |
| Pinocarvone            | 13.5833<br>0.760 | 819 | 820  | 7097      | 0.19   |                  |     |     |            | -       |                  |     |      |           | -      | 13.6667<br>0.710 | 808 | 810  | 5052      | 0.36   |
| Myrtenal               | 14.4167<br>0.780 | 932 | 932  | 8994      | 0.17   |                  |     |     |            | -       | 14.4167<br>0.790 | 876 | 876  | 7771      | 0.04   | 14,4167<br>0.720 | 921 | 921  | 9000      | 0.19   |
| cis-Sabinol            |                  |     |      |           | -      |                  |     |     |            | -       | 14.5<br>0.960    | 865 | 865  | 3826      | 0.31   |                  |     |      |           | -      |
| (-)-Myrtenyl acetate   |                  |     |      |           | -      |                  |     |     |            | -       | 17.1667<br>0.730 | 888 | 888  | 6532      | 0.10   |                  |     |      |           | -      |
| Pinocarveol            |                  |     |      |           | -      |                  |     |     |            | -       |                  |     |      |           | -      | 13.0833          | 816 | 817  | 4217      | 0.09   |

The Malaysian Journal of Analytical Sciences, Vol 14 No 1 (2010): 32 - 40 0.790

|   |                  |     | (Su | b-total 3 | 33.90%) |                  |     | (Su | b-total 3 | 33.98%) |                  |     | (Sul | o-total 1 | 2.58%) | 0.790            |     | (Sub | -total 22 | 63%) |
|---|------------------|-----|-----|-----------|---------|------------------|-----|-----|-----------|---------|------------------|-----|------|-----------|--------|------------------|-----|------|-----------|------|
| Cogguitamono hydrogonhon                    |                  |     |     |           |         |                  |     |     |           |         |                  |     |      |           |        |                  |     |      |           |      |
| <b>Sesquiterpene hydrocarbon</b> α-Humulene | 19.8333<br>0.690 | 943 | 943 | 8066      | 1.35    | 19.8333<br>0.680 | 940 | 940 | 7820      | 1.05    | 19.8333<br>0.670 | 935 | 935  | 7443      | 0.26   | 19.9167<br>0.600 | 945 | 945  | 7860      | 1.44 |
| δ-Cadinene                                  | 21.25<br>0.670   | 882 | 891 | 4419      | 0.80    | 21.25<br>0.670   | 869 | 875 | 4498      | 0.46    | 0.070            |     |      |           | -      | 21.25<br>0.580   | 879 | 885  | 5071      | 0.12 |
| Caryophyllene                               | 19.1667<br>0.680 | 891 | 891 | 1813      | 0.76    |                  |     |     |           | -       |                  |     |      |           | -      |                  |     |      |           | -    |
| α-Muurolene                                 | 20.3333<br>0.670 | 887 | 890 | 2150      | 0.72    | 20.3333<br>0.670 | 878 | 881 | 2190      | 0.24    |                  |     |      |           | -      | 20.4167<br>0.580 | 879 | 882  | 4412      | 0.16 |
| α- Gurjunene                                | 18.75<br>0.650   | 883 | 895 | 2145      | 0.67    |                  |     |     |           | -       |                  |     |      |           | -      |                  |     |      |           |      |
| α-Bergamotene                               | 19.4167<br>0.670 | 908 | 915 | 2630      | 0.41    | 19.4167<br>0.670 | 918 | 923 | 3162      | 0.35    |                  |     |      |           | -      | 19.5<br>0.590    | 925 | 930  | 3271      | 0.46 |
| γ- Muurolene                                | 21.0833<br>0.680 | 881 | 885 | 2517      | 0.39    | 21.0833<br>0.680 | 875 | 879 | 2521      | 0.13    |                  |     |      |           | -      |                  |     |      |           | -    |
| γ-Gurjunene                                 | 20.6667<br>0.670 | 886 | 893 | 1374      | 0.29    | 20.6667<br>0.670 | 891 | 896 | 1945      | 0.15    |                  |     |      |           | -      |                  |     |      |           | -    |
| Calamenene                                  | 21.25<br>0.700   | 846 | 847 | 5523      | 0.28    |                  |     |     |           | -       |                  |     |      |           | -      |                  |     |      |           | -    |
| trans-α-Bergamotene                         | 20.9167<br>0.690 | 822 | 845 | 1777      | 0.27    |                  |     |     |           | -       |                  |     |      |           | -      |                  |     |      |           | -    |
| α-Cubebene                                  | 18.25<br>0.660   | 872 | 876 | 3643      | 0.22    |                  |     |     |           | -       |                  |     |      |           | -      |                  |     |      |           | -    |
| <i>epi</i> -β-Santalene                     | 19.6667<br>0.670 | 867 | 870 | 3071      | 0.20    | 19.6667<br>0.670 | 913 | 913 | 6424      | 0.14    | 19.6667<br>0.660 | 906 | 906  | 5030      | 0.05   | 19.75<br>0.580   | 922 | 922  | 6667      | 0.20 |
| α-Calacorene                                | 21.5833<br>0.720 | 815 | 886 | 5478      | 0.13    |                  |     |     |           | -       |                  |     |      |           | -      |                  |     |      |           | -    |
| α-Santalene                                 |                  |     |     |           | -       | 19.1667<br>0.670 | 883 | 887 | 3562      | 0.59    | 19.1667<br>0.670 | 921 | 925  | 5613      | 0.28   | 19.1667<br>0.590 | 938 | 942  | 7830      | 0.55 |
| α-Selinene                                  |                  |     |     |           | -       | 20.5<br>0.680    | 898 | 906 | 1781      | 0.18    |                  |     |      |           | -      |                  |     |      |           | -    |
| Copaene                                     |                  |     |     |           | -       | 18.25<br>0.650   | 894 | 895 | 5825      | 0.16    | 18.25<br>0.650   | 876 | 877  | 5012      | 0.04   | 18.3333<br>0.580 | 883 | 884  | 5999      | 0.21 |
| $(Z,E)$ - $\alpha$ -Santalene               |                  |     |     |           | -       |                  |     |     |           | -       | 19.4167<br>0.670 | 916 | 929  | 7579      | 0.20   |                  |     |      |           | -    |
| β-Bisabolene                                |                  |     |     |           | -       |                  |     |     |           | -       | 20.9167<br>0.690 | 848 | 848  | 2817      | 0.13   |                  |     |      |           | -    |
| β-Santalene                                 |                  |     |     |           | -       |                  |     |     |           | -       | 20<br>0.660      | 912 | 912  | 4975      | 0.04   |                  |     |      |           | -    |
| Cyperene                                    |                  |     |     |           | -       |                  |     |     |           | -       | 3.000            |     |      |           | -      | 18.8333          | 868 | 874  | 2065      | 0.11 |

# M. A. A. Yahya et al: ANALYSIS OF ESSENTIAL OILS OF *ETLINGERA SPHAEROCEPHALA* VAR. *GRANDIFLORA* BY TWO-DIMENSIONAL GAS CHROMATOGRAPHY WITH TIME-OF-FLIGHT MASS SPECTROMETRY

| Germacrene D                                 |                  |     |     |          | -                 |                  |     |      |           | -                |                  |     |      |               | -               | 0.560<br>21.0833<br>0.590 | 864 | 893 | 2261       | 0.07               |
|--|------------------|-----|-----|----------|-------------------|------------------|-----|------|-----------|------------------|------------------|-----|------|---------------|-----------------|---------------------------|-----|-----|------------|--------------------|
|  |                  |     | (S  | ub-total | 6.49%)            |                  |     | (Sul | o-total 3 | .45%)            |                  |     | (Sub | -total 1.     | 00%)            | 0.570                     |     | (St | ıb-total î | 3.32%)             |
| Oxygenated sesquiterpene (±)-trans-Nerolidol | 21.9167          | 917 | 917 | 4964     | 0.22              | 21.9167          | 932 | 932  | 5064      | 0.59             |                  |     |      |               | _               |                           |     |     |            | _                  |
| Humulene oxide II                            | 0.800<br>22.9167 | 823 | 841 | 2891     | 0.10              | 0.820<br>22.9167 | 820 | 826  | 3607      | 0.11             |                  |     |      |               | _               |                           |     |     |            | _                  |
| Guaiol                                       | 0.740            |     |     |          | -                 | 0.740            |     |      |           | -                | 22.6667          | 875 | 877  | 4184          | 0.10            | 22.75                     | 856 | 859 | 3049       | 0.08               |
| Nerolidol                                    |                  |     |     |          | -                 |                  |     |      |           | -                | 0.770<br>21.9167 | 911 | 922  | 6255          | 0.04            | 0.660<br>22               | 912 | 919 | 5621       | 0.31               |
|  |                  |     | (S  | ub-total | 0.32%)            |                  |     | (S   | ub-total  | 0.70%)           | 0.800            |     | (Su  | b-total (     | 0.14 %)         | 0.700                     |     | (Su | ıb-total ( | 0.39%)             |
| Non-terpenic compound<br>1,13-Tetradecadiene | 27.1667<br>0.810 | 944 | 951 | 2487     | 0.09              |                  |     |      |           | -                |                  |     |      |               | -               |                           |     |     |            | -                  |
| 3,5-Dimethyloctane                           | 11<br>0.690      | 855 | 903 | 2437     | 0.04              | 11<br>0.680      | 870 | 913  | 2306      | 0.13             | 11<br>0.680      | 838 | 907  | 2344          | 0.04            | 11<br>0.660               | 851 | 899 | 2508       | 0.13               |
| Decamethylcyclopentasiloxane                 |                  |     |     |          | -                 | 13.25<br>0.850   | 802 | 802  | 8895      | 0.16             | 13.25<br>0.870   | 810 | 810  | 9272          | 0.04            |                           |     |     |            | -                  |
| Hexadecane                                   |                  |     |     |          | -                 | 16.0833<br>0.690 | 878 | 883  | 2365      | 0.05             | 16.0833<br>0.690 | 875 | 880  | 2970          | 0.02            |                           |     |     |            | -                  |
| (Z)-3-Hexenol                                |                  |     |     |          | -                 |                  |     |      |           | -                | 6.66667<br>1.080 | 924 | 924  | 4315          | 0.22            |                           |     |     |            | -                  |
| 2-Hexenal                                    |                  |     |     |          | -                 |                  |     |      |           | -                | 6.66667<br>0.940 | 939 | 939  | 7381          | 0.06            |                           |     |     |            | -                  |
| Undecane                                     |                  |     | (0  | 1 1      | - 0.12%           |                  |     | (6   | 1 , , 1   | - 0.24%          | 12.0833<br>0.680 | 859 | 859  | 2071          | 0.01            |                           |     | (6  | 1 , , 1,   | - 0.12%            |
| Total Rt                                     |                  | • / |     | ub-total | 0.13/.)<br>96.80/ |                  |     | (S   | ub-total  | 0.34%)<br>81.45% |                  |     | (St  | ıb-total<br>6 | 0.39/)<br>2.72/ |                           |     | (St | ıb-total ( | 0.13/.)<br>79.76/. |

R.t., retention time in the first dimension (min).
R.t., retention time in the second dimension (min).
S = similarity, R = reverse, P = probability.

### Conclusion

In comparison, the leaves of *Etlingera sphaerocephala* var. *grandiflora* yielded more oil percentage than others. The major compounds in each of the four oils of *E. sphaerocephala* var. *grandiflora* noticeably differed. These oils were rich in monoterpenes compared to the oils of *E. cevuga*, *E. elatior* and *E. punicea*.

# Acknowledgement

Thanks are due to the Center for Research and Innovation Management, Universiti Kebangsaan Malaysia for recording necessary data using the GCXGC-TOFMS instrument. We are also wish to thank the Ministry of Higher Education Malaysia and the Universiti Kebangsaan Malaysia for financial support through the Fundamental Research Grant Scheme UKM-ST-06-FRGS0110-2009.

#### References

- 1. Turner, I.M. (1995). A catalogue of the vascular plants of Malaya. Gardens' Bulletin Singapore. 47(2): 642-655.
- 2. Lim, C.K. (2001). Taxonomic notes on *Etlingera* Giseke (Zingiberaceae) in Peninsular Malaysia: the "*Achasma*" taxa and supplementary notes on the "*Nicolaia*" taxa. *Folia Malaysian*. 2(3): 141-178, 209-210.
- 3. Khaw, S.H. (2001). The genus *Etlingera* (Zingiberaceae) in Peninsular Malaysia including a new species. *Gardens' Bulletin Singapore*, 53: 191-239.
- 4. Holttum, R.E. (1950). The Zingiberance of the Malay Peninsula. Gardens' Bulletin Singapore. 13(1): 1-249.
- 5. Smith, R.M. (1986). New combinations in *Etlingera* Gisek (Zingiberaceae). *Notes Royal Botanic Garden Edinburgh*. 43: 243-254.
- 6. Poulsen, A.D. (2006). Etlingera of Borneo. Natural History Publications (Borneo). Kota Kinabalu
- 7. Lechat-Vahirua, I., Francois, P., Menut, C., Lamaty, G., Bessiere, J.M. (1993). Aromatic plants of French Polynesia. I. Constituents of three Zingiberaceae: *Zingiber zerumbet* Smith, *Hedychium coronarium* Koeing and *Etlingera cevuga* Smith. *Journal of Essential Oil Research*. 5: 55-59.
- 8. Zoghbi, M.D.G.B., Andrade, E.H.A. (2005). Volatiles of *Etlingera elatior* (Jack) R.M.Sm. and *Zingiber spectabile* Griff.: two Zingiberaceae cultivated in the Amazon. *Journal of Essential Oil Research.* 17: 209-211.
- 9. Faridahanim Mohd Jaafar, Che Puteh Osman, Nor Hadiani Ismail, Khalijah Awang (2007). Analysis of essential oils of leaves, stems, flowers and rhizomes of *Etlingera elatior* (Jack) R. M. Smith. *Malaysian Journal of Analytical Sciences*. 11: 269-273.
- 10. Tadtong, S., Wannakhot, P., Poolsawat, w., Athikomkulchai, S., Ruangrungsi, N. 2009. Antimicrobial activities of essential oil from *Etlingera puniceae* rhizome. *J Health Res*, 23(2): 77-79.

# EFFECT OF HTAB CONCENTRATION ON THE SYNTHESIS OF NANOSTRUCTURED ${\rm TiO_2}$ TOWARDS ITS CATALYTIC ACTIVITIES

(Kesan Kepekatan HTAB Terhadap Sintesis TiO<sub>2</sub> Nanostruktur Ke Atas Aktiviti Pemangkinannya)

Ruslimie C. A, Mohd Hasmizam Razali\* and Wan M. Khairul

Department of Chemical Sciences, Faculty of Science and Technology, Universiti Malaysia Terengganu, 21030, Kuala Terengganu, Terengganu, Malaysia

\*Corresponding author: mdhasmizam@umt.edu.my

#### **Abstract**

Titanium dioxide, TiO<sub>2</sub> photocatalyst was synthesised by microemulsion method under controlled hydrolysis of titanium butoxide, Ti(O(CH<sub>2</sub>)<sub>3</sub>)CH<sub>3</sub> in Hexadecyl Trimethyl Ammonium Bromide, HTAB. The effect of various concentrations of surfactant in the range between 0.01-1.0 M were focused on by investigating their morphology, crystallite size, crystalline phase and specific surface area. After observation on their degradation performance, 0.5 M concentration of HTAB presented as a optimum concentration to synthesis TiO<sub>2</sub> photocatalyst. These results also supported by XRD spectra which are exhibited size of photocatalyst in the range within 50-150 nm. As a result, the catalytic properties of the synthesised TiO<sub>2</sub> nanostructure was performed by exhibiting good behaviour in photocatalytically degraded atrazine, 2-chloro-4-(ethylamino)-6 (isopropylamino)-S-triazine to unharmful compounds in the environment.

Keywords: TiO<sub>2</sub>, microemulsion, photodegradation, atrazine.

### Abstrak

Fotopemangkin, titanium dioksida, TiO<sub>2</sub> telah disintesis melalui kaedah mikroemulsi di bawah kawalan hidrolisis titanium butoksida, Ti(O(CH<sub>2</sub>)<sub>3</sub>)CH<sub>3</sub> di dalam Heksadesil Trimetil Ammonium Bromida, HTAB. Kesan kepelbagaian kepekatan surfaktan dalam julat 0.01-1.0 M telah difokuskan di dalam kajian terhadap morfologi, saiz hablur, fasa kehablurannya dan luas permukaan spesifik. Selepas pemerhatian dan perbandingan dijalankan terhadap prestasi degradasinya, kepekatan 0.5 M HTAB telah menunjukkan kepekatan optimum untuk mesintesis fotopemangkin TiO<sub>2</sub>. Keputusan ini juga telah disokong oleh spektra XRD yang mana telah mempamerkan saiz fotopemangkin adalah di dalam julat di antara 50-150 nm. Hasilnya, ciriciri mangkin TiO<sub>2</sub> nanostruktur yang telah disintesis menunjukkan sifat yang baik sebagai fotopemangkin bagi menguraikan atrazina, 2-kloro-4-(etilamino)-(isopropilamino)-S-triazina kepada sebatian-sebatian yang tidak berbahaya di dalam alam sekitar.

Kata kunci: TiO<sub>2</sub>, mikroemulsi, fotopemangkinan, atrazina.

# Introduction

Titanium dioxide, TiO<sub>2</sub> photocatalyst has attracted great attention as a promising photocatalyst for photocatalytically degrade organic pollutant in the environment [1]. TiO<sub>2</sub> nanostructure is considered to be one of the promising materials due to its ideal physical and chemical properties such as environmental friendly, low cost, high oxidizing ability, long term stability and also exhibit high photocatalystic activity [2, 3]. However, their physical, chemical and photocatalytic activities are known to depend on its preparation methods such as by changing their calcinations temperature, time aging and pH of solution which may give affect on its performance [4, 5].

There are numerous methods known to synthesise TiO<sub>2</sub> including microemulsion which is believed to be very promising method to obtain nanosized TiO<sub>2</sub> particle with less agglomeration and flocculation. In addition, the surfactant in microemulsion will act as stabilized micro cavities to provide a cage-like effect that limits particle nucleation, growth and agglomeration [6]. However, the optimum concentration of surfactant in the microemulsion has become an argument among researchers because apparently it depends on the type of surfactant and preparation method that are used during synthesis process. The main objective of the study is to investigate the effect of various surfactant concentrations in synthesise TiO<sub>2</sub> towards degradation performance. The optimal surfactant concentration will promise great properties of TiO<sub>2</sub> nanoparticles and may have better capacity to degrade 2-chloro-4-(ethylamino)-6 (isopropylamino)-S-triazine or widely known as atrazine to unharmful compounds in the environment.

# Ruslimie et al: EFFECT OF HTAB CONCENTRATION ON THE SYNTHESIS OF NANOSTRUCTURED TiO<sub>2</sub> TOWARDS ITS CATALYTIC ACTIVITIES

### **Experimental**

### **Instruments**

The physical properties of the synthesised TiO<sub>2</sub> were characterized by Scanning Electron Microscopy, SEM (JEOL JSM-6360 LA). The specific surface area of TiO<sub>2</sub> particles (BET method), specific pore volume and average pore diameter (BJH method) of the samples were determined by using nitrogen adsorption-desorption isotherms using Quantachrome Autosorb Automated Gas Sorption. Meanwhile, the particles size of the TiO<sub>2</sub> powders was determined by X-Ray Diffraction, XRD (Rigaku, Miniflex II Desktop X-Ray Diffractometer).

### Reagents

The reagents used were Hexadecyl Trimethyl Ammonium Bromide, HTAB (Sigma - Aldrich), titanium butoxide (purity 97%, Sigma-Aldrich), cyclohexane (Hamburg Chemical), NaCl (Merck Schuchartdt) and ammonium hydroxide, NH<sub>4</sub>OH (Mallinckrodt). In addition, for catalytic studies, the selected pesticide namely Atrazine (Sigma-Aldrich) was used as standard. All of these chemicals were used as received without further purification.

#### General procedures

 $TiO_2$  nanoparticles were prepared according to 6:3:1 proportion as proposed and carried out in previous studies [7]. Microemulsion A and B consist 60 ml cyclohexane (Hamburg Chemical) as oil phase and 30 ml Hexatrimethyl Ammonium Bromide, HTAB (Sigma - Aldrich) as surfactant by varying their concentration 0.01, 0.05, 0.1, 0.5 and 1.0 M. As starting material, 10 ml of titanium (IV) butoxide,  $Ti(O(CH_2)_3)CH_3$  (purity 97%, Sigma-Aldrich) was added in microemulsion A, meanwhile ammonium hydroxide solution,  $NH_4OH$  (Mallinckrodt) 2 M as reducing agent in reagent B. After 30 min of stirring separately, both microemulsion were mixed in a beaker (100 ml) and followed by vibrated homogeneously in ultrasonicator (JAC Ultrasonic Cleaner, JAC 2010, 240~/50Hz/30 A) for 1 hour. This step was carried out to prevent agglomeration of  $TiO_2$  pigment in water.

Then, 10 ml of 5 M solution of sodium chloride, NaCl (Merck Schuchartdt) was added to microemulsion, followed by continuously vibrated in ultrasonicator for another 1 hour to ensure the mixture was completely mixed. The microemulsion, was then washed with 30 ml acetone before the product was annealed (Nabertherm, HTC 08/16, 400 V, 50/60 Hz) at 600° C for 4 hours. Next, the powders obtained were washed with 100 ml distilled water to remove the remaining NaCl, followed by dried in an oven at *ca.* 90°C for 12 hours to remove any excess water.

# Photocatalytic activity

The photocatalytic degradation of atrazine was performed by using 100 ml aqueous solution of atrazine (5 mg/l) (Sigma-Aldrich) and 0.1 g of synthesised  $TiO_2$  catalyst. The degradation mixture were stirred magnetically and irradiated by UV-light (302 nm, 230 V $\sim$ 50 Hz) for 1 hour to ensure their optimum thermodynamic stability. Every 5 ml of the aqueous suspension was collected at each 30 minutes interval during the irradiation and then was filtered on 0.10  $\mu$ m Milipore syringe filter (Whatman) to remove the catalyst. The samples were exposed for 4 hours under UV-light and analyzed by using UV-Vis spectrophotometer (UV-1601 PC, UV-Visible Spectrophotometer Shidmadzu) for the percentages of degradation determination.

### Results and discussion

# Morphological study

Figure 1 A to F indicate the SEM images of the  $TiO_2$  powders prepared by microemulsion method at various HTAB concentration. From the observation of Figure 1 A to D, the particle are slowly become less agglomerates. Sample A was carried out without HTAB as a comparison with others to show the significant of surfactant existence in the synthesis process. Figure 1 A shows the effect of microemulsion without existence of surfactant. It can be observed that without existence of surfactant in microemulsion, there are no covers by surfactant on the surface to hydrolyze the products and hence, no nanosize  $TiO_2$  can be obtained [8]. It is obviously noted that the ultrafine and nanosized particles cannot be achieved in the synthesis process without the present of surfactant.

However, at concentration of 0.5 M, the shape of TiO<sub>2</sub> particles becomes less agglomerates and uniformly shape. These observations are exposed to different water compositions in microemulsion which has played important roles. Therefore, according to Mohapatra *et al.*, 2006, at low HTAB concentration, the size of particles is increased. This might be due to the increasing size of water droplet which is produced by hydrolysis in the w/o microemulsion's water pool [9]. The high particles size of TiO<sub>2</sub> has caused by the increasing agglomeration process. The high agglomeration of particles is shown in Figure 1 A-D. However, one can observe that, their

agglomeration becomes gradually decrease with the decreasing of water content until it has reached the optimal concentration of HTAB which is 0.5 M.

Meanwhile, when HTAB concentration is more than  $0.5~\mathrm{M}$ , the particles become agglomerate again. Except for  $\mathrm{TiO_2}$  synthesised by  $1.0~\mathrm{M}$  of HTAB which has shown elongated structure compared to the other concentrations. This might be due to the viscosity of microemulsion has increased due to the high content of surfactant in microemulsion during synthetic steps. Hence, this condition caused the particles movement become difficult due to bridging of the surfactant and it was lead to the increasing of surface tension and particles size [10]. Therefore, the dispersion of powder in microemulsion is incompletely distributed and need to be improved under optimum concentration of HTAB, thus the ultrafine particles would be achieved.

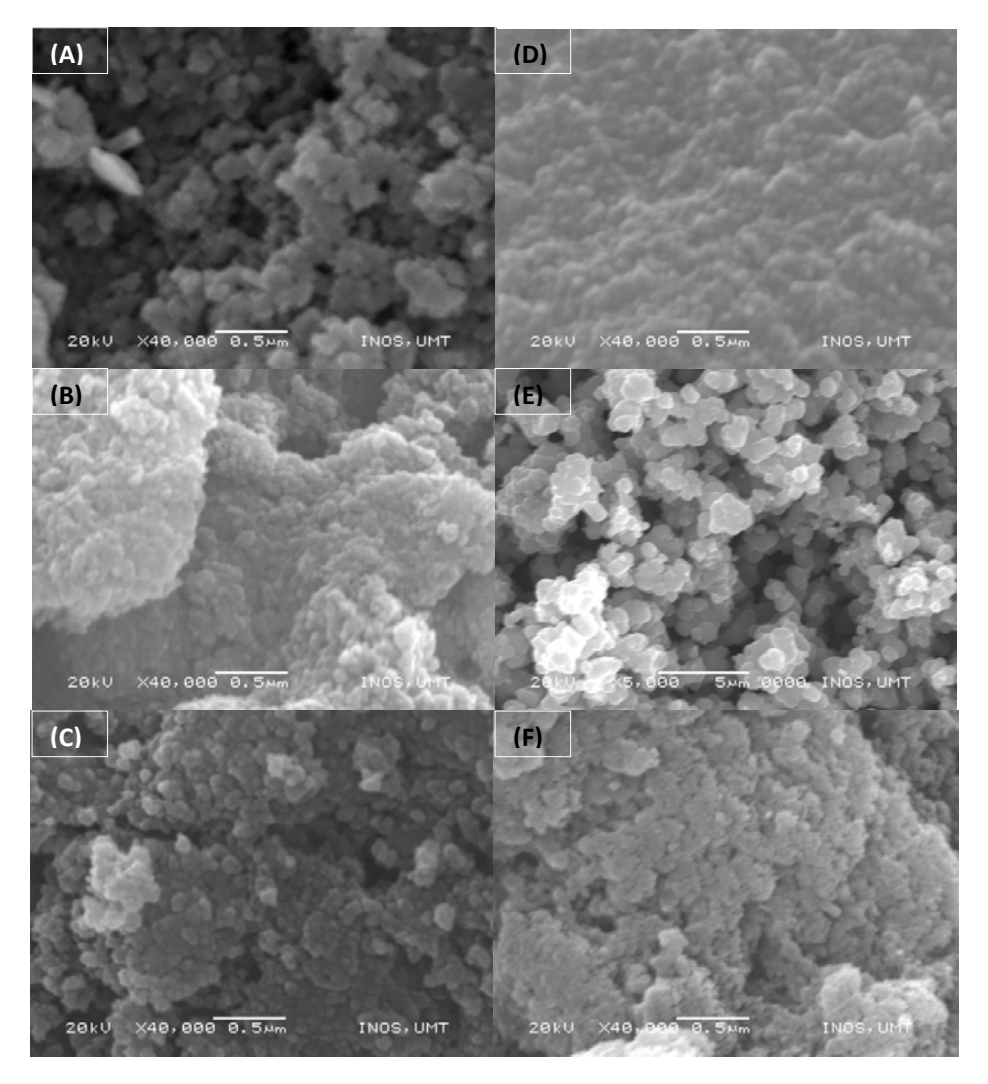


Figure 1: Morphological images effect of HTAB at (A) without HTAB, (B) 0.01, (C) 0.05, (D) 0.1, (E) 0.5 and (F) 1.0 M concentration.

# Crystal structure study

Figure 2 indicates X-ray diffraction pattern of  $TiO_2$  obtained from various HTAB concentrations. The XRD pattern revealed the effect of surfactant concentration on the phase change of  $TiO_2$  nanoparticles. It is clearly shown that diffraction peaks from concentration 0.01 to 0.5 M gradually transform to anatase phase completely. The change in the width of these diffraction peaks is related to the variation changes of crystallite size of the

# Ruslimie et al: EFFECT OF HTAB CONCENTRATION ON THE SYNTHESIS OF NANOSTRUCTURED TiO $_2$ TOWARDS ITS CATALYTIC ACTIVITIES

obtained powders. The major phase of all prepared particles is an anatase structure was observed at concentration 0.5 M HTAB. However, at concentration 1.0 M, the X-ray diffraction peak of the obtained  $TiO_2$  powders becomes broader which is apparently revealing the particles size of  $TiO_2$  to become increase again due to unsuitable and unideal concentration during synthesis process. The increase of the  $TiO_2$  particle size might be due to agglomeration on their surface. This X-ray diffraction spectra data are comparable to SEM morphological image which has proved that the optimal surfactant concentration is crucial in order to synthesis  $TiO_2$  at nanosize condition. Meanwhile, for synthesis  $TiO_2$  without using HTAB surfactant (0.0 M) exhibits undesired peak was appear at angle  $2\Theta$  =22 degree corresponding to the high agglomeration due to without ultrafine synthesis medium.

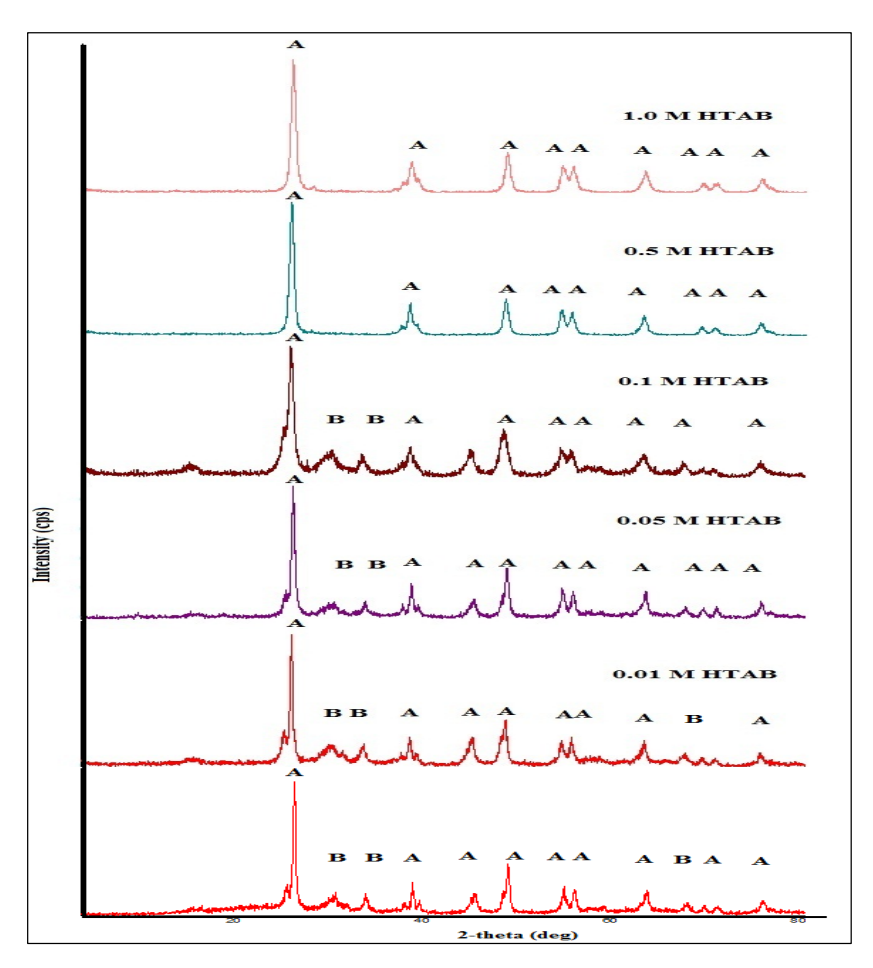


Figure 2: XRD spectra of TiO<sub>2</sub> nanoparticles synthesised at different HTAB concentration and were calcined at 500° C for 4 hours. (A: anatase, B: brookite).

Basically, the average particles size of  $TiO_2$  is calculated by using Scherer's equation on each the highest intensity diffraction peaks by following equation:

$$D = \frac{K\lambda}{\beta} \cos\theta$$
 Equation 1

Since D in the crystal size of the catalyst,  $\lambda$  the X-ray wavelength (1.54Å),  $\beta$  the full width half maximum, (FWHM) of the highest intensity diffraction peak, K is a coefficient (0.94 nm) and  $\Theta$  is the diffraction angle. An average particles size of around 40-140 nm was obtained for nanoparticles. Based on these results, 0.5 M concentration of HTAB surfactant was successfully synthesised in the smallest particles size. It might be due to X-ray diffraction peaks intensities of obtained TiO<sub>2</sub> which was increased and the Full Width Half Maximum, FWHM peak at  $2\Theta$ =25.3° became narrower with decreasing the composition of water ratio [11]. The peak at  $2\Theta$ =25.3° was chosen as a standard peak due to their well crystallite peak for TiO<sub>2</sub> appeared. In addition, Figure 3 clearly shows the effect of HTAB concentration on particles size of TiO<sub>2</sub>. This indicates the optimum value of HTAB concentration will determine the smallest size of particles. Hence, the best of particles size will be enhancing their percentage of degradation. Besides, physical properties of TiO<sub>2</sub> can be improved by varying their several parameters as well such as stirring time and pH of microemulsion in order to improve the performance of degradation process.

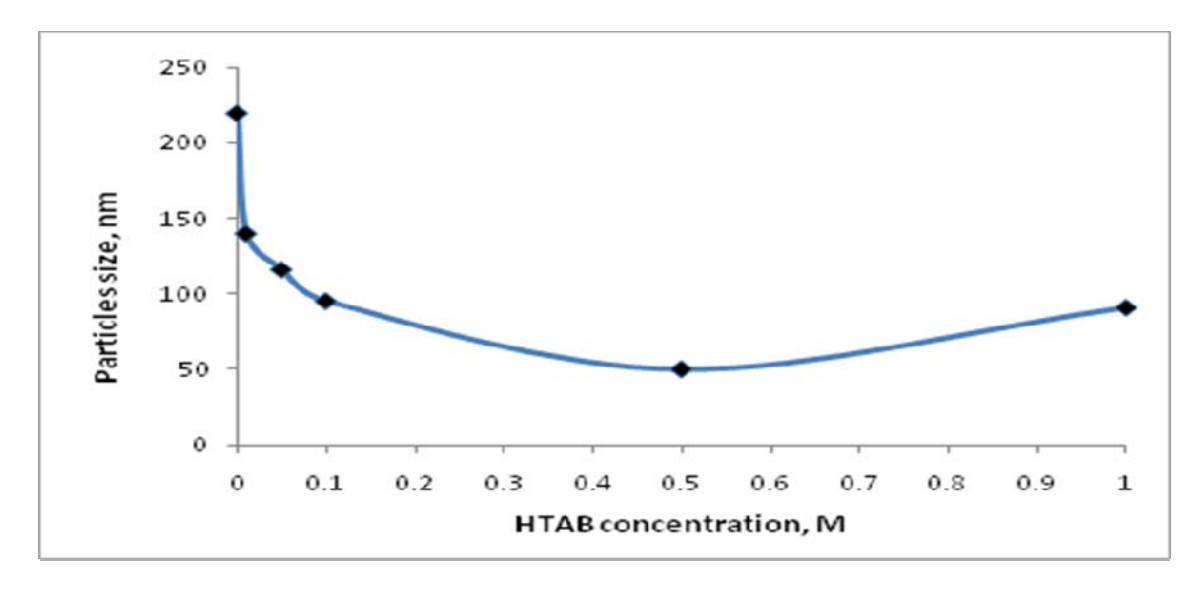


Figure 3: Variation in particles size of TiO<sub>2</sub> powders prepared at different surfactant concentration and were calcined at 500° C for hours.

# Surface area and pore volume analysis

Surface area and pore volume are crucial aspect in term of photocatalytic studies. Table 1 summarises the crystallite size, surface area and pore diameter of TiO<sub>2</sub> photocatalyst when synthesised by varying their surfactant concentrations. The specific surface area slightly increases from 15.22 to 76.66 m<sup>2</sup>/g as the concentration of HTAB surfactant is increased from 0.01 M to 0.5 M. Nevertheless, the specific surface area of synthesised TiO<sub>2</sub> is decreased with HTAB concentration at 1.0 M. The TiO<sub>2</sub> prepared at 0.5 M concentration of HTAB and calcined at 500°C for 4 hours exhibits the highest specific area of 76.66m<sup>2</sup>/g.

Generally, the specific surface area depends on the size and shape of the particles. Somehow, the different of surface area which observed is owing to the agglomeration of the particles even though their particle shape and size is similar [12]. Hence, according to Lu *et al.*, 2008, by the increasing the particle size, apparently it will decrease the surface area [13]. In addition, the pore diameter of TiO<sub>2</sub> synthesised without HTAB surfactant was show the lowest specific surface area, which is 15.22 m<sup>2</sup>/g. This resulted occurs due to absence of HTAB in the microemulsion during synthetic process. The presence of optimum concentration of HTAB not only controls the particles size and shape, but also increase the porosity of the materials [14].

Table 1: The profiles of the particles synthesised by varying their surfactant concentration in microemulsion and calcined at 500° C for 4 hours.

| HTAB concentration (M) | Crystallite size (nm)* | BET surface area (m²/g) | BJH adsorption-<br>desorption pore<br>surface area<br>(m²/g) | Crystallite phase |
|------------------------|------------------------|-------------------------|--|-------------------|
| 0.0                    | 150.6                  | 15.22                   | 20.11  | Anatase, brookite |
| 0.01                   | 139.5                  | 20.75                   | 36.91  | Anatase, brookite |
| 0.05                   | 115.9                  | 22.33                   | 47.92  | Anatase, brookite |
| 0.1                    | 95.1                   | 57.53                   | 62.77  | Anatase, brokite  |
| 0.5                    | 49.9                   | 76.66                   | 80.25  | Anatase           |
| 1.0                    | 90.8                   | 41.76                   | 38.47  | Anatase           |

<sup>\*</sup>Calculated by using Scherer equation.

While, the pore surface area of all synthesised  $TiO_2$  was determined by using Barret-Joyner-Halenda (BJH) adsorption-desorption method. The addition of HTAB surfactant has resulted the pore surface area to increase of which is within 20 to 80 m<sup>2</sup>/g. However, at the concentration of 1.0 M HTAB, the pore surface area drastically decrease to 38.5 m<sup>2</sup>/g. The decreasing of pore surface area is due to less pores formed in the catalyst surface. This phenomenon was attributed to the restricting effect of the microemulsion due to over loaded amount of HTAB surfactant to control their excess growth. Thus, the growth speed and synergistic control of  $TiO_2$  growth during synthetic process were inhibited and growth rate decreased accordingly [15]. Hence, the inhibition and restriction has caused the decreasing of surface area and pore surfacea area.

# Photocatalytic study

The catalytic activity of catalysts which are synthesised by various surfactant concentrations in order to investigate their catalytic behaviour towards atrazine. Figure 4 shows the percentage of atrazine's degradation when exposed for 4 hours under UV irradiation. Photodegradation of atrazine by using TiO<sub>2</sub> synthesised without HTAB was only able to degrade at 27%. This degradation is lower compared to the others which may due to their specific surface area. The limit of specific surface area will act as adsorption surface to reduce molecular oxygen on the Ti (III) sites to the superoxide radical anion. The surface to bulk ratio for a nanoparticles material is much greater than for material with larger grains, which yields large interface interaction between the solid and gaseous or liquid medium [16].

The enhancement of photodegradation activity is improved in the presence of HTAB. According to Lu *et al.*, 2009, HTAB not only helps in the spherical particle formation but it is also increases the surface area and visible light absorption [17]. Therefore, it should be an effective photocatalyst in the presence of HTAB and the optimum concentration of HTAB will enhance the performance of photodegradation activity.

In this study, obviously the percentages of photodegradation were increasing by the decreasingly degree of agglomeration. Somehow, high degree of agglomeration will affect the catalyst's surface area which mean will resulted low performance of degradation. Hence, the percentages of photodegradation in the presence of the synthesised TiO<sub>2</sub> catalyst by 0.01, 0.05, 0.1 and 0.5 M of HTAB increased gradually from 35, 39, 44 and 60 %. These findings are supported by SEM observations, which show the agglomeration of TiO<sub>2</sub> catalyst's surface slowly decreased by the increasing amount of surfactant in the microemulsion. Furthermore, phase content that clearly observed from XRD pattern plays vital important role in enhancing the rate of photodegradation [18]. Thus, at 0.01, 0.05 and 0.1 M concentration of HTAB, the broader, less crystalline and less intensity peaks are observed compared to the XRD spectrum which obtained from 0.5 M concentration of HTAB. According to these results, the highly diffract peaks may be attributed to agglomeration process. Meanwhile, the well-crystallite pattern as represented by 0.5 M of HTAB is corresponding to the anatase phase crystalline structure of these aggregated particles. Whilst, the existence of broader and so-called noise peaks are believed to be

attributed as brookite phase. The mixture of phase content is influenced by the percentages of degradation which also to the respect of impurities presence in the sample.

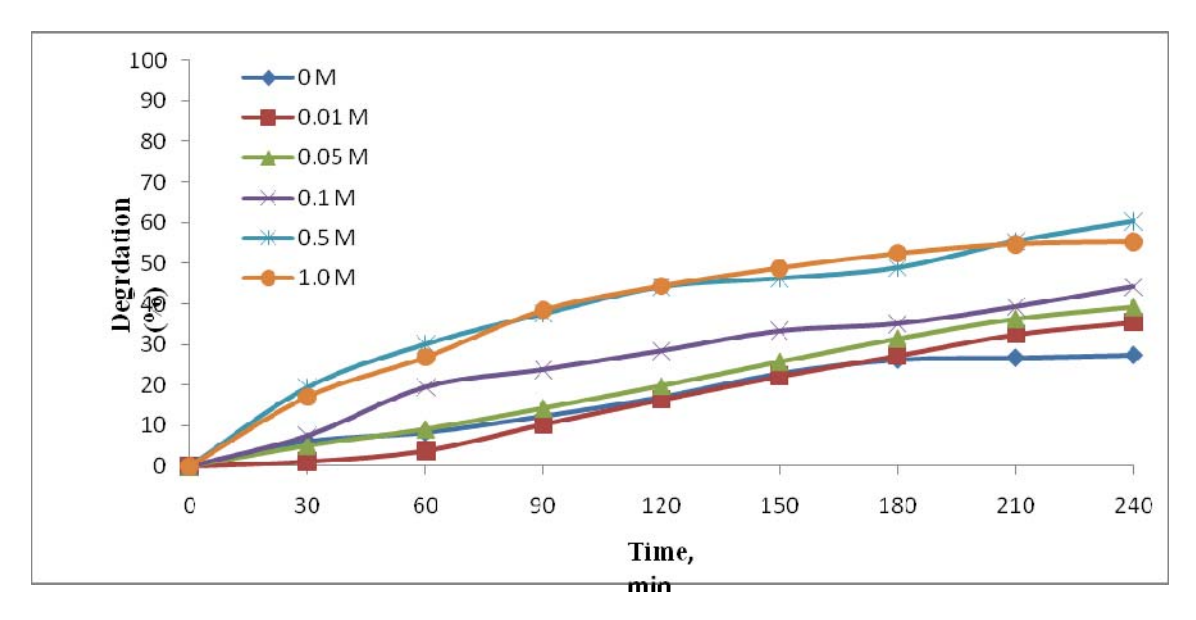


Figure 4: Effect of surfactant concentration towards percentages of photodegradation of atrazine by irradiated with UV for 4 hours.

Among all surfactant concentrations, 0.5 M surfactant shows the best photocatalytic activity by degrading 60 % of atrazine. Physical and chemical properties of all synthesised TiO<sub>2</sub> determined by SEM and XRD results proved that 0.5 M of HTAB has produced the aggregation of nanoparticles. The samples obtained at this concentration are all in the uniformly shape with the size particle in the average of 49.9 nm. This might be attributed to the narrower peaks, high crystalline and high intensity compared to the other peaks of other concentrations. The narrower peaks will produce high value of Full Width Half Maximum, FWHM value. Hence, by increasing the FWHM value the particles size will be decreased as suggested by Scherrer equation. In fact, less aggregation on surface of TiO<sub>2</sub> photocatalyst has caused the high specific surface area [19]. Hence, the interaction during photoreaction has taken place at maximum activity.

In addition, anatase crystallinity phase exhibits to produce high performance of degradation [20]. In addition, according to BET specific surface area has shows the surface area synthesised with 0.5 M of HTAB has the highest surface area compared with others. High surface area will enhancing the photodegradation process due to large surface area provided more area to react with atrazine and as well to produce hydroxyl radicals and superoxide radicals anions. Therefore, it can be assumed that the optimum concentration of surfactant in microemulsion leads to the formation of anatase phases. The nanoparticles in different phase formation observed as anatase phase is more stable at nanosized which resulted a higher photocatalytic activity compared to the bookite and rutile phase [21][22].

However, based on photodegradation result, it can be summarised that too high loading of surfactant in microemulsion will inhibit the formation of the desired nanoparticles. This is related to different size of water droplet in microemulsion with various concentration of HTAB [23]. In this report, 1.0 M HTAB is proven to contain an excessive amount of HTAB which prevent the formation of the ideally uniform shape. The observation was strongly agreed by SEM micrographs images, BET specific surface area and XRD spectrum result which show the degree of agglomeration of TiO<sub>2</sub> powders depends on the concentration of the aqueous solution. Thus, the most appropriate surfactant concentration in order to obtain spherical nanoparticles photocatalyst is 0.5 M HTAB.

# Ruslimie et al: EFFECT OF HTAB CONCENTRATION ON THE SYNTHESIS OF NANOSTRUCTURED TiO<sub>2</sub> TOWARDS ITS CATALYTIC ACTIVITIES

#### Conclusion

 $TiO_2$  nanoparticles with optimum surfactant concentration were successfully prepared via microemulsion method. This investigation concludes that agglomeration of  $TiO_2$  nanosized can be reduced by adding surfactant. However, the optimisation of surfactant concentration is essential for obtaining minimum  $TiO_2$  particle sizes. The increase of surfactant concentration significantly decreased the particles size of the prepared  $TiO_2$  by preventing agglomeration. The optimum concentration of surfactant needed is 0.5 M for synthesised  $TiO_2$ , which yield the size of the particles is 49.9 nm. As a result, photocatalytic activity of synthesised  $TiO_2$  by optimum surfactant concentration was successfully 60 % degraded atrazine.

# Ackowledgement

The authors would like to acknowledge Ministry of Higher Education Malaysia (MOHE) for Fundamental Research Grant Scheme, (FRGS), grant no. 59121, Ministry of Science, Technology and Innovation Malaysia (MOSTI) for National Science Fellowship (NSF) for postgraduate scholarship and E- Science Fund project vote no. 52027. The acknowledgement also goes to Department of Chemical Sciences, Faculty of Science and Technology, and Institute of Oceanography, INOS Universiti Malaysia Terengganu for research facilities and contribution in this research.

#### References

- 1. Kitano, M., Matsuoka, M., Ueshima, M. and Anpo, M. 2007. Recent Development in Titanium Oxide-based Photocatalysts. Applied Catalysis A: General, 325: 1-14.
- 2. Yu, J., Su, Y., Cheng, B. And Zhou, M. 2006. Effect of pH on the Microstructures and Photocatalytic Activity of Mesoporous Nanocrystalline Titania Powders Prepared via Hydrothermal Method. Journal of Molecular Catalyst A: Chemical, 258: 104-112.
- 3. Venkatachalam, N, Palanichamy, M. and Murugesan, V. 2007. Sol-gel Preparation and Characterisation of Nanosize TiO<sub>2</sub>: Its Photocatalytic Performance. Materials Chemistry and Physics, 104: 454-459.
- 4. Yu, J., Yu, H., Cheng B., Zhou, M. And Zhao, X. 2006. Enhanced Photocatalytic Activity of TiO<sub>2</sub> Powder (P25) by Hydrothermal Treatment. Journal Of Molecular Catalyst A: Chemical, 253: 112-118.
- 5. Lu, C.-H. and Wen, M.-C. 2008. Synthesis of Nanosized TiO<sub>2</sub> powders via a hydrothermal microemulsion process. Journal of Alloys and Compounds, 448: 155-158.
- 6. Lee, M. S., Lee, G.-D., Ju, C.-S. and Hong, S.-S. 2005b. Preparations of nanosized TiO<sub>2</sub> in reverse microemulsion and their photocatalytic activity. Solar Energy Materials and Solar Cells, 88: 389-401.
- 7. Wang, J., Sun, J., Bian, X. 2004. Preparation of Oriented TiO<sub>2</sub> Nanobelts by Microemulsion Technique. Material Science and Engineering, A 379: 7-10.
- 8. Timothy, J. M. 1999. Sonochemistry. *In an Introduction To The Uses of Power Ultrasound in Chemistry*. ed. R. G. Compton. Oxford University Press. New York: pp 1-39.
- 9. Mohapatra, P., Mishra, T. and Parida, K. M. 2006. Effect of Microemulsion Composition on Textural and Photocatalytic Activity of Titania Nanomaterial. Applied Catalysis A: General, 310: 183-189.
- 10. Chai, L.-Y., Yu, Y.-F., Zhang, G., Peng, B. and Wei, S.-W. 2007. Effect of Surfactant on Preparation TiO<sub>2</sub> by Pyrohydrolysis. Transaction of Nonferrous Metals Society of China, 17: 176-180.
- 11. Asim, N., Radiman, S. and bin Yarmo, M. A. 2007. Synthesis of WO<sub>3</sub> in Nanoscale With the Usage of Sucrose Ester Microemulsion and CTAB Micelle Solution. Materials Letters, 61: 2652-2657.
- 12. Zhanqi, G., Shaogui, Y., Na, T. and Cheng, S. 2007. Microwave Assisted Rapid and Complete Degradation of Atrazine using TiO<sub>2</sub> Nanotube Photocatalyst Suspensions. Journal of Hazardous Materials, 145: 424-430.
- 13. Lu, C.-H., Wu, W.-H. and Rohidas, B. K. 2008. Microemulsion-mediated Hydrothermal Synthesis of Photocatalytic TiO<sub>2</sub> Powders. Journal of Hazardous Materials, 154: 649-654.
- 14. Mishra, T., Hait, J., Aman, N., Gunjan, M., Mahato, B. and Jana, R. K. 2008. Surfactant Mediated Synthesis of Spherical Binary Oxides Photocatalytic With Enhanced Activity in Visible Light. Journal of Colloid and Interface Science, 327: 377-383.
- 15. Li, X., He, G., Xiao, G.,Liu, H. and Wang, M. 2009. Synthesis and morphology control of ZnO nanostructures in microemulsions. Journal of Colloid and Interface Science, 333: 465-473.
- Awitor, K. O., Rafqah, S., Géranton, G., Sibaud, Y., Larson, P. R., Bokalawela, R. S. P., Jernigen, J. D. and Johnson M. B. 2008. Photo-catalysis using titanium dioxide layers. Journal of Photochemistry and Photobiology A: Chemistry, 119: 250-254.
- 17. Lu, J., Bauermann, L. P., Gerstel, P., Heinrichs, U., Kopold, P., Bill, J. and Aldinger, F. 2009. Synthesis and characterization of TiO<sub>2</sub> nanopowders from peroxotitanium solutions. Materials Chemistry and Physics, 115: 142-146.

- Górska, P., Zaleska, A., Kowalska, E. Klimczuk, T., Sobczak, J. W., Skawarek, E., Janusz, W. and Hupka, J. 2008. TiO<sub>2</sub> Photoactivity in Vis and UV light: The Influence of Calcination Temperature and Surface Properties. Applied Catalyst B: environmental, 84: 440-447.
- 19. Deorsola, F. A. and Valluri, D. 2009. Study of the Parameters in the Synthesis of TiO<sub>2</sub> Nanospheres Through Reactive Microemulsion Precipitation. Powder Technology, 190: 304-309.
- 20. Janus, M., Tryba, B., Kusiak, E., Tsumura, T., Toyoda, M., Inagaki, M. and Morawski, A. W. 2008. TiO<sub>2</sub> nanoparticles with high photocatalytic activity under visible light. Catalysis Letters, 50: 177-183.
- 21. Lee, M. S., Park, S. S., Lee, G.-D., Ju, C.-S. and Hong S.-S. 2005. Synthesis of TiO<sub>2</sub> particles by reverse microemulsion method using nonionic surfactant with different hydrophilic and hydrophobic group and their photocatalytic activity. Catalysis Today, 101: 283-290.
- 22. Pu, Y., Fang, J., Peng, F., Li, B. & Huang, L. 2007. Microemulsion synthesis of nanosized SiO/TiO<sub>2</sub> particles and their photocatalytic activity. Chinese Journal of Catalysis, 28(3): 251-256.
- 23. Li, Z., Du, J., Zhang, J., Mu, T., Gao, Y., Han, B., Chen, J. and Chen, J. 2005. Synthesis of Single Crystal BaMoO<sub>4</sub> Nanofibers in CTAB Reverse Microemulsions. Materials Letters, 59: 64-68.

# Malaysian Journal of Analytical Sciences Vol 14 No 2 2010

|    |   | Page |
|----|---|------|
| 1. | HYDROLYSIS OF CHLORPYRIFOS IN AQUEOUS SOLUTIONS AT DIFFERENT TEMPERATURES AND pH (Hidrolisis Klorpirifos dalam Larutan Akueus pada Suhu dan pH Berbeza) Tay Joo Hui, Marinah Mohd Ariffin, Norhayati Mohd Tahir   | 50   |
| 2. | SPATIAL DISTRIBUTION OF <sup>210</sup> Pb ACTIVITY CONCENTRATIONS IN MARINE SURFACE SEDIMENTS WITHIN EAST COAST PENINSULAR MALAYSIA EXCLUSIVE ECONOMIC ZONE (EEZ) (Penyebaran <sup>210</sup> Pb Kepekatan Aktiviti di Dalam Sedimen Permukaan di Kawasan Zon Ekonomi Ekslusif Pantai Timur Semenanjung Malaysia) <i>Ahmad Sanadi Abu Bakar, Zaharudin Ahmad, Zaini Hamzah</i> | 56   |
| 3. | CARBOXYMETHYL CHITOSAN-Fe3O4 NANOPARTICLES: SYNTHESIS AND CHARACTERIZATION (Nanozarah Karboksimetil Kitosan-Fe3O4: Sintesis dan Pencirian) Nurul Hidayah Ahmad Safee, Md. Pauzi Abdullah, Mohamed Rozali Othman   | 63   |
| 4. | REMOVAL OF As(V) BY Ce(IV)-EXCHANGED ZEOLITE P USING COLUMN METHOD (Penyingkiran As(V) oleh Ce(IV)-Zeolit P Menggunakan Kaedah Turus)  Md Jelas Haron, Farha Abd Rahim, Mohd Zobir Hussein, Abdul Halim Abdullah, Anuar Kassim, S.M. Talebi   | 69   |
| 5. | ADSORPTION OF FORMULATED CHLORPYRIFOS ON SELECTED AGRICULTURAL SOILS OF TERENGGANU (Penjerapan Rumusan Klorpirifos ke atas Tanah Pertanian Terpilih di Terengganu) Tay Joo Hui, Marinah Mohd Ariffin, Norhayati Mohd Tahir  | 76   |
| 6. | CHLORPYRIFOS AND MALATHION RESIDUES IN SOILS OF A TERENGGANU GOLF COURSE: A CASE STUDY (Residu Klorpirifos dan Malathion Dalam Tanah di Padang Golf Terengganu: Satu Kajian Kes) Norhayati Mohd Tahir, Khaw Hock Soon, Marinah Mohd Ariffin, Suhaimi Suratman   | 82   |
| 7. | SYNTHESIS AND CHARACTERIZATION OF SEVERAL LAURYL CHITOSAN DERIVATIVES (Sintesis dan Pencirian Beberapa Terbitan Lauril Kitosan)  Nadhratun Naiim Mobarak, Md.Pauzi Abdullah   | 88   |
| 8. | EXTRACTION OF Eu (III) IN MONAZITE FROM SOILS CONTAINING 'AMANG' COLLECTED FROM KG GAJAH EX-MINING AREA (Ekstraksi Eu(III) Dalam Monazit Daripada Tanah Yang Mengandungi Amang Dari Kawasan Bekas Lombong Kg Gajah)  Zaini Hamzah, Nor Monica Ahmad, Ahmad Saat   | 100  |

# HYDROLYSIS OF CHLORPYRIFOS IN AQUEOUS SOLUTIONS AT DIFFERENT TEMPERATURES AND pH

(Hidrolisis Klorpirifos dalam Larutan Akueus pada Suhu dan pH Berbeza)

Tay Joo Hui<sup>1,2</sup>, Marinah Mohd Ariffin<sup>1</sup>, Norhayati Mohd Tahir<sup>1\*</sup>

<sup>1</sup>Environmental Research Group (ERG), Department of Chemical Sciences, Faculty of Science and Technology, Universiti Malaysia Terengganu (UMT), Mengabang Telipot, 21030 Kuala Terengganu, Terengganu, Malaysia.

<sup>2</sup>Faculty of Industrial Sciences and Technology (FIST), Universiti Malaysia Pahang (UMP), Lebuhraya Tun Razak, 26300 Gambang, Kuantan, Pahang Darul Makmur, Malaysia.

\*Corresponding author: hayati@umt.edu.my

#### Abstrak

Hidrolisis klorpirifos (O,O-diethyl-O-3,5,6-trichloro-2-pyridyl phosphorothionate) telah dikaji dalam media akues pada suhu dan keadaan pH yang berbeza. Pemalar kadar dan jangka hayat separa yang diperolehi menunjukkan bahawa klorpirifos lebih stabil dalam keadaan berasid. Kadar degradasi meningkat apabila nilai pH bertambah. Suhu juga mempengaruhi kadar hidrolisis. Hidrolisis klorpirifos dalam air mematuhi tindak balas tertib pertama. Jangka hayat separa klorpirifos dalam larutan akues adalah pendek (di antara 4.57 hingga 14.0 hari), dan ianya bergantung pada kepekatan asal klorpirifos dan jenis larutan akues. Kadar degradasi adalah perlahan dalam larutan 0.02M CaCl<sub>2</sub> dengan kepekatan asal klorpirifos yang tinggi. Perbandingan antara kadar hidrolisis dalam larutan air steril dan tidak steril tidak menunjukkan peranan biodegradasi yang ketara dalam air tidak disteril. Keputusan ini menunjukkan bahawa parameter pH sahaja tidak mencukupi untuk menjangkakan kadar hidrolisis klorpirifos.

**Katakunci:** Klorpirifos, hidrolisis, pestisid organofosforus

# Abstract

The hydrolysis of chlorpyrifos (O,O-diethyl-O-3,5,6-trichloro-2-pyridyl phosphorothionate) was investigated in buffered aqueous media at different temperature and pH conditions. Rate constants and half-life studies revealed that chlorpyrifos was relatively stable in acidic medium. The rate of degradation increased as the pH increased. Temperature showed a significant effect on the rate of hydrolysis. The hydrolysis of chlorpyrifos in water follows first-order kinetics. The half-life of chlorpyrifos in aqueous solutions was short (half-lives ranged from 4.57 to 14.0 days), depending on the initial concentration of chlorpyrifos and the type of the aqueous solutions. The rate of degradation was slower in the 0.02M CaCl<sub>2</sub> solution containing higher initial concentration of chlorpyrifos. Comparison between hydrolysis rate of chlorpyrifos in sterilized and non-sterilized water did not showed significant contribution of biodegradation component. These results indicate that pH alone cannot be used as a single parameter to predict hydrolysis of chlorpyrifos.

Keywords: Chlorpyrifos, hydrolysis, organophosphorus pesticide

# Introduction

Chlorpyrifos (O,O-diethyl-O-3,5,6-trichloro-2-pyridyl phosphorothionate) (Figure 1) is a broad-spectrum insecticide whose mode of activity is as a cholinesterase inhibitor. It is used to kill a wide variety of insects including cutworms, corn rootworms, cockroaches, grubs, flea beetles, flies, termites, fire ants, and lice by disrupting their nervous system. It is also used as a soil treatment (pre-plant and at planting), as a seed treatment and as a foliar spray, directed spray and dormant spray. Chlorpyrifos degradation is governed by both abiotic (e.g.: hydrolysis, photolysis) and biotic factors (e.g.: microbial degradation). After release in the aquatic compartment, degradation via hydrolysis is among the main transformation pathways for chlorpyrifos. Hydrolysis may occur at several reactive centres in the pesticide molecule, in the presence of OH or H<sub>2</sub>O acting as nucleophilic reagents [1].

# Tay Joo Hui et al: HYDROLYSIS OF CHLORPYRIFOS IN AQUEOUS SOLUTIONS AT DIFFERENT TEMPERATURES AND pH

The degradation pathway of chlorpyrifos in aquatic environments involves the breakdown of the thiophosphoric esters, forming 3,5,6-trichloropyridinol (TCP) and desethyl chlorpyrifos (DEC) as main metabolites.

The hydrolysis rate of chlorpyrifos in aquatic environments is influenced by environmental factors such as pH, temperature and other solution constituents. Reported hydrolysis half-lives (ranged from 18.9 to 120d) showed more rapid hydrolysis under alkaline conditions compared to neutral or acidic conditions [2]. The rate of hydrolysis was reported to increase an average of 3.5-fold and 5-fold for each 10°C rise in temperature by Meikle and Youngson in 1978 [3] and Noblet [4], respectively. The aqueous hydrolysis of chlorpyrifos may be catalyzed by dissolved copper ions [5] and free chlorine [3,6].

Surface water and groundwater quality may be affected by the widespread use of pesticides in the agricultural areas. As a widely used organophosphorus insecticide in Malaysia, there is a need to evaluate the fate of chlorpyrifos in the environment to which it may be applied. Most of the hydrolysis study of chlorpyrifos has been carried out in temperate zone, but there is still limited information on the fate and behaviour of chlorpyrifos in the tropical environment. The objective of this study was to investigate the hydrolysis of chlorpyrifos in aqueous media at different pH and temperatures.

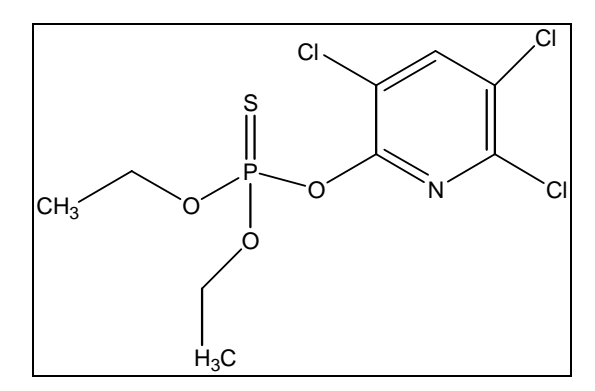


Figure 1: Structure of chlorpyrifos

# **Experimental**

Chlorpyrifos standard (>99.5% purity) were purchased from Sigma-Aldrich (Brand Riedel-de Haën). Stock solution was prepared by dissolving chlorpyrifos in acetonitrile. The effect of pH on the hydrolysis of chlorpyrifos was investigated using three triplicate sets of distilled water (50mL) fortified with 1.45mgL<sup>-1</sup> chlorpyrifos in tightly stoppered flasks. The pH of the samples was buffered at 4.0, 7.0 and 10.0. The initial concentration (C<sub>o</sub>) was measured immediately after sample preparation was completed. The samples were kept in constant temperature bath at 29±1°C. 5mL of samples were drawn, extracted three times with n-Hexane (10mL, 5mL and 5mL, respectively) and analyzed daily by using ThermoFinnigan GC fitted with AT<sup>TM</sup>-1 Capillary Column (0.25µm x 0.25mm x 30m Alltech) and a Nitrogen Phosphorus Detector (NPD). The column temperature was programmed from 125 to 230°C at rate of 30°C/min, held at 230°C for 6 min, the detector and injector temperatures were 300 and 200°C, respectively. The effect of temperature on hydrolysis of chlorpyrifos was also investigated using another set of samples (1.45mgL<sup>-1</sup> chlorpyrifos) buffered at pH 7.0 and incubated in thermostated water baths maintained at 20, 30 and 40±1°C. The concentrations of chlorpyrifos in the aqueous solution were then monitored daily as above. Hydrolysis of chlorpyrifos (initial concentration = 0.50, 1.00 and 1.80 mgL<sup>-1</sup>) in 0.02M CaCl<sub>2</sub> was also investigated at room temperature (29±1°C).

### **Results and discussion**

Chemical hydrolysis of chlorpyrifos at  $29\pm1^{\circ}$ C was investigated using buffered solutions at pH values 4, 7 and 10. All plots of the logarithm of the normalized concentration as a function of the reaction time (Figure 2) gives straight lines, indicating the reaction tends to be a pseudo-first-order reaction. The rate constants and half-lives (Table 1) indicate the relative fast degradation of chlorpyrifos in aqueous solution. The stability of chlorpyrifos decreased as the pH increased. The effect of temperature on rates of hydrolysis was also significant (Table 1, Figure 3). The half-life of chlorpyrifos in distilled water at pH 7.0 was 12.3 and 8.12 days at 16 and 40°C, respectively.

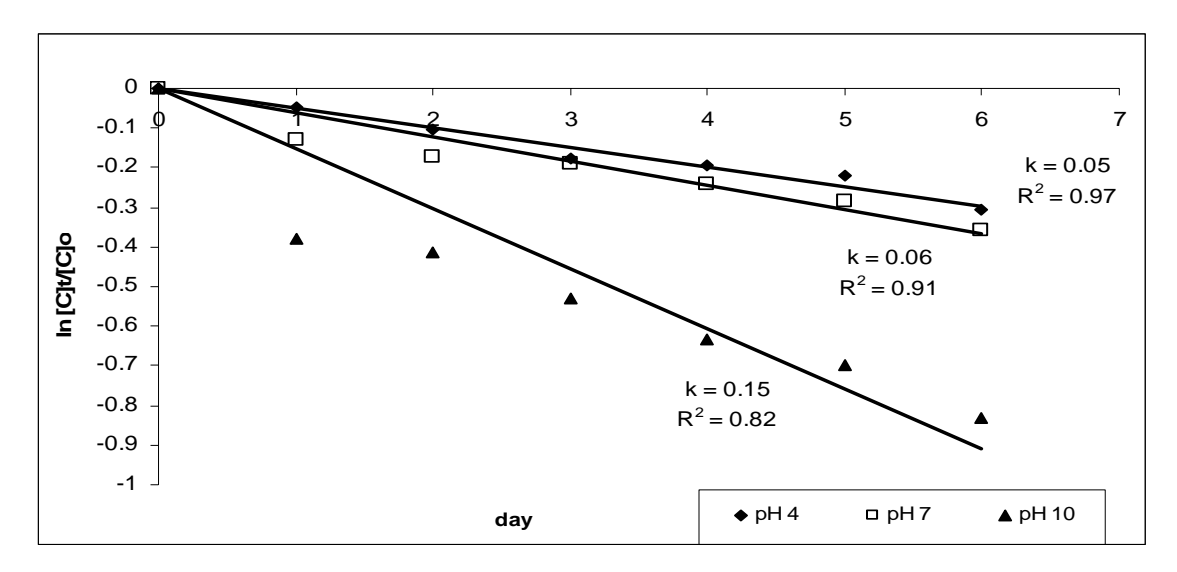


Figure 2: Hydrolysis kinetics of chlorpyrifos at various pH values at room temperature (29°C).

Table 1: Kinetic data for the hydrolysis of chlorpyrifos at various pH values and temperature.

|                                | рН   | Temperature (°C)  | k (d <sup>-1</sup> ) | t 1/2 (d) | $R^2$ |
|--------------------------------|--|-------------------|----------------------|-----------|-------|
|                                | Buffer pH 4  | 29 <u>+</u> 1     | 0.05                 | 14.0      | 0.97  |
|                                |  | 16 <u>+</u> 1     | 0.06                 | 12.3      | 0.92  |
| This study                     | Buffer pH 7  | 29 <u>+</u> 1     | 0.06                 | 11.3      | 0.91  |
| This study                     |  | 40 <u>+</u> 1     | 0.09                 | 8.12      | 0.92  |
|                                | Buffer pH 10   | 29 <u>+</u> 1     | 0.15                 | 4.57      | 0.82  |
|                                | Buffer pH 7 (RO water)   | 29 <u>+</u> 1     | 0.06                 | 11.9      | 0.94  |
| W [2]                          | Milli-Q water (Ci = $0.257 \mu \text{molL}^{-1}$ ) pH 6.50         | 23 <u>+</u> 2     | 0.01                 | 56.8      | -     |
| Wu [3]                         | Milli-Q water (Ci = $1.283 \mu \text{mol} \text{L}^{-1}$ ) pH 6.50 | 23 <u>+</u> 2     | 4.4x10 <sup>-3</sup> | 158       | -     |
| Noblet [4]                     | Buffer pH 8 (sterilized)   | 40                | 0.06                 | 11.2      | -     |
|                                | Buffer pH 4.7  | 25                | -                    | 63        | -     |
| Dow AgroSciences LLC [7]       | Buffer pH 6.9  | 25                | -                    | 35        | -     |
|                                | Buffer pH 8.1  | 25                | -                    | 23        | -     |
| Liu <i>et al</i> . [8]         | De-ionized water pH 5.72   | _                 | 0.02                 | 45.9      | -     |
| Deerasamee and<br>Tiensing [9] | De-ionized water pH 5.5  | Outdoor condition | -                    | 2.72      | -     |

-: not stated

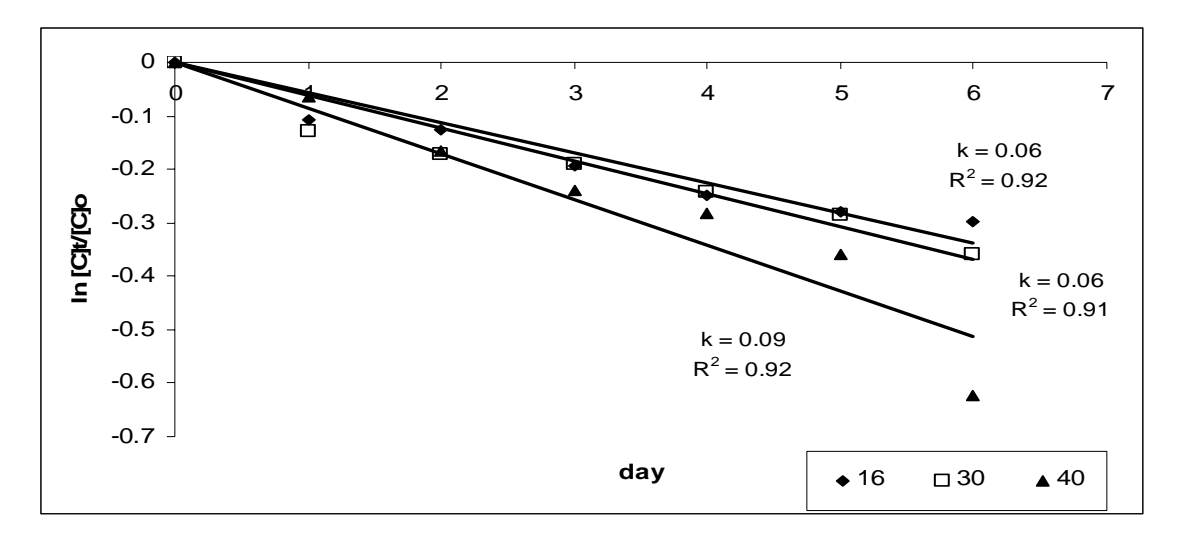


Figure 3: Hydrolysis of chlorpyrifos in pH 7 buffer at various temperatures.

For hydrolysis in 0.02M CaCl<sub>2</sub>, the results showed that degradation of chlorpyrifos still occurred very fast when the initial concentration of chlorpyrifos was low (0.5 mgL<sup>-1</sup>). However at higher initial concentration (1.8 and 1.0 mgL<sup>-1</sup>), the half-life for chlorpyrifos was 1.5-2 times longer (Table 2, Figure 4). Although the hydrolysis rates obtained in this study is relatively faster as higher concentration of CaCl<sub>2</sub> solution and higher experimental temperature had been chosen, but the trend is in agreement with previous study [3].

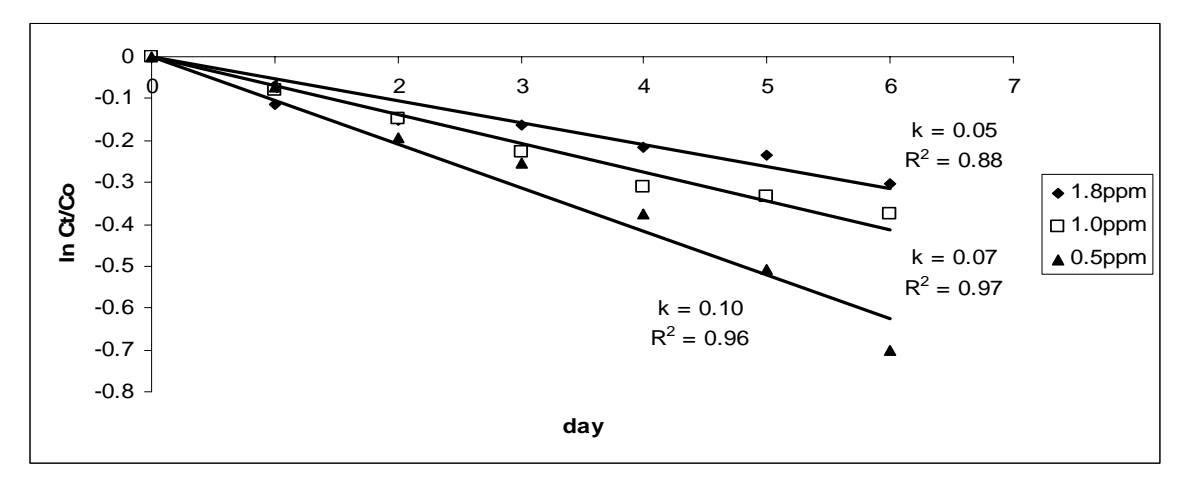


Figure 4: Hydrolysis of chlorpyrifos in 0.02M CaCl<sub>2</sub>.

|                       | This                   | study (0.02M C         | CaCl <sub>2)</sub>     | Wu (0.01   | M CaCl <sub>2</sub> )                                      |
|-----------------------|------------------------|------------------------|------------------------|--|--|
| Initial concentration | 1.80 mgL <sup>-1</sup> | 1.00 mgL <sup>-1</sup> | 0.50 mgL <sup>-1</sup> | $1.283 \mu \text{molL}^{-1} \approx 0.45 \text{ mgL}^{-1}$ | $0.257 \mu \text{molL}^{-1} \approx 0.09 \text{ mgL}^{-1}$ |
| Temperature (°C)      | 29 <u>+</u> 1          | 29 <u>+</u> 1          | 29 <u>+</u> 1          | 23 <u>+</u> 2  | 23 <u>+</u> 2  |
| k (d <sup>-1</sup> )  | 0.05                   | 0.07                   | 0.10                   | 0.01   | 0.01   |
| t <sub>1/2</sub> (d)  | 13.2                   | 10.1                   | 6.66                   | 60.3   | 52.9   |
| $R^2$                 | 0.88                   | 0.97                   | 0.96                   | -  | -  |

Table 2: Kinetic data for the hydrolysis of chlorpyrifos in 0.02M CaCl<sub>2</sub>.

-: not stated

The results obtained in this study showed faster hydrolysis rate for a comparable pH value and temperature condition compared to previous studies [3-4,7-8] (Table 1 and Table 2). In this study, only preliminary screening experiments were carried out to determine roughly the rates of hydrolysis at various pHs and temperatures, meanwhile majority of the reported data was derived from experiments that followed well-established hydrolysis test protocols which consist of a multi-level approach as described by Noblet [4]. As a comparison, hydrolysis test was performed with reverse osmosis water buffered at pH 7, however the half-life obtained was not significantly longer compared to non-sterile water (Table 1). On the other hand, a half-life of 2.72 days in deionized water (outdoor condition) has been observed in Thailand by Deerasamee and Tiensing [9], showing that the hydrolysis of chlorpyrifos is relatively faster in tropical environment. Besides, the chlorine, metals and other cations residue in distilled water may also responsible for the rapid hydrolysis of chlorpyrifos observed in this study [3,6]. Other experimental errors such as losses due to volatilization, adsorption onto glass surface [10] and pH changes might also resulted in higher hydrolysis rates.

# Conclusions

The hydrolysis of chlorpyrifos (O,O-diethyl-O-3,5,6-trichloro-2-pyridyl phosphorothionate) is greatly influenced by pH and temperature. Hydrolysis is slower in acidic condition and lower temperature. The hydrolysis of chlorpyrifos in different aqueous media follows first-order kinetics, with half-lives ranged from 4.57 to 14.0 days. Hydrolysis rate is slower in the 0.02M CaCl<sub>2</sub> solution containing higher initial concentration of chlorpyrifos. Comparison between sterilized and non-sterilized water suggested the contribution of biodegradation component. These results indicate that pH alone cannot be used as a single parameter to predict the hydrolysis of chlorpyrifos, other parameter such as temperature, metal content and water quality also showed significant effect on the hydrolysis rate.

# Acknowledgements

The financial support of the Research Management Centre of UMT through a research grant for postgraduate student is gratefully acknowledged.

# References

- 1. Zamy, C., Mazellier, P. & Legube, B. 2004. Analytical and kinetic study of the aqueous hydrolysis of four organophosphorus and two carbamate pesticides. Intern. J. Environ. Anal. Chem. Vol. 84, No.14-15; 1059-1068.
- 2. Racke, K.D. 1993. Environmental fate of chlorpyrifos. Reviews of Environmental Contamination and Toxicolovy, Vol 131. Springer-Verlag New York, Inc.
- 3. Wu, J. 2000. Interactions and transformations of chlorpyrifos in aqueous and colloidal systems. PhD dissertation. Iowa State University. Ames, Iowa. 126pp.
- 4. Noblet, J.A. 1997. Hydrolysis, sorption and supercritical fluid extraction of triazine and organophosphate pesticides. PhD dissertation. University of California, Los Angeles. 211pp.

# Tay Joo Hui et al: HYDROLYSIS OF CHLORPYRIFOS IN AQUEOUS SOLUTIONS AT DIFFERENT TEMPERATURES AND pH

- 5. Blanchet, P. & St-George, A. 1982. Kinetics of chemical degradation of organophosphorus pesticides: hydrolysis of chlorpyrifos and chlorpyrifos-methyl in the presence of copper(II). Pest. Sci. 13(1): 85-91.
- 6. Duirk, S.E. & Collette, T.W. 2006. Degradation of chlorpyrifos in aqueous chlorine solutions: Pathways, kinetics, and modeling. Environ. Sci. Technol. 40; 546-551.
- 7. Dow AgroSciences LLC. 2003. The Science Behind Chlorpyrifos: Physical/Chemical Properties. http://www.dowagro.com/chlorp/ap/science/prop.htm [accessed 26/11/07].
- 8. Liu, B., McConnell, L.L., & Torrents, A. 2001. Hydrolysis of chlorpyrifos in natural waters of the Chesapeake Bay. Chemosphere 44: 1315-1323.
- 9. Deerasamee, O. & Tiensing, T. 2007. Investigation of Organophosphorus Pesticide Degradation in Water Using Solid-phase Extraction followed by Gas Chromatography with Flame Photometric Detection. *Proceedings* in the 8<sup>th</sup>. National Graduate Research Conference on 7-8 Septempher 2007, Mahidol University, Salaya, Nakornpathom, Thailand.
- 10. Thomas, C. & Mansingh, A. 2002. Dissipation of Chlorpyrifos from Tap, River and Brackish Waters in Glass Aquaria. Environmental Technology, Vol 23, No.11: 1219-1227(9).

# SPATIAL DISTRIBUTION OF <sup>210</sup>Pb ACTIVITY CONCENTRATIONS IN MARINE SURFACE SEDIMENTS WITHIN EAST COAST PENINSULAR MALAYSIA EXCLUSIVE ECONOMIC ZONE (EEZ)

(Penyebaran <sup>210</sup>Pb Kepekatan Aktiviti di Dalam Sedimen Permukaan di Kawasan Zon Ekonomi Ekslusif Pantai Timur Semenanjung Malaysia)

Ahmad Sanadi Abu Bakar<sup>1</sup>, Zaharudin Ahmad<sup>1</sup>, Zaini Hamzah<sup>2</sup>

<sup>1</sup>Radiochemistry and Environment Group, Malaysian Nuclear Agency (Nuclear Malaysia), Bangi, 43000 Kajang, Selangor. <sup>2</sup>Faculty of Applied Sciences, Universiti Teknologi MARA (UiTM), 40450 Shah Alam, Selangor.

### Abstract

A sampling expedition into the East Coast Peninsula Malaysia Exclusive Economic Zone (EEZ) was carried in June 2008. Marine surface sediment samples were collected and the activity concentrations of <sup>210</sup>Pb have been determined. Its distribution was plotted and the findings show that the activity concentrations decline from north to south. On the other hand, the activity concentrations are increasing from west to east right to the edge of the EEZ. The <sup>210</sup>Pb activity concentrations were found to be in the range of 18.3 – 123.1 Bq/kg.

Keywords: Activity, lead, sediment, distribution, trend, EEZ

#### Abstrak

Ekspedisi persampelan ke kawasan Zon Ekonomi Ekslusif (EEZ) Pantai Timur Semenanjung Malaysia telah di buat pada bulan Jun 2008. Sedimen permukaan telah di ambil dan kepekatan aktiviti <sup>210</sup>Pb telah ditentukan. Taburannya telah di plotkan dan di dapati kepekatan aktiviti menurun dari utara ke selatan. Sebaliknya, kepekatan aktiviti telah meningkat dari barat ke timur sethingga kepenjuru EEZ. Kepekatan aktiviti <sup>210</sup>Pb di dapapti berada dalam julat 18.3 - 123.1 Bg/kg.

Kata kunci: Activiti, plumbum, sedimen, taburan, tren, EEZ

### Introduction

The East Coast Peninsular Malaysia Exclusive Economic Zone (EEZ) is an area between 1° 14.04' to 7° 48.92' N latitude and 102° 5.03' to 105° 48.77' E longitude. The area is approximately 1,150 km long and 417 km maximum width. The area is relatively shallow with maximum depth around 60 m to 70 m. Human activities in the area include fishing, tourism and oil exploration. The area is also a major shipping lane. These factors make the EEZ a good area to study the effects of human activities on the marine environment.

 $^{210}$ Po ( $T_{1/2}$  = 138 d, α) and  $^{210}$ Pb ( $T_{1/2}$  = 22.3 y, β) are both members of the  $^{238}$ U decay series.  $^{238}$ U is a naturally occurring radionuclide with a half-life of 4.5 billion years.  $^{210}$ Pb decays to  $^{210}$ Bi which then decays to  $^{210}$ Po. These radionuclides are recognised as tracers for natural processes and suitable in determining ocean processes [1]. For example,  $^{210}$ Pb has been extensively used to study environmental changes in different sedimentary environment and marine pollution [2].  $^{210}$ Pb is determined by counting its daughter  $^{210}$ Po which is α emitter. This method assumes secular equilibrium between  $^{210}$ Pb and  $^{210}$ Po. Radiochemical separation is employed to separate  $^{210}$ Po and the source is counted using alpha spectrometry counting system. The technique is widely used due to its lower detection limit, relatively inexpensive and requires small amounts of samples [3].

# **Materials and Methods**

The sampling of the EEZ area was done between 11 June 2008 and 26 June 2008. Sampling locations were arrayed in a grid of about 30 - 40 km between locations. This array allows good coverage of the EEZ with little blank spots. Seawater, core sediments and surface sediments were taken for various analyses. The surface sediment samples for <sup>210</sup>Pb analysis were taken using a Ponar grab sampler. Samples were put into a HDPE container and sealed for further analysis in the laboratory. Supporting data such as water depth, salinity, turbidity and temperature were also taken as supporting data.

The samples were then completely dried at 60°C in forced air oven. Grinding of the samples were done using Rocklabs and sieved using Fritsch Analysette 3 Pro siever. Two grams (2g) of sample were weighed and added

with ~6dpm <sup>209</sup>Po tracer. Acid leaching method using nitric acid (HNO<sub>3</sub>) and hydrochloric acid (HCl) was employed to digest the sample. Sample was filtered and the solution was heated until dryness. The solution was then dissolved in 0.5M hydrochloric acid and 0.1g ascorbic acid was added to the solution prior to deposition of <sup>210</sup>Po onto a silver disc for 24 hours.

The silver disc was counted for 24 hours using Ortec Octette+ Alpha Spectrometry System to determine <sup>210</sup>Po activity. The activity of <sup>210</sup>Pb was then calculated assuming secular equilibrium with <sup>210</sup>Po [4].

Table 1. Date of sampling and sampling location coordinates

| No. | Station | Date     | Latitude     | Longitude     | Water<br>Depth (m) |
|-----|---------|----------|--------------|---------------|--------------------|
| 1   | SF01    | 18.06.08 | 06° 13.99' N | 102° 19.00' E | 13                 |
| 2   | SF02    | 17.06.08 | 06° 50.04' N | 102° 47.04′ E | 47                 |
| 3   | SF03    | 17.06.08 | 07° 05.03' N | 103° 04.99' E | 50                 |
| 4   | SF04    | 17.06.08 | 07° 25.98' N | 103° 26.01' E | 61                 |
| 5   | SF05    | 16.06.08 | 06° 56.09' N | 103° 56.04′ E | 62                 |
| 6   | SF06    | 16.06.08 | 06° 42.14' N | 103° 35.17' E | 52                 |
| 7   | SF07    | 16.06.08 | 06° 10.00' N | 103° 01.00' E | 45                 |
| 8   | SF08    | 18.06.08 | 05° 52.10' N | 102° 51.92′ E | 34                 |
| 9   | SF09    | 20.06.08 | 05° 22.06' N | 102° 21.97' E | 47                 |
| 10  | SF10    | 14.06.08 | 05° 48.20' N | 103° 48.98′ E | 55                 |
| 11  | SF11    | 14.06.08 | 06° 06.16′ N | 104° 09.11′ E | 72                 |
| 12  | SF12    | 14.06.08 | 06° 32.01' N | 104° 22.11′ E | 59                 |
| 13  | SF13    | 13.06.08 | 06° 16.98' N | 105° 16.99' E | 55                 |
| 14  | SF14    | 13.06.08 | 05° 57.15' N | 104° 58.13′ E | 56                 |
| 15  | SF15    | 12.06.08 | 05° 29.08' N | 104° 29.02' E | 61                 |
| 16  | SF16    | 12.06.08 | 05° 18.50' N | 104° 12.60′ E | 60                 |
| 17  | SF17    | 20.06.08 | 04° 54.12' N | 103° 42.98' E | 54                 |
| 18  | SF18    | 11.06.08 | 04° 28.14' N | 103° 49.98' E | 40                 |
| 19  | SF19    | 22.06.08 | 03° 37.07' N | 103° 41.08' E | 23                 |
| 20  | SF20    | 22.06.08 | 03° 55.10' N | 104° 00.05′ E | 50                 |
| 21  | SF21    | 23.06.08 | 04° 22.16′ N | 104° 22.07' E | 65                 |
| 22  | SF22    | 23.06.08 | 04° 44.19' N | 104° 38.44′ E | 66                 |
| 23  | SF23    | 12.06.08 | 05° 08.10' N | 105° 12.90' E | 67                 |
| 24  | SF24    | 23.06.08 | 03° 32.08' N | 104° 36.00′ E | 62                 |
| 25  | SF25    | 24.06.08 | 03° 09.14' N | 104° 09.04′ E | 41                 |
| 26  | SF26    | 26.06.08 | 02° 56.13' N | 103° 49.97' E | 20                 |
| 27  | SF27    | 24.06.08 | 02° 16.94' N | 104° 16.97′ E | 30                 |
| 28  | SF28    | 24.06.08 | 02° 39.18' N | 104° 38.91′ E | 58                 |
| 29  | SF29    | 25.06.08 | 02° 00.55' N | 104° 41.97′ E | 46                 |
| 30  | SF30    | 25.06.08 | 01° 48.04' N | 104° 15.03' E | 14                 |

Quality assurance was complied by using reference material IAEA-368 Marine Sediment. The reference material was processed in the same batch as the samples and the activity concentration of <sup>210</sup>Pb was compared to the certified value.

# **Results and Discussion**

The activity concentration of <sup>210</sup>Pb in surface sediments in the sampling area is shown in Table 2.

Table 2. Activity concentration of <sup>210</sup>Pb in surface sediments other physical data

|          |                           | m .              | G 11 1/           |           |
|----------|---------------------------|------------------|-------------------|-----------|
| Location | <sup>210</sup> Pb (Bq/kg) | Temperature (°C) | Salinity<br>(psu) | Turbidity |
| SF01     | $123.1 \pm 0.2$           | 30.38            | 33.34             | 5.267     |
| SF02     | $24.4 \pm 0.1$            | 27.33            | 34.49             | 4.450     |
| SF03     | $28.7 \pm 0.1$            | 27.30            | 34.43             | 4.300     |
| SF04     | $46.1 \pm 0.1$            | 27.16            | 34.48             | 4.050     |
| SF05     | $64.4 \pm 0.1$            | 26.90            | 34.43             | 10.753    |
| SF06     | $48.3 \pm 0.1$            | 26.80            | 34.52             | 4.150     |
| SF07     | $31.4 \pm 0.1$            | 27.04            | 34.47             | 3.450     |
| SF08     | $52.4 \pm 0.3$            | 26.92            | 34.42             | 3.300     |
| SF09     | $57.0 \pm 0.1$            | 26.45            | 34.40             | 4.250     |
| SF10     | $43.6 \pm 0.1$            | 27.38            | 34.27             | 3.300     |
| SF11     | $49.3 \pm 0.1$            | 27.31            | 34.17             | 3.200     |
| SF12     | $88.1 \pm 0.1$            | 27.65            | 34.19             | 3.767     |
| SF13     | $122.5 \pm 0.2$           | 29.32            | 33.88             | 4.367     |
| SF14     | $99.0 \pm 0.1$            | 28.87            | 34.03             | 3.833     |
| SF15     | $63.4 \pm 0.1$            | 27.77            | 34.14             | 3.950     |
| SF16     | $34.1 \pm 0.1$            | 27.10            | 34.13             | 3.600     |
| SF17     | $45.3 \pm 0.2$            | 26.54            | 34.43             | 3.650     |
| SF18     | $43.0\pm0.2$              | 26.52            | 34.16             | 3.250     |
| SF19     | $18.3 \pm 0.1$            | 29.44            | 34.02             | 2.700     |
| SF20     | $44.7 \pm 0.2$            | 26.56            | 34.37             | 3.100     |
| SF21     | $39.0 \pm 0.1$            | 25.57            | 34.49             | 3.633     |
| SF22     | $53.2 \pm 0.1$            | 25.54            | 34.47             | 3.250     |
| SF23     | $69.1 \pm 0.1$            | 26.66            | 34.21             | 3.800     |
| SF24     | $45.3 \pm 0.2$            | 25.41            | 34.56             | 3.380     |
| SF25     | $42.7 \pm 0.1$            | 26.16            | 34.50             | 3.750     |
| SF26     | $35.0 \pm 0.1$            | 28.16            | 34.18             | 3.050     |
| SF27     | $49.7 \pm 0.7$            | 29.12            | 34.06             | 3.050     |
| SF28     | $60.4 \pm 0.1$            | 25.55            | 34.63             | 3.500     |
| SF29     | $49.6 \pm 0.1$            | 27.86            | 34.22             | 3.450     |
| SF30     | $60.4 \pm 0.1$            | 29.49            | 33.78             | 15.267    |

# **Spatial Distribution**

The spatial distribution was plotted using ArcGIS and the distribution is shown in Figure 1.

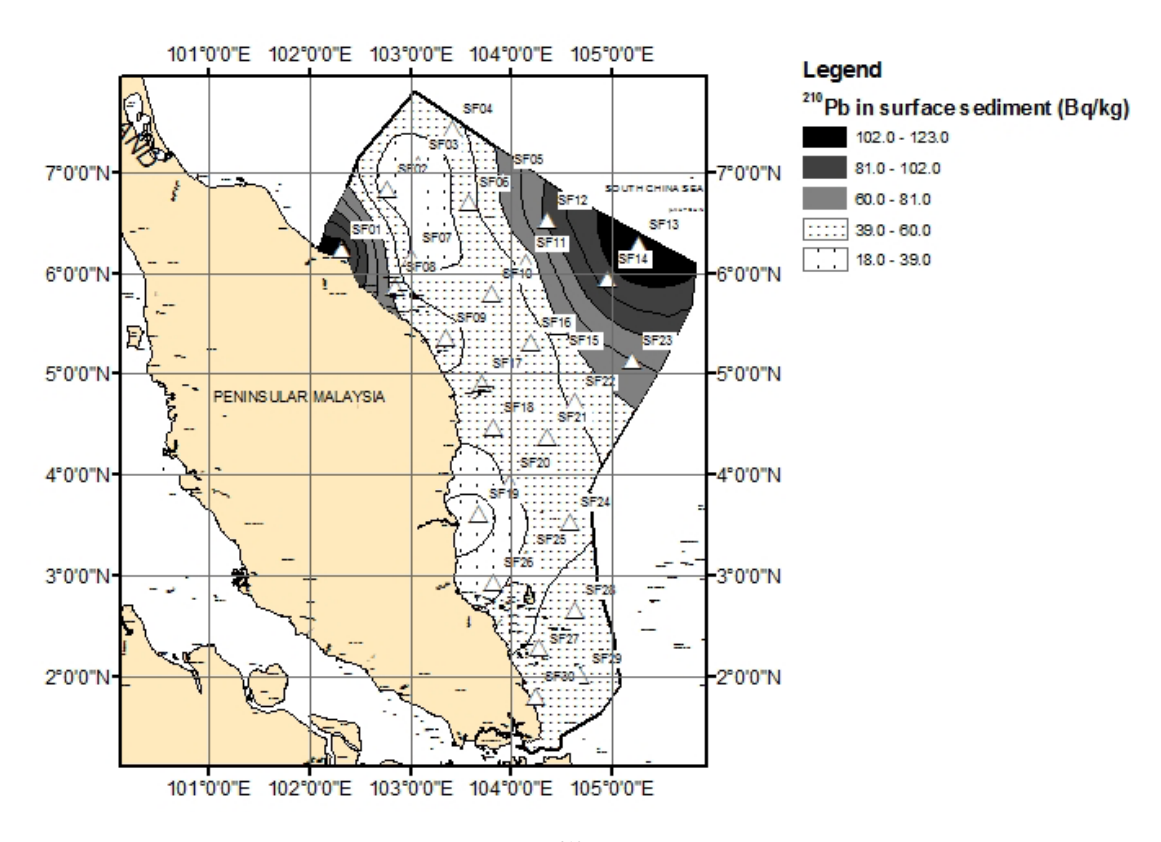


Figure 1: Spatial distribution of <sup>210</sup>Pb in surface marine sediments

The activity concentrations of  $^{210}\text{Pb}$  in surface marine sediments show a slightly declining trend from north to south. This trend is similar to those observed in the previous study in 2003 [5]. This is especially true to sampling sites in the coastal area. The highest activity concentration is found at station SF01 (123.1  $\pm$  0.2 Bq/kg). This is due to input from terrestrial source as the station is very close to the river Sungai Kelantan. The lowest activity was found to be in station SF19 (18.3  $\pm$  0.1 Bq/kg). This station is close to Pekan coastal area which is about 25 km from the mouth of Sungai Pahang. The low activity concentration observed was rather surprising given that previous study at the mouth Sungai Pahang showed much higher activity concentration [5]. This might be due to minimal sediment transport from Sungai Pahang to the station site, which means little fresh sediment being introduced to the area.

The activity concentration from west to east, which is from coastal area towards open seas initially showed a declining trend. This is expected as less input of  $^{210}\text{Pb}$  from terrestrial sources as it further away from land, and thus less  $^{210}\text{Pb}$  activity concentration in surface sediments. However, from about 140 km from shore onwards (stations SF12, SF15, SF23, SF14 and SF13) the  $^{210}\text{Pb}$  activity concentration show an increasing trend. The furthest station is SF13 which is 261 km from land. Yet this station showed the second highest activity concentration of all the stations (122.5  $\pm$  0.2 Bq/kg). This level of activity concentration is similar to those in SF01. Terrestrial input from natural process cannot explain such high level of activity concentration. It could be that such high activity concentration is lithogenic to that area.  $^{226}\text{Ra}$  activity concentration needs to be determined to calculate the ratio between  $^{210}\text{Pb}$  and  $^{226}\text{Ra}$ . The ratio between  $^{210}\text{Pb}$  and  $^{226}\text{Ra}$  can help in determining whether the  $^{210}\text{Pb}$  activity concentration is of lithogenic or anthropogenic origin [1]. The activity

concentration of <sup>210</sup>Pb observed could also be caused by human activities such as oil exploration. Human activities would also cause elevated heavy metal contents in the area. Therefore further analysis need to be carried out to determine the cause of this high <sup>210</sup>Pb activity concentration.

# Correlation with physical data

A Pearson correlation of <sup>210</sup>Pb and the physical data as presented in Table 2 was done using SPSS. No significant correlation was found between the parameters. This means <sup>210</sup>Pb activity concentration found was not affected by physical parameters as tabulated in Table 2.

Table 3: Correlation (R) value between <sup>210</sup>Pb and various physical parameters

|                   | Temperature | Salinity | OBS   | Depth |
|-------------------|-------------|----------|-------|-------|
| <sup>210</sup> Pb | 0.037       | 0.498    | 0.033 | 0.134 |

# Comparison to other studies

Table 4: <sup>210</sup>Pb activity concentration in surface marine sediments at various locations

| Area<br>(Sampling Date)             | Min <sup>210</sup> Pb<br>(Bq/kg) | Max <sup>210</sup> Pb<br>(Bq/kg) | Reference  |
|-------------------------------------|----------------------------------|----------------------------------|------------|
| South China Sea (2008)              | 18.3                             | 123.1                            | This Study |
| South China Sea (2003)              | 35.3                             | 144.2                            | [5]        |
| Straits of Malacca (2004)           | 7.3                              | 136.0                            | [6]        |
| Sabah & Sarawak<br>Waters<br>(2004) | 13.5                             | 220.2                            | [7]        |
| Kuala Selangor                      | 7.6                              | 43.6                             | [8]        |
| Kapar                               | 0.1                              | 36.0                             | [9]        |

In comparison, the current study does not show any significant differences of <sup>210</sup>Pb activity concentration against the previous study carried out at same area. This shows that there is no major change in natural processes and human activities between 2003 and 2008 in the area that could affects the marine environment.

Compared to Straits of Malacca, the results obtained in this study is slightly lower. This could be due to fact that the South China Sea being less an enclosed system compared to Straits of Malacca [10]. This would lead to more sediment movement in South China Sea compared to Straits of Malacca. There are also more rivers and more human activities in the West Coast Peninsula Malaysia that could lead to more terrestrial input into Straits of Malacca.

The <sup>210</sup>Pb activity concentration is Sabah & Sarawak waters are significantly higher compared to this study. This could be due to the various rivers in Sabah and Sarawak that contribute to terrestrial input into the sea.

# **Ouality Control of Data**

The reference material IAEA-368 Marine Sediment was used as a quality control and quality assuarance to evaluate the quality of data obtained. The reference material was processed and analysed alongside the samples. The result obtained then compared with the certified value (IAEA-368  $23.2 \pm 1.8$  Bq/kg).

Table 5: Results of IAEA-368 analysis

| Reference Sample | Measured Value | U-Score |  |  |
|------------------|----------------|---------|--|--|
| 1                | $23.0 \pm 1.0$ | 0.09    |  |  |
| 2                | $22.9 \pm 1.0$ | 0.13    |  |  |
| 3                | $23.2 \pm 1.0$ | 0.02    |  |  |
| 4                | $23.8 \pm 1.1$ | 0.27    |  |  |
| 5                | $25.6 \pm 1.1$ | 1.09    |  |  |
| 6                | $23.2 \pm 1.0$ | 0.02    |  |  |
| 7                | $24.1 \pm 1.1$ | 0.44    |  |  |
| 8                | $22.9 \pm 1.0$ | 0.13    |  |  |
| 9                | $27.6 \pm 1.2$ | 1.96    |  |  |
| 10               | $24.0 \pm 1.1$ | 0.36    |  |  |
| 11               | $26.8 \pm 1.2$ | 1.63    |  |  |
| 12               | $25.6 \pm 1.1$ | 1.12    |  |  |
| 13               | $24.2 \pm 1.1$ | 0.46    |  |  |
| 14               | $22.4 \pm 1.0$ | 0.37    |  |  |
| 15               | $23.6 \pm 1.1$ | 0.20    |  |  |
| 16               | $24.1 \pm 1.1$ | 0.42    |  |  |
| 17               | $25.8 \pm 1.2$ | 1.21    |  |  |
| 18               | $26.1 \pm 1.2$ | 1.33    |  |  |
| 19               | $27.2 \pm 1.2$ | 1.80    |  |  |

The majority of U-score calculated are below 1.64. This means that the <sup>210</sup>Pb measured in the reference material does not differ significantly with the certified value.

Table 6: Physical Meaning of the U-Score Values

| Condition       | Probability            | Status   |  |  |
|-----------------|------------------------|--|--|--|
| u < 1.64        | Greater than 0.1       | The reported value does not differ significantly from the certified value                |  |  |
| 1.95 > u > 1.64 | Between 0.1 and 0.05   | The reported value probably does not differ significantly from the certified value       |  |  |
| 2.58 > u > 1.95 | Between 0.05 and 0.01  | It is not clear whether the reported value differ significantly from the certified value |  |  |
| 3.29 > u > 2.58 | Between 0.01 and 0.001 | The reported value is probably significantly different from the certified value          |  |  |
| u > 3.29        | Less than 0.001        | The reported value significantly differs from the certified value                        |  |  |

# Conclusion

The activity concentration of <sup>210</sup>Pb in surface sea sediments in coastal area of the East Coast Peninsula Malaysia Exclusive Economic Zone (EEZ) are generally similar to those observed in previous studies. The high activity concentration of <sup>210</sup>Pb in the most eastern part of the EEZ require further analysis of <sup>226</sup>Ra and heavy metals to determine whether the high <sup>210</sup>Pb activity concentration is the result of natural processes or due to human activities

# Acknowledments

Funding from MOSTI, under ScienceFund 04-03-01-SF0020 is gratefully acknowledged. The authors would also like to thank the captain and crews of KL PAUS for their assistance during sampling expedition and staff members of the Radiochemistry and Environment Group for their support and technical assistance throughout this study.

### References

- Theng, T. L., Zaharudin, A., & Che Abd Rahim, M. (2003). Estimation of sedimentation rates using <sup>210</sup>Pb and <sup>210</sup>Po at the coastal water of Sabah, Malaysia. *Journal of Radioanalytical and Nuclear Chemistry*, 256 (1) 115-120
- 2. Tanner, A., Pan, M., Mao, Y., & Yu, K. (2000). γ-Ray Spectometric and α-Counting Method Comparison for the Determination of Pb-210 in Estuarine Sediments. *J. Applied Spectroscopy*, **54**, 1143-1146.
- 3. Zaborska, A., Carroll, J., Papucci, C., & Pempkowiak, J. (2007). Intercomparison of alpha and gamma spectrometry techniques used in Pb-210 geochronology. *J. Environment Radioactivity*, **93**, 38-50.
- 4. Edgington, N. D., & John, R. A. (1975). *Determination of the activity of Lead -210 in Sediments and soils*. Ann Arbor, MI: NOAA.
- 5. Zaharudin, A., Zal U'yun, W. M., Yii, M. W., Norfaizal, M., Jalal, S., Kamarozaman, I. (February 2006). Laporan Projek Pembangunan Data Asas Keradioaktifan Marin di Malaysia, Jilid I: Perairan Pantai Timur Semenanjung Malaysia, MINT/L/2006/8. Bangi: Malaysian Nuclear Agency.
- 6. Zaharudin, A., Zal U'yun, W. M., Yii, M. W., Norfaizal, M., Jalal, S., Kamarozaman, I., et al. (December 2006). Laporan Projek Pembangunan Data Asas Keradioaktifan Marin di Malaysia, Jilid II: Perairan Pantai Barat Semenanjung Malaysia, MINT/L/2006/48. Bangi, Kajang: Malaysian Nuclear Agency.
- 7. Zaharudin, A., Yii, M. W., Norfaizal, M., Jalal, S., Kamarozaman, I., & Sanadi, A. (2007). *Laporan Projek Pembangunan Data Asas Keradioaktifan Marin di Malaysia, Jilid III: Perairan Sabah dan Sarawak, NUKLEARMALAYSIA/L/2007/6.* Bangi, Kajang: Malaysian Nuclear Agency.
- Choong, C. C., Zaharudin, A., & Che Abd Rahim, M. (2006). Vertical Profile of <sup>210</sup>Pb in the sediment core
  of Kuala Selangor, Malaysia. *Proceedings International Conference SKAM19 & MyCat2*, (pp. 3A1 (1-7)).
  Malacca.
- 9. Che Abd Rahim, M., Zaharudin, A., & Tan, Y. S. (2006). <sup>210</sup>Po dan <sup>210</sup>Pb di persekitaran marin Stesen Janakuasa Elektrik Kapar, Selangor. *Malaysian Journal of Analytical Sciences*, **10** (1), 47-54.
- 10. Ibrahim, Z., & Tanagi, T. (2003). The influence of the Andaman Sea and South China Sea on water mass in the Straits of Malacca. *Proceedings of the first joint seminar on coastal oceanography, 14-16 December 2003.* Chiang Mai, Thailand.

# CARBOXYMETHYL CHITOSAN-Fe<sub>3</sub>O<sub>4</sub> NANOPARTICLES: SYNTHESIS AND CHARACTERIZATION

(Nanozarah Karboksimetil Kitosan-Fe<sub>3</sub>O<sub>4</sub>: Sintesis dan Pencirian)

Nurul Hidayah Ahmad Safee, Md. Pauzi Abdullah\*, Mohamed Rozali Othman

School of Chemistry Science and Food Technology, Faculty of Science and Technology, Universiti Kebangsaan Malaysia, 43600 Bangi, Selangor Darul Ehsan

\*Corresponding author: mpauzi@ukm.my

#### Abstract

In this study, carboxymethyl chitosan bound  $Fe_3O_4$  magnetic nanoparticles (CC- $Fe_3O_4$  NPs) was synthesized by the binding of carboxymethyl chitosan (CC) onto the surface of  $Fe_3O_4$  magnetic nanoparticles, which was prepared by coprecipitating method. The CC- $Fe_3O_4$  nanoparticles was characterized by transmission electron microscopy (TEM), X-ray diffractometer (XRD), vibrating sample magnetometer (VSM), Nucleus Magnetic Resonans (NMR) and Fourier Transform Infra Red (FTIR). TEM studies confirmed that the  $Fe_3O_4$  and CC- $Fe_3O_4$  particles have a particle size ranges from 9.73-12.30 nm and 9.70-12.50 nm, respectively. The magnetic properties of the  $Fe_3O_4$  particles were verified using VSM. Their saturation magnetization, remnant magnetization and coercivity were 61.0 emu/g, 2.70 emu/g and 38.20 G, respectively. FTIR studies showed the appearance of peaks at 1629 cm<sup>-1</sup> and 1397 cm<sup>-1</sup> which were characteristic of COOM (M = metal ions) bands, indicating the formation of the iron carboxylate.

Keywords: Carboxymethyl chitosan, magnetic nanoparticles

#### Abstrak

Dalam kajian ini, karboksimetil kitosan berikat dengan nanozarah magnetik Fe<sub>3</sub>O<sub>4</sub> telah disintesis dengan pengikatan karboksimetil kitosan (CC) terhadap permukaan nanozarah magnetik Fe<sub>3</sub>O<sub>4</sub>, yang disediakan melalui kaedah kopemendakan. Nanozarah CC-Fe<sub>3</sub>O<sub>4</sub> kemudian dicirikan dengan Transmisi Elektron Mikroskopi (TEM), Pembelauan Sinar-X (XRD), Magnetometer Getaran Sampel (VSM), Resonans Magnetik Nukleus (RMN) dan Infra Merah Transformasi Fourier (FTIR). Analisis TEM menunjukkan Fe<sub>3</sub>O<sub>4</sub> dan CC-Fe<sub>3</sub>O<sub>4</sub> mempunyai julat saiz zarah di antara 9.73-12.30 nm dan 9.70-12.50 nm. Sifat kemagnetan Fe<sub>3</sub>O<sub>4</sub> menunjukkan nilai pemagnetan tepu, pemagnetan sisa dan daya paksa sebanyak 61.0 emu/g, 2.70 emu/g dan 38.20 G. Analisis FTIR pula menunjukkan kehadiran puncak pada 1629 cm<sup>-1</sup> dan 1397 cm<sup>-1</sup> yang merupakan ciri jalur COOM (M = ion logam), menunjukkan pembentukan ferum karboksilat.

Kata Kunci: Karboksimetil kitosan, nanozarah magneti.

# Introduction

Chitosan,  $poly(1\rightarrow 4)$ -2-amino-2-deoxy-D-glucan, is a polyaminosaccharide with many significant biological (biodegradable, biocompatible, bioactive) and chemical properties (polycationic, hydrogel, reactive groups such as OH and  $NH_2$ ). All of these properties make chitosan and its derivatives widely used in many biomedical fields [1]. Carboxymethylated chitosan has received more and more attention because of its good water solubility, and it is more convenient to be applied in medicine because it fits the neutral environment of the human body [2,3]. Nano-sized carriers could not be separated easily from the contaminated waste streams by filtration or centrifugation. Magnetic nano-carriers can be easily manipulated by an external magnetic field and hence should be suitable as the support of adsorbents [4]. In this study, carboxymethyl chitosan bound  $Fe_3O_4$  magnetic nanoparticles was synthesized by the binding of carboxymethyl chitosan (CMC) onto the surface of  $Fe_3O_4$  magnetic nanoparticles. These  $Fe_3O_4$  and carboxymethyl chitosan- $Fe_3O_4$  nanoparticles were characterized by TEM, XRD, VSM, FTIR and  $^1H$ -NMR, respectively.

### **Experimental**

# Chemicals

Chitosan used as raw material was supplied by ChitoChem Company. It is of medical grade and has degree of acetylation of more than 90%. FeCl $_3$  and FeSO $_4.7H_2O$  were purchased from BDH Chemicals Ltd . Carbodiimide were supplied by Aldrich. Monochloroacetic acids were purchased from MERCK-Schuchardt. All chemicals were of analytical grade reagents and used as supplied.

# Preparation of Fe<sub>3</sub>O<sub>4</sub> Nanoparticles

Nanosized magnetite was prepared by controlled chemical co-precipitation of Fe<sup>2+</sup> and Fe<sup>3+</sup> (1:2 ratio) from ammoniacal medium at 80° C under nitrogen atmosphere. In a typical experiment, 0.02 mol of ferrous sulphate and 0.04 mol of FeCl<sub>3</sub> were dissolved in 200 ml of de-ionized and de-oxygenated water. The resulting solution was vigorously stirred and heated to 80° C under nitrogen atmosphere. Subsequently about 12 ml of 25% ammonia solution was injected into the flask and stirring was continued for another 20 minutes to allow the growth of the nanoparticles. The solution was then cooled to room temperature and the resulting particles were centrifuged followed by repeated washing with distilled water. The pH of the suspension was brought to neutral by the addition of dilute HCl, and the particles were rewashed with distilled water [5].

# Preparation of Carboxymethyl Chitosan

Carboxymethyl chitosan was prepared by method as suggested by Sun et.al [6]. Chitosan (10g), sodium hydroxide (10g), isopropanol (50 ml) and water (50 ml) were added into a flask to swell and alkalize at 50°C for 1 h. The monochloroacetic acid (15 g) was dissolved in isopropanol (20 ml), added into the reaction mixture drop-wise for 30 min and reacted for 4 h at the same temperature, then stopped by adding 70% ethyl alcohol (250 ml). The solid was filtered and rinsed in 70-90% ethyl alcohol, and vacuum dried at room temperature. The product was Na salt CC (Na-CC). Na-CC (1 g) was suspended in 80% ethyl alcohol aqueous solution (100 ml), hydrochloric acid (10 ml, 37%) was added and stirred for 30 min. The solid was filtered and rinsed in 70-90% ethyl alcohol to neutral, vacuum dried. The products were the H-form CC (H-CC).

# Preparation of Fe<sub>3</sub>O<sub>4</sub> Bound Carboxymethyl Chitosan

The binding of carboxymethyl chitosan was conducted following Chang and Chen [7] method but the difference is carboxymethylchitosan used was N,O-carboxymethylchitosan. Approximately, 1 g of  $Fe_3O_4$  nanoparticles was added to 20 ml of buffer A (0.003 M phosphate, pH 6, 0.1 M NaCl). Then, the reaction mixture was shaked for 60 min after adding 5 ml of carbodiimide solution (0.025 gml<sup>-1</sup> in buffer A). Finally, 25 ml of carboxymethyl chitosan solution (50 mg ml<sup>-1</sup> in buffer A) was added and the reaction mixture was shaked for 2 hours. The chitosan-bound  $Fe_3O_4$  nanoparticles were recovered from the reaction mixture by magnetic bar. The magnetic particles were then washed with water and ethanol.

# Characterization of Fe<sub>3</sub>O<sub>4</sub> Bound Carboxymethyl Chitosan

The determination on functional group of chitosan, carboxymethyl chitosan (CC),  $Fe_3O_4$  and  $CC-Fe_3O_4$  nanoparticles were performed using FTIR. Carboxymethyl chitosan (CC) was analysed by NMR 400 MHz to determine position of carboxymethylation took placed. The morphology of the magnetic particles was characterized by TEM. TEM analysis was carried out by placing a drop of the ethanol-dispersed magnetic nanoparticle aqueous solution onto a copper grid and allowing the solution to evaporate in air at room temperature. Before sample withdrawal, it was sonicated for 30 min to obtain a better dispersion. XRD measurement was carried out on an X-ray diffractometer ( $Cu K\alpha$ ,  $\lambda$ =0.1542 nm). Magnetic properties of  $Fe_3O_4$  and  $CC-Fe_3O_4$  nanoparticles was measured by using Vibrating Sample Magnetometer.

# **Result and Discussion**

# **FTIR Analysis**

The IR results of chitosan, were summarised in Table 1, shows the basic characteristic of chitosan at : 3430 cm<sup>-1</sup> (O-H stretch) and N-H stretch, 2924 cm<sup>-1</sup> (C-H stretch), 1642 cm<sup>-1</sup> (C=O stretch), 1148 cm<sup>-1</sup> (bridge-O-stretch), and 1079 cm<sup>-1</sup> (C-O stretch) [8,9]. Sodium carboxymethyl chitosan (Na-CC) shows peak at 1603 cm<sup>-1</sup> indicating of appearence of –COONa group. H-form carboxymethyl chitosan (H-CC) shows appearence of peak at 1726 cm<sup>-1</sup> representing the carboxylate C=O asymmetric stretching. The signal at 1394 cm<sup>-1</sup> could be assigned to the symmetric stretching vibration of carboxylate C=O [10]. The peak of 577 cm<sup>-1</sup> is typical characteristic of Fe–O group in Fe<sub>3</sub>O<sub>4</sub>. Appearance of the peaks at 1629 cm<sup>-1</sup> and 1397 cm<sup>-1</sup> shows that binding of carboxymethyl chitosan with Fe<sub>3</sub>O<sub>4</sub> has occured. These two peaks were characteristic of COOM (M= metal ion) band, indicated that carboxyl groups in CC reacted with the surface hydroxide groups of Fe<sub>3</sub>O<sub>4</sub> particles, resulting in the formation of the iron carboxylate [11].

# <sup>1</sup>H-NMR Analysis

In the <sup>1</sup>H NMR spectrum of carboxymethyl chitosan as shown in Fig.1, the signal at 2.00 ppm can be attributed to the hydrogen atoms of the methyl from acetamide groups. The signal at 3.15 ppm corresponds to the

hydrogen bonded to the carbon atom C2 of the glucosamine ring, while the signals between 3.72 and 3.91 ppm correspond to the hydrogen atoms bonded to carbons C3, C4, C5 and C6 of the glucopyranose. The signal between 4.26-4.55 ppm corresponds to the protons of 3- and 6-substituted carboxymethyl (–O–CH<sub>2</sub>–COOD) of carboxymethyl chitosan [12]. The hydrogen bonding to carbon C1 gives the signals at 4.8 ppm. Moreover, the resonance signal of the protons from N-CH<sub>2</sub>-COOD groups could be found at 3.29 ppm. This result indicated that the amino groups were partly carboxymethylated along with hydroxyl groups [13].

| Type of Vibration Type (cm <sup>-1</sup> ) of derivatives | O-H, N-H<br>stretch | C-H<br>stretch | C=O<br>asym<br>stretch | C=O sym<br>stretch | C-O/C-N<br>stretch   | Fe-O<br>stretch |
|---|---------------------|----------------|------------------------|--------------------|----------------------|-----------------|
| Chitosan  | 3430                | 2924           | 1642                   | -                  | 1148                 | -               |
| Na-CC   | 3430                | 2912           | 1603                   | -                  | 1079<br>1148<br>1078 | -               |
| H-CC  | 3435                | 2929           | 1726                   | 1394               | 1151                 | -               |
| CC-Fe <sub>3</sub> O <sub>4</sub>                         | 3411                | 2929           | 1629                   | 1397               | 1070<br>1024         | 577             |

Table 1: FTIR results of Chitosan, Na-CC, H-CCand CC-Fe<sub>3</sub>O<sub>4</sub>

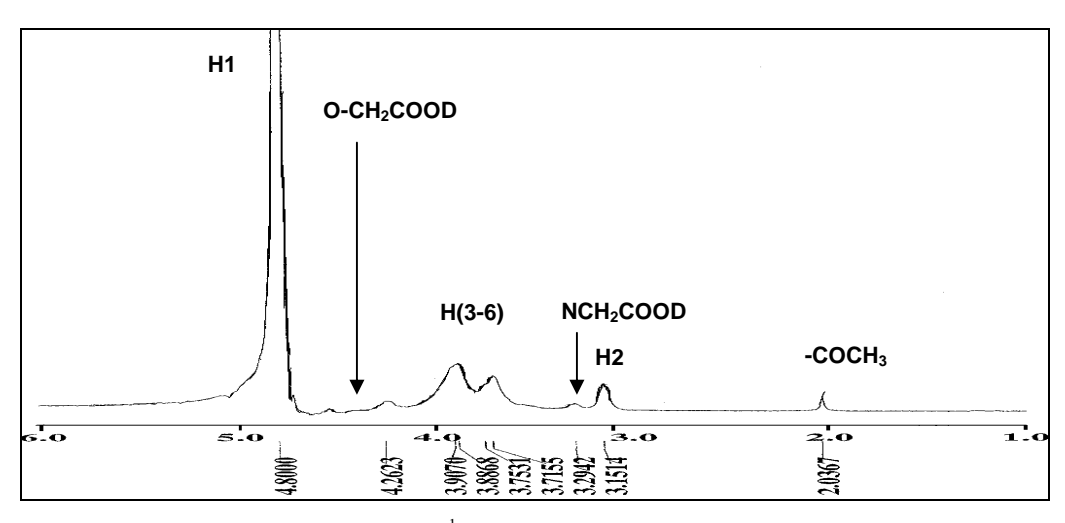


Figure 1: <sup>1</sup>H-NMR Spectrum of H-CC in D<sub>2</sub>O.

# **TEM Analysis**

It can be seen from TEM micrograph (Fig.2) that the resulting magnetic  $Fe_3O_4$  nanoparticles were almost spherical or ellipsoidal. It was clear that the  $Fe_3O_4$  nanoparticles had a diameter range of 9.73-12.30 nm. After binding with carboxymethyl chitosan Fig.2b the particles remained discrete with a diameter range of about 9.70-12.50 nm. This revealed that the coating process did not significantly result in the agglomeration and the change in size of the particles. This could be attributed to the reaction occurring only on the particle surface [7]. However, there is a little aggregation in the  $Fe_3O_4$  nanoparticles coated with carboxymethyl chitosan.

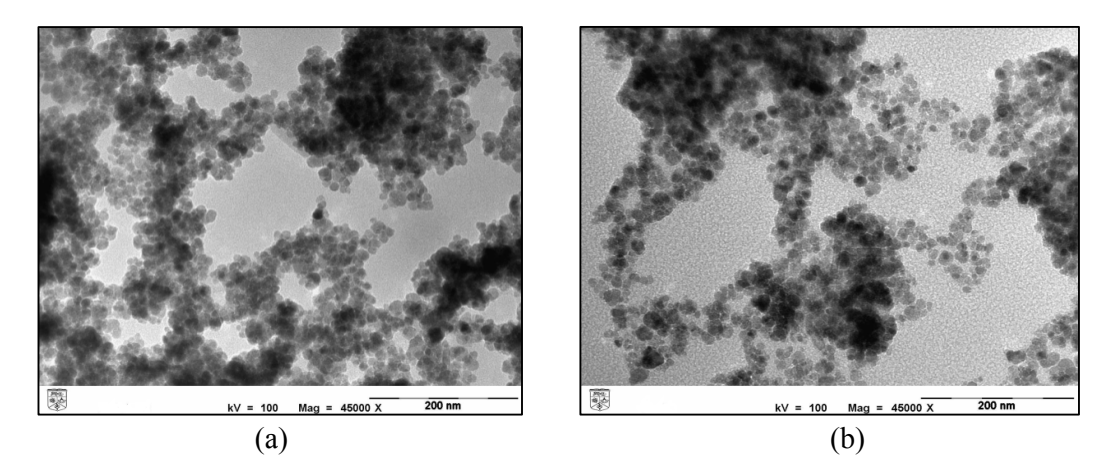


Figure 2: TEM micrographs of the Fe<sub>3</sub>O<sub>4</sub>(a) and CC-Fe<sub>3</sub>O<sub>4</sub>(b) nanoparticles

# **Magnetic Properties**

The magnetic hysteresis loop at room temperature of the  $Fe_3O_4$  and CC- $Fe_3O_4$  nanoparticles is shown in Figure 3.  $Fe_3O_4$  has saturated magnetization (Ms) about 61.00 emu/g. The remanence (Mr) and coercivity (Hc) of  $Fe_3O_4$  nanoparticles were 2.70 emu/g and 38.20 G, respectively. The saturated magnetization (Ms) of CC- $Fe_3O_4$  was 43.69 emu/g (51.4 emu/g)[14] when considering the carboxymethyl chitosan content. The significantly decrease Ms value of CC- $Fe_3O_4$  is attributed due to the existence of a magnetically inactive surface layer and some diamagnetic contribution from the carboxymethyl chitosan [15,16].

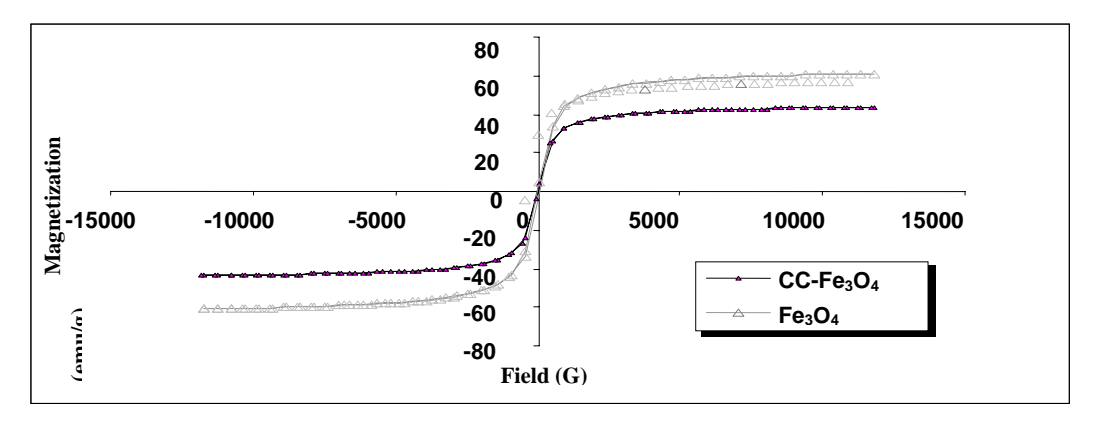


Figure 3: Magnetic hysteresis loop of  $\ Fe_3O_4$  and  $CC\text{-}Fe_3O_4$  nanoparticles.

# **XRD Pattern**

The presence of crystalline structure of  $Fe_3O_4$  and CC-  $Fe_3O_4$  nanoparticles was comfirmed by XRD. The diffractogram is shown in Fig. 4. There are six diffraction peaks for  $Fe_3O_4$  and CC-  $Fe_3O_4$ : (2 2 0), (3 1 1), (4 0 0), (4 2 2), (5 1 1) and (4 4 0), which is the standard pattern for crystalline magnetite with spinel structure

[17]. These peaks reveal that the resulting nanoparticles were pure Fe<sub>3</sub>O<sub>4</sub> with a spinel structure. The binding process of CC and Fe<sub>3</sub>O<sub>4</sub> did not result in the phase change of Fe<sub>3</sub>O<sub>4</sub>.

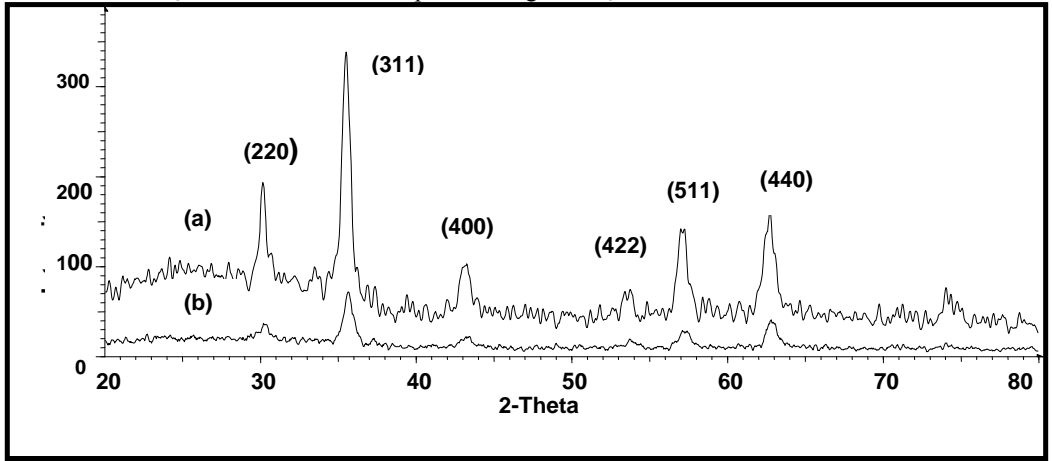


Figure 4: XRD pattern of Fe<sub>3</sub>O<sub>4</sub>(a) and CC- Fe<sub>3</sub>O<sub>4</sub>(b) nanoparticles.

### Conclusion

H-CC bound  $Fe_3O_4$  nanoparticles with diameter 9.70-12.5 nm was prepared in this study by the binding of carboxymethylated chitosan on  $Fe_3O_4$  nanoparticles via carbodiimide activation. The saturated magnetization of CC- $Fe_3O_4$  nanoparticles could reach 43.69 emu/g. This magnetic chitosan nanoparticles have a good potential to remove metal ions such as iron and manganese which are the problem of drinking water in Malaysia.

### Acknowledgement

The authors wish to thank PPSKTM, UKM for the instrumentations and the Ministry of Sciences, Technology and Innovation (MOSTI) for supported this work by its grant 02-01-02 SF0125.

### References

- Ding, P., Huang, K.L. & Li, G.Y. Kinetics of adsorption of Zn(II) ion on chitosan derivatives. 2006. Int. J. Biol. Macromol. 39: 222–227.
- Zhang L., Guo J. & Peng X., Jin Y.Preparation and release behavior of carboxymethylated chitosan/alginate microspheres encapsulating bovine serum albumin. 2004. J. Appl. Polym. Sci. 92: 878-882.
- 3. Chen X.G. & Park H.J., Chemical characteristics of *O*-carboxymethyl chitosans related to the preparation conditions. 2003. *Carbohyd. Polym.* 53: 355-359.
- 4. Chang, Y.C., Chang, S.W. & Chen, D.H. 2006. Magnetic chitosan nanoparticles: Studies on chitosan binding and adsorption of Co(II) ions. *Reactive & Functional Polymer* 66: 335-341.
- 5. Mohapatra, S., Pal, D., Ghosh, S. K. & Pramanik, P. 2007. Design of Superparamagnetic Iron Oxide Nanoparticle for Purification of Recombinant Proteins. Journal of Nanoscience and Nanotechnology 7: 1–7.
- Sun, G., Chen, X., Li, Y., Zheng, B., Gong, Z., Sun, J., Chen, H., Li, J. & Lin, W. 2008. Preparation of Holeoyl-carboxymethyl-chitosan and the function as a coagulation agent for residual oil in aqueous system. Front. Mater. Sci. China. 2(1): 105–112.
- Chang, Y.C. & Chen, D.H. 2005. Preparation and adsorption properties of monodisperse chitosan-bound Fe<sub>3</sub>O<sub>4</sub> magnetic nanoparticles for removal of Cu(II) ions. *Journal of Colloid and Interface Science* 283: 446–451.
- 8. Brugnerotto, J., Lizardi, J., Goycoolea, F.M., Arguelles-Monal, W., Desbrieres, J. and Rinaudo, M. 2001.An infrared investigation in relation with chitin and chitosan characterization. *Polymer* 42: 3569–3580
- 9. Shigemasa, Y., Matsuura, H., Sashiwa, H. and Saimoto, H. 1996. Evaluation of different absorbance ratios from infrared spectroscopy for analyzing the degree of deacetylation in chitin. *International Journal of Biological Macromolecules* 18: 237–242.

# Nurul Hidayah Ahmad Safee et al: CARBOXYMETHYL CHITOSAN-Fe<sub>3</sub>O<sub>4</sub> NANOPARTICLES: SYNTHESIS AND CHARACTERIZATION

- 10. El-Sherbiny, I.M.2009. Synthesis, characterization and metal uptake capacity of a newcarboxymethyl chitosan derivative. *European Polymer Journal* 45: 199–210.
- 11. Xu, X.Q., Shen, H., Xu, J. R. and Li,X.J.2004. Aqueous-based magnetite magnetic fluids stabilized by surface small micelles of oleolysarcosine. *Applied Surface Science* 221(1-4): 430-436.
- 12. Ragnhild, J., Hjerde, N., Varum, K.M., Grasdalen, H., Tokura, S. and Smidsrod, O. 1997. Chemical composition of *O*-(carboxymethyl)-chitins in relation to lysozyme degradation rates. *Carbohydrate Polymers* 34:131–139.
- 13. de Abreu, F.R. & Campana-Filho S.P. Characteristics and properties of carboxymethylchitosan. Carbohydrate Polymers 75: 214–221.
- 14. Zhu, A., Yuan, L., & Liao, T. 2008. Suspension of Fe<sub>3</sub>O<sub>4</sub> nanoparticles stabilized by chitosan and *o*-carboxymethylchitosan. International Journal of Pharmaceutics 350: 361–368.
- Morales, M.P., Veintemillas-Verdaguer, S., Montero, M.I., Serna, C.J., Roig, A., Casas, L.I., Martínez, B. & Sandiumenge, F. 1999. Surface and internal spin canting in γ-Fe2O3 nanoparticles. Chemistry of Materials 11(11): 3058-3064.
- 16. Iglesias O. & Labarta A. 2001. Finite-Size and surface effects in maghemite nanoparticles: Monte Carlo simulations. Phys. Rev. B 63, 184416-1/184416-11.
- 17. Ma, Z.Y., Guan, Y.P., Liu, H.Z., 2005. Synthesis and characterization of micronsized monodisperse superparamagnetic polymer particles with amino groups. *J. Polym. Sci. A: Polym. Chem.* 43: 3433–3439.

# REMOVAL OF As(V) BY Ce(IV)-EXCHANGED ZEOLITE P USING COLUMN METHOD

(Penyingkiran As(V) oleh Ce(IV)-Zeolit P Menggunakan Kaedah Turus)

Md Jelas Haron\*<sup>1</sup>, Farha Abd Rahim<sup>1</sup>, Mohd Zobir Hussein<sup>1</sup>, Abdul Halim Abdullah<sup>1</sup>, Anuar Kassim<sup>1</sup>, S.M. Talebi<sup>2</sup>

<sup>1</sup>Chemistry Department, Universiti Putra Malaysia, 43400 Serdang, Selangor, Malaysia <sup>2</sup>Department of Chemistry and Environmental Science, University of Isfahan, 81744 Isfahan, Iran

\*Corresponding author: mdjelas@science.upm.edu.my

#### Abstract

Zeolite P was modified by ion exchange with Ce(IV) cation (Ce4ZP) and its performance for removal of As(V) anion using column method is described. The removal of As(V) was strongly depending on the bed depth, influent flow rate and initial As(V) concentration. The increase in bed depth enable more water can be treated, but with a slight reduction in adsorption capacity. At lower flow rate, the quantity of treated water and adsorption capacity were found to increase. At higher influent concentrations, better adsorption capacity was observed. The theoretical service times evaluated from bed depth service time (BDST) model for different flow rates and influent As(V) concentrations shows good correlation with the experimental data.

**Keywords**: Arsenate, BDST model, Ce(IV)-zeolite P, column, adsorption

#### **Abstrak**

Zeolite P telah diubahsuai secara penukaran ion dengan kation cerium (IV) (Ce4ZP) dan kebolehannya untuk penyingkiran anion As(V) menggunakan kaedah turus dilaporkan. Penyingkiran As(V) bergantung kepada ketinggian turus, kadar aliran masuk dan kepekatan awal As(V). Penambahan ketinggian turus menghasikan lebih banyak air yang dapat dirawat tetapi ia merendahkan sidikit muatan jerapan. Pada kadar aliran masuk yang rendah, kuantiti air yang dirawat dan muatan jerapan meningkat. Sample air dengan kepekatan arsenik lebih tinggi menghasilkan muatan jerapan yang lebih tinggi. Jangka masa operasi turus yang dikira dari model BDST hampir sama dengan jangka masa operasi yang didapati secara eksperimen.

Kata kunci: Arsenat, model BDST, Ce(IV)-zeolit P, turus, jerapan

# Introduction

Arsenic is harmful to man and living organisms and a suspected carcinogen [1]. It enters the environment through anthropogenic activities such as petroleum refineries, fossil fuel power plants and non-ferrous smelting as well as through natural weathering of arsenic rock. Arsenic is also used in many industries such as in wood treatment that use the largest amount of arsenic compounds, lead shot, storage batteries, semiconductors, pesticides and fertilizers [2]. The arsenic levels in many international standards for drinking water and industrial waste effluent have been lowered to 0.01 mg L<sup>-1</sup> and 0.05 mg L<sup>-1</sup>, respectively [3-4]. Conventional precipitation methods for arsenic removals using iron and aluminum salts have not been successful to meet these drinking and effluent standards for arsenic due to the solubility of the resultant products. On the other hand, adsorption appears to be one of the promising methods for removal of arsenic from water [5]. Among these processes, the removal of As(V) using metal oxides such as antimony and manganese [6], iron hydroxide [7] and iron coated catalysts [8] have been studied.

Zeolites are crystalline, hydrated aluminosilicate minerals containing exchangeable alkaline and alkaline earth metal cations, in particular, sodium, potassium, magnesium and calcium as well as water molecules in their structural frameworks. The compounds are based on three dimensional networks of AlO<sub>4</sub> and SiO<sub>4</sub> tetrahedra linked to each other by sharing all the oxygen atoms [9]. Since zeolites have a permanent negative charge on their surface, they have no affinity for anions. Recent studies have shown that modification of zeolites with certain cations resulted in sorbents with a strong affinity for many anions [10]. Cationic-surfactant-modified zeolites have been shown to remove arsenate from aqueous solutions [11]. Since the presence of the arsenate anion in water covers a wide pH range, the removal of As(V) by zeolites could be enhanced after loading them with various metal cations such as aluminium [12] and iron [13]. Cerium hydroxide has been

known to adsorb As(V) effectively from aqueous solution. Recently hydrous cerium oxide was shown to possess a high anion exchange capacity for As(V) [14]. Furthermore cerium doped iron oxide adsorbed As(V) at a higher capacity than alumina [15]. Our previous study showed that Ce(IV)-exchanged Zeolite P could sorb As(V) at higher capacity than several cerium- and zeolite-based adsorbents using batch method [16].

This paper describes the use of Ce(IV)-exchanged Zeolite P (Ce(IV)ZP) to sorb As(V) from aqueous solution using column method. Parameters investigated were effect of bed depth, flow rate and also initial influent concentration. The evaluation of column performance and analysis of breakthrough curves were done by the Bed Depth ServiceTtime (BDST) model [17]. The BDST approach was used for prediction of breakthrough time and exhaust time of column bed under different flow rate and influent concentration. All experiments for column method were performed at room temperature (25±2 °C).

#### **Experimental**

Zeolite P prepared from rice husk silica was donated by the Ibnu Sina Institute, University Technology Malaysia. Ce(IV)-loaded Zeolite P (Ce4ZP) was prepared by stirring of Zeolite P (5.0 g) in 45 cm³ of 0.1 mol L¹ ceric ammonium nitrate (Merck) in distilled water at 90 °C for 24 h. The Zeolite was separated from the solution by vacuum filtration rinsed with distilled water and oven dried at 60 °C for 24 h. The concentration of Ce(IV) in the supernatant was determined using ICP-AES model Perkin-Elmer Plasma 1000. The loading capacity of Ce(IV) in Zeolite P was found to be 170 mg g¹ [16]. A stock solution of As(V), 1000 mg/L, was prepared by dissolving NaH<sub>2</sub>AsO<sub>4</sub>.7H<sub>2</sub>O (Sigma) in distilled water. Test As(V) sample solutions were prepared by dilution of the stock solution.

The Ce4ZP adsorbent was packed inside borosilicate glass columns (Omnifit USA) with internal diameter of 10 mm and length of 100 mm equipped with teflon frit. The experiments were conducted in the up flow mode. The As(V) spiked water was pumped through the packed bed of Ce4ZP with a double reciprocating piston pump (model Pharmacia P 50). The effect of process parameters such as bed height, inlet flow rate, initial As(V) concentration were studied. The effluent samples were collected in a glass test tubes at definite interval using a fraction collector (model Pharmacia GradiFrac) and analyzed for As concentration using ICP-AES (model Perkin Elmer 1000). The As(V) spiked water was allowed to pass through Ce4ZP bed in up flow mode at a flow rate of 0.5 mL/min. The bed depths of 1.0, 1.5 and 2.0 cm and initial As(V) concentration of 25 mg/L were selected for experimental evaluation of column parameters. The effect of flow rate on As(V) removal was studied at 0.5 and 1 mL/min for a fixed bed depth of 1.0 cm and As(V) concentration of 25 mg/L. The performance of Ce4ZP at a bed depth of 1.0 cm was also evaluated at a higher As(V) concentration of 50 mg/L at 0.5 mL/min.

#### **Results and Discussion**

#### **Effect of Column Bed Height**

The breakthrough curves which is the plots  $C/C_0$  as a function of lapse time of water treated for an initial As(V) concentration of 25 mg/L for three different bed depths of 1.0, 1.5 and 2.0 cm at a flow rate of 0.5 mL/min are shown in Fig. 1. For the low bed depth, the breakthrough curve is steeper showing faster saturation of the bed. The point on the breakthrough curve at which arsenic concentration reaches its maximum allowable value for wastewater of 0.05 mg/L (corresponding to  $C/C_0 = 0.002$  or 0.2% of the influent concentration) was taken as 'breakthrough point' and the value of  $C/C_0 = 90\%$  was taken as 'exhaustion point'. The time corresponding to breakthrough and exhaustion points with respective volumes of water treated are shown in Table 1. The data showed that the increase in bed depth increased the volume of treated water at breakthrough and exhaustion points. This could be due to the availability of more adsorbent binding sites with the increase of bed depth [18]. However reduction in adsorption capacity of As(V) was observed with increased bed heights which could be due more active sites of the adsorbent may be remained inaccessible for adsorption of As(V) ions [19].

#### Effect of initial As(III) concentration

The performance of Ce4ZP column for influent As(V) concentrations of 25 and 50 mg/L for the bed depth of 1.0 cm at 0.5 mL/min are shown in Fig. 2 and the breakthrough and the exhaustion data are shown in Table 1. The breakthrough time and time of exhaustion for 50 mg/L As(V) concentration obtained were 120 and 220 min, respectively which are lower compared the values of 180 and 360 min for corresponding concentration of 25 mg/L. The quantities of treated water at breakthrough were also reduced to 60 mL for 50 mg/L concentration, compared to 90 ml for 25 mg/L As(V) concentration. However the column adsorption capacities obtained was higher for higher concentrations. A decrease in breakthrough as well as time of exhaustion at higher initial

concentration may be due to the rapid exhaustion of the adsorption sites since a higher concentration gradient caused a faster transport of ions as a result of increase in diffusion coefficient [20].

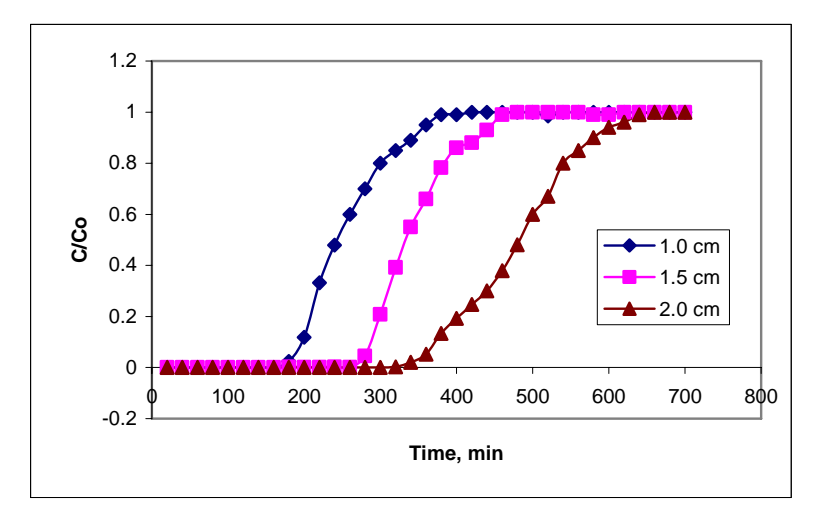


Fig. 1 Breakthrough curves of As(V) adsorption on Ce4ZP for different bed depths (initial As(V) conc. = 25 mg/L, flow rate = 0.5 mL/min).

| Table 1. | The volumes water | treated at different be | d depths, initial As( | V) concentrations and flow rates |
|----------|-------------------|-------------------------|-----------------------|----------------------------------|
|----------|-------------------|-------------------------|-----------------------|----------------------------------|

| Bed<br>depth<br>(cm) | Initial<br>concentrat<br>ion<br>mg/L | Flow<br>rate<br>ml/min | Break-<br>through<br>time (min) | Time of exhaustio n (min) | Volume of<br>water treated<br>at<br>breakthrough | Volume of<br>water treated<br>before<br>exhaust (ml) | Adsorptio<br>n capacity<br>(mg/g) |
|----------------------|--------------------------------------|------------------------|---------------------------------|---------------------------|--|--|-----------------------------------|
|                      |                                      |                        |                                 |                           | (ml)   |  |                                   |
| 1.0                  | 25                                   | 0.5                    | 180                             | 360                       | 90   | 180  | 6.8                               |
| 1.5                  | 25                                   | 0.5                    | 260                             | 440                       | 130  | 220  | 6.4                               |
| 2.0                  | 25                                   | 0.5                    | 380                             | 560                       | 190  | 280  | 5.9                               |
| 1.0                  | 50                                   | 0.5                    | 120                             | 220                       | 60   | 110  | 8.1                               |
| 1.0                  | 25                                   | 1.0                    | 80                              | 260                       | 40   | 130  | 4.3                               |

## Effect of flow rate

The effect of flow rate was investigated at 0.5 and 1.0 mL/min for an influent As(V) concentration of 25 mg/L, bed depth of 1.0 cm and column diameter of 1 cm. The breakthrough curves for different flow rates are shown in Fig. 3. The quantity of water treated at breakthrough point and exhaust point are shown in Table 1. There is a reduction in the adsorption capacity of Ce4ZP with increase in flow rate. This may be due to relatively low contact time between the adsorbate and adsorbent there by reducing the diffusion of As(V) ions into pores of Ce4ZP [21]. Also, at higher flow rates, the movement of adsorption zone along the bed is faster which in turn reducing the time for adsorption of As(V) ions on adsorbent bed.

## Bed depth service time model (BDST)

According to Hutchins only three column tests are necessary to collect data required for column design using BDST model. The bed depth (x) and service time (t) can be express as [17]:

$$t = ax + b \tag{1}$$

where

$$a = \text{slope} = \frac{N_0}{C_0 V} \tag{2}$$

$$b = \text{intercept} = \frac{1}{KC_0} \ln \left( \frac{C_0}{C_B} - 1 \right)$$
 (3)

where  $C_0$  = initial solute concentration (mg/L);  $C_B$  desired solute concentration at breakthrough (mg/L);  $K_B$  adsorption rate constant (L/mg min);  $K_B$  adsorption capacity (mg solute/L sorbent);  $K_B$  = bed depth of sorbent (cm);  $K_B$  = linear flow velocity of feed to bed (cm/min); and  $K_B$  = service time of column under above conditions (min).

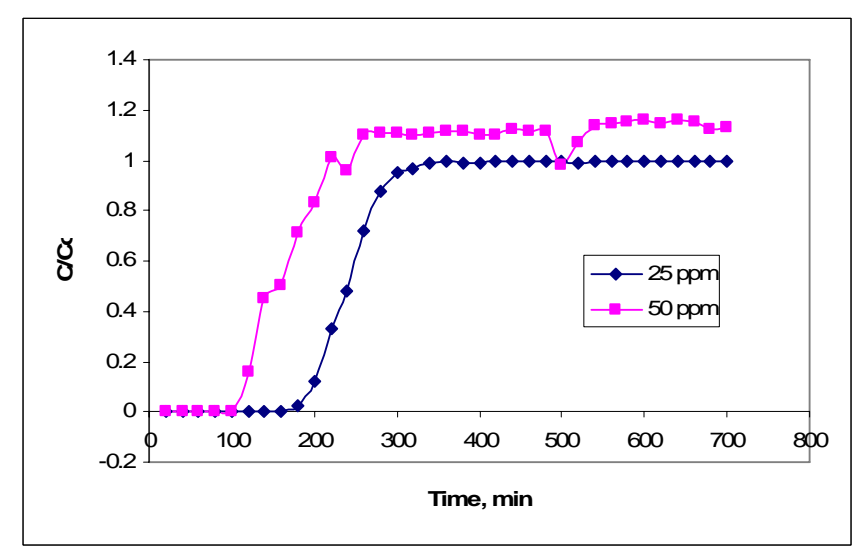


Fig. 2 Effect of initial concentrations on the breakthrough curves for As(V) adsorption on Ce4ZP. Bed depth = 1.0 cm and flow rate = 0.5 mL/min.

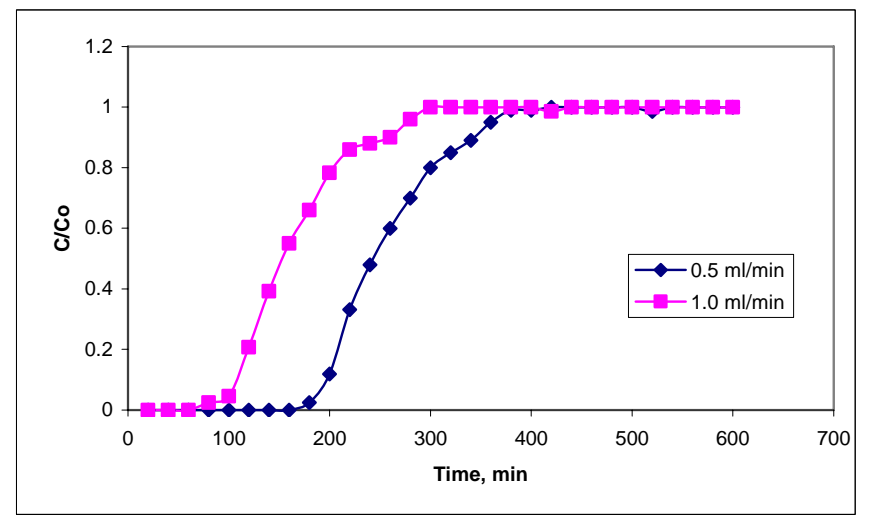


Fig. 3 Effect of flow rates on the breakthrough curve of As(V) adsorption on Ce4ZP. Bed depth = 1.0 cm and initial As(V) conc. = 10 mg/L.

From breakthrough times corresponding to  $C/C_0 = 0.002$  (0.2% saturation) and the exhaust times corresponding to  $C/C_0 = 0.9$  (90% saturation) for bed depth of 1.0, 1.5 and 2 cm, a plots service time versus bed depth for 0.2% breakthrough and 90% saturation of Ce4ZP bed were made and given in Fig. 4. The equations of these lines are:

$$t = 200x + 153.33$$
 (90% saturation) (4)

$$t = 200x - 26.667$$
 (0.2% saturation) (5)

Since those lines were parallel the equations can be used to predict the service time at breakthrough and at exhaustion for different flow rates and initial influent concentrations for practical used as discussed below [17].

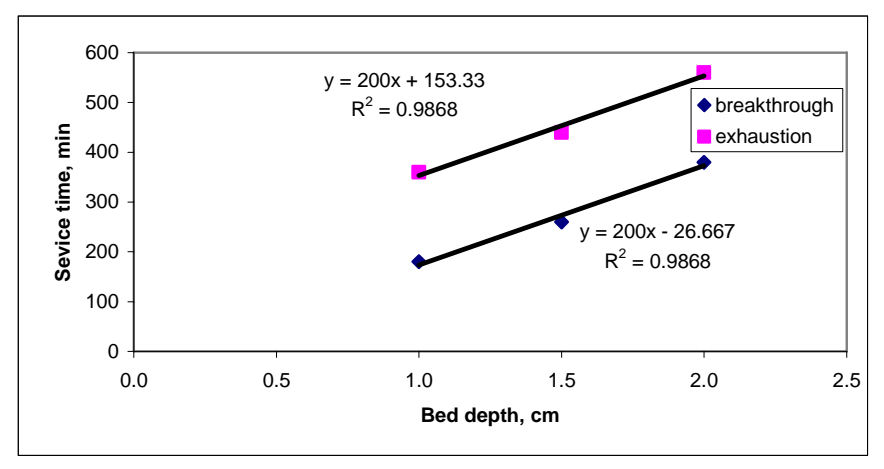


Fig. 4. Bed depths versus service time plot at 0.2% and 90% saturation of Ce4ZP fixed bed. Initial As(V) 25 mg/L, flow rate 0.5 mL/min.

## Prediction of service times of columns under new operating conditions using BDST model

#### New flow rate

According to BDST approach (equation 1), if the value of slope ' $a_1$ ' is determined for one flow rate ' $f_1$ ', value of ' $a_2$ ' for the other flow rate ' $f_2$ ' can be calculated as [21]:

$$a_2 = a_1 \frac{f_1}{f_2} \tag{6}$$

In this case the value of intercept 'b' is not affected significantly with flow rates. For flow rates of 1.0 mL/min, the calculated value of ' $a_2$ ', is 100. With this value the BDST equation for flow rate of 1.0 mL/min can be written as:

$$t = 100x + 153.33$$
 (for 90% saturation) (7)

$$t = 100x - 26.667$$
 (for 0.2% saturation) (8)

From Eqs. (7) and (8), the breakthrough and exhaust times for new flow rate of 1.0 mL/min at a bed depth of 1.0 cm were calculate and presented in Table 2. The data show that the experimental and theoretical values are well comparable with error less than 10%.

#### **New concentration**

From the BDST equation of the experimental data of a solute concentration  $C_1$ , it is also possible to predict the equation for another concentration  $C_2$  as [17]

$$a_2 = a_1 \frac{C_1}{C_2} \tag{9}$$

$$b_2 = b_1 \frac{C_1}{C_2} \frac{\ln(C_2/C_F - 1)}{\ln(C_1/C_B - 1)}$$
(10)

where  $a_I$  is the slope at concentration  $C_I$ ;  $a_2$  the new slope at concentration  $C_2$ ;  $b_I$  the intercept at concentration  $C_I$ ;  $b_2$  the new intercept at concentration  $C_2$ ;  $C_F$  the effluent concentration at influent concentration  $C_I$  is the effluent concentration at influent concentration  $C_I$ . For As(V) concentration of 50 mg/L, the values of  $a_2$  and  $b_2$  calculated from Eqs. (9) and (10) at breakthrough are 100 and -3.63 and for exhaust are 100 and 80.56, respectively. The equations of service time/bed depth for the new concentration can be written as

$$t = 100x + 80.56$$
 (for 90% saturation) (11)

$$t = 100x - 3.65 \quad \text{(for breakthrough)} \tag{12}$$

The theoretical exhaust time and breakthrough calculated from Eqs. (11) and (12) are 96 and 180 min, respectively, which are comparable to the experimental values (with errors less than 10%) as shown in Table 2. These equations can be used to prediction service times for different As(V) influent concentrations with acceptable accuracy.

Table 2 Comparison of the experimental service times with theoretical service times predicted using BDST model

| Flow   | Influent concentration | Break        | kthrough time<br>min |       | Ex           | khaust time<br>min |           |
|--------|------------------------|--------------|----------------------|-------|--------------|--------------------|-----------|
| ml/min | mg/L                   | Experimental | Theoretical          | Error | Experimental | Theoretical        | Error (%) |
| 1.0    | 25.0                   | 80           | 73                   | 8     | 260          | 253                | 3         |
| 0.5    | 50.0                   | 100          | 96                   | 3     | 200          | 180                | 9         |

#### Conclusion

The adsorption of As(V) on Ce4ZP in a fixed bed, was observed strongly depending on the influent flow rate, initial concentration and bed depth of column. Increase in bed depth enable more water can be treated, but with a slight reduction in column capacity. The quantity of treated water and adsorption capacity were found higher at a lower flow rate. At higher influent concentration, the adsorption capacity was higher. The service times predicted from the theoretical BDST equations agreed well with the service time obtained experimentally at different concentration and flow rate. The results suggest the practical applicability of Ce4ZP in As(V) removal in fixed bed columns.

#### Acknowledgements

We acknowledge the support of the Ministry of Science, Technology and Innovation for financial support, and Institute Ibnu Sina, University Technology Malaysia for donating Zeolite P.

#### References

- 1. Cantor KP, Drinking water and cancer. Cancer Causes Control 8:292-308 (1997).
- 2. Brooks WE, Miner. Commodity Summ. U.S. Geol. Surv. p. 23 (2007).
- 3. Johannesson M, The Market Implication of Integrated Management for Heavy Metals Flows for Bioenergy Use in the European Union, Kalmar University, Kalmar, Sweden, p. 115 (2002).

- 4. Huang CP, Pan JR, Lee M and Yen S, Treatment of high-level arsenic-containing wastewater by fluidized bed crystallization process. *J. Chem. Technol. Biotechnol.* **82**:289-294 (2007).
- 5. Leis M, Casey RJ and Caridi D, The management of arsenic wastes: problems and prospects. *J. Hazardous Materials* **B76:** 125-138 (2000).
- Galer JM, Delmas R and Loos-Neskovic C in: Progress in Ion Exchange: Advances and Applications, A Dyer, MJ Hudson, PA Williams (Eds.), The Royal Society of Chemistry, U.K., p. 187 (1997).
- 7. Raven KP, Jain A, and Loeppert RH, Arsenite and arsenate adsorption on ferrihydrite: Kinetics, equilibrium, and adsorption envelop. *Env. Sci. Technol.* 32:344-349 (1998).
- 8. Huang JG and Liu JC, Enhanced removal of As(V) from water with iron-coated spent catalyst. *Sepn. Sci. Technol.* 32: 1557-1569 (1997).
- 9. Bhatia S, Zeolite catalysis: Principles and applications, CRC Press, Florida, (1990).
- 10. Li Z, Anghel I and Bowman RS, Sorption of oxyanions by surfactant-modified zeolite. *J. Dispersion Sci. Technol.* **19:** 843-857 (1998).
- 11. Campos V and Buchler PM, Anionic sorption onto modified natural zeolites using chemical activation. *Environ. Geol.* **52:**1187-1192 (2007).
- 12. Xu YH, Ohki A and Maeda S, Removal of arsenate, phosphate and fluoride ions by aluminum-loaded Shirasu-zeolite. *Toxicol. Environ. Chem.* **76:** 111-119 (2000).
- 13. Elizalde-González MP, Mattusch J, Einicke WD and Wennrich R, Sorption on natural solids for arsenic removal. *Chem. Eng. J.* **81:**187-195 (2001).
- 14. He G, Yang J, Yu X and Yue Y, Assessment of arsenic removal from drinking water by new adsorbent. *Research Report from the National Institute for Environmental Studies, Japan*, **166:**4044 (2001)
- 15. Zhang Y, Yang M, Mindou X, He H and Wang DS, Arsenate adsorption on Fe-Ce bimetal oxide adsorbent: Role of surface properties. *Environ. Sci. Technol.* **39**:7246-7253 (2005).
- 16. Md Jelas Haron, Farha Ab Rahim, Abdul Halim Abdullah, Mohd Zobir Hussein and Anuar Kassim, Kinetic and Thermodynamic of Arsenic Sorption by Cerium(IV)-exchanged Zeolite P, in Recent Advances in Ion Exchange Theory and Practice (Proceedings of IEX 2008), M. Cox (Ed.), Cambridge, 2008, pp 291-299.
- R.A. Hutchins, New method simplifies design of activated-carbon system, Am. J. Chem. 80 (1973) 133– 138.
- 18. K. Vijayaraghavan, J. Jegan, K. Palanivelu, M. Velan, Removal of nickel(II) ions from aqueous solution using crab shell particles in a packed bed up-flow column, J. Hazard. Mat. **113B** (1–3) (2004) 223–230.
- 19. P.B. Bhakat, A.K. Gupta, S. Ayoob, Feasibility analysis of As(III) removal in a continuous flow fixed bed system by modified calcined bauxite (MCB), Journal of Hazardous Materials, **B13**9 (2007) 286–292.
- 20. Z. Aksu, F. G"onen, Biosorption of phenol by immobilized activated sludge in a continuous packed bed: prediction of breakthrough curves, Proc. Biochem. **39** (2003) 599–613.
- 21. D.C.K. Ko, J.F. Porter, G. McKay, Optimised correlations for the fixed-bed adsorption of metal ions on bone char, Chem. Eng. Sci. **55** (2000) 5819–5829.

# ADSORPTION OF FORMULATED CHLORPYRIFOS ON SELECTED AGRICULTURAL SOILS OF TERENGGANU

(Penjerapan Rumusan Klorpirifos ke atas Tanah Pertanian Terpilih di Terengganu)

Tay Joo Hui<sup>1,2</sup>, Marinah Mohd Ariffin<sup>1</sup>, Norhayati Mohd Tahir<sup>1\*</sup>

<sup>1</sup>Environmental Research Group (ERG), Department of Chemical Sciences, Faculty of Science and Technology, Universiti Malaysia Terengganu (UMT), Mengabang Telipot, 21030 Kuala Terengganu, Terengganu. <sup>2</sup>Faculty of Industrial Sciences and Technology (FIST), Universiti Malaysia Pahang (UMP), Lebuhraya Tun Razak, 26300 Gambang, Kuantan, Pahang Darul Makmur.

\*Correspondence author: hayati@umt.edu.my

#### Abstrak

Penjerapan insektisid klorpirifos (rumusan kormersil berjenama Kensban®, 20% bahan aktif) pada tiga jenis siri tanah (0-25cm) dari kebun sayur-sayuran di negeri Terengganu, Malaysia telah dikaji menggunakan kaedah penjerapan kelompok. Analisis insektisid dijalankan menggunakan kaedah kromatografi gas dilengkapkan dengan pengesan nitrogen and fosforus. Keputusan menunjukkan bahawa tanah yang mengandungi lebih banyak jirim organik dan lempung mempunyai keupayaan menjerap insektisid yang lebih kuat. Selain itu, pH tanah juga mempengaruhi keupayaan penjerapan insektisid di mana penjerapan adalah lebih tinggi pada tanah yang mempunyai nilai pH yang rendah. Secara keseluruhannya, kandungan jirim organik , kandungan lempung dan pH memainkan peranan yang penting dalam penjerapan insektisid klorpirifos. Walau bagaimanapun, tidak boleh dinafikan bahawa keupayaan penjerapan yang diperolehi dalam kajian ini mungkin juga dipengaruhi oleh interaksi di antara klorpirifos, pelarut, pengemulsi, air dengan tapak penjerapan tanah memandangkan klorpirifos yang digunakan adalah formulasi komersil.

Kata kunci: penjerapan, klorpirifos, insektisid organofosforus, tanah pertanian, GC-NPD

#### Abstract

In this study, the adsorption of commercially formulated chlorpyrifos (trade name Kensban®, 20% a.i.) in three soil samples (0-25cm depths) collected from vegetable farms in the state of Terengganu, Malaysia has been investigated using a batch technique. Analysis of the insecticide was carried out using gas chromatography equipped with nitrogen and phosphorus detector. Result indicated that, soils contained higher organic matter and clay content exhibited a much stronger adsorption affinity for the insecticide. In addition, soil pH was also observed to play a role in influencing the adsorption affinity of this insecticide where a higher adsorption was observed for soils with lower pH values. Results from this study clearly showed that, in agreement with previously reported studies, soil properties particularly organic matter content, clay content and pH play an important role in controlling the sorption behaviour of chlorpyrifos insecticide. However, it must be conceded that the measured adsorption in this study might also be influenced by a number of processes occurred in the soil, such as complex interaction between chlorpyrifos, solvent, emulsifier, water and the soil sorption sites since the applied chlorpyrifos was a commercial formulation.

Keywords: adsorption, chlorpyrifos, organophosphorus insecticide, agricultural soil, GC-NPD

#### Introduction

Chlorpyrifos (O,O-diethyl-O-3,5,6-trichloro-2-pyridyl phosphorothionate) (Figure 1) is a broad-spectrum insecticide whose mode of activity is as a cholinesterase inhibitor. It is used to kill a wide variety of insects including cutworms, corn rootworms, cockroaches, grubs, flea beetles, flies, termites, fire ants, and lice by disrupting their nervous system. It is also used as a soil treatment (pre-plant and at planting), as a seed treatment and as a foliar spray, directed spray and dormant spray. It has been speculated that the bioaccumulation ability of chlorpyrifos and other organophosphorus pesticides in living tissues may spell a potential environment risk to marine organisms and humans [1]. Recently, the U.S. Environmental Protection Agency (USEPA) and the manufacturers of chlorpyrifos have agreed to eliminate nearly all-household applications of chlorpyrifos, but agriculture use continues [2]. Because of its low water solubility and relatively high log K<sub>ow</sub> (Table 1), the sorption of chlorpyrifos will play a crucial role in determining its fate and transport in the environment. This adsorption process in turn, is influenced by the soil properties, chemical nature of the insecticide and also climatic factors.

## Tay Joo Hui et al: ADSORPTION OF FORMULATED CHLORPYRIFOS ON SELECTED AGRICULTURAL SOILS OF TERENGGANU

Although the sorption behaviour of this insecticide has been well studied under temperate climate, similar information under tropical climate is still limited, especially on formulated chlorpyrifos. Several reports have been published in recent years on the dissipation of chlorpyrifos in Malaysian soils [3-4] but very limited report on adsorption study. The objective of this study was to investigate the adsorption of chlorpyrifos in selected agricultural soils of Malaysia in order to provide data to assess the potential risk of pollution to the environment.

Figure 1: Structure of chlorpyrifos.

Table 1: The physical and chemical properties of chlorpyrifos.

| Insecticide  | Melting point (°C) | Molecular<br>weight | Vapour pressure<br>(mPa at 25°C) | Water solubitily (ppm at 25°C) | Log K <sub>ow</sub><br>(at 25°C) |
|--------------|--------------------|---------------------|----------------------------------|--------------------------------|----------------------------------|
| chlorpyrifos | 41-43              | 350.6               | 3.35                             | 2                              | 4.98                             |

#### Materials and methods

Three surface (0-25cm) soil samples were obtained from vegetable farms in Marang (*Nami* and *Chempaka* series) and Kuala Terengganu (*Sabrang* series). Bulk soils were air-dried, ground and passed through a 2mm sieve. Subsamples of freshly collected soils were dried at 110°C until there is no significant change in weight (approx. 24h) to determine the initial soil moisture content. Soil pH was determined in a 1:2.5 soil/water suspension; soil organic matter (OM) by Walkley and Black's Titration Method [5]; particle size distribution by using pipette method; clay mineralogy analysed using Philiphs X-ray diffraction system.

The commercial formulation of chlorpyrifos (trade name Kensban®) which contains 20% of active ingredient was used in this study. All insecticide solutions were prepared in 0.02M calcium chloride and its concentration was determined by using ThermoFinnigan Gas Chromatography (GC) fitted with  $AT^{TM}$ -1 Capillary Column (0.25 $\mu$ m x 0.25mm x 30m Alltech) and a Nitrogen Phosphorus Detector (NPD). The column temperature was programmed from 125 to 230°C at rate of 30°C/min, held at 230°C for 6 min, the detector and injector temperatures were 300 and 200°C, respectively. Adsorption study was carried out using a batch equilibrium method. Triplicate samples of the air-dried soil (1g) were equilibrated with 5ml of insecticide solutions (initial concentration,  $C_i$ = 0-25 mg/L), shaken for 2h and 24h, allowed to stand followed by centrifugation. The clear supernatants obtained were extracted three times using n-Hexane (10mL, 5mL and 5mL, respectively) and analysed for their insecticide content using GC-NPD technique described above. The amount of insecticide adsorbed by the soil was estimated as the differences between that initially present in solution ( $C_i$ ) and that remaining after equilibration with soil ( $C_e$ ).

#### Results and discussion

The physicochemical properties of the soils are given in Table 2. The *Chempaka* soils was observed to have significantly lower (p<0.05) pH value compared to other soil series. Results showed that all soil studied exhibited similar OM content and statistical analysis showed the differences were insignificant (p>0.05). Clay mineral analysis showed that muscovite-3, kaolinite and gibbsite is the most abundant mineral in soil samples.

| Soil     | moisture content (%) | pH in<br>water | pH in<br>CaCl <sub>2</sub> | %<br>OM | %<br>sand | %<br>clay | %<br>silt | texture       | Clay<br>mineralogy* |
|----------|----------------------|----------------|----------------------------|---------|-----------|-----------|-----------|---------------|---------------------|
| Chempaka | 20.4                 | 4.52           | 4.07                       | 2.08    | 30.1      | 31.7      | 38.2      | Clay loam     | M, K, Q             |
| Sabrang  | 13.9                 | 4.91           | 4.34                       | 1.92    | 69.6      | 10.1      | 20.3      | Sandy<br>Loam | M, K, G, Q          |
| Nami     | 15.7                 | 5.32           | 4.51                       | 1.94    | 48.5      | 10.2      | 41.3      | Loam          | K, G, Q             |

Table 2: Physicochemical properties of soil samples.

The adsorption isotherms for chlorpyrifos in the soil samples are shown in Figure 2 and Figure 3. Two different equilibration times (2h and 24h) has been chosen for comparison. The distribution coefficient ( $K_d$ ), which represents the partitioning of the insecticide between liquid ( $C_e$ ) and solid phases ( $C_s$ ) in equilibrium and typically known as a linear adsorption isotherm, was calculated using equation  $C_s = K_d C_e$ . The empirical Freundlich adsorption isotherm ( $C_s = K_f C_e^{-1/n}$ ), which allows the evaluation of experimental constants  $K_f$  and n, was also calculated using the lineariased form of the equation ( $L_s = L_s =$ 

Table 3: Distribution coefficient  $(K_d)$  and Freundlich constants  $(K_f$  and n) for adsorption of chlorpyrifos on various soil samples.

| Equilibration time (hour) | Soil     | $K_{d}$ | $R^2$ | $K_{\mathrm{f}}$ | n     | $\mathbb{R}^2$ |
|---------------------------|----------|---------|-------|------------------|-------|----------------|
|                           | sabrang  | 195     | 0.62  | 153              | 1.36  | 0.32           |
| 2h                        | chempaka | 241     | 0.76  | 200              | 1.26  | 0.56           |
|                           | nami     | 185     | 0.30  | 0.71             | -0.21 | 0.30           |
|                           | sabrang  | 289     | 0.69  | 700              | 0.56  | 0.38           |
| 24h                       | chempaka | 346     | 0.42  | 82.0             | 6.29  | 0.00           |
|                           | nami     | 231     | 0.84  | 493              | 0.57  | 0.83           |

The adsorption capacity of the soils towards chlorpyrifos was evaluated by comparing the values of  $K_d$  obtained. The isotherm was S-type for all samples investigated indicating a low herbicide-soil affinity at low herbicide concentrations. However, once the chlorpyrifos molecule begins to adsorb it is easier for additional amounts to become stabilized on the soil surface and lead to enhanced affinity of the soil surface for chlorpyrifos with increasing amounts adsorbed. Great difference between  $K_d$  values obtained using 2h and 24h equilibration time

<sup>\*</sup>M = Muscovite-3, K = Kaolinite, G = Gibbsite, Q = Quartz

## Tay Joo Hui et al: ADSORPTION OF FORMULATED CHLORPYRIFOS ON SELECTED AGRICULTURAL SOILS OF TERENGGANU

indicated that the adsorption of formulated chlorpyrifos is characterized by a rapid initial process, followed by a slower stage and needed longer time to reach equilibrium.

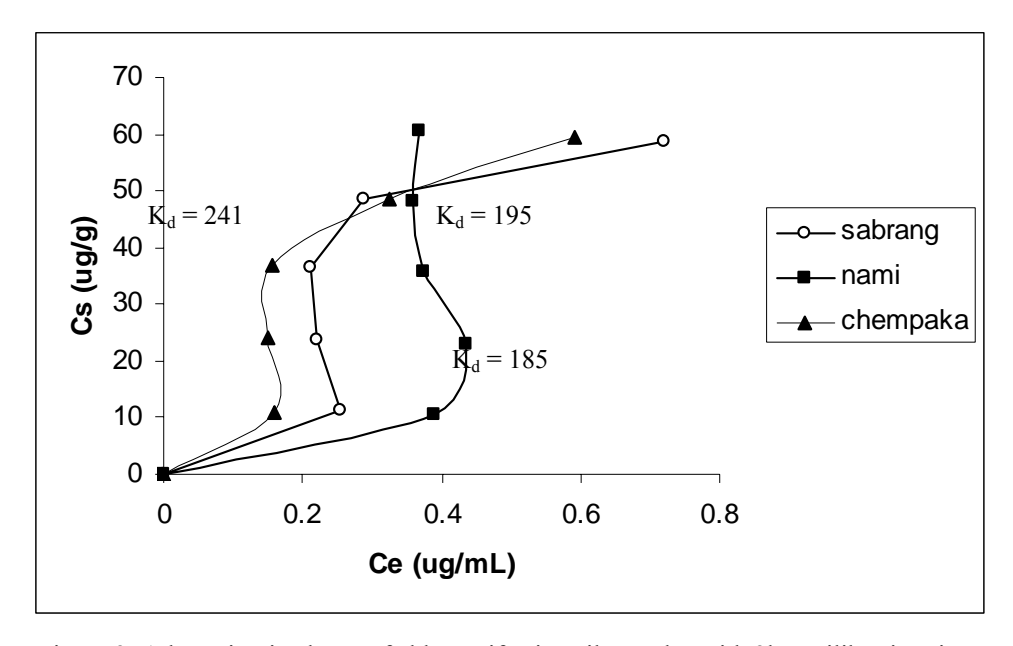


Figure 2: Adsorption isotherm of chlorpyrifos in soil samples with 2h equilibration time.

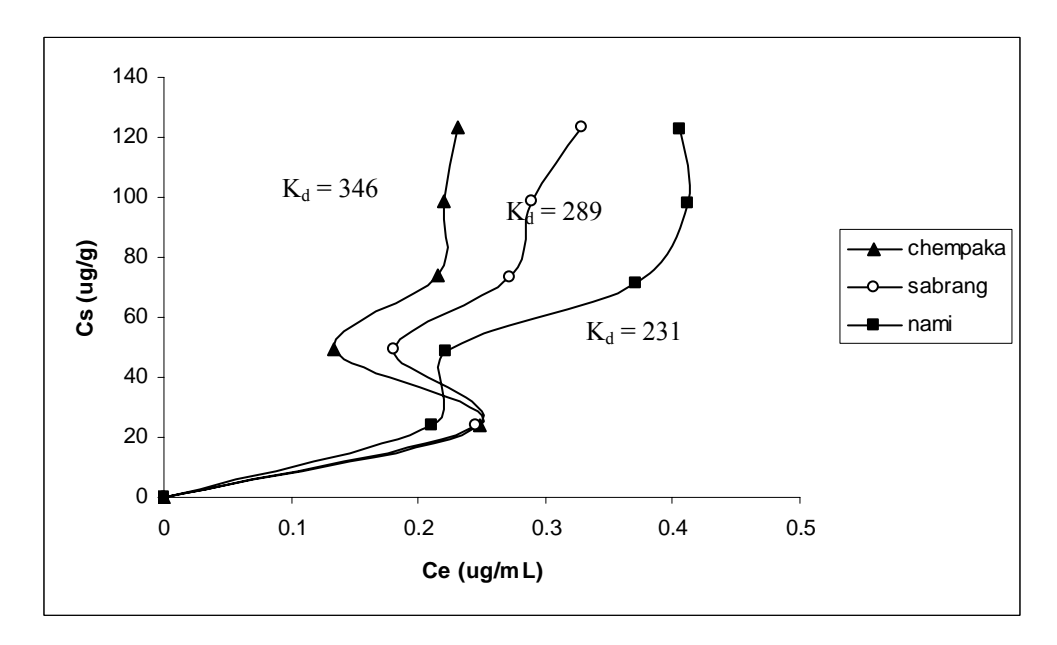


Figure 3: Adsorption isotherm of chlorpyrifos in soil samples with 24h equilibration time.

In order to assess the factors that affect the adsorption of formulated chlorpyrifos by soil, the  $K_d$  values were correlated with the soil properties (Table 4). *Chempaka* soil with higher OM and lower pH exhibited the highest value of  $K_d$  (for both 2h and 24h equilibration time) compared to *Sabrang* and *Nami* soil series. OM has been reported to be one of the major factors that influence the extent of pesticide adsorption on soils and results obtained in this study are in agreement with earlier reports [6-8]. The correlation coefficient was found to be 0.96 and 0.81 for 2h and 24h adsorption, respectively, indicating strong positive correlation between OM and adsorption even though the OM content in soil samples was low.

It has also been reported that for soils with low OM content the interactions of pesticides with soil inorganic matrix may become more important [9]. Correlation analysis between  $K_d$  and % clay in this present study gives value of 0.99 and 0.86 for 2h and 24h equilibration time, indicating strong correlation between clay content and adsorption affinity of chlorpyrifos. However, the correlation was not statistically significant (p>0.05). Interaction study of acephate (an organophophorus insecticide) with montmorillonite (a mineral of the group of smectites) by Gonzalez-Pozuelo *et al.* in 1991 [10] showed that the pesticide is adsorbed into the interlayer space of the smectite forming a stable complex. Similar finding had been reported by Hernández-Soriano *et al.* [9], in which the adsorption of malathion (an organophophorus insecticide) was enhanced for clayey soils. However, soil samples used in this study are dominated by kaolinite, gibbsite, muscovite-3 (mica group) and quartz which do not contain the microporous structure that is present in montmorillonite. Haderlein and Schwarzenbach [11] found a specific adsorption of nitroaromatic compounds (NACs) to the silanol surface sites of kaolinite. They proposed that an electron donor-acceptor complex (i.e., a  $\pi$  complex) between electron donor functions at the siloxane surface and the aromatic ring system of the NAC is responsible for the observed specific adsorption. This may also be a plausible mechanism for the adsorption of the uncharged chlorpyrifos investigated in this study.

Table 4: Correlation coefficients between K<sub>d</sub> values and soil parameter.

| Coil nomenton           |                       | r                      |
|-------------------------|-----------------------|------------------------|
| Soil parameter          | 2h equilibration time | 24h equilibration time |
| % organic matter        | 0.96                  | 0.81                   |
| % clay                  | 0.99                  | 0.86                   |
| pH in CaCl <sub>2</sub> | -0.98                 | -0.99*                 |

<sup>\*:</sup> correlation is significant at the 0.05 level.

Study by Van Emmerik *et al.* [2] showed that the adsorption of chlorpyrifos on gibbsite is dependent on pH (adsorption decreased when pH increased) but only has little effect on chlorpyrifos adsorption by kaolinite. The result obtained in this present study showed that soil with lower pH (*Chempaka* series) exhibited higher adsorption capacity for chlorpyrifos, with correlation coefficient of -0.98 and -0.99 between K<sub>d</sub> and pH (for 2h and 24h equilibration time, respectively). The reduction in chlorpyrifos adsorption as the pH increases might be due to an increase in negative surface charge at the edges of clay.

However, it must be conceded that the measured adsorption in this study may also involve a number of other processes that occurred in the soil because the chlorpyrifos applied was a commercial formulation containing aromatic hydrocarbons as a co-solvent. Complex interaction between chlorpyrifos, solvent, emulsifier, water and the soil sorption sites may have occurred, in which chlorpyrifos and solvent may compete for the same sorption sites. Since chlorpyrifos has greater affinity for solvent than water (Log  $K_{ow} = 4.98$ ), solvent adsorption at soil surface may also enhance chlorpyrifos adsorption at that site. Therefore, the measured sorption may be the result of simple sorption, competitive or cooperative sorption involving chlorpyrifos and solvent. Comparison with previous studies using non-formulated chlorpyrifos (Baskaran et al., 2003; Huang, 1999) showed that formulated chlorpyrifos exhibited higher adsorption coefficient (Kd). This result indicated that the presence of additive(s) in commercial formulation could enhance chlorpyrifos adsorption at soil surface.

## Tay Joo Hui et al: ADSORPTION OF FORMULATED CHLORPYRIFOS ON SELECTED AGRICULTURAL SOILS OF TERENGGANU

#### **Conclusions**

Results obtained in present study indicated the influences of soil organic matter content, clay content and soil pH on the adsorption of formulated chlorpyrifos in selected Terengganu agricultural soils. In general, soils with higher organic matter content, higher clay content and lower pH value exhibited stronger adsorption affinity for the insecticide. Consistent with previously reported work, soil properties particularly organic matter content, clay content and pH play an important role in controlling the sorption behaviour of chlorpyrifos. However, the measured adsorption in this study may also involve a number of processes that occurred in the soil because the chlorpyrifos applied was a commercial formulation. Complex interaction between chlorpyrifos, solvent, emulsifier, water and the soil sorption sites may have occurred, in which solvent may enhance chlorpyrifos adsorption at that site. Although formulated chlorpyrifos is mainly used for environmental fate studies rather than sorption studies, results obtained in this study suggest that mechanisms for sorption of formulated chlorpyrifos should also be more thoroughly investigated as sorption processes will undoubtedly influence the fate of this pesticide in the environment.

## Acknowledgements

The financial support of the Research Management Centre of UMT through a research grant for postgraduate student (Vote No: 63912) is gratefully acknowledged. The manuscript benefitted from the comments of an anonymous reviewer.

#### References

- 1. Kale, S.P., Carvalho, F.P., Raghu, K., Sherkhane, P.D., Pandit, G.G., Mohan Rao, A., Mukherjee, P.K. & Murthy, N.B.K. 1999. Studies on degradation of 14C-chlorpyrifos in the marine environment. *Chemosphere* 39(6): 969-976.
- 2. Van Emmerik, T.J., Angove, M.J., Johnson, B.B. & Wells, J.D. 2007. Sorption of chlorpyrifos to selected minerals and the effect of humic acid. *J. Agric. Food Chem.* 55: 7527-7533.
- 3. Ngan, C.K., Cheah, U.B., Wan Abdullah, W.Y., Lim, K.P. & Ismail, B.S. 2005. Fate of chlorothalonil, chlorpyrifos and profenofos in a vegetable farm in Cameron Highlands, Malaysia. *Water, Air, and Soil Pollution: Focus* 5: 125-136.
- 4. Chai, L.K., Mohd-Tahir, N. & Hansen, H.C.B. 2009. Dissipation of acephate, chlorpyrifos, cypermethrin and their metabolites in a humid-tropical vegetable production system. *Pest. Manag. Sci.* 65: 189-196.
- 5. Moris, N. & Singh, M.M. 1971. Manual of Laboratory Method of Chemical Soil Analysis. Rubber Research Institute of Malaysia. Kuala Lumpur, 1980. Pp13-15.
- 6. Baskaran., S., Kookana., R.S. & Naidu, R. 2003. Contrasting behaviour of chlorpyrifos and its primary metabolite, TCP (3,5,6-trichloro-2-pyridinol), with depth in soil profiles. *Aunstralian Journal of Soil Research* 43: 749-760.
- 7. Yu, L.Y., Wu, X.M., Li, S.N., Fang, H., Zhan, H.Y. & Yu, J.Q. 2006. An exploration of the relationship between adsorption and bioavailability of pesticides in soil to earthworm. *Environmental pollution* 141: 428-433.
- 8. Valverde García, A., Socías Viciana, M., González Pradas, E. & Vilafranca Sánchez, M. 1992. Adsorption of chlorpyrifos on Almería soils. *The Science of the Total Environment*, 123/124: 541-549.
- 9. Hernández-Soriano, M.C., Mingorance, M.D., Peña, A. 2007. Interaction of pesticides with a surfactant-modified soil interface: Effect of soil properties. *Colloids and Surfaces A: Physicochem. Eng. Aspects* 306: 49-55.
- 10. Arienzo, M., Sánchez-Camazano, M., Crisanto Herrero, T. & Sánchez-Martín, M.J. 1993. Effect of organic cosolvents on adsorption of organophosphorus pesticides by soils. *Chemosphere* 27(8): 1409-1417.
- 11. Clausen, L., Fabricis, I. & Madsen, L. 2001. Adsorption of pesticides onto quartz, calcite, kaolinite, and  $\alpha$ -Alumina. *J. Environ. Qual.* 30: 846-857.

# CHLORPYRIFOS AND MALATHION RESIDUES IN SOILS OF A TERENGGANU GOLF COURSE: A CASE STUDY

(Residu Klorpirifos dan Malathion Dalam Tanah di Padang Golf Terengganu: Satu Kajian Kes)

Norhayati Mohd Tahir\*, Khaw Hock Soon, Marinah Mohd Ariffin, Suhaimi Suratman

Environmental Research Group (ERG),
Department of Chemical Sciences, Faculty of Science and Technology,
Universiti Malaysia Terengganu, Mengabang Telipot, 21030 Kuala Terengganu, Malaysia

\*Corresponding author: hayati@umt.edu.my

#### Abstract

A preliminary study was conducted to determine the residues of organophosphorus insecticides, Chlorpyrifos and Malathion, in soils of a local 18-hole golf course in order to evaluate their dissipation rate and half-life values under field condition. Soils samples were collected from 18 stations (greens) three times within a period of one month after its application. The insecticide residues were extracted using soxhlet technique and determined using gas chromatography fitted with a nitrogen phosphorus detector (GC-NPD). Results obtained indicated that dissipation of these insecticides were fairly fast, with amount dissipated within 30 days ranging from 65.0 to 96.6 % for chlorpyrifos and 63.5 to 95.8% for malathion. The dissipation of these insecticides from the soils seemed to follow a first order kinetic with half-life values ranging from 3.4 to 15.3 days with average of 6.5 days and 6.8 to 31.3 days with average of 13.5 days for chlorpyrifos and malathion, respectively. It appears that soil physico-chemical properties such as organic matter content, pH, particle size distribution, cationic exhange capacity and moisture content do not exert an influence on the dissipation of these insecticides.

Keywords: chlorpyrifos, malathion, residues in soils, golf course, Kuala Terengganu

#### **Abstrak**

Satu kajian awal telah dilakukan bagi menentukan residu insektisid organofosforus, Klorpyrifos dan Malathion, dalam tanah padang golf 18-lubang tempatan bagi menilai kadar lesapan dan separuh-hayat insektisid tersebut pada keadaan lapangan. Sampel tanah diambil dari 18 stesen ('greens') sebanyak tiga kali sepanjang satu bulan selepas racun tersebut digunakan. Residu insektisid diekstrak dengan menggunakan teknik soxhlet dan ditentukan dengan kromatografi gas dengan pengesan nitrogen fosforus (GC-NPD). Keputusan yang didapati menunjukkan lesapan insektisid ini adalah cepat, iaitu dalam jangkamasa 30 hari, 65.0 hingga 96.6 % klorpirifos dan 63.5 hingga 95.8% malathion telah melesap. Kelesapan kedua-dua insektisid ini dari tanah adalah mengikut kinetik tertib pertama dengan nilai separuh-hayat masing-masing di antara 3.4 hingga 15.3 hari dengan purata 6.5 hari dan 6.8 hingga 31.3 hari dengan purata 13.5 hari, bagi klorpirifos dan malathion. Kajian ini juga menunjukkan ciri fizik-kimia tanah seperti kandungan bahan organik, pH, taburan saiz partikel, kapasiti penukaran kation dan kandungan lembapan tidak mempengaruhi lesapan insektisid-insektisid tersebut.

Kata kunci: klorpirifos, malathion, residu dalam tanah, padang golf, Kuala Terengganu

#### Introduction

The demand for golf is rapidly expanding worldwide and the number of golf courses around the world has increased tremendously; for instance, it is estimated that in the United States alone, there are approximately 16,000 golf courses across the country [1]. In the South East Asian countries of Thailand, Malaysia, Indonesia and the Philippines, the popularity of golf has led to the spread of golf tourism in these countries where golf courses has become a central part of many hotels and resorts development projects. In Malaysia, it is also now becoming a trend to use golf courses as a central part of many new housing development projects; in Kuala Terengganu alone, there are at least two housing developments with such concept.

Golf courses are highly managed locations. Generally, turf grass receives almost daily applications of irrigation water and frequent applications of fertilizers in order to stimulate plant growth. In addition pesticides are used in large quantities on turf grass to control damage caused by insects, weeds and fungus-borne diseases. All these additions are needed in order to maintain a high quality turf grass playing surface. Golf course is often presumed to be a significant contributor to nonpoint source water pollution and an increased attention on the possible environmental effects of chemical applications on golf courses has occurred with the increase in

## Norhayati Mohd Tahir et al: CHLORPYRIFOS AND MALATHION RESIDUES IN SOILS OF A TERENGGANU GOLF COURSE: A CASE STUDY

public's concern for the environment. This has led to several studies being conducted worldwide particularly in the United States on these issues [2-12].

This paper presents results of a preliminary study conducted to determine residues of organophosphorus insecticides, Chlorpyrifos and Malathion, in soils of a local 18-hole golf course in order to evaluate their dissipation rate and half-life values under field condition. It is hope that the findings reported would provide some baseline information on the fate of pesticides applied on golf courses.

#### **Experimental**

#### Study area and sampling sites

The 18 holes golf course is located in Tok Jembal, approximately 15km north of Kuala Terengganu. The golf course was built on a reclaimed municipal landfill. The site was initially a swamp land used by Kuala Terengganu municipal as their landfill site and when the landfill was decommissioned, it was reclaimed and converted into a golf course in the late 90's. The golf course is actually part of a housing development project known as Kuala Terengganu Golf Resort managed by KT Golf Resort Berhad, a subsidiary of UDA Holdings Sdn Bhd. A variety of pesticides are applied to the turfgrass on this golf course (Table 1) and two types of insecticide was chosen for this study *viz*. malathion and chlorpyrifos.

Pesticides Trade Name Active Ingredients Classification Insecticides ACM DIAZINON Diazinon 55% CH MALAXION Malathion 88% **DURSBAN 75** Chlorpyrifos 21.2% Chlorpyrifos 46.3%, Cypermethrin 4.6% KONSEP 550 Herbicides Fluroxypyr, 1-Methyl Heptyl Ester 29.6% STARANE 200 **FUSILADE** Fluazifop-butyl 26% (pyridyloxyl phenoxy propionic ester) **MEWAHTOX** 2,4- Butyl Ester 45% Fungicides Ultracide 0.3EC Methidation 20.6% **KENLATE** Benomyl 24.7% TERAZOLE 25EC Etridiazole 24.7% TERRACHLOR 75 wp Quintozene 75% Cuprawit 85wp Copper oxychloride 85% (metallic copper 50%) CH MANCOZEB Zinc 62%, Manganese ion 16% Carbendazim 50% Bavistin (BASF)

Table 1. List of pesticides used on the golf course

Surface soils (0-5 cm) were collected from a total of 18 sampling sites (Fig. 1) using metal spades; each sampling site represents one green. Samplings were carried out three times, *viz.* one day (1<sup>st</sup> sampling), fifteen days (2<sup>nd</sup> sampling) and thirty days (3<sup>rd</sup> sampling) after pesticide application. The soils collected were packed in plastic bags and transported immediately to the laboratory and once in the laboratory, they were kept cool in the fridge until further analysis to minimise degradation. Analysis of pesticides in soils was carried out using a method based on USEPA method 3542B [13]. Briefly, pesticides were soxhlet extracted using 1:1 mixture of hexane and acetone for 12hrs and the extracts concentrated using rotary evaporator. Determination and quantification of the two pesticides were carried out using gas chromatography fitted with nitrogen phosphorus detector (GC-NPD) based on the retention times compared to that of external malathion and chlorpyrifos standards.

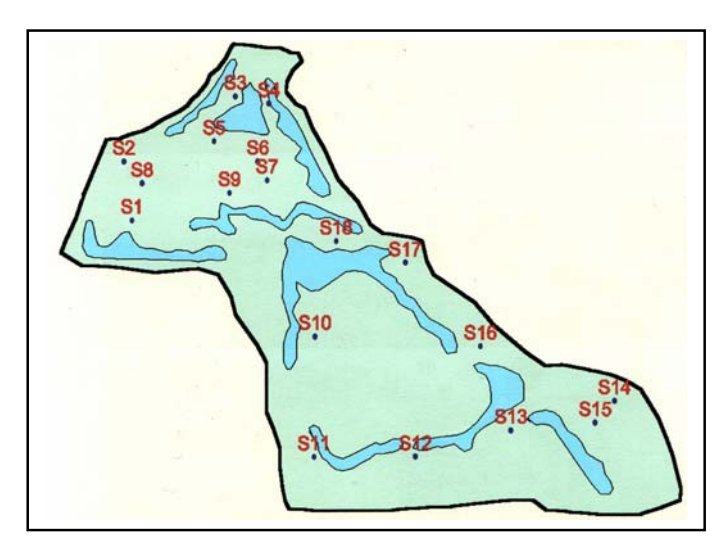


Figure 1. Locations of soil sampling stations

The GC-NPD operating conditions were modified slightly from the recommended method in order to improve separation of the two peaks of interest (Fig 2) and they were as follows: 2  $\mu$ l extract was injected onto ETX-5 column (30m x 0.25 mm i.d; 0.25 $\mu$ m filmed thickness); injection temperature was set at 250°C; column temperature was programmed in the following manner: hold at 120°C for 2 min, first temperature ramp of 120 - 170°C at 20°C min<sup>-1</sup> followed by the second and third temperature ramp of 170 - 180°C at 0.5°C min<sup>-1</sup> and 180 – 270°C at 30°C min<sup>-1</sup> before maintaining at 270°C for 1 min resulting in a total run time of 28.5 mins; helium was used as the carrier gas with a flow rate at 1.0ml. min<sup>-1</sup>; detector temperature was set at 300°C. Recoveries of malathion and chlorpyrifos from six replicates of soils fortified with 10  $\mu$ g/g (soil dry weight) insecticide standards was between 88.5 to 99.9% and 78.5 to 85.6% with mean recovery of 95.1% ( $\pm$ 3.7%) and 83.4 % ( $\pm$ 2.6%), respectively. Recoveries obtained for malathion were within those recommended by the EPA method (>85%). Recoveries for chlorpyrifos on the other hand were slightly below those recommended by EPA (85%) but are still acceptable since method reproducibility is very good.

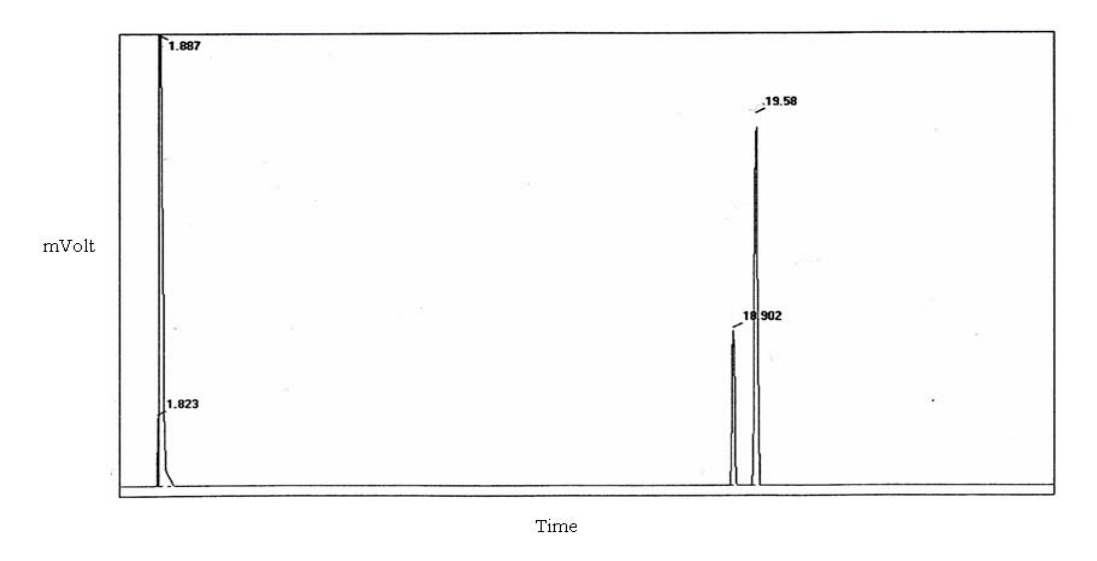


Figure 2. Typical chromatogram of malathion (18. 90 min) and chlorpyrifos (19.58) obtained

Physical characteristics, viz. particle size analysis (PSA), total organic content, cationic exchange capacity (CEC), moisture content and pH were determined using procedure described by Lim, H.K. [14].

#### **Results and Discussion**

Table 2 shows the results of soil physical-chemical characteristics. Soil texture for the whole course is sandy with very low silt and clay content. Generally, soil organic carbon content was low whilst the moisture content of the course was relatively high; very small variation of organic carbon and moisture content were found in these soils and statistical analysis showed that the variation between the 18 greens were insignificant. On the hand, the soil pH and CEC values showed significant variation (p<0.05) with sampling stations. The pH values ranged from 3.48 to 4.65 with mean value of 4.25; generally these soils were in the acidic range and it is not surprising that the greens on this golf course were regularly limed by the green keeper as part of the turf treatment and management. The CEC was found to range from 0.0257 to 0.0766 cmol/kg. Very strong correlation between these two soils parameters (r= 0.95) was found and this is generally an indication that pH exerts a strong influence on the CEC of the soils.

Soil characteristicsResultsOrganic matter content\* $2.85 \pm 0.08\%$ Moisture content\* $10.3 \pm 0.19\%$ Soil textureSandy (<2.23  $\pm$  0.66% silt+clay content)pH\*4.25 + 0.29

0.0579 + 0.0173 cmol/kg

Table 2. Physical-chemical characteristics of turf soils

Cationic exchange capacity\*

Table 3 summarises the results obtained for chlorpyrifos and malathion residues in soils within 30 days after their application on the greens while Figure 3 and 4 shows their distribution in soils with sampling stations for the three samplings.

 Days after application
 Malathion / ppm
 Chlorpyrifos / ppm

 0
 0.08 - 2.36
 0.74 - 2.24

 15
 0.02 - 0.09
 0.08 - 0.43

 30
 0.02 - 0.05
 0.02 - 0.18

Table 3. Concentration range of chlorpyrifos and malathion residues in soils

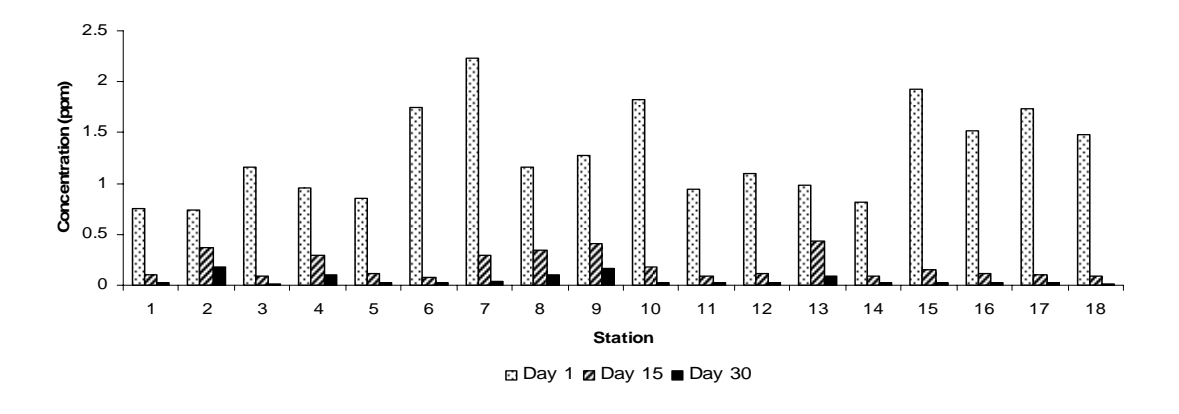


Figure 3. Concentration of chlorpyrifos residues in soils for a period of 30 days after application

<sup>\*</sup> Mean value

Statistical analysis (ANOVA) shows that differences observed between stations were insignificant (p>0.05) whilst significant differences were obtained (p<0.05) between the three samplings for both insecticides. These results show a fairly rapid dissipation of the two insecticides under field condition where 65.0-96.6% of the chlorpyrifos and 63.5-95.8% of the malathion have dissipated from the top soils within 30 days after their application. Correlation analysis between measured soil physical-chemical characteristics and the insecticides concentrations and their dissipation rates suggests that these parameters do not play an important role in influencing the dissipation of the two insecticides from the soils.

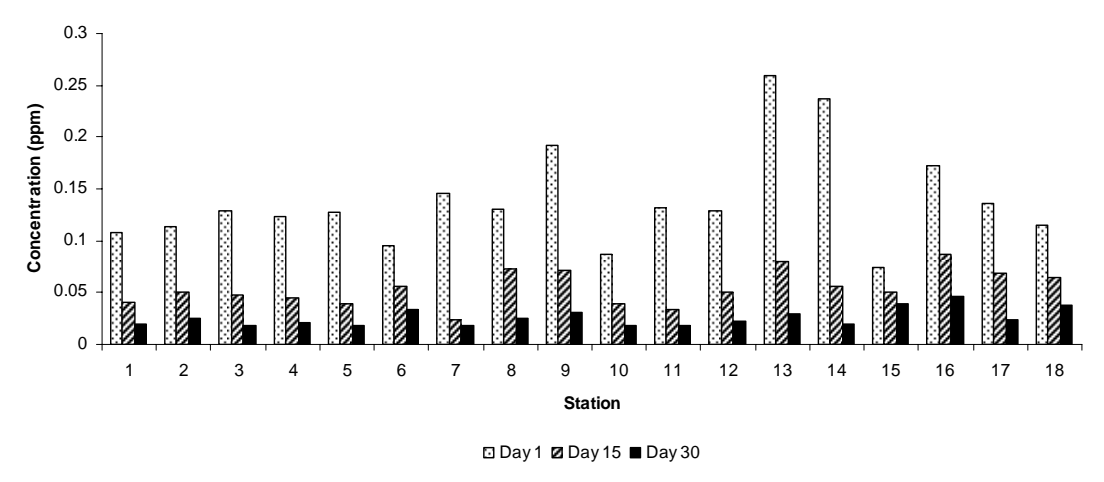


Figure 4. Concentration of malathion residues in soils for a period of 30 days after application

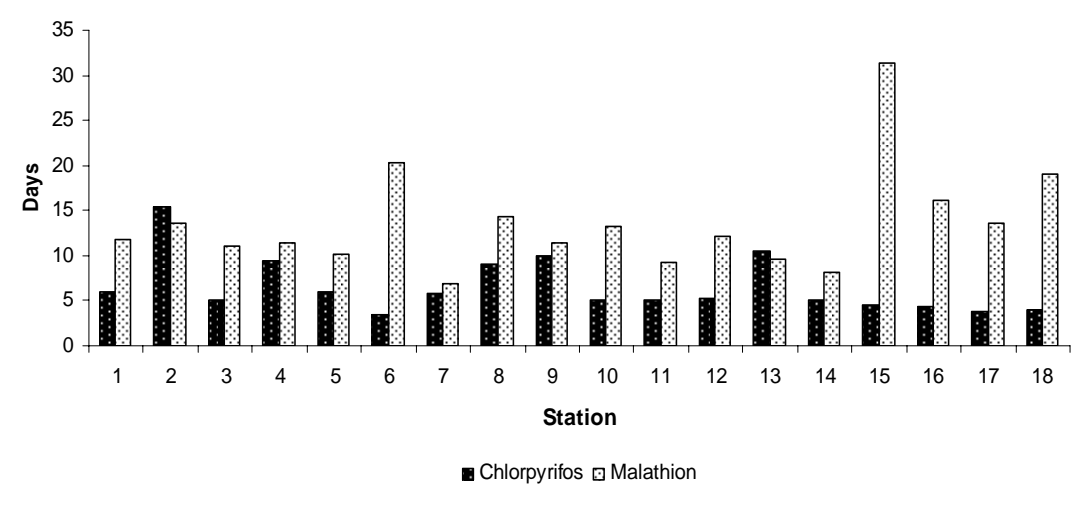


Figure 5. Half-life of chlorpyrifos and malathion under field condition

Using the data obtained, the half-lifes of chlorpyrifos and malathion were calculated assuming the dissipation reaction follows a first order reaction kinetic. The equation used was  $C=C_oe^{kt}$  where C is the concentration of insecticide after time t,  $C_o$  is the apparent initial concentration, k is the rate constant and t is time in days. A plot of ln C against time would yield a negative slope; the rate constant can thus be obtained from the slope. Good linearity was obtained with  $R^2$  value greater than 0.95 for all the stations suggests that the dissipation rate for these two insecticides actually follows the first order kinetic.

## Norhayati Mohd Tahir et al: CHLORPYRIFOS AND MALATHION RESIDUES IN SOILS OF A TERENGGANU GOLF COURSE: A CASE STUDY

For first order reaction, the half-life  $(t_{1/2})$  of a given insecticide is calculated using the equation,  $t_{1/2} = 0.693/k$ . In this study, the half-life for chlorpyrifos was relatively short with values ranging from 3.4 to 15.3 days with mean value of  $6.5 \pm 3.1$  days while for malathion, a significantly longer half-life was obtained with values ranging from 6.8 to 31.3 days with mean value of  $13.5 \pm 5.6$  days (Figure 5).

#### Conclusions

Results show that dissipation of the two insecticides were relatively fast with chlorpyrifos dissipating faster than malathion under field conditions. It was estimated that 65.0-96.6% of chlorpyrifos and 63.5-95.8% malathion dissipated after 30 days of application to the soils. The dissipation rate of these insecticides appeared to follow a first order kinetic with half-life values ranging from 3.4 to 15.3 days for chlorpyrifos and 6.8 to 31.3 days for malathion. Mean half-life calculated for the two insecticides was 6.50 and 13.5 days, respectively. It appears that soil physico-chemical properties *viz.* organic matter content, pH, particle size distribution, cationic exhange capacity and moisture content do not exert an influence on the dissipation of these insecticides.

#### Acknowledgement

The financial support from the Department of Chemical Sciences for the final year project student (KHS) is gratefully acknowledged. The cooperation given by the KT Golf Resort management is much appreciated. Assistance of Mr. Ruziman, Muzafeq, Aszrul and Mrs. Asbah is also acknowledged.

#### References

- National Golf Foundation (2003). Golf facilities in the U.S. 3<sup>rd</sup>. ed. The National Golf Foundation, Jupiter, Fl., USA, 41pp.
- 2. Larsboa, M., Aamlidb, T. S., Perssona, L., Jarvis, N. (2008). Fungicide Leaching from Golf Greens: Effects of Root Zone Composition and Surfactant Use. J Environ Qual., 37: 527-1535.
- 3. Metcalfe, T. L., Dillon, P. J., Metcalfe, C. D. (2008). Detecting the Transport of Toxic Pesticides from Golf Courses into Watersheds in the Precambrian Shield Region of Ontario, Canada. Environmental Toxicology and Chemistry. 27:811-818.
- 4. Kohler, E.A., Poole V.L., Reicher, Z.J., Turco, R.F. (2004). Nutrient, metal, and pesticides removal during storm and nonstorm events by a constructed wetland on an urban golf course. Ecological Engineering, 23:285-298.
- 5. Cai, Y., Cabrera, J. C., Georgiadis, M., Jayachandran, K. (2002). Assessment of arsenic mobility in the soils of some golf courses in South Florida. The Sci. of Total Environ. 291:123-134.
- 6. Mazlin, M., Lee Y. H., Hazirah, M.N. (2001). Water quality of discharge from a golf course and its effect on the Langat River: Towards an intergrated river management. Malays. J. Anal. Sci. 6(1):157-161.
- 7. Starrett, S.K., Christians, N.E., Austin, T. Al. (2000). Movement of herbicides under two irrigation regimes applied to turfgrass. Advances in Environ. Res. 4:169-176
- 8. Starrett, S.K., Christians, N.E., Austin, T. Al. (1996). Movement of herbicides under two irrigation regimes applied to turfgrass. J. Environ. Qual. 25(3):566-571.
- 9. Horst, G.L., Shea, P.J., Christians, N.E., Miller, D.R., Stuefer-Powell, C.L., Starrett, S.K. (1996). Pesticide dissipation under golf course fairway conditions. Crop Sci., 36:362-370.
- 10. Cisar, J.L., Snyder, G.H., (1996). Mobility and persistence of pesticides applied to a USGA green, III: Organophosphate recovery in clippings, thatch, soil, and percolate. Crop Sci. 36:1433-1438.
- 11. Smith, A.E., Bridges, D.C. (1996). Movement of certain herbicides following application to simulated golf course greens and fairways. Crop Sci. 36:1439-1445.
- 12. Matthews, S.L. (1995). Mercury Contamination of golf courses due to pesticide use. Bull. Environ. Contam. Toxicol. 55:390-398.
- 13. EPA Standard Methods (1997). Compilation of EPA Samplings and Analytical Methods. Third edition, Keith, L. (ed). ISBN 1-5667-0170-8.
- 14. Lim, H.K. (1975) Working manual for soil analysis. Ministry of Agriculture Malaysia, Kuala Lumpur.

## SYNTHESIS AND CHARACTERIZATION OF SEVERAL LAURYL CHITOSAN DERIVATIVES

(Sintesis dan Pencirian Beberapa Terbitan Lauril Kitosan)

Nadhratun Naiim Mobarak, Md.Pauzi Abdullah\*

School of Chemical Sciences and Food Technology, Faculty of Science and Technology, Universiti Kebangsaan Malaysia, 43600 UKM Bangi, Selangor Darul Ehsan, Malaysia

\*Corresponding author: mpauzi@ukm.my

#### Abstract

Three derivatives of chitosan namely lauryl chitosan, lauryl succinyl chitosan and lauryl carboxymethyl chitosan had been synthesized in this study. The synthesis of lauryl carboxymethyl chitosan and lauryl succinyl chitosan require two steps of reaction whereas for lauryl chitosan only one step was required. Lauryl carboxymethyl chitosan was prepared by reacting chitosan with monochloroacetic acid to form carboxymethyl chitosan. The synthesis of lauryl succinyl chitosan involved the reaction between chitosan with succinic anhydride to form succinyl chitosan. After that, the carboxymethyl chitosan and succinyl chitosan were reacted with dodecanal to form lauryl carboxymethyl chitosan and lauryl succinyl chitosan, respectively. The addition of lauryl group onto the derivative aim at producing chitosan derivatives having both hydrophobic and hydrophillic properties. The chemical structures of the derivatives were characterized by Fourier Transform Infrared (FTIR), <sup>1</sup>H Nuclear Magnetic Resonance (<sup>1</sup>H NMR) and Elemental Analysis (CHNS). In the IR spectrum of carboxymethyl chitosan and succinyl chitosan, peaks at 1645-1630 cm<sup>-1</sup>, representing C=O were clearly seen. After the substitution of lauryl group on the derivatives, the presence of peaks at 2930-2860 cm<sup>-1</sup> indicates the C-H stretching of lauryl group. The presence of lauryl group was further supported by the presence of peaks at about 0.8-1.7 ppm in the <sup>1</sup>H NMR spectra that assigned for hydrogen that attached to lauryl group. Elemental analysis was used to compare the derivatives prepared with the theoretical values.

Keywords: Hydrophilic, Hydrophobic and Chitosan.

#### Abstrak

Tiga terbitan kitosan iaitu lauril kitosan, lauril karboksimetil kitosan dan lauril suksinil kitosan telah di sintesis. Proses penyediaan lauril karboksimetil kitosan dan lauril suksinil kitosan melibatkan dua langkah tindak balas manakala lauril kitosan hanya melibatkan satu langkah tindakbalas. Lauril karboksimetil kitosan disediakan dengan mensintesis karboksimetil kitosan terlebih dahulu melalui tindak balas kitosan dengan asid monokloroasetik. Manakala lauril suksinil kitosan pula disediakan dengan mensintesis suksinil kitosan terlebih dahulu melalui tindakbalas di antara kitosan dengan suksinil anhidrida. Kemudian, karboksimetil kitosan dan suksinil kitosan ditindakbalaskan dengan dodekenal untuk menghasilkan lauril karboksimetil kitosan dan lauril suksinil kitosan. Penambahan kumpulan lauril pada terbitan yang terhasil adalah bertujuan untuk menghasilkan terbitan kitosan yang mempunyai kedua-dua sifat iaitu sifat hidrofilik dan hidrofobik. Terbitan kitosan tersebut telah dicirikan dengan menggunakan Spektroskopi Inframerah (FTIR), Resonan Magnetik Nukleus (RMN) dan analisis unsur (CHNS). Berdasarkan data FTIR, bagi terbitan karboksimetil kitosan dan suksinil kitosan, terdapat puncak pada 1645-1630 cm<sup>-1</sup> yang menunjukkan kehadiran kumpulan C=O. Namun begitu, setelah kemasukkan kumpulan lauril pada terbitan tersebut terdapat kehadiran puncak pada 2930-2860 cm<sup>-1</sup> yang menunjukkan regangan C-H pada kumpulan lauril. Puncak ini juga hadir pada spektrum FTIR bagi lauril kitosan. Kehadiran kumpulan lauril pada ketiga-tiga terbitan seterusnya disokong dengan kehadiran puncak pada 0.8-1.7 ppm pada spektrum H-NMR. Analisis CHNS digunakan untuk membandingkan peratus unsur dalam terbitan yang disintesis dengan nilai teori.

Kata kunci: Hidrofilik, hidrofobik dan kitosan.

## Introduction

Chitosan were obtained from partial deacetylation of chitin. It compose of  $\beta$ -(1,4)-2-amino-2-deoxy-D-glucopyranose(GLcNAc) residues. Previous studies proved that chitosan have various properties such as antibacterial, non-toxicity, biodegradability, haemocompatible and biocompatibility. All of these properties make it become an attractive biomaterial [1]. However, chitosan has poor solubility in water. In order to improve its water solubility, some chemical modification of chitosan was carried out [2]. Chemical structure of chitosan contains two hydroxyls and one amino group. The general reaction for formation

of lauryl derivatives chitosan was shown in Figure 1 and all chitosan derivatives had been synthesized were listed in Table 1.

In the past, many studies had been focused on improvement of the solubility of chitosan e.g. the insertion of hydrophilic group onto chitosan where the derivatives that had formed such as carboxymethyl chitosan, succinyl chitosan, hydroxylalkyl and many more [2]. Besides that, insertion of the hydrophobic group onto chitosan had formed the derivatives such as N-pentyl-chitosan, N-pentylidene-chitosan and many more [3]. Insertion of both groups also can be done into chitosan [4, 5, 6, 11].

In this study, substitution of both hydrophobic and hydrophilic groups into chitosan structure were performed. The derivatives studied were lauryl chitosan, lauryl carboxymethyl chitosan and lauryl succinyl chitosan. The derivatives were characterized by means of Fourier Transform Infra Red (FTIR) spectroscopy, <sup>1</sup>H Nuclear Magnetic Resonance Spetroscopy (<sup>1</sup>H-NMR) and elemental analysis (CHNS).

$$\begin{array}{c|c}
CH_2OH \\
OH \\
OH
\end{array}$$

$$\begin{array}{c|c}
CH_2OA \\
OA \\
OA
\end{array}$$

$$\begin{array}{c|c}
CH_2OA \\
OA \\
OA
\end{array}$$

$$\begin{array}{c|c}
NB_1B_2
\end{array}$$
Chitosan Derivatives

Figure 1: General reaction for formation of lauryl chitosan derivatives

| Derivatives of chitosan             | Reaction step                           | A  | $B_1$         | $\mathrm{B}_2$  |
|-------------------------------------|---|--|---------------|---|
| Lauryl Chitosan                     | Lauryl aldehyde                         | -Н   | -H            | -CH <sub>2</sub> (CH <sub>2</sub> ) <sub>10</sub> CH <sub>3</sub> |
| Lauryl<br>Carboxymethyl<br>Chitosan | Monochloacetic acid     Lauryl aldehyde | -CH <sub>2</sub> COOH  | -H            | -CH <sub>2</sub> (CH <sub>2</sub> ) <sub>10</sub> CH <sub>3</sub> |
| Lauryl Succinyl<br>Chitosan         | Succinic anhydride     Lauryl aldehyde  | - С(ОН)Н<br>(СН <sub>2</sub> ) <sub>10</sub> СН <sub>3</sub> | -COCH₂CH₂COOH | -Н  |

Table 1: All chitosan derivatives synthesized

#### Materials and methods

## Reagents

Chitosan powder was supplied by Chito-chem Sdn Bhd., Malaysia. All commercially available solvents and reagents were used without further purification.

## Preparation of chitosan derivatives

#### Preparation of Lauryl Chitosan

Lauryl chitosan was prepared according to the Muzzarelli et al. [14] and Ramos et al. method [6]. Chitosan (1g) was suspended in a water-methanol 1:1 mixture (100 mL), lauryl aldehyde (1.5g) was added and stirred for 30 min. Reduction was carried out with sodium borohydride solution (0.5 g dissolve in 10 ml of water) for 2h with mechanical stirring. The preparation was left overnight. The reaction mixture was then neutralized with HCl 5M solution and the lauryl chitosan was precipitated with methanol. The precipitate was filtered and washed with 90% methanol/water, methanol, hexane and acetone.

### Preparation of Lauryl Carboxymethyl Chitosan

Carboxymethyl chitosan was prepared was prepared according to oleh Chen & Park method [7]. Chitosan (10g), sodium hydroxide (10g), isopropanol (50 mL) and water (50 mL) were added into a flask to swell and alkalize at a 50°C for 1 h. The monochloroacetic acid (15 g) was dissolved in isopropanol (20 mL), added into the reaction mixture drop-wise for 30 min and reacted for 4 h at the same temperature, then stopped by adding 70% ethyl alcohol (200 mL). The solid was filtered and rinsed in 70%, 80%, 90% ethyl alcohol, and dried at room temperature. The product was Na salt Carboxymethyl Chitosan. (Na-CC). Addition of lauryl group to Carboxymethyl Chitosan was done according to the method preparation of lauryl chitosan.

#### Preparation of Lauryl Succinyl Chitosan

Succinyl chitosan (SC) was prepared according to Zhu et al. method [8]. However, the solvent had been changed from acetone to ethanol during the rinsing process of precipitates. 1 g of chitosan was dissolved into 200 mL distilled water and then transferred into a flask. Succinic anhydride (0.2 g) was dissolve in acetone (20 mL) and added into the flask by drop-wise for 30 min at room temperature, and then the reaction was left for 4 h at 40°C. The reaction mixture was cooled to room temperature. The mixture precipitated in an excess of ethanol, was filtered to remove the solvent, and then washed with 70%, 80%, 90% ethanol, and dried at room temperature. Addition of lauryl group to succinyl chitosan was done according to the method preparation of lauryl chitosan.

#### Result and discussion

### Synthesis of chitosan derivatives

The introduction of a hydrophobic alkyl chain onto chitosan and its derivatives leads to the formation of chitosan derivatives with two group which are hydrophilic and hydrophobic group. In this study, the introduction of lauryl group where C12 chain gives rise to formation of lauryl chitosan (LC), lauryl carboxymethyl chitosan (LCC) and lauryl succinyl chitosan (LSC). All of these derivatives, namely carboxymethyl and succinyl act as hydrophilic moities while lauryl groups as hydrophobic one.

## **Characterization of derivatives**

Structure of chitosan and its derivatives were confirmed by FTIR spectra. The FTIR spectra of chitosan, carboxymethyl chitosan (CC), succinyl chitosan (SC), lauryl chitosan (LC), lauryl carboxymethyl chitosan (LCC) and lauryl succinyl chitosan (LSC) were given in Fig. 2a ,2b, 2c,2d, 2e and 2f. The main bands observed in the infrared spectrum of chitosan (Fig. 2a) were: (i) a broad band due to the stretching of O-H and N-H bond centred at 3429 cm<sup>-1</sup>, (ii) a band centred at 2923 cm<sup>-1</sup> corresponding to the stretching of C-H bonds; (iii) a band centred at 1642 cm<sup>-1</sup> which is attributed to the stretching of C-O bonds of the acetamide groups, named as amide I band; (iv) a band at 1377 cm<sup>-1</sup> due to the symmetric deformation of CH<sub>3</sub>; (vi) the amide III band at 1321cm<sup>-1</sup>; (vii) the band corresponding to the polysaccharide skeleton, including the vibrations of the glycoside bonds, C-O and C-O-C stretching, in the range 1148–896 cm<sup>-1</sup> [9].

## Nadhratun Naiim Mobarak & Md. Pauzi Abdullah: SYNTHESIS AND CHARACTERIZATION OF SEVERAL LAURYL DERIVATIVES

Based on the IR spectra of carboxymethyl chitosan (Fig. 2b), it was found that absorption bands appear at 1634 cm<sup>-1</sup> and 1406 cm<sup>-1</sup> while for succinyl chitosan (Fig. 2c) absorption bands appear at 1646 cm<sup>-1</sup> and 1402 cm<sup>-1</sup>. Both bands are due to asymmetric and symmetric stretching vibration of C=O, indicating a successful substitution of carboxyl groups. Stretching vibration of C=O for succinyl chitosan are higher compared to carboxymethyl chitosan because the carbonyl group in the succinyl chitosan are in the form of amide while carbonyl group in the carboxymethyl chitosan are in the form of carboxylate salts [10].

Lauryl group was attached covalently to the amino groups of chitosan and carboxymethyl chitosan while for succinyl chitosan, lauryl group was attached at the hydroxyl group. The IR spectra for native chitosan and the derivatives were compared. Substitution of lauryl group onto chitosan, carboxymethyl chitosan or succinyl chitosan leads to two absorption band around 2923 and 2855cm<sup>-1</sup> for C-H stretching. Besides that, bands where observed at 1527 cm<sup>-1</sup>, 1530 cm<sup>-1</sup> and due to deformation for amines. It proves that the substitution of chitosan by lauryl group occurred at N position for chitosan and carboxymethyl chitosan [10].

In addition, by comparing IR spectrum of lauryl chitosan(Fig. 2d), lauryl-CC (Fig. 2e) and lauryl-SC (Fig. 2f) with IR spectrum of chitosan (Fig. 2a), carboxymethyl chitosan (Fig. 2b), succinyl chitosan (Fig. 2c), the two peaks at 1074 and 1030 cm<sup>-1</sup> in the derivatives were attributed to the methyl rocking and C-CH<sub>3</sub> stretching vibration respectively of the lauryl group. All of these are evidences suggest that the hydrophilic group and hydrophobic group were introduced to chitosan [4].

The  $^1$ H NMR spectra of CC, LCC, SC, LSC and LC were given in Fig. 3a, 3b, 3c, 3d and 3e.  $^1$ H NMR spectra of lauryl chitosan (Fig. 3e):  $^1$ H NMR (CDCl<sub>3</sub>),  $\delta$ =4.81(H1),  $\delta$ =3.11(H2),  $\delta$ = 3.40-3.66 (H3, H4, H5, H6),  $\delta$ = 2.01 (NCOCH<sub>3</sub>),  $\delta$ = 0.89 (-NH-R-CH<sub>3</sub>;R=alkyl chain),  $\delta$ =1.27-1.65 (-(CH<sub>2</sub>)<sub>n</sub>-CH<sub>3</sub>) [10, 12, 4, 13].  $^1$ H NMR spectra of carboxymethyl chitosan (Fig. 3a):  $^1$ H NMR (D<sub>2</sub>O),  $\delta$ =4.80(H1),  $\delta$ =3.12(H2),  $\delta$ = 3.69-3.86 (H3, H4, H5, H6),  $\delta$ = 2.01 (NCOCH<sub>3</sub>),  $\delta$ = 3.69-3.86 (O-CH<sub>2</sub>-COO).  $^1$ H NMR spectra of lauryl carboxymethyl chitosan (Fig. 3b), there was a peak as follows:  $^1$ H NMR (CDCl<sub>3</sub>),  $\delta$ = 0.88 (-NH-R-CH<sub>3</sub>;R=alkyl chain),  $\delta$ =1.26-1.62 (NH-(CH<sub>2</sub>)<sub>11</sub>-CH<sub>3</sub>) [10, 12, 4, 13].

While  $^1H$  NMR spectra of succinyl chitosan (Fig. 3c):  $^1H$  NMR (D<sub>2</sub>O),  $\delta$ =4.88(H1),  $\delta$ =3.12(H2),  $\delta$ =3.66-3.82 (H3, H4, H5, H6),  $\delta$ =1.92 (NCOCH<sub>3</sub>),  $\delta$ =2.45-2.55(NCO-CH<sub>2</sub>-COOH).  $^1H$  NMR spectra of lauryl succinyl chitosan (Fig. 3d), there was a peak as follows:  $^1H$  NMR (CDCl<sub>3</sub>),  $\delta$ =0.89 (-O-R-CH<sub>3</sub>;R=rantai alkil),  $\delta$ =1.26-1.60 (O-CH(OH)(CH<sub>2</sub>)<sub>10</sub>-CH<sub>3</sub>),  $\delta$ =3.56 (O-CH(OH)-R)) [10, 12, 4, 13].  $^1H$ -NMR data showed that the, lauryl group bound to N atom for lauryl chitosan and lauryl carboxymethyl chitosan. While lauryl group bound to O atom for lauryl succinyl chitosan.

The degrees of substitution were calculated by comparing the C and N ratio obtained from element analysis in each derivative. The increase in the C/N ratio indicates the increasing carbon in monosaccharides include one nitrogen. For example, in the case of carboxymethylation, carboxymethyl group includes 2 carbons; therefore, the degree of carboxymethylation was estimated from the increasing-molar ratio/2 [11]. While, the substitution of lauryl group involve 12 carbons; so the degree of laurylation was estimated from the increasing-molar ratio/12. The degrees of carboxymethylation, succinylation and laurylation were shown in Table 2. Between all the three derivatives, lauryl chitosan show the highest degree of substitution (DS). This is because; lauryl chitosan only involved one step of preparation while lauryl carboxymethyl chitosan and lauryl succinyl chitosan was higher than the lauryl chitosan.

Table 2: Elemental Analyses and the Degree of Substitution (DS) of Chitosan Derivatives

|                                  | Found | d %  |      |      |
|----------------------------------|-------|------|------|------|
| Derivatives                      | С     | N    | C/N  | DS   |
| Chitosan                         | 38.51 | 7.24 | 6.20 |      |
| Carboxymethyl Chitosan           | 28.90 | 5.33 | 6.33 | 0.03 |
| Succinyl Chitosan                | 36.08 | 5.47 | 7.69 | 0.37 |
| Lauryl Chitosan                  | 40.60 | 5.18 | 9.14 | 0.25 |
| Lauryl Carboxymethyl<br>Chitosan | 31.44 | 4.56 | 8.04 | 0.14 |
| Lauryl Succinyl chitosan         | 32.27 | 4.35 | 8.65 | 0.08 |

#### Conclusion

Three derivatives of chitosan had been synthesized namely lauryl chitosan, lauryl succinyl chitosan and lauryl carboxymethyl chitosan by introducing lauryl group into chitosan, carboxmethyl chitosan or succinyl chitosan. The chemical structures of the three derivatives were characterized by FTIR, <sup>1</sup>H NMR and elemental analysis. IR studies confirmed the appearance of C=O and lauryl group at chitosan derivatives. It also supported by <sup>1</sup>H-NMR data. These indicate hydrophobic and hydropholic group was attached to the chitosan derivatives.

#### Acknowledgement

The authors wish to thank PPSKTM, UKM for the instrumentations and the Ministry of Sciences, Technology and Innovation (MOSTI) for supported this work by its grant 02-01-02 SF0125.

#### References

- 1. Ma, G., Yang, D., Kennedy, J.F. & Nie, J. 2008. Synthesize and characterization of organic-soluble acylated chitosan. *Carbohydrate Polymers*. 75: 390-394.
- 2. Rinaudo, M. 2006. Chitin and chitosan: Properties and application. *Progress in Polymer Science*.31: 603-632.
- 3. Kurita, K., Mori, S., Nishiyama, Y. & Harata, M. 2002. N-Alkylation of chitin and some characteristics of the novel derivatives. *Polymer Bulletin*.48:159-166.
- 4. Sui, W., Wang, Y., Dong, S. & Chen, Y. 2008. Preparation and properties of an amphiphilic derivative of succinyl-chitosan. *Colloids and Surfaces A: Physicochem. Eng. Aspects.* 316: 171-175.
- 5. Tikhonov, V.E., Stepnova, E.A, Babak, V.G., Krakyukhina, M.A., Brezin, B.B. & Yamskov, I.A. 2008. *Reactive & Functional Polymers*. 68: 436-445.
- 6. Ramos, V.M., Rodriguez, N.M., Rodriguez, M.S., Heras, A. & Agullo, E. 2003. Modified chitosan carrying phosphonic and alkyl groups. *Carbohydrate Polymers*. 51:425-429.
- 7. Chen, X.G. & Park, H.J. 2003. Chemical characteristics of O-carboxymethyl chitosans related to the preparation conditions. *Carbohydrate Polymers* 53: 355-359.
- 8. Zhu, A., Yuan, L. & Lu, Y. 2007. Synthesis and aggregation behavior of N-succinyl-O-carboxymethylchitosan in aqueous solutions. Colloids Polymer Science 285:1535-1541.
- 9. Elsabee, M.Z, Morsi, R.E. & Al-Sabagh, A.M. 2009. Surface active properties of chitosan and its derivatives. *Colloids and Surfaces B: Biointerfaces*, 74:1-16.

## Nadhratun Naiim Mobarak & Md. Pauzi Abdullah: SYNTHESIS AND CHARACTERIZATION OF SEVERAL LAURYL DERIVATIVES

- 10. Pavia, D.L., Lampman, G.M., & Kriz, G.S. 2001. "Introduction to spectroscopy", third edition/Ed.
- 11. Miwa, A., Ishibe, A., Nakano, M., Yamahira, T., Itai, S., Jinno, S., & Kawahara, H. 1998. Development of Novel Chitosan Derivatives as Micellar Carriers of Taxol. *Pharmaceutical Research*. 15(12):1844-1850.
- 12. Zhang, C., Ping, Q., Zhang, H. & Shen, J. 2003. Synthesis and characterization of water soluble O-succinyl-chitosan. *European Polymer Journal* 39 1629-1634.
- 13. Aiping, Z., Lanhua, Y. & Yan, L. 2007. Synthesis and aggregation behavior of N-succinylocarboxymethylchitosan in aqueous solutions. *Colloid Polym Sci* 285: 1534-1541.
- 14. Muzzarelli, R.A.A,Frega, N., Miliani, M.,Muzzarelli, C. & Cartolari, M. 2000. Interaction of chitin, chitosan, N-lauryl chitosan and N-dimethylaminopropyl chitosan with olive oil. *Carbohydrate Polymers* 43:263-268.

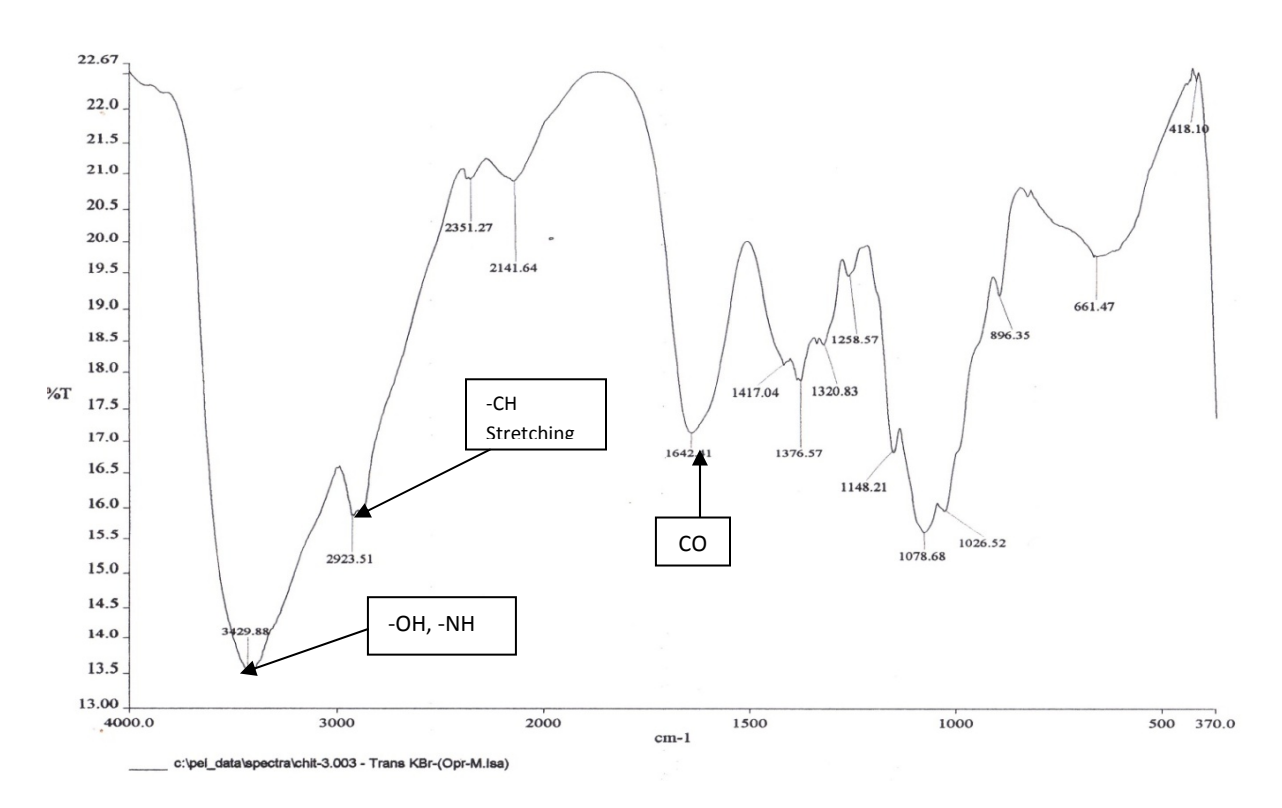


Fig 2a: FTIR spectrum of Chitosan

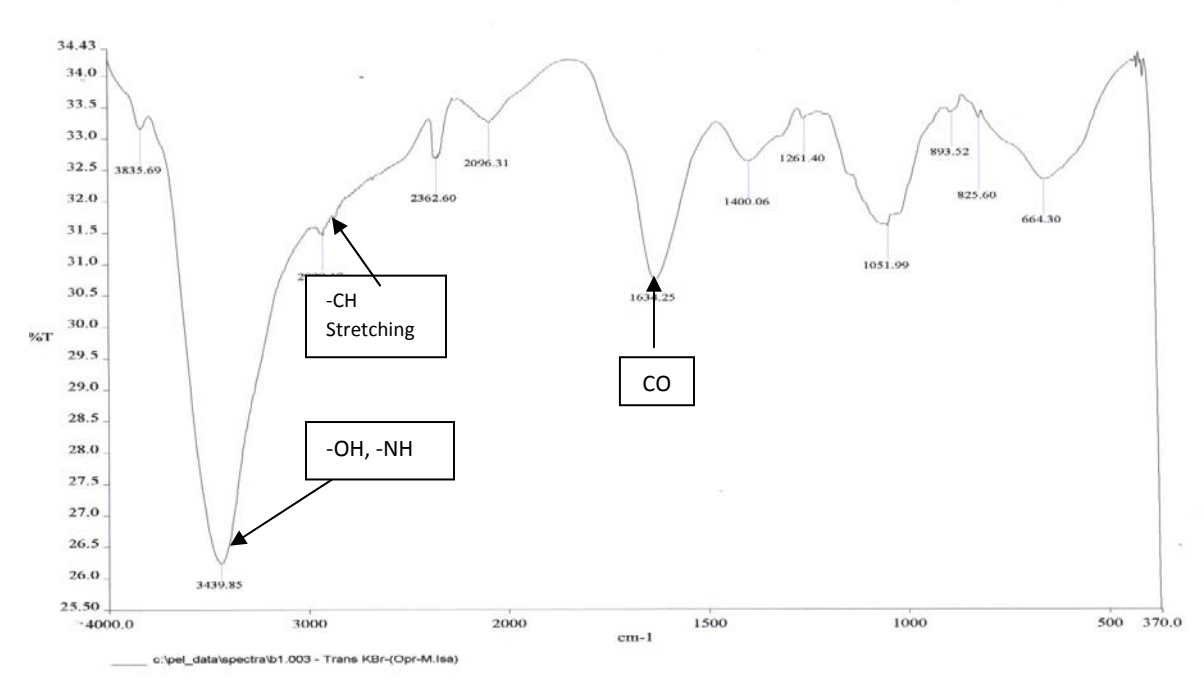


Fig. 2b: FTIR spectrum of Carboxymethyl Chitosan

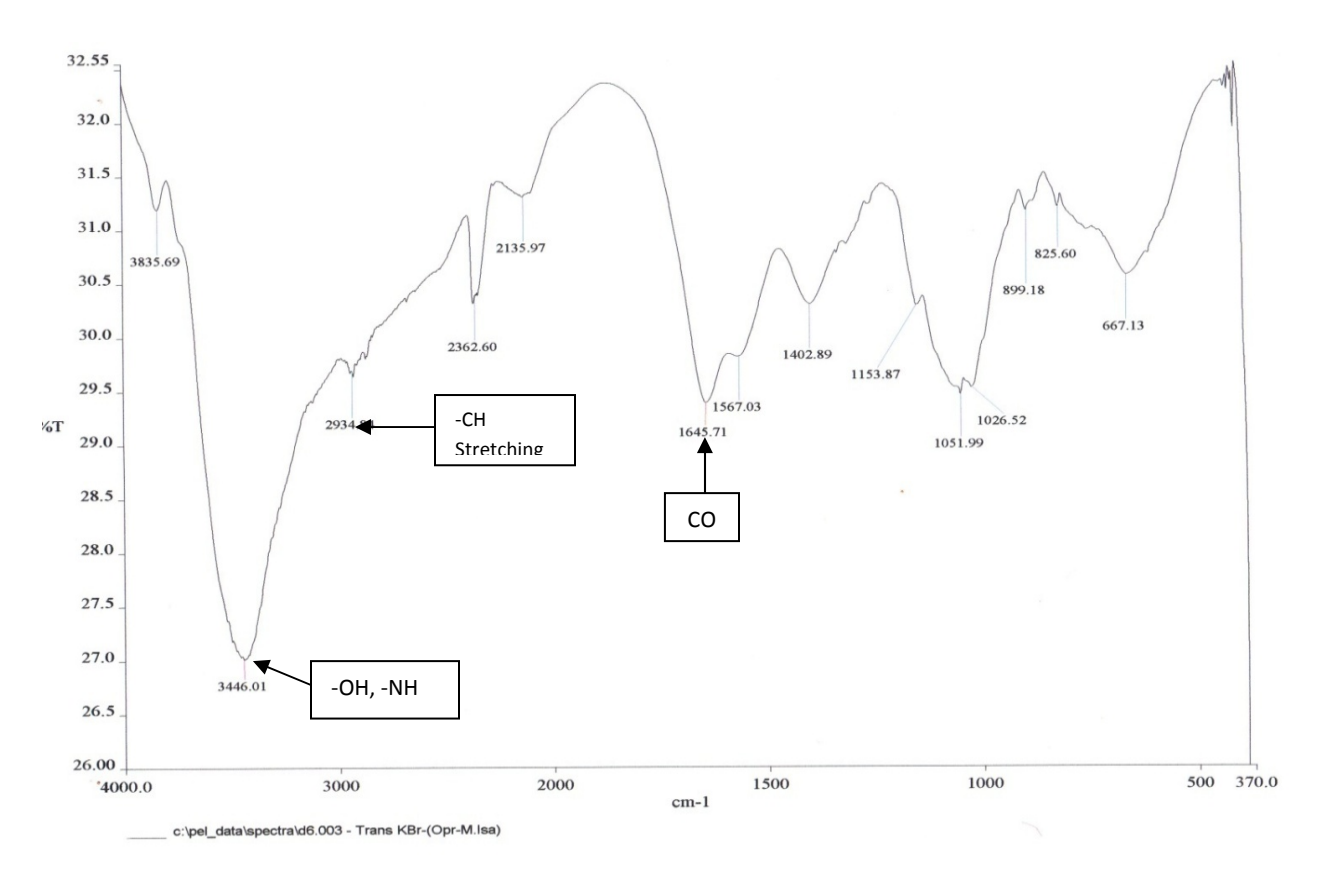


Fig 2c: FTIR spectrum of Succinyl Chitosan

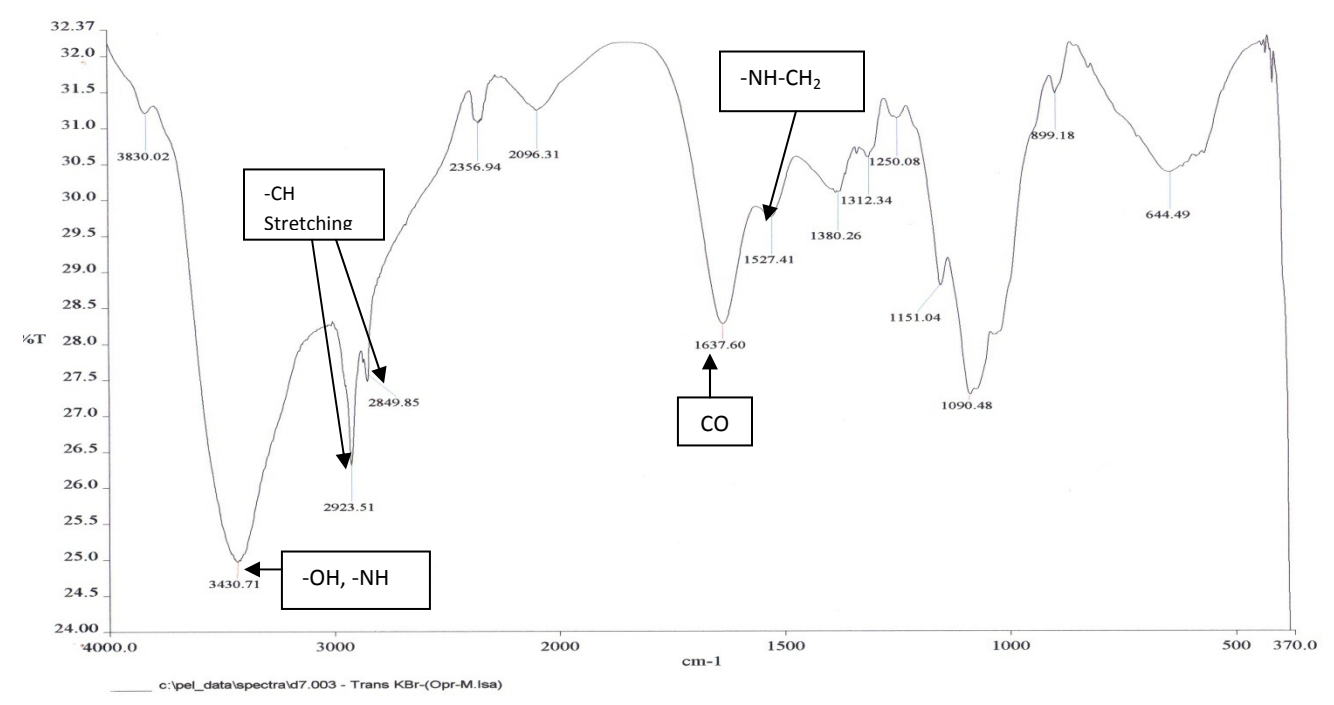


Fig 2d: FTIR spectrum of Lauryl Chitosan

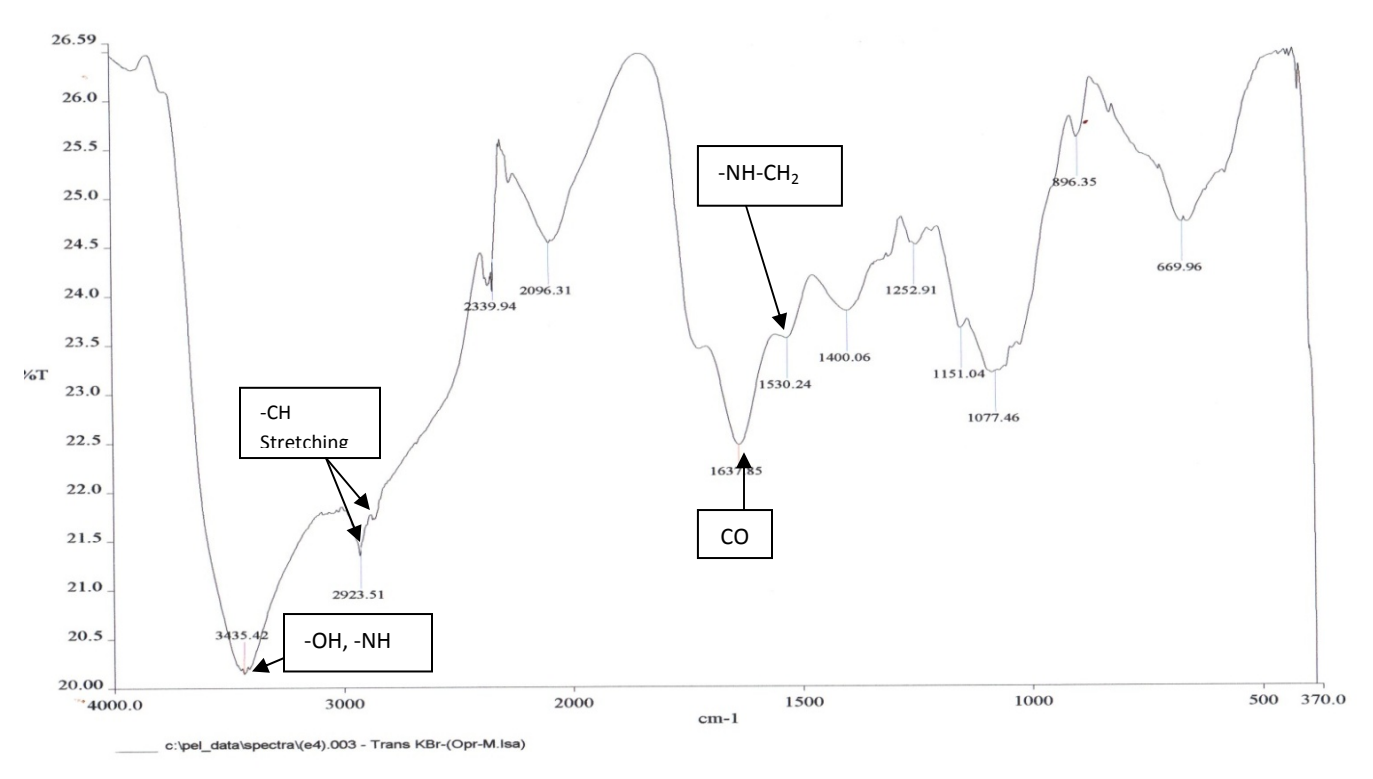


Fig 2e: FTIR spectrum of lauryl carboxymethyl chitosan

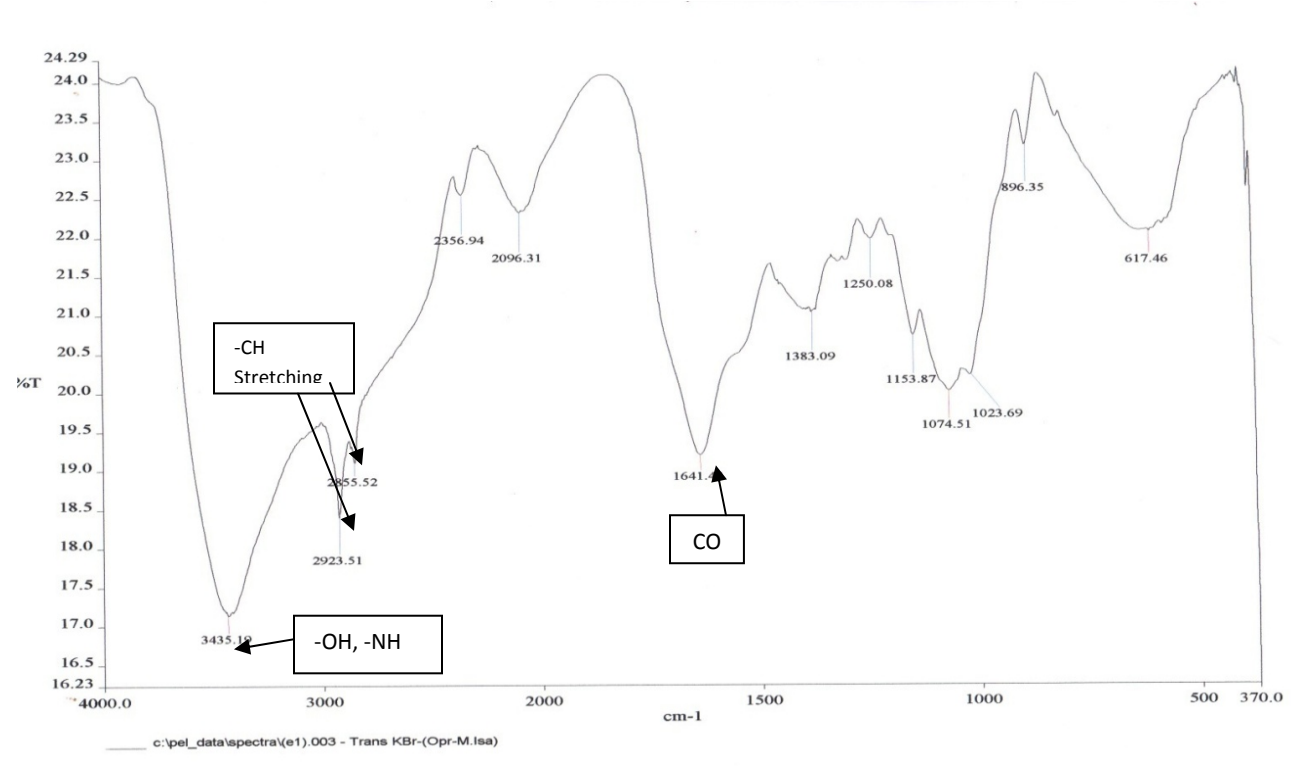


Fig 2f: FTIR spectrum of lauryl succinyl chitosan

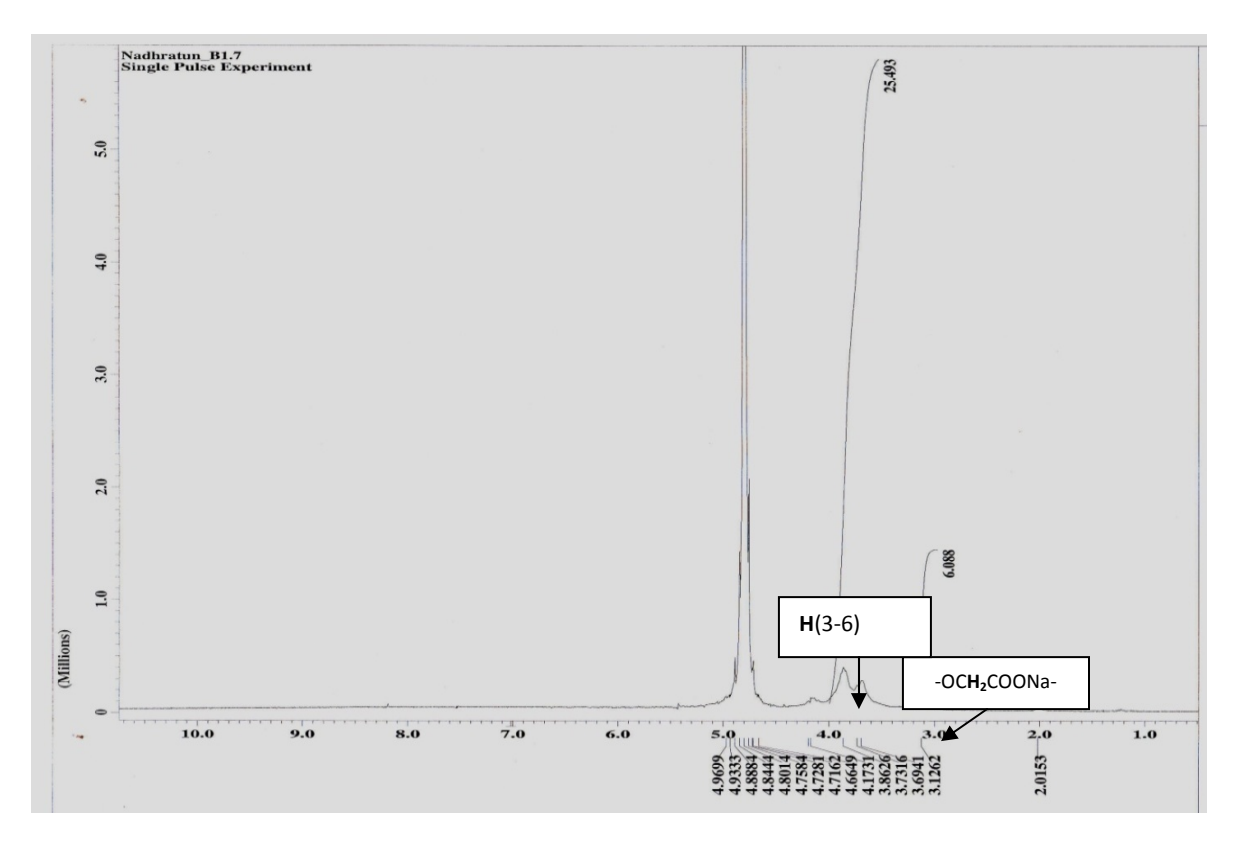


Fig 3a: NMR spectrum of carboxymethyl chitosan

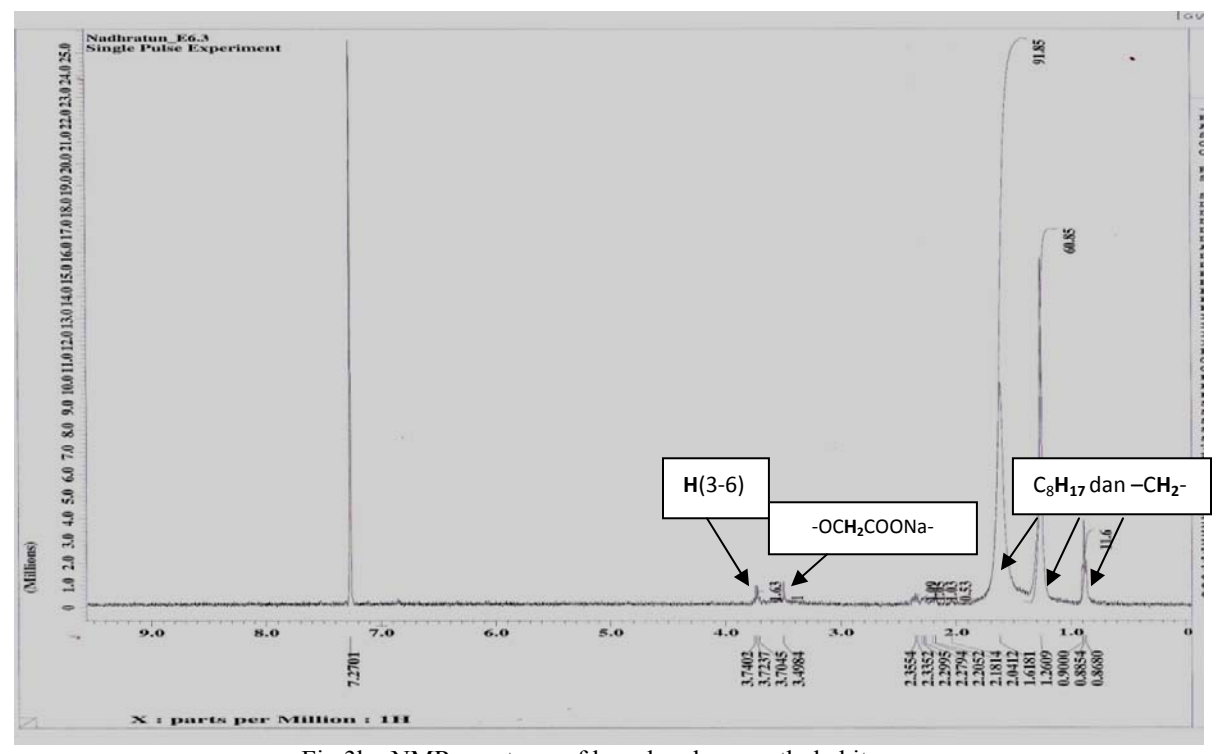


Fig 3b: NMR spectrum of lauryl carboxymethyl chitosan

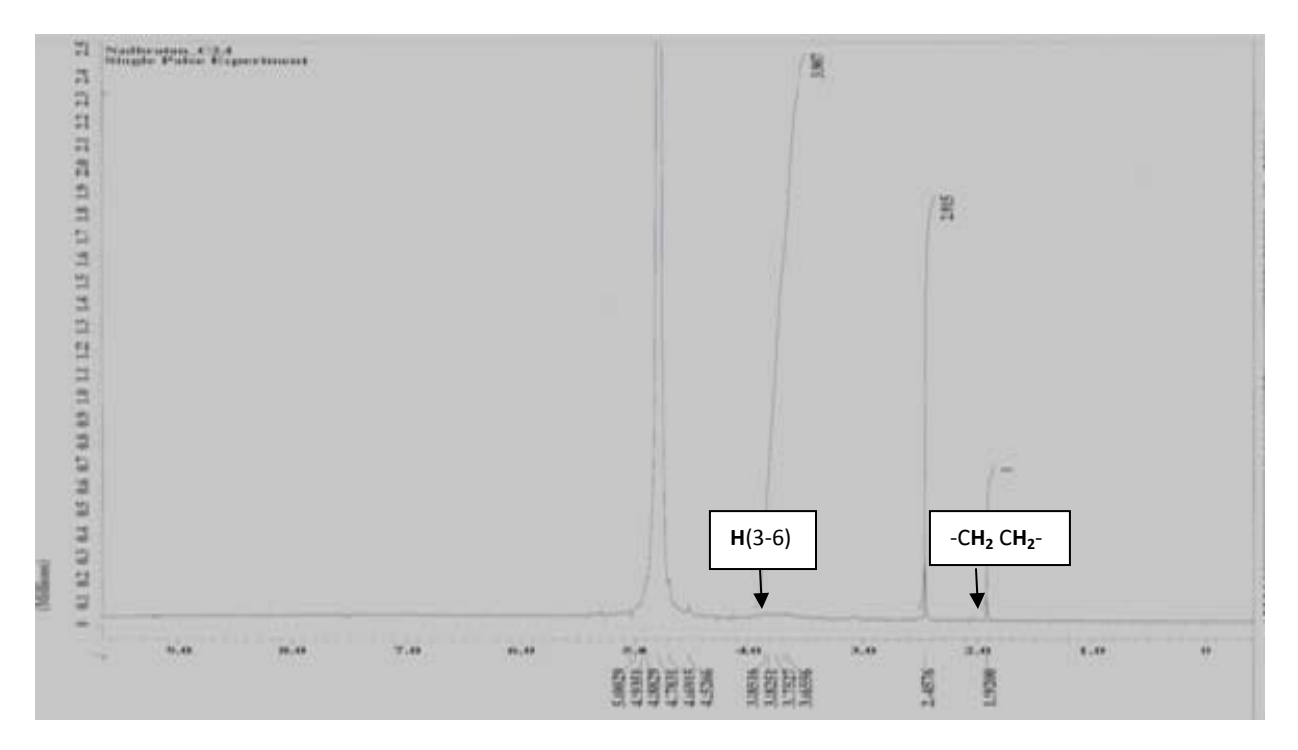


Fig 3c: NMR spectrum of succinyl chitosan

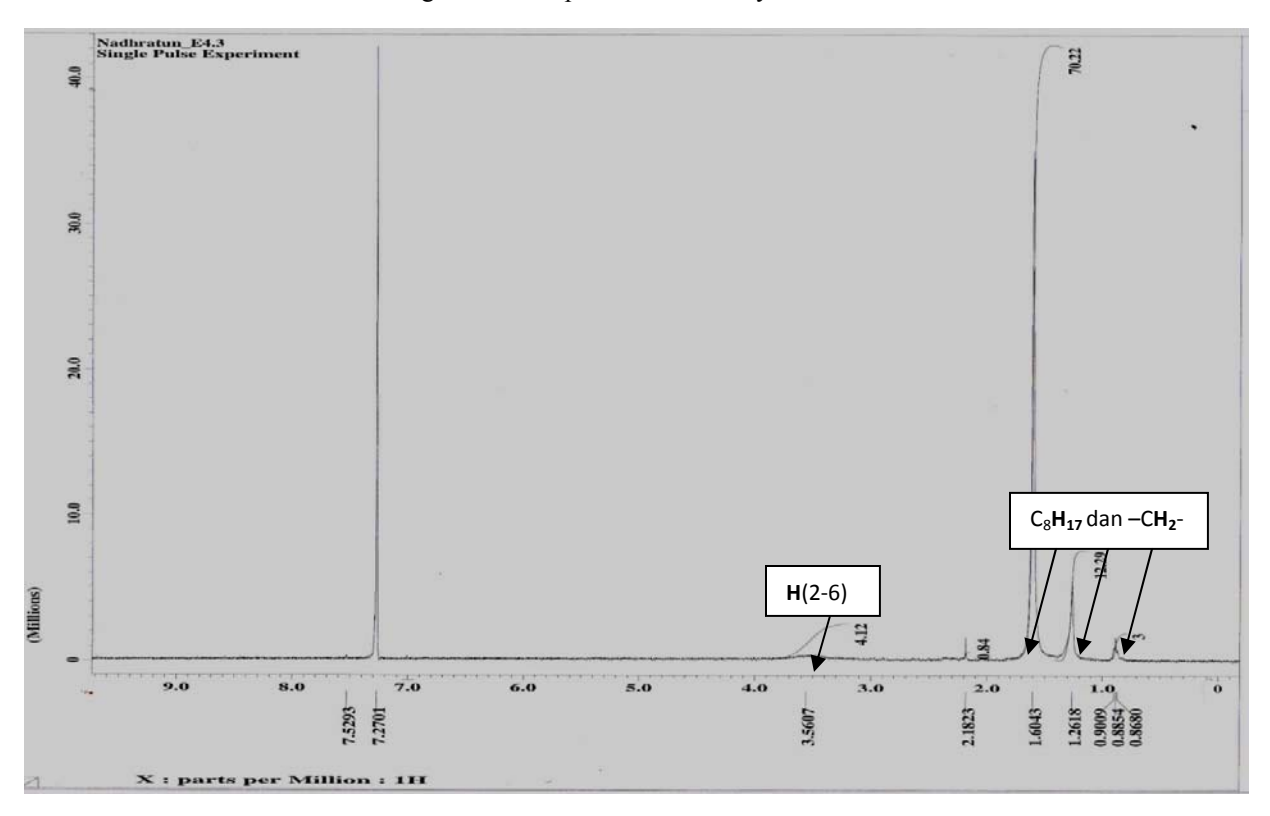


Fig 3d: NMR spectrum of lauryl succinyl chitosan

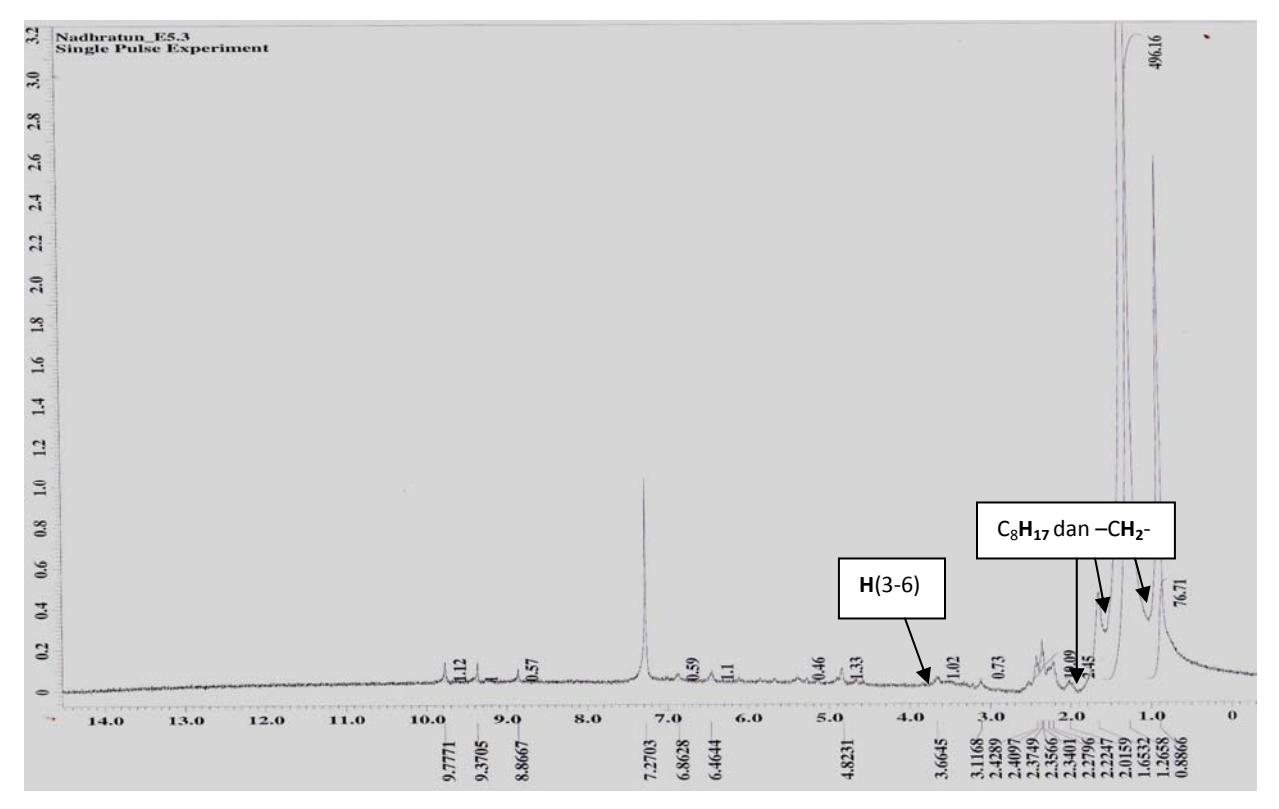


Fig 3e: NMR spectrum of lauryl chitosan

# EXTRACTION OF Eu (III) IN MONAZITE FROM SOILS CONTAINING 'AMANG' COLLECTED FROM KG GAJAH EX-MINING AREA

(Ekstraksi Eu(III) Dalam Monazit Daripada Tanah Yang Mengandungi Amang Dari Kawasan Bekas Lombong Kg Gajah)

Zaini Hamzah<sup>1</sup>, Nor Monica Ahmad<sup>1\*</sup>, Ahmad Saat<sup>2</sup>

<sup>1</sup>Faculty of Applied Sciences, <sup>2</sup>Institute of Science (IOS), Universiti Teknologi MARA (UiTM), 40450 Shah Alam, Selangor Darul Ehsan, Malaysia

\*Corresponding author: normonica@gmail.com

#### Abstract

Malaysia was once a major tin exporting country. One of the by-products of the tin-mining activities is tin-tailing which known as `amang` very rich in rare earth elements, especially the lanthanides which are present as a mixture of phosphate minerals, mainly as ilmenite, xenotime and monazite. In this study, Kg Gajah in Kinta Valley occupying the State of Perak was chosen as a study area, since this area used to be the largest mining area in the 60's and 70's. The soil samples were separated using wet separation technique followed by magnetic separation. The monazite was then digested using a mixture of HF/HNO<sub>3</sub> acids. The digested sample was extracted for its cerium content. The extraction behaviour of cerium in those samples has been investigated as a function of Cyanex 302 concentration in diluents and the time taken to reach the equilibrium. Extractant of bis(2,4,4-trimethylpentyl)-mono-thiophosphinic acid (Cyanex302) in n-heptane was used throughout the analysis. Aqueous phase from extraction was analyzed spectrometrically using Arsenazo (III) while organic phase was subjected to rotavapour followed by analysis by FTIR. The aim of this study is to have the best concentration for Cyanex302 in order to extract as much as possible of Europium and to confirm the transfer of Eu (III) to the Cyanex 302 as an extractant. Result from UV/VIS shows that 0.7 M is the best concentration of Cyanex 302 for the Eu (III) extraction from samples. Result from FTIR confirmed the structure of Cyanex302 has been replaced by Ce(IV).

Keyword: `Amang`, Rare earth elements (REE), Cyanex302, Arsenazo III

#### Abstrak

Malaysia pernah menjadi negara pengekspot timah yang utama. Salah satu dari hasil sampingan aktiviti lombong bijih timah ialah tahi bijih yang dikenali sebagai 'amang' yang kaya dengan unsur nadir bumi, terutamanya lantanid yang wujud sebagai campuran mineral fosfat, terutamanya ilminit, xenotim dan monazit. Di dalam kajian ini, Kg Gajah dalam kawasan Lembah Kinta di negeri Perak telah dipilih sebagai kawasan kajian, memandangkan kawasan ini pernah menjadi kawasan lombong timah terbesar dalam tahun 60an dan 70an. Sampel tanah diasingkan menggunakan teknik pemisahan basah dikuti dengan pemisahan magnet. Monozit kemudiannya dihadhamkan menggunakan campuran asid HF/HNO<sub>3</sub>. Sampel yang telah hadham telah diekstrak kandungan europiumnya. Sifat pengekstrakan europium di dalam sample tersebut telah dikaji sebagai fungsi kepekatan Cyanex 302 di dalam pelarut dan juga masa yang diambil untuk mencapai keseimbangan. Pengekstrak bis(2,4,4-trimethylpentyl)-monothiophosphinic acid (Cyanex 302) dalam toluen telah digunakan sepanjang analysis. Fasa akuas dari pengektrakan ini telah dianalisis secara spektrometri menggunakan Arsenazo (III), manakala fasa organik telah dikeringkan menggunakan rotavapour sebelum dianalisis menggunakan spektrometer FTIR. Objektif kajian ini adalah untuk mendapatkan kepekatan terbaik bagi Cyanex 302 untuk mengekstrak sebanyak mungkin europium, dan memastikan pemindahan Eu ke dalam Cyanex 302. Hasil analisis UV/VIS menunjukan bahawa 0.7 M adalah merupakan kepekatan terbaik Cyanex 302 untuk ekstraksi Eu dari sampel. Hasil analisis FTIR mengesahkan bahawa struktur Cyanex 302 telah pun digantikan oleh Ce(IV).

Kata kunci: 'Amang', unsur nadir bumi, Cyanex 302, Arsenazo III

#### Introduction

Worobiec *et al* [1] and Walsh [2] have reported that beach sand and rock is a mineral resources other than exmining area. However, former tin mining areas contained minerals which will be economically beneficial to the mineral industries. Tin ores were processed using a physical property (wet processing technique or smelting process) to recover the tin. 'Amang' is a widely accepted term in Malaysia for the heavy mineral rejects which

## Zaini Hamzah et al: EXTRACTION OF Eu (III) IN MONAZITE FROM SOILS CONTAINING 'AMANG' COLLECTED FROM KG GAJAH EX-MINING AREA

remain after tin oxide (cassiterite) has been extracted from tin ore [3]. The remaining ('amang') were left there since not many people knew their uses. Nowaday, 'amang' is becoming more important since one can recover valuable heavy minerals from it. Some examples of heavy minerals are monazite ([Ce, La, Nd, Gd, Th] PO<sub>4</sub>), zircon (ZrSiO<sub>4</sub>), ilmenite (FeOTiO<sub>2</sub>), xenotime (YPO<sub>4</sub>) and struverite (Nb.Ta.TiO<sub>2</sub>) which have various uses in minerals industries [4].

High grade (99.99%) europium oxide has important uses as red phosphor in television screen and in computer monitors, compact fluorescent light bulbs, X-ray and tomography scans, X-ray screen, high intensity mercury vapour lamps, neutron scintillations, charge particle detectors and optically read memory systems. Europhium is one of the least abundant of the rare earth elements, accounting for only 0.05-0.10% of the total rare earth content in its ores [5, 6].

Solvent extraction is generally used as the separation method for rare earth metals [7]. Extracting agents of industrial importance include tri-n-butyl phosphate, dimethyl heptyl methyl phosphonate, di (2-ethylhexyl) phosphoric acid, 2-ethylhexyl phosphoric acid mono 2-ethylhexyl ester, tetra decyl phosphoric acid and naphtenic acid [8]. Lanthanide elements are well chelated by phosphorous compounds such as phosphoric acid and phosphonic acid [9]. Cyanex302 consists of bis-(2,4,4-trimethylpentyl) mono-thiophosphinic acid, tris-alkylphosphine oxide, bis-(2,4,4-trimethylpentyl) phosphinic acid, bis-(2,4,4-trimethylpentyl)-dithiophosphinic acid, and other unknown components. A lot of work has been done on rare earth ion extraction from hydrochloric acid, nitric acid and sulfuric acid media using Cyanex302 as and extractant [10].

The use of organic dyes for the spectrometric determination of actinides including uranium, in various materials has been reported to be simple and selective. Among these, the sodium salt of Arsenazo-III has been reported to be more sensitive than other chromogenic reagents this type, such as Arsenazo-1and thorane. In other words, by specifying the pH it is possible to use Arsenazo-III very selectively. It is a commercial product, equally soluble in both water and dilutes mineral acids [11]. Arsenazo-III is a dye that forms a colored complex with europium in an acidic solution at pH 3.

A portion of the minerals were then extracted for the europium content within the minerals and the analysis was done using UV/VIS and FTIR. The aim of this study is to study the effect of Cyanex302 concentration to the extraction of Eu(III) in monazite type minerals, to confirm the ion exchange mechanism in solvent extraction and to validate the method used for the extraction procedure.

## **Experimental**

The spectrophotometric analysis was performed on a UV/VIS spectrophotometer Perkin Elmer Lambda 35. Hanna Instrument pH213 microprocessor pH meter calibrated daily with pH 4.0 and 7.0 buffer were used to measure the acidity of solution and pH of buffer. About 40 mg of monazite was digested using sand bath using a mixture of HF:HNO<sub>3</sub> until the sample is turning to yellowish clear solution.. To make sure that the solutions are free from the undissolved particulates, it was then brought to the centrifuge for 2000 rpm within 7 minutes and filtered before diluted to 50.0 mL of volumetric flask. A 20.0 mL aliquot of prepared sample was pipette to the 100.0 mL of volumetric flask together with 10 mL of buffer, 10 mL NaCl and was top up with sodium citrate to the required volume for pH adjustment. Cyanex302 in n-heptane and toluene were used as extractants which were set at 0.1, 0.3, 0.4, 0.5, and 0.7 M for the organic phase. Sodium citrate and citric acid were used as a buffer while NaCl used to maintain the ionic strength of solution. Mixtures of organic and aqueous phases were shaken in the separating funnel for 5 minutes and allowed to reach the equilibrium within 5 minutes, 15 minutes and 30 minutes each. Then 0.05 % w/v of Arsenazo (III) was added to the aqueous phase for the spectrometry analysis by UV/VIS spectrometer.

#### **Calibration**

Working solution of europium was made by diluting the stock solution to the 0.1, 0.2, 0.3, 0.5, 0.7 and 0.8 for the calibration curve.

#### Recovery

A recovery test was performed using a known amount of analyte added to be sample and the analysis then performed and after the addition so that the amount received can be calculated [12, 13].

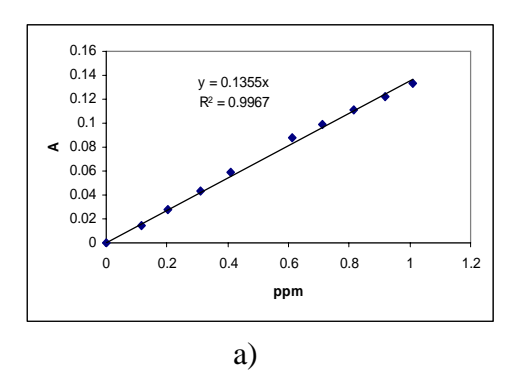
### **Extraction Eu(III) from Heavy Minerals**

The pure europium was prepared in an aqueous phase and extracted using Cyanex302 diluted in toluene. Varying the concentrations of Cyanex302, we will find the best Cyanex302 concentration which extract most Eu(III) into the organic phase. The amount of Eu(III) extracted was measured by the concentration Eu(III) left in the aqueous phase. This concentration was determined using UV/Vis spectrometer by adding Arsenazo (III) into the aqueous phase to produce the colour which is related to the concentration of Eu(III) in the sample.

#### **Results and Discussion**

## **Calibration and Linearity**

The standard solution was prepared in de-ionized water and buffer (citric acid/sodium citrate pH 2.2) to maintain pH ant 2.2 and 3 for toluene and n-heptane respectively. Figure 1a and 1b show the calibration curve for standard addition methods, respectively. The correlation coefficient for the calibration curve is 0.9967 while the correlation coefficient for the standard addition method is equal to 1 which is considered as a good linearity. Both curves can be used for estimating the concentration of Eu in the solution.



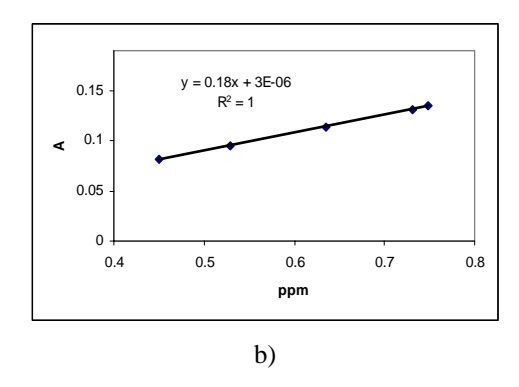


Figure 1: Linearity of the study represents by (a) Calibration curves and (b) standard addition method

### Recovery

Table 1 show the recovery of the laboratory fortified blank and laboratory fortified matrix. Laboratory fortified blank gives recovery in the range of 100.00 to 108.57 percent. The recoveries of fortified matrix range from 82.30 to 110.45.

Table 1: The percent recovery for laboratory fortified blank of sample spiked with standard europium

| Spiking level (ppm) | Fortified Blank % Recovery | Fortified Matrix % Recovery |
|---------------------|----------------------------|-----------------------------|
| 0.11                | 100.00                     | 110.45                      |
| 0.21                | 102.86                     | 94.30                       |
| 0.31                | 108.57                     | 97.72                       |
| 0.41                | 102.86                     | 96.24                       |
| 0.51                | 108.57                     | 82.30                       |

## Eu (III) extraction: Extraction as a function of pH

Figure 2 shows the extraction of europium as a function of the pH. Figure 2(a) shows the extraction of different pH using n-heptane as Cyanex302 diluents. It can be seen that the highest distribution ratio which lead to the highest percent extraction is at pH 3. However for the extraction using toluene as diluent, the highest distribution ratio is at pH 2.2. This pH value agreed with Ohashi *et al*, [7] finding, that is at pH 2.2, it could extract higher amount of europium even though their study is using cloud point extraction by di(2-ethylhexyl)phosphoric acid and Triton X-100.

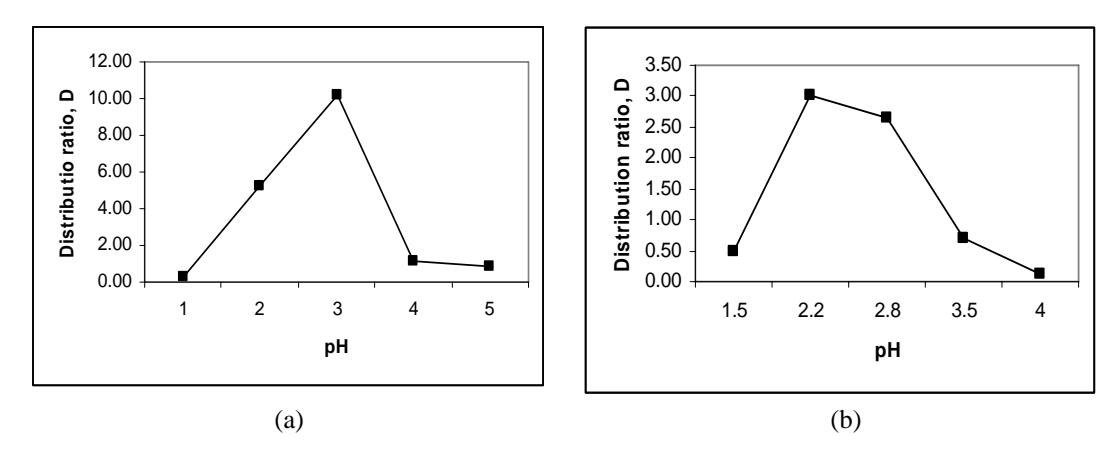


Figure 2: Effect of pH on the distribution ratio of Europium by (a) n-heptane (b) toluene

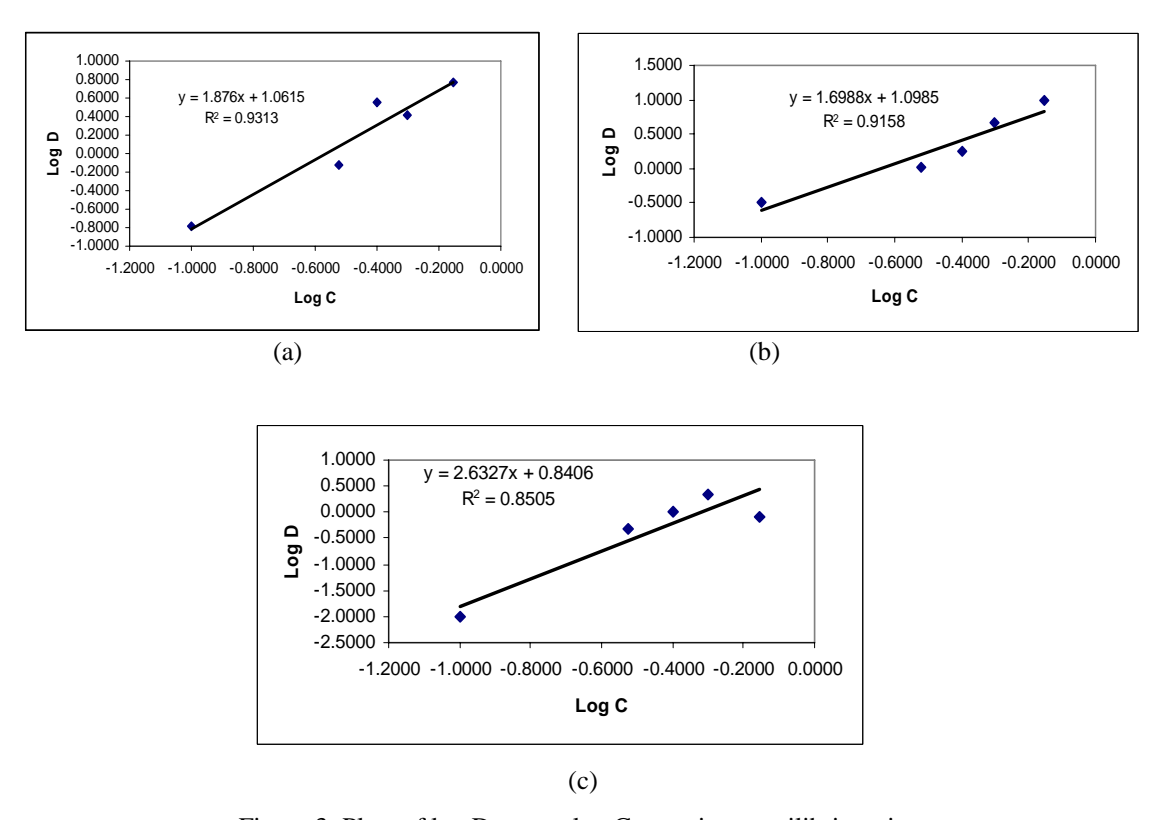


Figure 3: Plots of log D versus log C at various equilibrium time

### **Nature of the extracted species**

The nature of the extracted complex species was analyzed using the Log D versus Log C plots as suggested by Sarkar *et al* [14, 15] and Ajgaonkar *et al* [16]. In this study, the plot of log D versus log C as shown in Figure 3, show slopes of 1.876, 1.699 and 2.633 for 5, 15 and 30 minutes, respectively. However, the percent extraction was found greater in 15 minutes equilibrium time, thus indicating the best equilibrium time for europium extraction is 15 minutes.

The concentrayion of Cyanex302 were found to affect the amount of europium extracted from the aqueous phase. The higher the Cynex302 concentration, the more the europium ion will be transfered to the organic phase.

| Concentration of extractant | 5 minutes<br>(%) | 15 minutes<br>(%) | 30 minutes (%) |
|-----------------------------|------------------|-------------------|----------------|
| 0.1 ppm                     | 14.13            | 24.74             | 0.97           |
| 0.3 ppm                     | 43.00            | 51.12             | 33.10          |
| 0.4 ppm                     | 78.44            | 64.24             | 51.45          |
| 0.5 ppm                     | 72.56            | 82.35             | 67.96          |
| 0.7 ppm                     | 85.54            | 90.82             | 44.65          |

Table 2: Effect of equilibrium time to the extraction of europium

Distribution coefficient of Eu(III) increases with the increase of concentration of the extractant [17]. In other study, it was found that a decrease in the concentration of Cyanex302 will give lower disribution ratio values [14, 15].

## Extraction of Eu (III) from monazite samples

Table 3 shows the percent europium being extracted from two monazite samples (from Kg Gajah and Beh Minerals Sdn. Bhd., Perak) done in duplicates. It seems that the amount of europium extracted (in percent) from these monazites are comparable.

| Sample                 | Amount Extracted (%) |
|------------------------|----------------------|
| Kg. Gajah 1            | 64.89                |
| Kg. Gajah 2            | 62.20                |
| Beh Minerals Sdn Bhd 1 | 50.03                |
| Beh Minerals Sdn Bhd 2 | 57.78                |

Table 3: Percent extraction of europium from duplicates samples

## **Spectroscopy analysis**

The replacement of other element by europium in Cyanex302 can be proved by analysis with IR spectroscopy as shown in Figures 4a and 4b. This is well agreed by Ramachandran *et al* [18], Muhammad Idiris Saleh *et al* [19], Francis *et al* [20] Biswas *et al* [21, 22].

The IR spectra of europium complex with Cyanex302 and pure extractant were analyzed for a comparison. Cyanex302 spectrum shows two absorption bands at about 2950 cm<sup>-1</sup> and 2280 cm<sup>-1</sup> which indicates that the acids contains characteristics P(S)OH group. The bands at 750 and 905 cm<sup>-1</sup> indicate the P=S group and P-O stretching vibration in the P-O-H bond, respectively. In the spectra of Eu-Cyanex302 complex, the bands due to P(S)OH group are absent. These observations suggests when Cyanex302 molecule forms a complex with europium, the hydrogen atom of P-O-H is displaced by other ion [23].

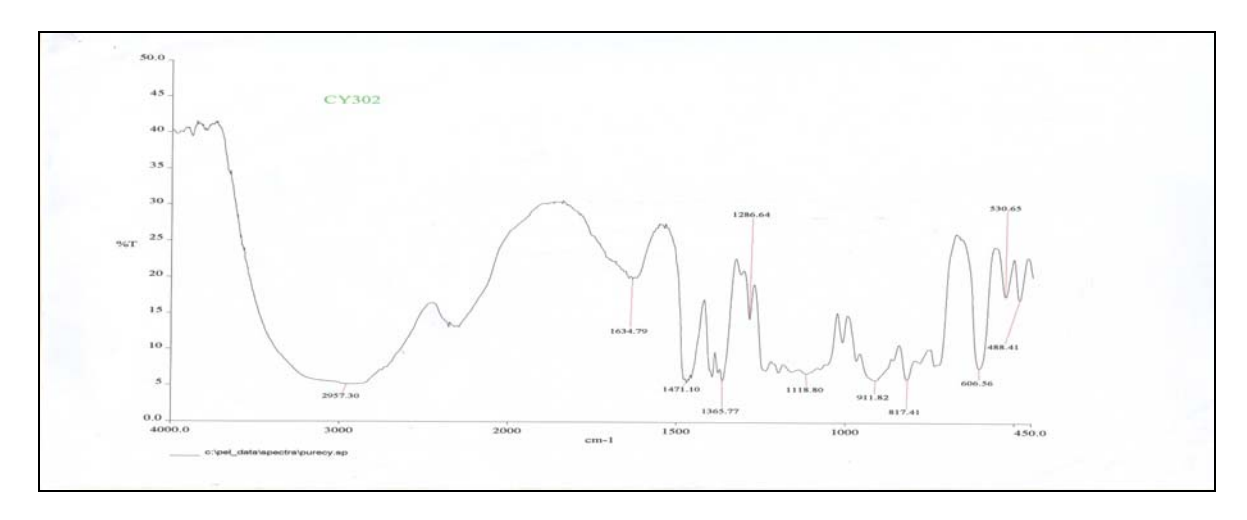


Figure 4a: FTIR spectrum of pure Cyanex302

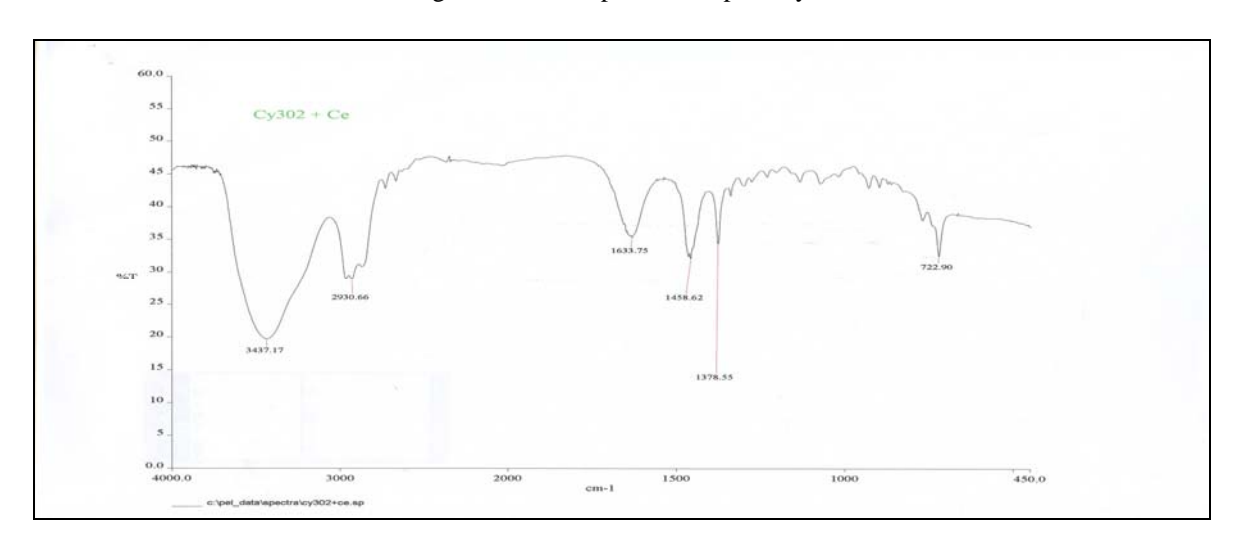


Figure 4b: FTIR spectrum of Eu-Cyanex302 complex

## Conclusion

Increasing the extractant concentrations will result in a better distribution ratio, D. It extracts more Eu(III) from monazite samples. The best concentration of Cyanex 302 for Eu(III) extraction in this study is 0.7 M at pH 2.2 for 15 minutes equilibrium time.

### Acknowledgement

The authors would like to thank RMI (UiTM) and Faculty of Applied Sciences UiTM for the support given and MOSTI for funding this project under Science Fund (03-01-01-sf0084).

## References

- 1. Worobiec, A., Stefaniak, E.A., Potgieter-Vermaak, S., Sawlowicz, Z., Spolnik, Z., Van Grieken, R. (2007). Characterisation of concentrates of heavy mineral sands by micro-Raman spectrometry and CC-SEM/EDX with HCA. *Applied Geochemistry*, **22**, 2078-2085
- 2. Walsh, J.A. (2007). The use of scanning electron microscope in the determination of the mineral composition of Ballachulish slate. *Materials Characterization*, **58**, 1095-1103.

- 3. Hu, S. J., Kandaiya, S. and T.S. Lee (1995). Studies of the radioactivity of amang effluent. *Applied Radiation and Isotopes*, **46**, 147-148.
- 4. Zaini Hamzah, Nor Monica Ahmad and Ahmad Saat (2009). Determination of heavy minerals in "amang" from Kampong Gajah ex-mining area. *The Malaysian J. Analytical Sciences*, **13(2)**, 184-203.
- 5. Morais C.A. and Ciminelli V.S.T. (1998). Recovery of europium from a rare earth chloride solution. *Hydrometallurgy* **49**, 167-177.
- 6. Morais C.A. and Ciminelli V.S.T. (1998). Recovery of europium by chemical reduction of a commercial solution of europium and gadolinium chloride. *Hydrometallurgy* **60**, 247-253.
- 7. Ohashi A., Hashimoto T., Imura H. and Ohashi K (2007). Cloud point extraction equilibrium of lanthanum (III), europium (III) and lutetium (III) using di(2-ethylhexyl)phosphoric acid and Triton X-100. *Talanta* **73**, 893-898.
- 8. Redling K (2006). Rare earth elements in agriculture with emphasis on animal husbandry. PhD thesis Ludwig-Maximilians-UniversitatMunchen, Germany.
- 9. Gracia Valls, R. Hrdlicka, A. Perutka, J. Havel, J. Deorka, N. V. Tavlarides, L. L. Munoz, M. and Valiente, M. (2001). Separation of rare earth elements by high performance liquid chromatography using a covalent modified silica gel column. *Analytica Chimica Acta*, **439**, 247-253.
- 10. Wu, D. Xiong, Y. Li, D. and Meng, S. (2005). Interfacial behavior of Ctanex302 and kinetics of lanthanum extraction. *Journal of Colloid and Interface Science*, 290, 235-240.
- 11. Khan, M. H. Warwick, P. and Evans, N. (2006). Spectrometric determination of uranium with arsenazo III in perchloric acid. *Chemosphere*, **61**, 1165-1169.
- 12. Gioia, M. G. Di Pietra, A. M. and Gatti, R. (2002). Validation of spectrometric method for determination of iron (III) impurities in dosage form. *Journal of Pharmaceutical and Biomedical Analysis*, **29**, 1159-1164.
- 13. Md. Pauzi Abdullah and Mohamad Nasir Othman (2007). Validation of an extraction technique based on Tributyl Phosphate for the determination of Pb(II) in water, *The Malaysian Journal of Analytical Sciences*, **11**(2), 361-369.
- 14. Sunil G.S. and Puroshattam M.D. (1999). Solvent extraction separation of antimony (III) and bismuth (III) with bis(2,4,4-trimethylpentyl) monothiophosphinic acid (Cyanex 302). *Separation and Purification Technology*, **15**, 131-138.
- 15. Sunil G.S. and Puroshattam M. D. (2000). Solvent extraction separation of Gold with Cyanex 302 as extractant. *Journal of the Chinese Chemical Society*, 47, 869-873.
- 16. Ajgaonkar, H.S. Puroshattam, M.D (1997). Solvent extraction separation of iron (III) and aluminium (III) from other elements with Cyanex 302. *Talanta*. **44**, 563-570.
- 17. Zhifeng Z, Hongfei L, Fuqiang G, Shulan M, Deqian L. (2008). Synergistic extraction and recovery of Cerium (IV) and Fluorin from sulfuric solutions with Cyanex 923 and di-2-ethylhexyl phosphoric acid. *Separation of Purification Technology*, **63**, 348-352.
- 18. Ramachandran Reddy, B. Rajesh Kumar, J. Phani Raja, K and Varada Reddy, A. (2004). Solvent extraction of Hf(IV) from acidic chloride solutions using Cyanex 302. *Minerals Engineering*, **17**, 939-942.
- 19. Muhammad Idiris Saleh, Md. Fazlul Bari, Bahruddin Saad. (2002), Solvent extraction of lanthanum(III) from acidic nitrate-acetato medium by Cyanex 272 in toluene. *Hydrometallurgy*, **63**, 75-84.
- 20. Tania F, Prasada Rao, T. Reddy, M.L.P. (2000). Cyanex 471X as extractant for the recovery of Hg(II) from industrial wastes. *Hydrometallurgy*, **57**, 263-268.
- 21. Biswas, R.K. and Begum, D.A. (1998). Solvent extraction of tetravalent titanium from chloride solution by di-2-ethylhexyl phosphoric acid in kerosene. *Hydrometallurgy*, **49**, 263-274.
- 22. Biswas, R.K. and Begum, D.A. (1998). Solvent extraction of Fe<sup>3+</sup> from chloride solution by D2EHPA in kerosene *Hydrometallurgy*, 50, 153-163.
- 23. Reddy B. R, Kumar J. R. Raja K.P. and Reddy A. V (2004). Solvent extraction of Hf(IV) from acidic chloride solution using Cyanex302. *Minerals Engineering*, 17, 939-942.